High-resolution organic petrography of the Toarcian Posidonia Shale of Germany and the western Netherlands: Study of the organo-mineral microfacies variations, reconstruction of the depositional environments and construction of a depositional model

Dissertation

der Mathematisch-Naturwissenschaftlichen Fakultät

der Eberhard Karls Universität Tübingen

zur Erlangung des Grades eines

Doktors der Naturwissenschaften

(Dr. rer. nat.)

vorgelegt von

Olga Gorbanenko

aus Semipalatinsk,

Kasachstan

Tübingen

2015

Gedruckt mit Genehmigung der Mathematisch-Naturwissenschaftlichen Fakultät der Eberhard Karls Universität Tübingen.

Tag der mündlichen Qualifikation: 11.08.2015

Dekan:	Prof. Dr. Wolfgang Rosenstiel
1. Berichterstatter:	Prof. Dr. Hervé Bocherens
2. Berichterstatter:	Prof. Dr. James Nebelsick

DECLARATION

I hereby declare that I alone wrote the doctoral work herewith submitted under the title "High-resolution organic petrography of the Toarcian Posidonia Shale of Germany and the western Netherlands: Study of the organo-mineral microfacies variations, reconstruction of the depositional environments and construction of a depositional model", that I used only the sources and materials cited in the work, and that all citations, whether word-for-word or paraphrased, are given as such.

I declare that I adhered to the guidelines set forth by the University of Tübingen to guarantee proper academic scholarship (Senate Resolution 25.05.2000).

I declare that these statements are true and that I am concealing nothing. I understand that my false statements can be punished with a jail term of up to three years or a financial penalty.

Olga Gorbanenko

ABSTRACT

High-resolution organic petrological analysis was carried out on more than 150 core bituminous shale samples of the Posidonia Shale (Toarcian, Lower Jurassic) from three sedimentary basins: the West Netherlands Basin, the Lower Saxony Basin and the South German Basin. This study is subdivided into three main parts: the identification of the organic microfacies variations in order to reconstruct paleoenvironmental conditions of the Posidonia Shale sedimentation, the maturity evaluation of the Posidonia Shale from three sedimentary basins and the construction of the deposition model of the Posidonia Shale.

The results of the organic petrography reveal that the organo-mineral microfacies defined by maceral composition and associated mineral groundmass show a wide range of variations related to the content of individual liptinite of marine origin and terrestrial macerals (macerals of vitrinite and inertinite groups and sporinite). The modifications in composition are considered as a potential indicator of different changes in depositional environments. In addition, much attention has been paid to the origin of the bituminite, which comprises most of the hydrocarbon-rich source rocks.

All defined organo-mineral microfacies are poorly correlated laterally between sedimentary basins. Only those from wells E and M (the West Netherlands Basin) show a resemblance. Organo-mineral microfacies from each investigated area contain a specific type of bituminite. Particularly, bituminite V has been observed in high concentration only in wells from the West Netherlands Basin, while the content of bituminite II increased significantly in wells from the Lower Saxony Basin, and bituminite III is well-represented in the Posidonia Shale from southern Germany.

The second part of the study evaluates the maturity of the Posidonia Shale. Vitrinite reflectance analysis has been used. In samples of those wells where appropriate vitrinite particles were not found, the Tmax parameter of Rock-Eval pyrolysis was used instead. The maturity of the Posidonia Shale from the West Netherlands Basin (0.4 %VRr) and southern Germany (0.4 %VRr) is defined as an early mature stage, whereas that of the Posidonia Shale from the Lower Saxony Basin (0.5–0.6 %VRr) reaches the mature stage. Exceptionally high vitrinite reflectance values are shown by Posidonia Shale in well B (3.2-3.6 %VRr) from the Lower Saxony Basin. In this case, organic matter maturity corresponds to the post-mature stage.

In order to study the changes in optical properties of the macerals from mature to post-mature Posidonia Shale, two wells, A and B, were chosen. The distance between the two wells is 44 km. This part of the study demonstrates that the telalginite bodies (named post-mature telalginite), bituminite I (post-mature bituminite I) and bituminite II (post-mature bituminite II), sporinite (post-mature sporinite) in post-mature Posidonia Shale are still recognisable on the basis of their morphology. This will help to extend the scope of application of maceral analysis in such post-mature black shale and will allow a better integration of the results of organic petrology in the field of exploration geology.

The third part is devoted to elaboration of a depositional model of Posidonia Shale. This part of the study is focused on the deposition of the organic matter and the main factors favouring its accumulation and preservation.

To improve the quality of the interpretation, two types of graphical visualisation of the petrographic results are proposed, primarily based on several factors controlling the deposition of the organic matter. Among these, the most important are primary biomass productivity in the marine environment and transported adjoining terrestrial organic matter, biological degradation related to bacterial activity, and oxygenation of the bottom water. The first type of graphical representation is a ternary diagram focusing on the paleoenvironments in the water column. The liptodetrinite, alginite and bituminite contents have been used to characterise the different paleoenvironments which reflect not only the content of oxygen in the water column but also the dynamic conditions.

The second type of graphical representation used is a scatter plot, assessing the paleoenvironmental conditions in the sediments. In order to evaluate the relationships between different types of organo-mineral microfacies and paleoenvironmental conditions, an Oxidation Index and a maceral Degradation Index are proposed. These indices display the degree of preservation of the macerals from the highly degraded to well preserved macerals, provide information on the origin of organic matter and permit recognition of the precursors of degraded organic matter (AOM).

For each of the investigated sedimentary basins, a depositional model of the organic matter sedimentation is proposed. These results reveal that the deposition and preservation of the organic matter are governed not only by the morphology of the sea floor, circulation of the water masses, but by changes in environments over time which enable both the biomass productivity and rapid burial of the organic matter in the anoxic ocean floor sediments. These environments are triggered not by an instant and continuous rise of the sea level, but more by sea-level fluctuations induced by alternate periods of dry and wet climates.

KURZFASSUNG

Hochauflösende organische petrologische Analyse wurde an mehr als 150 verschiedenen Bohrkernproben des Posidonienschiefers (Toarcium, Unterjura) aus drei Sedimentbecken angewendet: dem Westniederländischen Becken, dem Niedersächsischen Becken und dem Süddeutschen Becken. Diese Studie ist in drei Hauptbereiche unterteilt: die Bestimmung der Variationen der organischen Mikrofazies, um die Ablagerungsbedingungen des Posidonienschiefers zu rekonstruieren, die Bestimmung des Reifegrades der Posidonienschiefer aus den drei Sedimentbecken und die Entwicklung des Ablagerungsmodells des Posidonienschiefers.

Das Ergebnis der organischen Petrographie zeigt, dass die organo-mineralische Mikrofazies, die durch die Zusammensetzung der Macerale und der dazugehörigen mineralischen Grundmasse gekennzeichnet ist, eine große Streuung aufweist die in Abhängikeit zum Gehalt einzelner Liptinite mariner Herkunft und terrestrischer Macerale (Macerale aus der Vitrinit- und Inertinitgruppe und Sporinit) steht. Abwandlungen in der Zusammensetzung sind als potentielle Indikatoren von verschiedenen Änderungen in den Ablagerungsmilieus zu betrachten. Zudem wurde das Augenmerk auf die Herkunft des Bituminits gelenkt, der in den meisten mit Kohlenwasserstoff angereicherten Muttergesteinen enthalten ist.

Alle definierten organo-mineralischen Mikrofazies lassen sich schlecht zwischen den Sedimentbecken korrelieren. Lediglich die Bohrungen E und M (Westniederländisches Becken) weisen Ähnlichkeiten auf. Die organo-mineralische Mikrofazies von allen untersuchten Gebieten enthalten einen speziellen Bituminit Typ. Während Bituminit V mit hohen Konzentrationen nur in den Bohrungen des Westniederländischen Beckens beobachtet wurde, stieg der Gehalt an Bituminit II erheblich in den Bohrungen des Niedersächsischen Beckens an. Der Bituminit III wiederum, war besonders stark im Posidonienschiefer des Süddeutschen Beckens vertreten.

Der zweite Teil der Arbeit beschäftigt sich mit der Reife des Posidonienschiefer. Die Analyse der Vitrinitreflexion wurde hierfür angewendet. In den Proben, in denen keine geeigneten Vitrinitpartikel gefunden werden konnten, wurde stattdessen der Tmax-Parameter der Rock-Eval Pyrolyse verwendet. Die Reife des Posidonienschiefer des Westniederländischen Beckens (0.4%VRr) und des Süddeutschen Beckens (0.4%VRr) sind gekennzeichnet durch das Stadium der beginnenden Erdöl-Enstehung wohingegen die organische Materie der Posidonienschiefer des Niedersächsischen Beckens (0.5-0.6%VRr) reif ist (Hauptstadium der Erdölgeneration). Besonders hohe Vitrinitreflexionswerte zeigt der Posidonienschiefer der Bohrung B (3.2-3.6%VRr) des Niedersächsischen Beckens. In diesem Fall entspricht die Reife des organischen Materials dem Stadium der Trockengas Bildung.

Um die Veränderungen der optischen Eigenschaften der Macerale des Posidonienschiefers von dem Hauptstadium der Edölgeneration bis zum Stadium der Trockengas Bildung zu studieren, wurden zwei Bohrungen A und B ausgewählt. Der Abstand zwischen den Bohrungen beträgt 44 km. Dieser Teil der Arbeit zeigt, dass die Telalginit-Körper („postmature“ Telalginit genannt), Bituminit I (“postmature“ Bituminit I) und Bituminit II („postmature“ Bituminit II), Sporinit („postmature“ Sporinit) im Stadium der Trockengas Bildung des Posidonienschiefers anhand ihrer Morphologie immer noch erkennbar sind. Dies wird helfen, den Geltungsbereich der Maceralanalyse für solche Schwarzschiefer mit hohem Inkohlungsgrad zu erweitern und eine bessere Einbindung der Ergebnisse der organischen Petrologie im Bereich der Explorationsgeologie ermöglichen.

Der dritte Part widmet sich der Ausarbeitung eines Ablagerungsmodells vom Posidonienschiefer. Dieser Teil der Studie befasst sich mit der Ablagerung des organischen Materials and den Hauptfaktoren, die seine Anreicherung und Erhaltung begünstigen.

Um die Qualität der Interpretation zu verbessern, wurden zwei Arten von graphischen Darstellungen vorgeschlagen die hauptsächlich auf einige Faktoren basieren, welche die Ablagerung des organischen Materials beeinflussen. Darunter die primäre Produktivität der Biomasse im marinen Milieu und das hinzugefügte terrestrische organische Material, die biologische Zersetzung abhängig von der bakteriellen Aktivität sowie die Sauerstoffzufuhr des Bodenwassers.

Die erste Art der graphischen Darstellung ist ein Ternärdiagramm, das sich auf die Paläoablagerungsbedingungen in der Wassersäule konzentriert. Die Gehalte an Liptodetrinit, Alginit und Bituminit wurden verwendet, um die verschiedenen Ablagerungsbedingungen zu charakterisieren, die nicht nur den Sauerstoffgehalt in der Wassersäule widerspiegeln, sondern auch seine dynamischen Verhältnisse.

Die zweite Art der graphischen Darstellung ist eine Punktwolke zur Beurteilung der Paläoablagerungsbedingungen in den Sedimenten. Um die Zusammenhänge zwischen den verschiedenen organo-mineralischen Mikrofazies und Paläoablagerungsbedingungen auszuwerten, wurden ein Oxidationsindex und ein Maceral-Degradationsindex vorgeschlagen. Diese Indexe zeigen den Erhaltungszustand der Macerale, von stark zersetzten bis gut erhaltenen Maceralen, geben Auskunft über die Herkunft und Aussgangsstoffe des zersetzten organischen Materials (AOM).

Für jedes untersuchte Sedimentbecken wurde ein Ablagerungsmodell vorgeschlagen. Diese Resultate zeigen, dass die Ablagerung und Erhaltung des organischen Materials nicht nur von der Morphologie des Meeresbodens und der Bewegung der Wassermassen beherrscht werden, sondern auch durch langfristige Veränderungen des Milieus welche die Produktivität der Biomasse und die schnelle Einbettung des organischen Materials in anoxischen Sedimenten des Meeresbodens ermöglichen. Dieses Umfeld wird nicht durch einen kurzfristigen und fortwährenden Anstieg des Meeresspiegels ausgelöst, sondern vielmehr durch Meeresspiegelschwankungen, herbeigeführt, die auf abwechselnde Trocken - und Feuchtklimaperioden beruhen.

TABLE OF CONTENTS

LIST OF FIGURES

LIST OF TABLES

LIST OF ABBREVIATIONS

WNB – the West Netherlands Basin

LSB – the Lower Saxony Basin

SGB – the South German Basin

TOC – Total Organic Carbon, %

HI – Hydrogen Index, mg HC/g TOC

OI – Oxygen Index, mg CO_2/g TOC

KEYWORDS

Posidonia Shale, bituminous shale, Toarcian, Lias epsilon, Germany, West Netherlands, high-resolution organic petrography, organo-facies variations, depositional environments, depositional model, organic geochemistry, maturation, liptinite macerals, oil-prone macerals, meta-sporinite, meta-telalginite, meta-bituminite

ACKNOWLEDGEMENTS

This PhD thesis is a part of my life that has lasted for a bit more than three years. During this period I have met many different people. I would hereby like to acknowledge everyone who has supported me in various stages of my research and, of course, many thanks to those without whom this work would have been impossible.

It gives me great pleasure to acknowledge my supervisors at Tübingen University, Prof. Hervé Bocherens and Prof. James Nebelsick, for their invaluable discussions and good advice. I consider it an honour to work with Dr. B. Ligouis (Laboratory for Organic Petrology (LAOP), Rümelinstr. 23, 72070 Tübingen). Bertrand, thank you very much for your support of my study, scientific guidance, assistance in providing the microphotographs and for your introduction to the fascinating world of organic petrography of bituminous shale. Moreover, thank you for sharing with me the unpublished geochemical and petrographic results and microphotographs on Posidonia Shale from southern Germany, which are integrated in this work. I appreciate the help of Tabea Schmid and Miriam Vogler in the sample preparation for the microscopic work.

This thesis would not have been possible without the financial support of Shell International Exploration and Production B.V., Netherlands (UI35306). In particular, I would like to thank my project coordinators, Dr. Matthias Keym, Dr. Femke Vossepoel and Ghassen Chaari. Thank you very much for your valuable help in the solving of those many administrative problems which occurred during my studies. My sincere thanks go to Dr. Erdem Idiz and Dr. Erik Tegelaar for their constructive discussions, their encouragement and insightful comments. I am very grateful to Dr. Johan Weijers, Dr. Jos Pureveen and Dr. Rolande Dekke for introduction and assistance in sample preparation for biomarker analysis.
I would also like to thank ExxonMobil Production Deutschland GmbH and Shell Erdgas Beteiligungsgesellschaft mbH for the permission to share the data.

I am grateful to Prof. Hugh Jenkyns and Prof. Joe Cartwright at Oxford University for their fruitful discussions. Many thanks are extended to Dr. Micha Ruhl, who carried out the Rock-Eval analysis for me, as well as Matteo Paganoni and Martino Foschi. I thank all of you for your positive and friendly attitude. I would like to thank O.R. Green, who helped me to accomplish the powdering of 150 samples within 3 days.

Many thanks go to my friends, Flora Schilt, Mereike Stahlschmidt, Alvise Barbieri, Magnus Haaland, Haydar Martinez and Saman Heydari: thank you very much for your support and for all the fun we had in the past years.

Last but not least, I would like to express my sincere gratitude to my nearest and dearest, who have always stood by me throughout my life, for their continued support in different situations and for their encouragement.

CHAPTER 1. INTRODUCTION

Contents

1.1. A problem statement

Organic petrology is a subject with a broad scope originating from coal petrography, which dates back to the end of the 19th century as a branch of Earth Science (Stach *et al.*, 1982). With the increasing economic interest in fossil fuels, organic petrology has extended its application to the field of petroleum geology (Taylor *et al.*, 1998; Suárez-Ruiz, 2012). Basically, the petrographic evaluation of the maturity of the source rocks and a qualitative description of the composition of organic matter have been used.

In recent decades, the role of organic petrology has increased. It is frequently used in conjunction with results of geochemical analysis in order to provide insight into understanding the composition of kerogen. The different ability of kerogen to generate hydrocarbon reflects the variability in chemical composition of the organic matter (Huc, 1990). Organic matter, in terms of organic petrography, can be described by using macerals, which represent the highest level of chemical organisation of organic matter (Hutton and Rob, 1994). The occurrence of the specific maceral assemblages is closely linked to the different paleoenvironments in which this organic matter was deposited and preserved. Using not only qualitative, but quantitative methods, organic petrology enables light to be shed on the origin of some organic components (bituminites and liptodetrinite), which are linked to the generation properties of the source rocks, and to reconstruct the depositional environments, triggering the sedimentation of organic-rich sediments. Specifically, this method is essential in those sediments in which sedimentological transition is not obviously marked by lithological differences present at subsurface cutting and logs (Leckie *et al.*, 1990; Pasley and Hazel, 1989).

Deposition of Posidonia Shale is considered as a cause of a global oceanic anoxic event (OAE), which was recorded not only in Europe, but in Canada, Alaska, Japan, Australia, Madagascar and Argentina (Farrimond *et al.*, 1989). In Western and Central Europe, the Posidonia Shale is one of the most widespread of bituminous shale formations. It is also known as “Schistes carton” in France (Paris Basin, Aquitaine Basin, Chalhac and Causses Basin), “Jet Rock” in England (Yorkshire Basin, Cleveland Basin) and “Posidionienschiefer” in Germany (German Basin and Swiss Basin) (Röhl and Schmid-Röhl, 2005).

Many scientists have shown a particular interest in this bituminous shale formation, acting as an economically important source rock of the most oil and gas accumulations in

northern Germany, the Paris Basin, Upper Rhine Graben and the Netherlands (Littke *et al*., 1991). As an understanding of the origin of organic-rich sediments during the Early Toarcian period requires a multidisciplinary approach, much research is devoted to the investigation of the Posidonia Shale from a geological, paleontological, paleoecological, sedimentological, geochemical point of view. However, few attempts have been successful in the detailed quantitative organic petrological investigation of the organic constituents of the Posidonia Shale. Moreover, for the first time, high-resolution organic petrography is carried out on the Toarcian bituminous shales from the Netherlands.

Although a global anoxic event resulted in the deposition of Posidonia Shale, the properties of the bituminous shales vary significantly from one sedimentary basin to another. This evidence requires more detailed understanding of the depositional environments and processes of organic matter deposition, accumulation and preservation.

This study presents a detailed description of organo-mineral microfacies of Posidonia Shale from the West Netherlands Basin, the Lower Saxony Basin and the South German Basin. For the first time, high-resolution organic petrology has been used to describe organo-mineral microfacies, defining individual macerals which act as a sensitive indicator of different conditions and to define petrographic indices in order to reconstruct depositional environments of the Posidonia Shale. In addition, this takes the lid off the origin of amorphous organic matter, which is still little understood.

1.2. Location of the studied areas

For this study, wells from the West Netherlands Basin (WNB), the Lower Saxony Basin (LSB) and the South German Basin (SGB) were selected (Fig. 1-1). The West Netherlands Basin is situated in the southwestern part of the Netherlands and the adjacent offshore areas (Wong, 2007) (Fig. 1-1). This basin is bounded to the south by the London-Brabant Massif, forming the boundary with the Roer Balley Graben to the southeast. It borders the Ijmuiden High/Zandvoort Ridge, which separates WNB from the Central Netherlands Basin to the northeast and the Broad Fourteens Basin to the northwest (van Balen *et al*., 2000). The WNB is one of the set basins which were separated from the bigger extensive South Permian Basin in the Triassic time and was later inverted in the Late Jurassic/Early Cretaceous time (Betz et al., 1987; Ziegler, 1990; Wong, 2007).

The Lower Saxony Basin (LSB) is a relatively small, approximately E-W trending basin within the greater South Permian Basin. It is 270 km long and 70 km wide, and is bounded to the north by the stable Pompeckj Block and to the west by the Central Netherlands

High (Betz *et al*., 1987; Kockel *et al*., 1994)). To the south, the LSB is limited by the stable Münsterland block and the Harz mountains, and to the east it is bordered by the N-S trending Jurassic Gifhorn Trough (Betz *et al*., 1987).

Finally, the third studied area is the Swabian Basin which belongs to the South German Basin. The latter is a part of an intracratonic basin, which remains an isosceles triangle (Geyer *et al*., 2011). To the west, the basin is bordered by the Upper Rhine Graben, to the northeast with the Tertiary vulcanites of the Vogelsberg mountains and by a NW-SE striking fault system. The southern border is formed by the Molasse Basin and the folded Subalpine molasse of the French Alps.

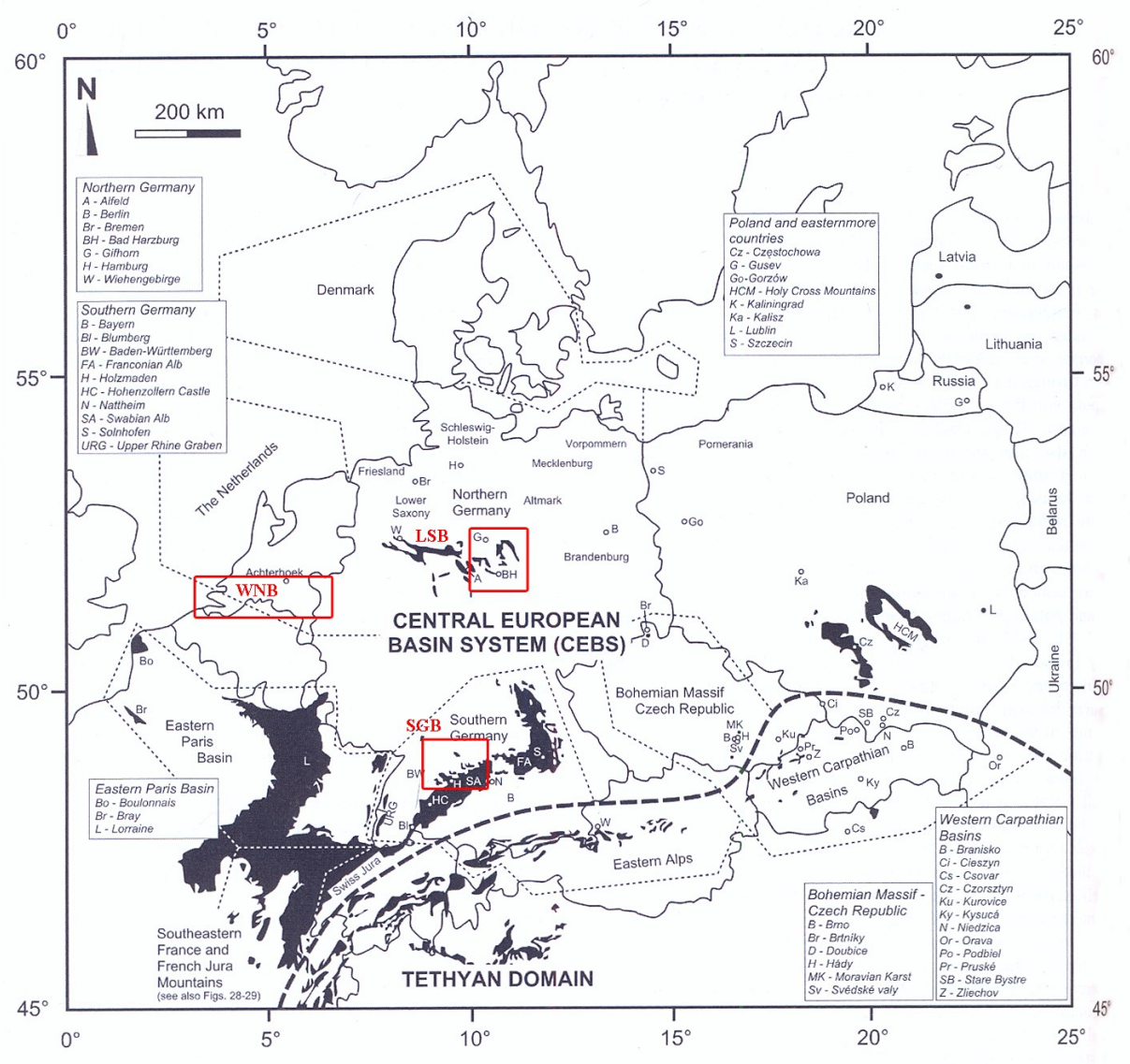

Fig. 1-1: Location of investigated areas (Modified after McCann, 2008).
On the map: WNB – West Netherlands Basin; LSB – the Lower Saxony Basin; SGB-SouthGerman Basin.

1.3. Aims and objectives of the study

This study is a comprehensive organic petrological characterisation of the Posidonia Shale and its depositional environments from three sedimentary basins: the West Netherlands Basin, the Lower Saxony Basin and the South German Basin. The main objectives of this study are the following:

- to identify and characterise the organo-mineral microfacies in each of the aforementioned sedimentary basins, using high-resolution organic petrography;
- to understand the lateral and vertical organo-microfacies variations;
- to interpret the results obtained by organic petrography in conjunction with geochemical analysis;
- to reconstruct the depositional environments and develop the hypothesis on their origin and evolution;
- to construct the depositional model of sedimentation of the Posidonia Shale

The goals can be fulfilled by providing the results on a microscopic level, using qualitative and quantitative methods of high-resolution organic petrography. Petrographic investigations were performed on the Posidonia Shale block samples, polished perpendicular to the bedding in both reflected light and fluorescence mode in order to increase the quality of the work. To better understand the paleoenvironments which control the deposition of organic-rich sediments, a specific graphic representation of the results is proposed.

1.4. Literature overview

1.4.1. Geology of the investigated sedimentary basins

The geological history of the Jurassic from the West Netherlands Basin has been studied by Heybroek (1974), Van Wijhe (1987), Ziegler (1990) and Wong (2007). During the last decade, several authors have published detailed works on the Lower Jurassic source rocks (Bodenhausen and Ott, 1981; De Jager *et al*., 1996; van Balen *et al.*, 2000). The first estimation of expected petroleum resources in the Netherlands was made by Muntendam-Bos *et al*. (2009).

General investigations on the geological evolution of Lower Saxony were undertaken by Boigk (1968), Stadler and Teichmüller (1971), Betz *et a*l. (1987), Ziegler (1990), Baldaschuhn *et al*. (1991) and Kockel *et al*. (1994). However, most of the research was conducted as a consequence of increased interest in the economically profitable oil and gas

fields (Boigk *et al*., 1974; Plein, 1985; Düppenbecker and Welte, 1989; Binot *et al*., 1993; Kockel *et al*., 1994). Some of the workers attempted to understand the high thermal anomaly occurring in the vicinity of the lacoliths (Bartenstein *et al*., 1971; Koch and Arnemann, 1975; Deutloff *et al*., 1980; Brauckmann, 1984; Buntebarth, 1985; Teichmüller and Teichmüller, 1985; Büchner, 1986; Littke and Rullkötter, 1987; Rullkötter *et al*., 1988; Schmitz and Wenzlow, 1990; Leischner *et al*., 1993). These investigations used vitrinite reflectance measurements as a tool for maturity assessment.

The geological history of southern Germany has been described by Ziegler (1990), Walter (2007) and Geyer *et al*. (2011). Detailed micropalaeontological, biostratigraphical and sedimentological work on Lower Toarcian core sections in southwestern Germany was carried out by Riegraf (1985). In his work, the author provided a detailed microfacies description of the Lower Toarcian, complemented with numerous paleoenvironmental data. More recent works by Röhl and Schmid-Röhl (2005) depicted a sequential stratigraphic interpretation of the deposition of the Posidonia Shale from the South German Basin, based on sedimentological, geochemical and paleoecological data.

1.4.1. Petrographic and geochemical characterisation of organic matter in bituminous shales

Much work has been done on the geochemical and petrographical analysis of the composition of the organic matter of bituminous shaless, including the Posidonia Shale (Alpern and Cheymol, 1978; Kauffman, 1978; Küspert, 1983; Tissot *et al*., 1987; Rullkötter and Marzi, 1988; Leythaeuser et al., 1988; Röhl and Schmid-Röhl, 2005; Bernard *et al*., 2012). Many hypotheses have been put forward regarding its origin. These hypotheses have been established mainly from geological, organic petrological and geochemical investigations. The geochemical and petrological properties of liptinite macerals, which are the dominant organic constituents of bituminous shaless, were reported by Stach (1953), Durand *et al*. (1972), Huc (1977), Espitalié *et al*. (1977), Teichmüller and Ottenjann (1977), Littke and Rullkötter (1987); Stasiuk and Goodarzi (1988), Peniguel *et al*. (1989), Hollander *et al*. (1991) and Prauss *et al*. (1991). Many of these studies were devoted to the petrographic properties of the liptinite group as a main oil-prone component in bituminous shale (Leythaeuser *et al*., 1988; Littke and Rullkötter, 1987; Stasiuk, 1994).

It is evident that Early Toarcian bituminous shaless seem to be well-investigated. However, some of the proposed theories' hypotheses of their formation and depositional

models have been inter-inconsistent and the factors controlling the sedimentation of Early Toarcian bituminous shaless are still a subject of hot debate.

1.4.2. Existing depositional models of black shales

As black shales have a high oil generation potential, numerous authors have attempted to understand the main factors triggering the deposition of the organic-rich sediments. In the '70s, the point of view about the origin of black shales underwent a revolutionary change after the start of the Deep Sea Drilling Project (DSDP). The origin of black shales was linked to the global anoxic event (AOE), originally defined by Schlanger and Jenkyns (1976). Although this concept does not explain the variation in paleoenvironmental conditions launching the sedimentation of bituminous shales, it does not invalidate the concept. However, it requires the individual adaptation of the scenario of black shale deposition in the case of each of the investigated sedimentary basins (Lipson-Benitah et al., 1990).

Many created depositional models describe physical and chemical factors, such as sea bottom relief, origin of the oxygen-minimum zone, water mass distribution, position of the redox boundary, climate, cloud streamers indicating offshore winds. However, fewer attempts have been made regarding the variability of the origin of organic matter and biomass productivity. Some of the authors turned to the modern analogies of black shale sedimentary basins in order to provide insight into and understanding of black shale sedimentation. Some of the created models were based on a deep, enclosed basin with a positive water balance in the case of bituminous shale (Caspers, 1957; Degens and Ross, 1974; Demaison and Moore, 1980); a deep borderland basin with an indicated O_2 minimum (e.g. S. California) (Demaison and Moore, 1980; Smith and Hamilton, 1983; Thompson et al., 1985); Western continental slope; coastal upwelling (e. g. Peru, Namibia) (Demaison and Moore, 1980; Rosenberg *et al*., 1983; Arntz *et al*., 1991); shallow stratified basin (e.g. Baltic Sea) (Goldman, 1924); Rosenberg, 1977)) and coastal/intertidal zone (e.g. lagoons, tidal flats) (Jørgensen and Revsbech, 1985).

However, some processes occurred only in the past and have no analogies in recent times. Although many models exist to describe the deposition and accumulation of bituminous shales, in this study the main focus of attention lies on the examination of four basic models (“silled basin” model, “irregular bottom topography” model, “expanding puddle” model, “upwelling” model), which were later supported or invalidated by many other

authors (Küspert, 1983, Riegraf, 1985; Röhl and Schmid-Röhl, 2005; Trabucho-Alexandre *et al*., 2012).

1.4.2.1. "Silled basin" model

The "silled basin" model was proposed by Pompeckj (1901) (Fig. 1-2A). This model is based on the modern Black Sea deep-water basin with restricted circulation and anoxic bottom waters caused by a topographic barrier. This model was further developed by Sielacher (1982), Küspert (1983) and others. The occurrence of anoxic events in this model is explained only by the physical characteristics, but not necessarily by stratification of water masses or an euxinic water column, that causes it to fail compared to other existing models (Trabucho-Alexandre *et al*., 2012).

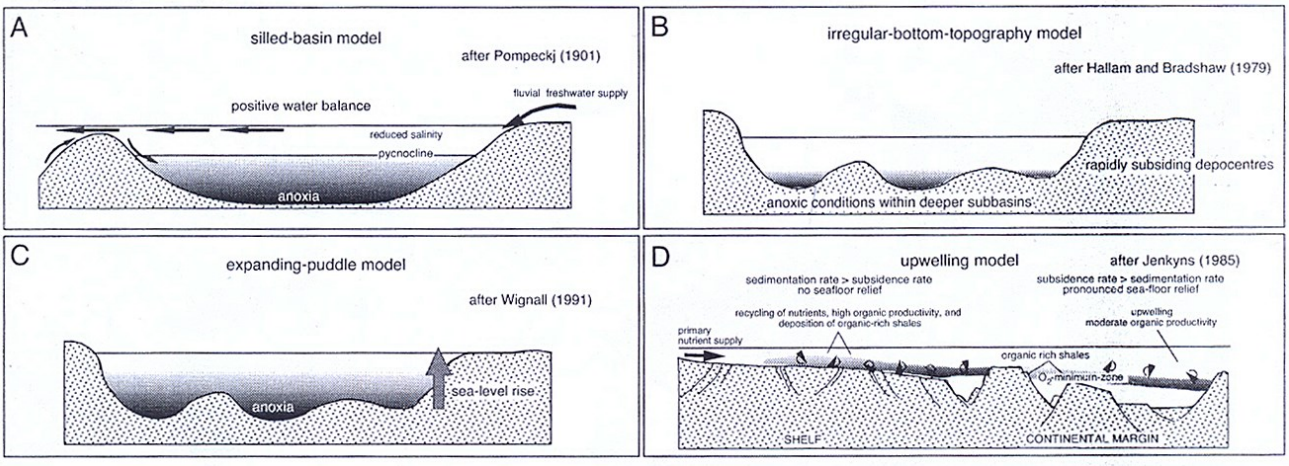

Fig. 1-2: Models describing the details of the deposition of Lower Toarcian black shales.
A) the "silled basin" model; B) The "irregular bottom topography" model; C) the "expanding puddle" model; D) The "upwelling" model (Modified after Röhl and Schmid-Röhl, 2005).

1.4.2.2. "Irregular bottom topography" model

The "irregular bottom topography" model was introduced by Hallam and Bradshaw (1979) and demonstrates the reconstruction of a pronounced sea-floor relief in the Central European Basin (Fig. 1-2B). The "expanding puddle" model, as an extended version of the previously described model, explains progressive onlapping of black shale facies during the Early Toarcian transgression (Fig.1-2C). However, the authors attempted to explain the occurrence of black shale by one global anoxic event. Moreover, this model is an oversimplification of the existing variety of environments and processes which led to the occurrence of organic-rich sediments (Trabucho-Alexandre *et al.,* 2012).

1.4.2.3. "Upwelling" model

Jenkyns (1985) proposed the "upwelling" model, which has been further discussed in the works of Jenkyns and Clayton (1997) and Jenkyns *et al*. (2001) (Fig. 1-2D). According to this model, upwelling at the northern Tethyan margin led to enhanced water surface productivity and caused an expansion of the oxygen-minimum layer, which spread into the Central European Basin during transgression and launch of black shale sedimentation.

1.4.2.4. "Shallow water" model

The "shallow water" model was proposed by Schlager (1981), in which a slow rise in sea level led to stagnation. This model is based on the existence of a permanent stable stratification of the water column over the shelf and the absence of bottom currency (Trabucho-Alexandre *et al.,* 2012). It was further developed by Wignall (1991), Wignall and Newton (2001), later by Röhl and Schmid-Röhl (2005). It was renamed the "transgressive chemocline" model, which explains facies distribution, more precisely, onlapping of black shale facies and transgressive nearshore black shales in the Central European Basin during the Early Toarcian period.

Although numerous existing published works relate to the depositional environments of bituminous shaless, the details and key triggers of organic-carbon deposition are still poorly understood. Moreover, the processes favouring the formation of the Posidonia Shale in each of the investigated sedimentary basins differ and should be examined individually.

CHAPTER 2. GEOLOGICAL FRAMEWORK OF THE INVESTIGATED AREAS

Contents

2.1. General outline

In the Late Triassic-Jurassic time, the structural outline of Western and Central Europe changed dramatically. That reorganisation, caused by a major tectonic event — the break-up of the supercontinent Pangea, occurred in the course of several extension phases, followed by a period of tectonic quiescence (Wong, 2007).

The Early Jurassic period was a period of a tectonic quiescence. It is characterised by regional thermal subsidence, caused by salt movements, which, in turn, controlled the distribution of Jurassic depocentres of sedimentation (Ziegler, 1988; Wong, 2007). At that time, a set of smaller sedimentary basins, such as the West Netherlands Basin, the Lower Saxony Basin, occurred from a single extensive Southern Permian Basin in northern Germany and the South German Basin, which was a northern margin of paleocean Tethys, in the south. Contemporaneously, transgression of epicontinental seas flooded cratonic interiors during high stands of sea level, triggering sedimentation of the well-known source rocks Posidonia Shale.

The Toarcian time was characterised by a cyclical rise in the sea level, probably related to the waxing and vanishing of the ice sheets of Siberia (Littke, 1993). In Western and Central Europe, the facies pattern was strongly influenced by the interference of the colder, lower-salinity Arctic, and the warmer, higher-salinity Tethys waters, as well as by the continued influx of clastics from eastern sources (Fig. 2-1). This was accompanied by a commensurate run-off of fresh water from the land areas (Littke, 1993). This particularity reflected on the diversity and distribution of macro- and microfauna and, as a consequence, on the characteristics of the Posidonia Shale as a source rock.

In the investigated area, the Posidonia Shale appeared as a large outcrop in southern Germany, but smaller and more scattered sets of outcrops in northern Germany. However, it is completely overlapped by younger sediments in the Netherlands, where the Posidonia Shale was penetrated only by wells (Farrimond *et al*., 1988). The thickness of the Posidonia Shale also varies, depending on the area of deposition. For instance, in northern Germany, the thickness of the Posidonia Shale succession is much higher than in southern Germany (Littke, 1993). Evidently, taking into account all particularities of the Posidonia Shale deposition in the different sedimentary basins, a description of geological, tectonic and stratigraphical features will be presented individually in order to avoid oversimplifications.

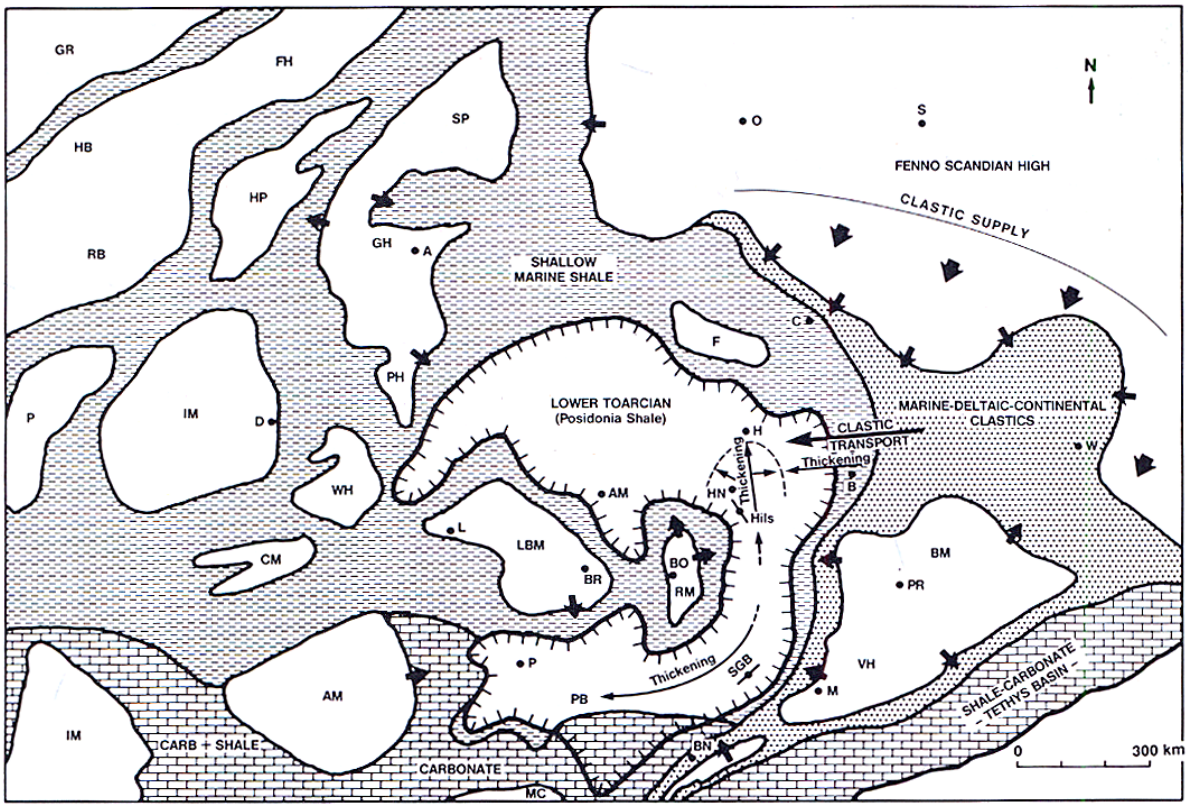

Fig. 2-1: Sinemurian-Aalenian paleogeographic map showing principal sedimentary facies distribution in Western and Central Europe (Modified after Ziegler, 1982; Littke, 1993).
Emergent areas: AM-Armorican Massif; BM-Bohemian Massif; F-Fünen High: GH, Grampian Highlands; LBM-London-Brabant Massif; MC-Massif Central; PB-Paris Basin; PH-Pennine High; RM-Rhenish Massif; SP-Shetland Platform; VH-Vindelician High; WH-Welsh High. Cities: A, Aberdeen; AM, Amsterdam; B, Berlin; BN, Bern; BO, Bonn; BR, Brussels; C, Copenhagen; H, Hamburg; HN, Hannover; L, London; M, Munich; O, Oslo.

2.2. The West Netherlands Basin

2.2.1. Geological setting

Generally, the evolution of the West Netherlands Basin (WNB) governed by tectonic events can be subdivided into four stages:

(1) *Late Carboniferous–Late Permian stage*. At the beginning of this stage, the basin was situated to the north of the London-Brabant Massif and displayed subsidence, however, this trend changed at the time of Variscan orogeny, which caused uplift of the area and widely distributed erosion. Sediments corresponding to this stage consist of basal hot shale and coal-bearing strata, which gave the latter a way to the younger red-beds series (van Balen *et al*., 2000).

(2) *Late Permian–Middle Jurassic stage.* This stage is also well-known as the Prerift stage. In Late Permian, WNB formed a relatively stable block. The sedimentary succession

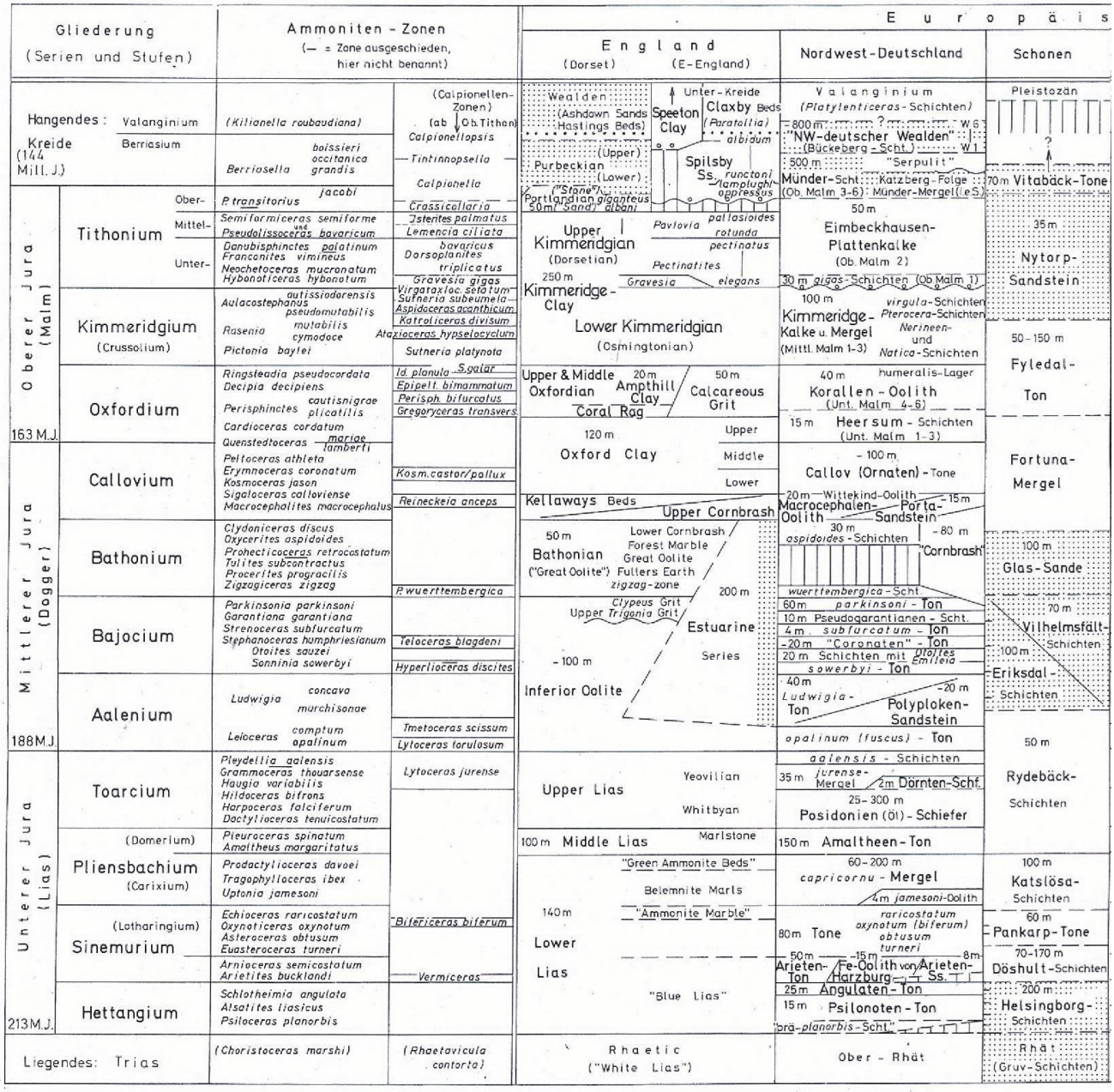

Fig. 2-2: Correlation between the Jurassic regional subdivisions of Western Europe and international stratigraphic chart (Modified after Brinkmann and Kayser, 1991).

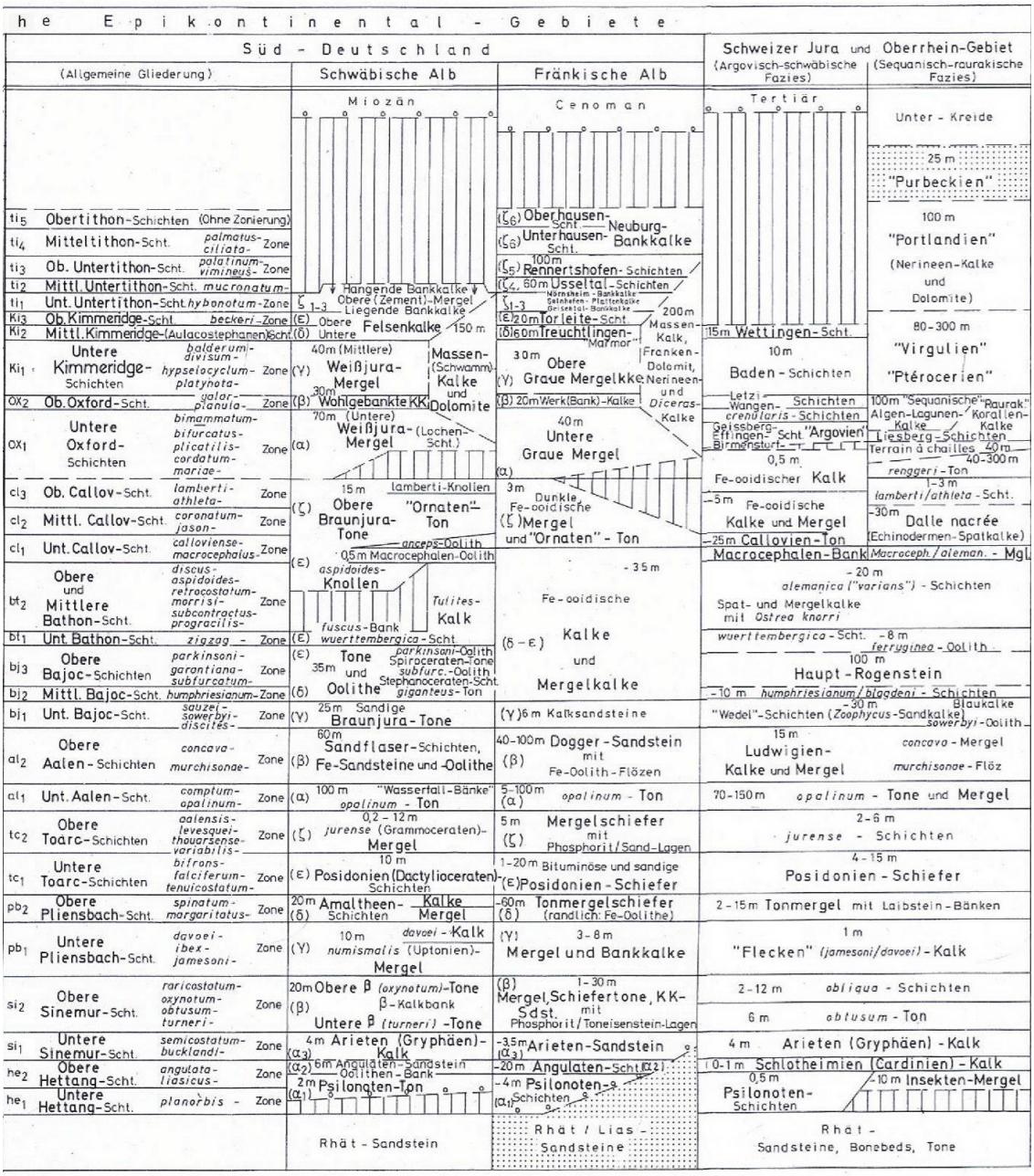
he Epikontinental-Gebiete
Süd-Deutschland
(Allgemeine Gliederung)
Schwäbische Alb
Fränkische Alb
Schweizer Jura und (Argovisch-schwäbische Fazies)
Oberrhein-Gebiet (Sequanisch-raurakische Fazies)
Miozän
Cenoman
Tertiär
Unter-Kreide
"Purbeckien"
"Portlandien"
(Nerineen-Kalke und Dolomite)
"Virgulien"
"Ptérocerien"
Wettingen-Schicht
Baden-Schichten
Macrocephalen-Bank
Haupt-Rogenstein
Ludwigien-Kalke und Mergel
Posidonien-Schiefer
"Flecken" (jamesoni/davoei)-Kalk
Arieten (Gryphäen)-Kalk
Schlotheimien (Cardinien)-Kalk
Psilonoten-Schichten
Insekten-Mergel
Rhät-Sandsteine, Bonebeds, Tone
Rhät/Lias-Sandsteine

comprises fluvial and aeolian sandstones of the Upper Rotliegend group, which was later followed by claystone, siltstone and carbonate of the Zechstein Group. The thickness of sediments increased towards the Zandvoort Ridge. The uplift event in the Late Permian period was changed by regional thermal subsidence in the Early Triassic period. The previous extensional phase in the earliest Rhaetian caused the marine transgression across large parts of Europe. Once, in the Earliest Hettangian to Earliest Toarcian, basin circulation became restricted, a dysaerobic condition governed the sedimentation. Evidently, the well-oxygenated condition changed into oxygen-depleted, which was re-established in the latest Toarcian and Aalenian, when a series of marine silty and oolitic mudstone was deposited. The next phase of uplift led to a decrease of the thickness of the Buntsandstein subgroup (Fig. 2-2) (Ziegler, 1990; van Balen *et al*., 2000). In the Middle Triassic–Early Jurassic time, tectonic movement triggered the occurrence of a faulting system; this caused differential subsidence of various parts of the basin. The West Netherlands Basin and Roer Valley Graben developed in NW–SE to NNW–SSE directions.

(3) *Late Jurassic–Early Cretaceous* stage. Rifting processes, occurring at that time, caused the differentiation and thickness variation in different parts of the basin. This stage was accompanied by repeated igneous activity, mainly occurring in the southeastern part of the WNB (van Balen *et al*., 2000; Herngreen *et al*., 2003; McCann, 2008).

(4) *Late Cretaceous–Quaternary stage.* The last stage of basin evolution is characterised by inversion of the WNB, which was governed by compressive stress. As a consequence of this tectonic event, numerous faults occurred in that period of basin evolution. The majority of those fault zones displayed reverse movements. At the beginning of the Paleogene period, the subsidence of the WNB increased (van Balen *et al*., 2000). The Roer Valley Graben were strongly inverted during the Late Cretaceous (Sybhercynian/Laramide phase), eroding most of the Jurassic and Cretaceous deposits. In the transition zones between the Roer Valley Graben and the WNB, distinct structural NNW–SSE and WNW–ESE fault directions occurred (Fig. 2-3; 2-4) (van Balen *et al.,* 2000).

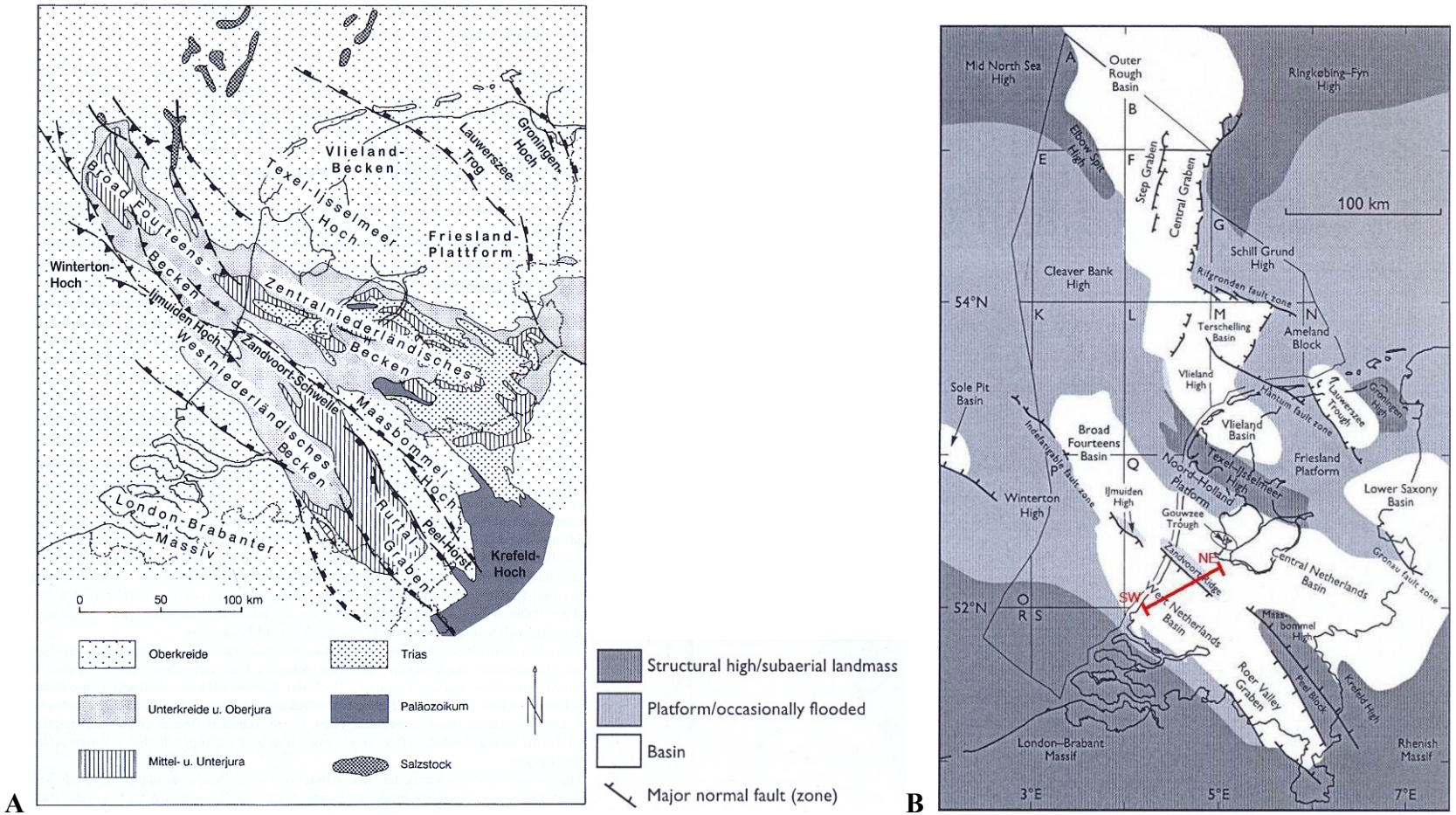

Fig. 2-3: Geological map (A) and tectonic map (B) of the West Netherlands Basin (Modified after Walter, 2007; McCann, 2008).
Geological map: Salzstock-Salt stock; Paläozoicum-Paleozoic; Trias-Triassic; Mittel and Unterjura – Middle and Lower Jurassic; Unterkreide u. Oberjura – Lower and Upper Jurassic; Oberkreide – Upper Cretaceous. The other main tectonic elements on Map A are identical to those on Map B.

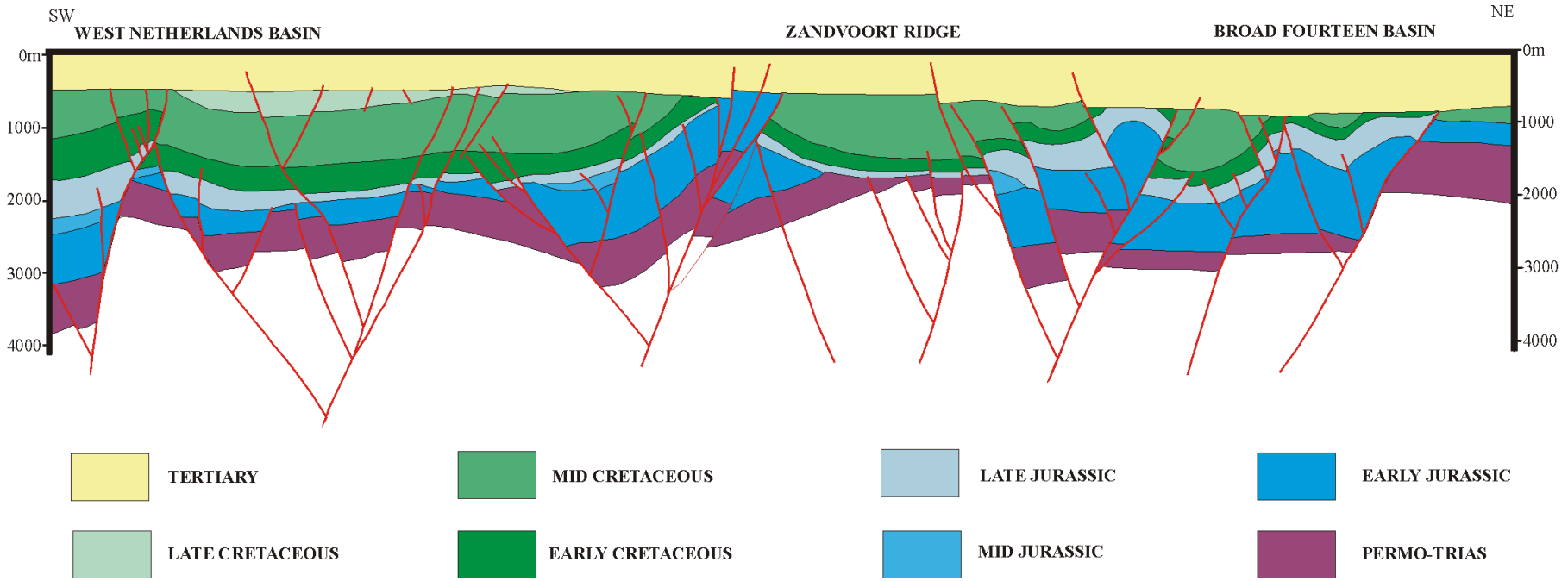

Fig. 2-4: Stratigraphic cross-section across the West Netherlands Basin. See Fig. 2-3 for the location of the cross-section (Modified after Ziegler, 1990).

2.2.2. Tectonic features

The West Netherlands Basin (WNB) has a Caledonian Crystalline basement, which is deeply buried and has been encountered only in the offshore area (van Bergen and Sissingh, 2007; De Jager and Geluk, 2007). This basement is unconformably covered by the transitional complex of the Middle Devonian–Early Carboniferous deposited in horsts and grabens occurring in the last phase of Caledonian orogeny horsts and grabens. This transitional complex is covered by Late Paleozoic-Mesozoic-Cenozoic sedimentary rocks. The geological record comprises more than 10 km of sediments, despite numerous unconformities (De Jager and Geluk, 2007).

The WNB is fragmented by numerous smaller and bigger tectonic elements trending in a NW–SE direction. To the south, it is bordered by the NW–SE- to NNW–SSE-striking Roer Valley Graben, which developed in the Jurassic time (Fig. 2-3; Fig. 2-4). Large faults in the WNB occurred during the Carboniferous–Permian time and were later reactivated in the different phases of tectonic evolution of the basin. Salt movement events led to the development of depocentres of Jurassic deposition (McCann, 2008).

2.2.3. Stratigraphy

The Posidonia Shale succession is the most widely distributed and important source rock in the Netherlands, appearing in the depth interval between 830 m and 3055 m (van Bergen *et al*., 2013). Its thickness varies from 30 to 60 m across the West Netherland Basin, diminishing towards the basin margins and bounding heights (Wong, 2007; Pletsch *et al*., 2010). The irregular character of the Posidonia Shale distribution indicates that an erosion event occurred as a consequence of the Late Carboniferous inversion (Pletsch *et al.,* 2010)

Generally, the Posidonia Shale is a part of the Alterna Group, represented by a dark grey to brownish-grey bituminous claystone (Fig. 2-5). Within this formation, the composition of the bituminous shaless varies, indicating different paleoenvironmental conditions during its deposition (van Bergen et al., 2013). Evidently, the geochemical properties and organic petrographic characteristic may also differ within one the Posidonia Shale succession.

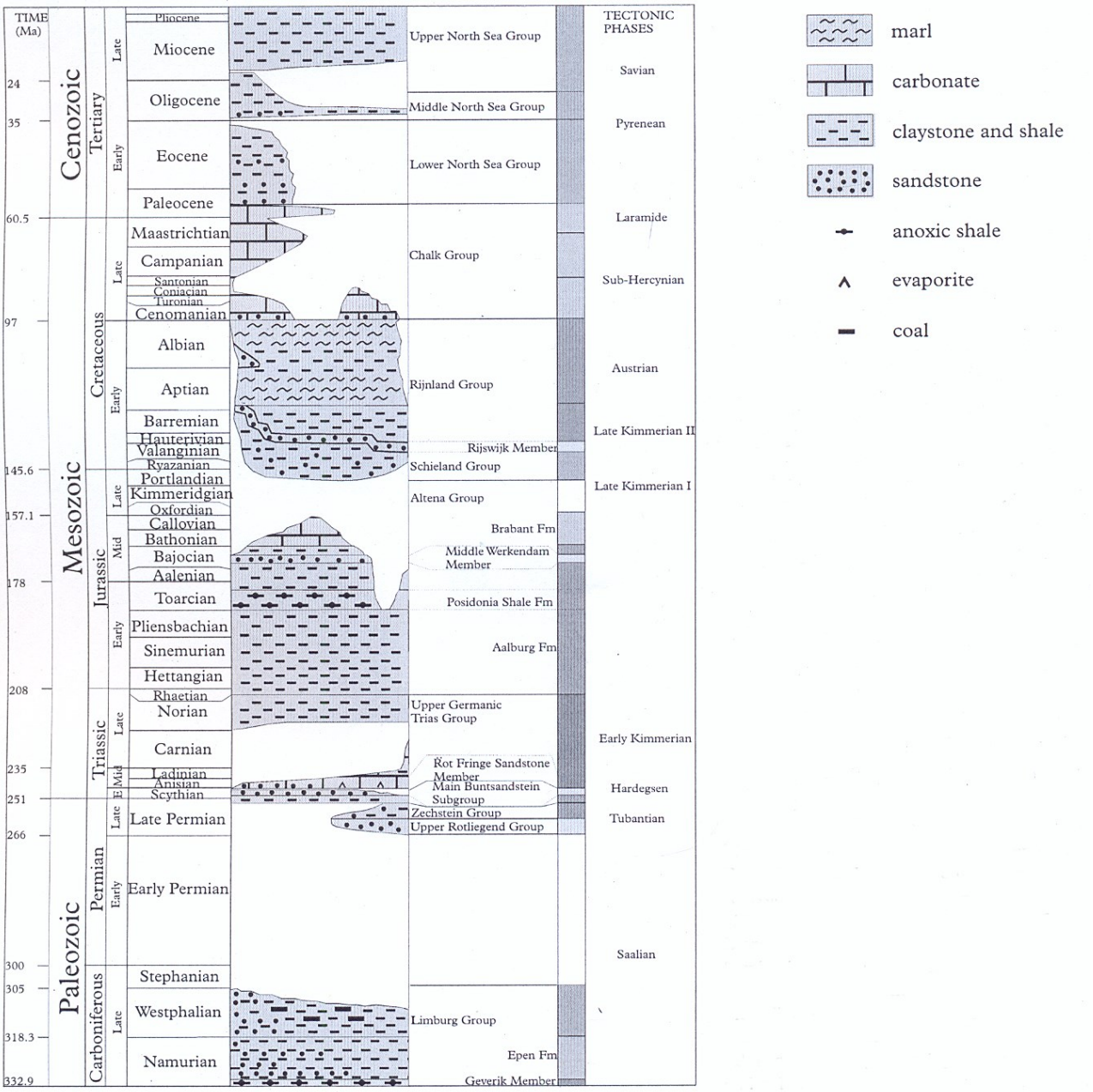

Fig. 2-5: Chronostratigraphic chart and facies variations in the West Netherlands Basin (Modified after McCann, 2008).

2.3. The Lower Saxony Basin

2.3.1. Geological setting

The geological evolutionary history of the LSB, which can be subdivided into four stages, started from the Late Triassic time when the LSB separated from the South Permian.

(1) In the period from the *Late Triassic to the Early Jurassic*, the North Sea–German–Polish Basin was differentiated into small ridges and troughs, which created smaller sedimentary basins, including LSB. At that stage, the territory was affected by a stress regime, indicating the development of the North Sea rift system. The LSB came into evidence in the occurring NNE–SSW trending systems (Betz *et al*., 1987; Kockel *et al*., 1994). Corresponding sediments consisted of terrestrial lacustrine and fluvio-deltaic clastic series. In Early Jurassic, the time of tectonic activity changed into a time of quiescence. Progressing subsidence of the basin triggered the expansion of transgression from the Scottish Highlands into northern Germany, which led to the re-establishment of marine conditions (Ziegler, 1990). Throughout the LSB, Early Jurassic sediments consist of open marine dark coloured organic-rich bituminous shale with interbedded limestone layers and concretions. These sediments contain a rich fauna of ammonites.

(2) The *Middle Jurassic–Early Cretaceous* stage was characterised by tectonically-induced changes of the relative sea level. At this stage, a series of WNW–ESE striking horsts and grabens developed. These grabens were filled with a thick series of sedimentary rocks, in which depositional environments changed alternatively from open marine to shallow marine, to hypersaline and to lacustrine (Kockel *et al*., 1994). The Pompeckj Block, Brabant, Rheinish and Bohemian massifs, which acted as a major source of clastic influx, were uplifted above erosional level. The marine connection between the South German Franconian Platform and the NW European Basin was interrupted as a consequence of wrench-induced uplift of the Rhenish Massif (Ziegler, 1982). The condition of sedimentation changed again to open marine at the end of this stage (Betz *et al*., 1987).

(3) In the *Late Cretaceous* time, the inversion tectonic in the LSB basin involved the basement and was accompanied by the uplift of the pre-Permian unconformity surface. Late Permian Zechstein salts (Middle-Late Permian) acted as detachment planes in which a fault system was developed (Betz *et al*., 1987). In the centre of LSB a number of Cretaceous plutonic laccoliths (Bramsche, Vlotho, Uchte, Nordhorn & Apeldorn) ascended at the beginning of the inversion, causing thermal anomalies in adjacent sediments and an injection

of hydrothermal fluids (Teichmüller and Teichmüller, 1950; Teichmüller and Teichmüller, 1951; Stadler and Teichmüller, 1971; Koch and Arnemann, 1975; Deutloff *et al*., 1980; Kockel *et al*., 1994; Petmecky *et al*., 1999; Kus *et al.*, 2005; Senglaub *et al*., 2005).

(4) The *Tertiary* sedimentary rocks were deposited on the northeastern and western margins of the LSB and were partly eroded in the Oligocence and Miocene time (Kockel *et al.,* 1994). Present-day stress appears only in the Rhenish Massif and in areas adjacent to the LSB. Fault systems formed during this period are oriented in a NW–SE direction (Betz *et al.,* 1987).

2.3.2. Tectonic features

The Lower Saxony Basin is a pull-apart basin with pre-Permian Caledonian-Hercynian basement and overlying it the Permian-Mesozoic-Cenozoic sedimentary cover with a total thickness of 8 000 km (Betz *et al*., 1987; Walter, 2007). The LSB includes numerous rhomboidal sub-basins, separated by NNW–SSE-trending transitional zones (Betz *et al.,* 1987). The complex structures and fault assemblages of this basin were formed due to repeated reactivations, which took place in a different time of its tectonic evolutionary history. The structure profile across LSB is evidently complicated by multiple tectonic elements, fault systems, intrusive bodies and salt diapirs (Fig. 2-6; 2-7).

Tectonically, the north-west of the investigated region is adjacent to the Niedersachsen Tectogene, which is, in turn, bordered by the Pompeckj Block to the north-east and by the Munster Upper Cretaceous Syncline to the west-south (Fig. 2-7; 2-8). This tectogene was formed in the Jurassic period and changed into a sedimentary basin (Niedersachsen Basin) in the Cretaceous time. In Upper Jurassic, the area of Niedersachsen Tectogene was affected by a salt diapir event and inverted in the Late Cretaceous period (Walter, 2007).

The Pompeckij Block is located between Aller-Linie in the SSE and Ringköbing-Fünen High to the north (Fig. 2-7). It includes NNE–SSW-trending grabens filled with Lower–Middle Jurassic sediments and salt diapirs striking in a NW–SE or from NNE–SSW to N–S direction (Betz *et al.,* 2007). Prignitz Wall is situated to the NE of the investigated area and bordered by the NW–SE striking Almark Horse to the south-west and S–E-striking Brandenburg Horse to the north-east. It is developed in a NW–SE direction and filled, as well as the Niedersachsen Basin, with sediments from Permian to Lower Cretaceous and was inverted in the Late Cretaceous (Walter, 2007).

The Grimmen region is bordered to the north by the Rügen Horse, which occurred at the end of the Later Cretaceous period (Fig. 2-7). In the Grimmen region, sediments deposited up to the Cretaceous time were later eroded in Late Cretaceous, consequently, outcropping the Jurassic deposits (Walter, 2007).

Smaller tectonic elements (fault system) are oriented in a NNE–SSW direction and, in places, WNW–ESE. They were formed at the time of rapid subsidence (Kimmeridgian to Aptian) (Petmecky *et al*., 1999). Fault systems appearing during inversion in the Late Cretaceous became reactivated by NW–SE direction convergent wrenching (Betz *et al.,* 1987).

2.3.3. Stratigraphy

The Jurassic in northern Germany extends over an area of 100 000 km^2. However, it crops out only in the southern part of the Lower Saxony Basin comprising 1 % of all Jurassic sediments (McCann, 2008).

Within a 100 m sequence of Toarcian sedimentary rocks, the Posidonia Shale has a thickness of 25–70 m (Kockel *et al*., 1994; McCann, 2008). The thickness of this succession increases towards the northwestern part of the LSB. The Posidonia Shale appears in the depth interval of between 250 and 1300 m (McCann, 2008). It is represented by open marine facies, nevertheless, which to the north-east is interfringed with shallow marine sand and adjacent terrestrial sediments (McCann, 2008). Specifically, the Posidonia Shale consists of organic-rich mudstone or limestone of a dark grey to grey colour. The straugraphic features with distribution of ammonite zones are depicted in Fig. 2-2 and 2-8

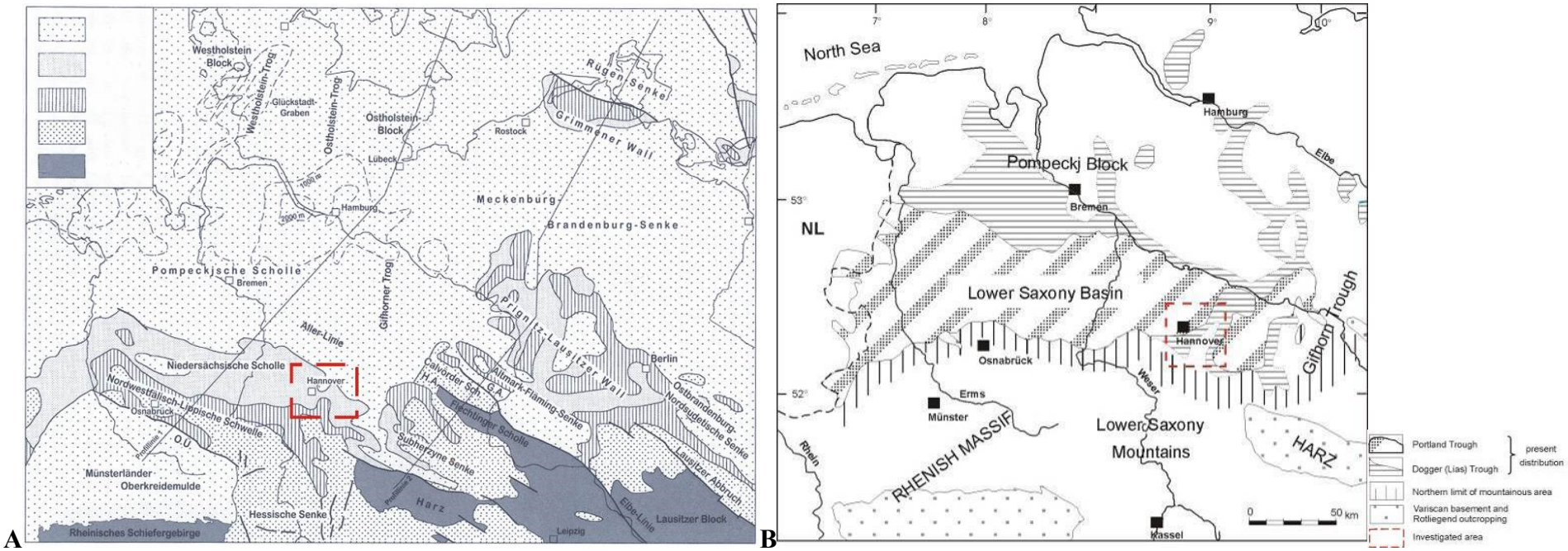

Fig. 2-6: Geological map (A) and tectonic framework (B) of the investigated area (red square) and its vicinity (Modified after Betz *et al*., 1987; Walter, 2007).
Legend: Präzechstein - Pre-Zechstein (Pre-Middle Permian); Trias - Triassic; Jura - Jurassic; Unterkreide - Lower Cretaceous; Oberkreide - Upper Cretaceous. Selected main tectonic structures on the map: Münsterlander Oberkreidemulde – Münster Upper Cretaceous depression; Niedersächsische Scholle (Niedersächsisches Tektogen) – Niedersachsen horse; Pompeckjsche Scholle – Pompeckj horse; Fünen- Moen- Hoch – Fünen- Moen High; Rügen Senke – Rügen depression; Grimmener Wall – Grimmen Wall; Meckenburg- Brandenburg-Senke – Meckenburg- Brandenburg Syncline; Prignitzer Wall – Prignitz Wall; Altmark- Fläming-Senke – Altmark- Fläming depression; Flechtinger Scholle – Flechting horse; Subherzynes Becken – Sub-Hercynian Basin.

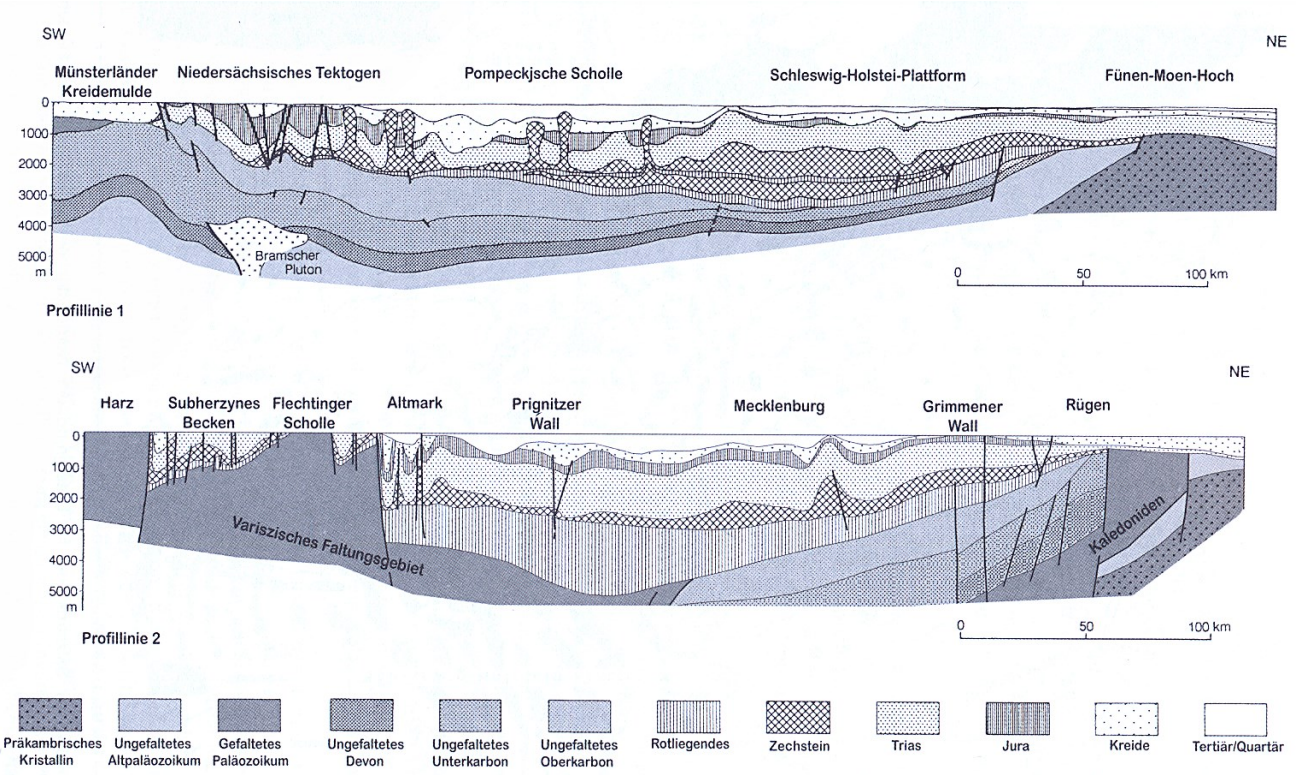

Fig. 2-7: Two geological profiles across the investigated area in the Lower Saxony Basin; see Fig. 2-6 for their location (Modified after Walter, 2007).
Legend: Präkambrisches Kristallin – Pre-Cambrian basement; Ungefaltetes Altpaläozoikum – unfolded Lower Paleozoic; Gefaltetes Paläozoikum – folded Paleozoic; Ungefaltetes Devon – unfolded Devonian; Ungefaltetes Unterkarbon – unfolded Lower Carboniferous; Ungefaltetes Oberkarbon – unfolded Upper Carboniferous; Rotliegendes – Rotliegend; Zechstein – Zechstein (Middle-Late Permian); Trias – Triassic; Jura – Jurassic; Kreide – Cretaceous; Tertiär/Quartär – Tertiary/Quaternary. For the tectonic structures, see Fig. 2-6.

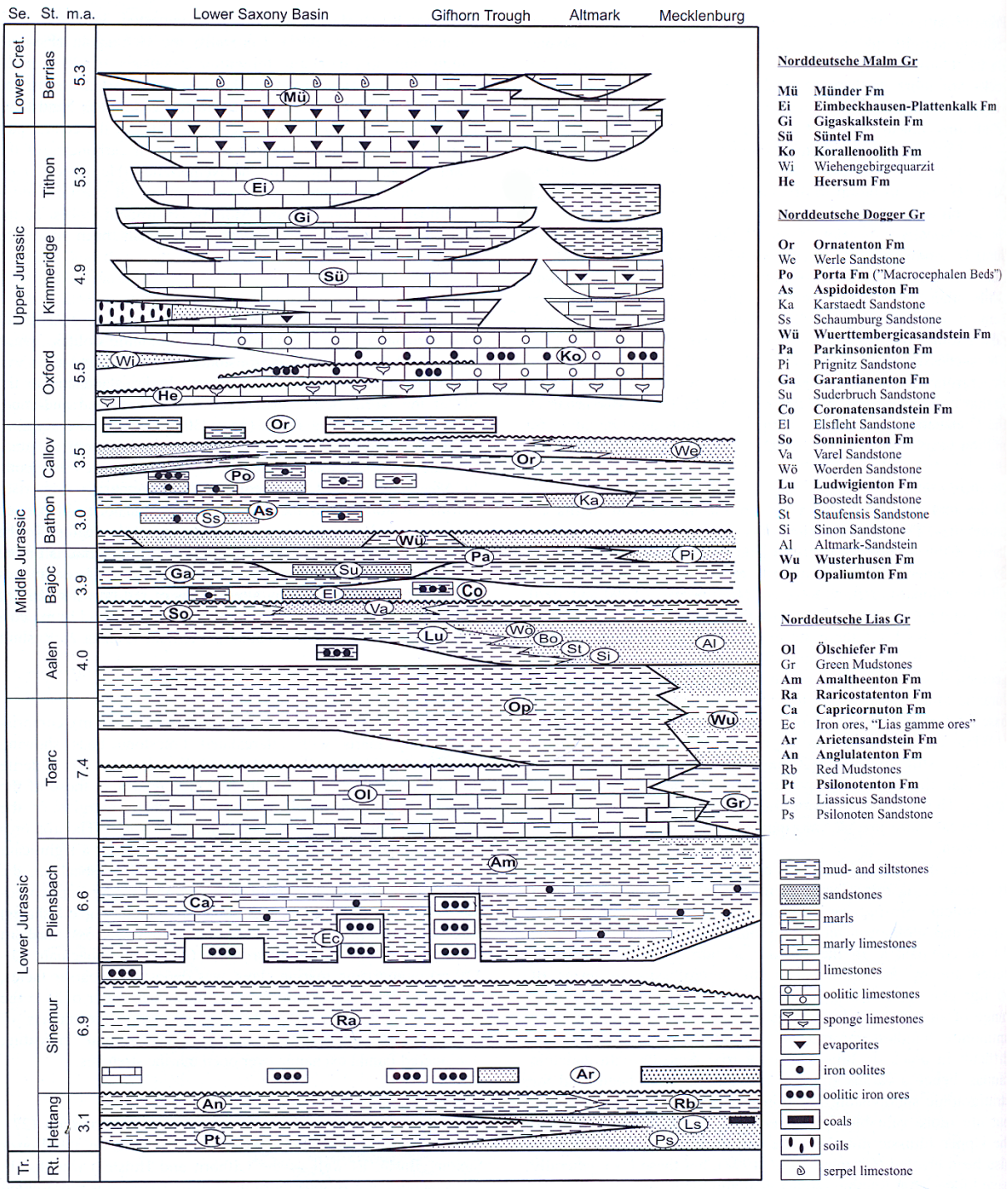

Fig. 2-8: Chronostratigraphic chart illustrating the Jurassic stratigraphy and the vertical and lateral lithofacies variations in the Lower Saxony Basin (modified after McCann *et al.*, 2008).

2.4. The South German Basin

2.4.1. Geological setting

As for the previous two basins, the geodynamic evolution of southern Germany can be subdivided into four stages as well (Walter, 2007; McCann, 2008).

(1) *Late Permian–Early Jurassic* stage. In the Late Permian time, the area of southern Germany was uplifted as a consequence of the Variscan tectonic phase. Evidently, the corresponding sediments comprised of conglomerates, arkose sandstones and sandstones, were deposited in intermountain sedimentary basins. These basins were subsided under increasing pressure from the Bohemian massif. However, in the Stockheim and Erbendorf areas, the Rotliegend sediments are represented by coal seams. The total thickness of the Stefanian and Rotliegend deposits in southern Germany range from 100 to 2000 m in depressions and small basins (Walter, 2007; McCann, 2008).

The Late Permian Zechstein sea transgression led to sedimentation of dolomites, green mudstones and marls, whose thickness together varies from 200 m in the north of the South German Basin up to 5 m in the southwestern area (Geyer *et al*., 2011). Later, these marine sediments were changed by continental reddish sandstones and conglomerates of Buntsandstein series (Fig. 2-2). In the Early-Middle Triassic period, a new phase of transgression took place (Walter, 2007). The paleoenvironments changed from brackish marine to shallow marine (McCann, 2008). Accordingly, anhydride, gypsum and salt sediments, with an average thickness of 50 m, were covered by limestones and marls. In the Early Jurassic, marine transgression reached its maximum. The PSF of southern Germany was deposited at the peak of this transgression (Littke et al., 1991).

(2) *Middle Jurassic–Early Cretaceous* stage. In the middle of the Brown Jurassic (Dogger), in the Frankian Alb and eastern Swabian Alb, fine-grained brown sandstones with iron ooliths were deposited, which in turn, were covered by mudstones and silty marls (Table 2-1; Fig. 2-2). In the Upper Jurassic time after a transgression, as a consequence, limestones and marls were deposited, and covered by coral and oolith limestones and dolomites. At the beginning of the Cretaceous period, these sediments were affected by karst processes. In addition, at that time the tectonic style of southern Germany began to change, leading to fragmentation of the investigated and adjacent areas. The Bohemian Massif was uplifted, whereby the fault systems occurred, trending in a NW–SE direction.

Table 2-1: Chronostratigraphic chart of Jurassic of South Germany (Modified after Beurlen et al., 1992).

Stufen-bezeichnungen			Schwaben		Franken	
Oberer (Weißer) Jura = Malm	Tithonium (Ober-Kimmeridgium)	ζ	Hangende Bankkalke Zementmergel Liegende Bankkalke	Trümmeroolith und Korallenkalk	Neuburger Schichten Rennertshofener Schichten Usseltalschichten Mörnsheimer Schichten Solnhofener Plattenkalk Geisentalschichten	
	Kimmeridgium	ε	Oberer Felsenkalk und Bankkalk	Massiger Schwammkalk	Plumper Felsenkalk und Plattenkalk	Felsenkalk und Frankendolomit
		δ	Quaderkalk (Aulacostephanusschichten)		Treuchtlinger Marmor (Aulacostephanusschichten)	
		γ	Mittlere Weißjuramergel		Uhlandikalk Obere graue Mergelkalke	
	Oxfordium	β	Wohlgeschichteter Kalk		Werkkalk	
		α	Unterer Weißjuramergel (Impressamergel) Transversariuskalk		Untere graue Mergelkalke Glaukonitbank	
Mittlerer (Brauner) Jura = Dogger	Callovium	ζ	Oberer Braunjuraton	Lambertiknollen Ornatenton Macrocephalenoolith	Ornatenton Macrocephalenschichten	
	Bathonium	ε		Aspidoideston	Variansschichten Württembergicaschichten	
	Bajocium	δ	Parkinsonioolith Oolithische Laibsteinschichten und Tone		Parkinsonischichten Stephanoceratenschichten	
		γ	Sandige Braunjuratone (Sowerbyischichten)		Sowerbyischichten	
	Aalenium	β	Sandflaserschichten mit Sandstein und Eisenoolith (Ludwigienschichten)		Eisensandstein, Doggersandstein	
		α	Wasserfallschichten Unterer Braunjuraton (Opalinuston)		Opalinuston	
Unterer (Schwarzer) Jura = Lias	Toarcium	ζ	Oberer Liasmergel (Jurensismergel)		Jurensisschichten	
		ε	Posidonien- oder Ölschiefer		Posidonienschichten	
	Pliensbachium	δ	Oberer Liaston (Amaltheenton)		Costatenmergel mit Toneisensteinknollen Amaltheenton	
		γ	Unterer Liasmergel (Numismalismergel)		Numismalisschichten	
	Sinemurium	β	Unterer Liaston (Oxynoten- und Raricostatenschichten)		Turneri- und Raricostatenschichten	
		α	Arietenkalk		Arietenschichten, z. T. Arietensandstein	
	Hettangium		Angulatensandstein Psilonotenschichten		Angulatensandstein Psilonotenschichten / Rät-Lias-Übergangsschichten	

(3) *Late Cretaceous* stage. At the beginning of the Late Cretaceous stage, sediments between the Frankian Alb and western part of the basin were eroded. Contemporaneously, the Later Upper Cretaceous sea expanded from the southern Molasse basin towards the Frankian Alb. The sediments deposited in the Regensburg area were composed of glauconite sands, whereas in the north of South Germany, fluval limnic sediments were more common. The latter, as a consequence of the further sea expansion, were changed by marine sandstones, siltstones, marls and limestones (Mc Cann, 2008).

(4) *Tertiary–present* stage. The structural configuration of the present-day southern Germany was formed during this stage. Eustatic sea-level fluctuation induced regression in the beginning, which later changed by regional transgression from the area of Frankian into

the Swabian Alb. In the area of southern Germany, sedimentation changed from a clastic regime to a limnic deposition. Tertiary sediments can be observed on the peaks of the mountains or/and in karst gaps, including tertiary faunal remains. In addition, Upper Miocene limnic sandstones, mudstones and brown coals were deposited on the western side of the Bavarian Forest to the north of the Regensburg, Ries and Steinheimer Basins. As a final episode in the geological evolution of southern Germany, regional volcanism occurred in the Upper Rhein Graben and Swabian Alb (Walter, 2007; Geyer et al., 2011).

2.4.2. Tectonic features

Tectonically, the investigated area is limited by the following tectonic elements: to the north-west, it is bordered by the Stromberg and Löwensteiner Synclines, to the north-north-west it borders with the Triassic sedimentary basin, to the north-east it is limited by the Steigerwald (Sattel) Anticline and, to the south, by the Swabian Alb (Fig. 2-9).

Specifically, the investigated area is a part of the northern edge of the mountain range of the Swabian Alb, which stretches across southwestern Germany over a length of approximately 220 km from Lake Bodensee in the south-west to the impact crater of the Nördlinger Ries in the north-east (Kaufmann and Romanov, 2007). It has a height of between 700 and 1000 m (Walter, 2007). The landscape represents a tilted plateau, which gently dips towards the Danube River in the south. The western part of this plateau consists of the sedimentary rocks of White Jurassic ß and the middle and eastern parts, in turn, of White Jurassic σ and Ɛ respectively (Malm) (Table 2-1). The upper step of the Swabian Alps is comprised of sandstones and marls of Brown Jurassic (Dogger) (Table 2-1). At the western edge of the Swabian Alps, the tectonic element — namely the Hercynian Hohenzollern Graben — striking in a NW–SE direction, can be recognised (Fig. 2-9, 2-10). This Graben is 30 km in length and its width comprises only 1.5 km. Another tectonic element, the Urach-Kircheimer Volcanic domain, which occurred in Miocene, is situated in the middle of the Swabian Alps. It has a surface of 30x50 km. Its chimney is filled with tuff and basalts. After eruptions which took place several times, the paleoenvironment changed, giving way to the sedimentation of the marly limestones, limestones and sapropelic sedimentary rocks. These sediments are famous for their well-preserved plant prints.

Between the Swabian and the Frankian Alb, the Nördlinger Ries impact crater is clearly recognised (Fig.2-9, 2-10). It has a round form of 26 km in diameter. In the south, it reaches a height of 100 m, in the north it has the shape of a flat wall.

To the south of the Triassic domain, the Frankian depression (Furche) strikes parallel to the Swabian Alb. It consists of narrow graben and synlines of 3 – 4 km in width. Almost parallel to each other, the Neckar-Jagst-Furche, the Swabian-Frankian Anticline and the Swabian-Frankian lineament are located to the north of the Swabian Alb. The lineament of the Filder Graben is situated between the Swabian-Frankian Sattel and the Swabian-Frankian lineament, striking in a WSW–ENE direction (Fig. 2-10).

In this area, anticlines and synclines are fragmented by fault systems in three different directions. The first fault system is oriented in a NNW–SSW direction, whereas the other strikes in a NW–SE direction and occurred during the Hercynian Orogeny. Finally, the third fault system trends in a WSW–ENE direction, fragmenting the base of the Variscan basement and younger overlay of sedimentary rocks.

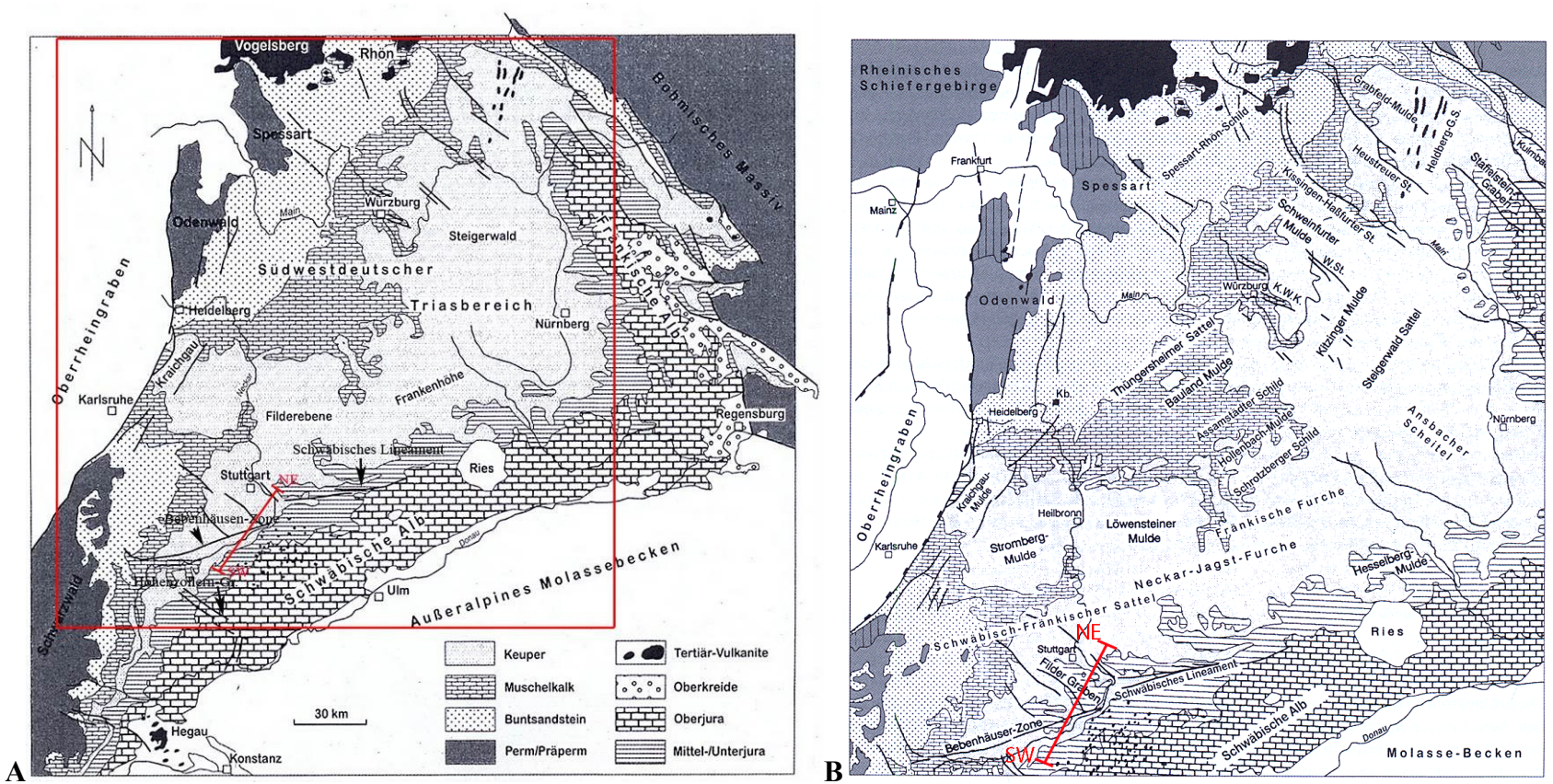

Fig. 2-9: Geological map showing the main geological structures of the South German Basin (Modified after Walter, 2007).
A), General overview; B) Detailed view. Legend: Perm/Präperm – Permian/Pre-Permian; Buntsandstein - Lower Triassic series; Muschelkalk - Middle Triassic series; Keuper - Upper Triassic series; Mittel-/Unterjura - Middle/Lower Jurassic; Oberjura - Upper Jurassic; Oberkreide - Upper Cretaceous; Tertiär-Vulkanite - Tertiary volcanites. *Tectonic elements*: Schwäbische Alb - Swabian Alps; Nördlinger Ries - impact crater Nördlinger Ries; Uracher Vullkangebiet - Urach volcanic area; Swäbisches Lineament – Swabian lineament; Swäbisch-Fränkischer Sattel - Swabian-Frankian Anticline; Fränkische Furche - Frankian depression; Stromberg Mulde - Stromberg syncline; Löwensteiner Mulde - Löwensteiner syncline; Steigerwald Sattel - Steigerwald Anticline.

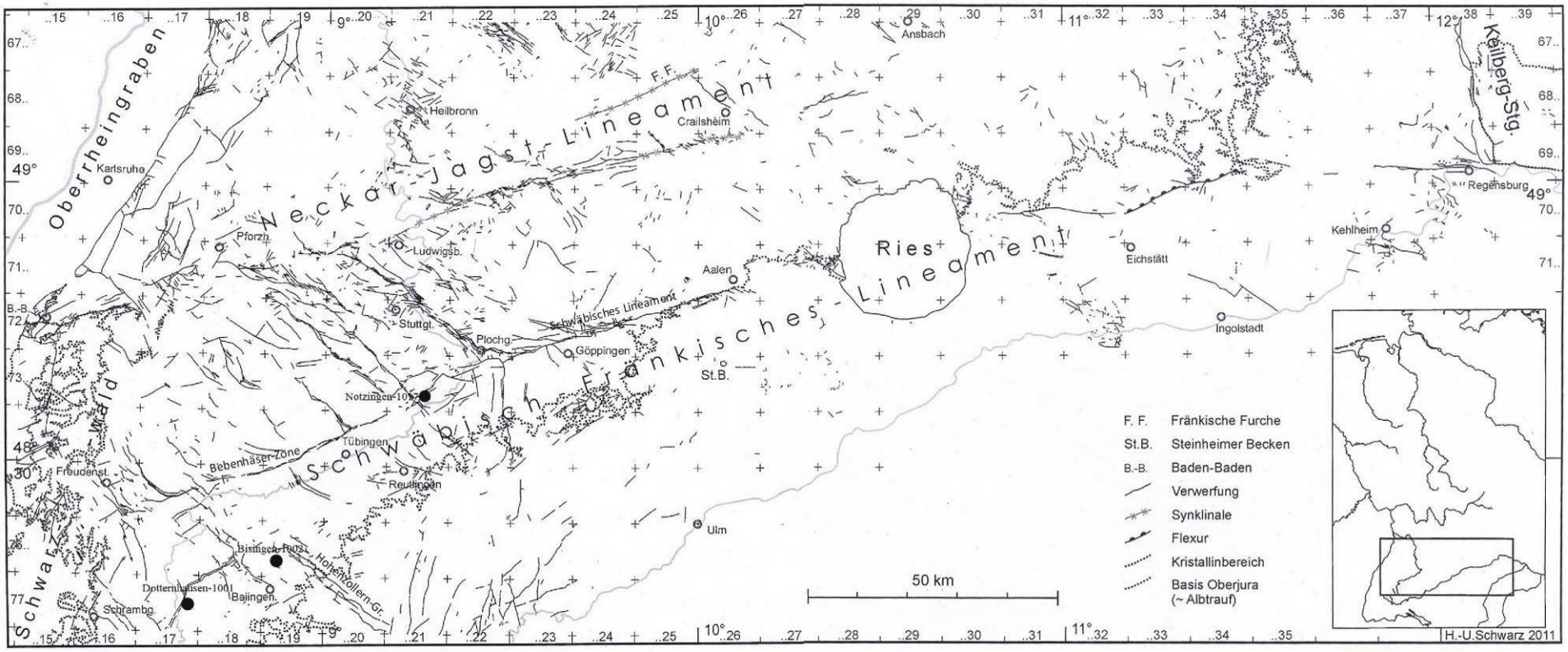

Fig. 2-10: The Swabian-Franconian fault pattern with schematic location of the investigated wells (Modified after Schwarz, 2012).

2.4.3. Stratigraphy

The major Posidonia Shale outcrop is located in southern Germany (Figs. 2-11 – 2-13). It became famous for well-preserved faunal remains such as ichthyosaurs, fishes, giant crinoid colonies, numerous cephalopods, etc. In addition, scientific attention has been attracted by the high concentration of coccoliths, representing the first mass bloomings of the coccolithophorid algae in Earth's history (McCann, 2008).

Generally, the PS is divided into three ammonite zones: the *tenuicostatum*, *falciferum* and *bifrons* (Fig. 2-14). These zones in turn consist of ammonite subzones. A gradual transition between lower zones, consisting of marls and mudstones, and bituminous shales of the middle *falciferum* zone, is defined as the consequence of a rapid transgression and subsidence of the basin (Riegraf, 1985). The bituminous shales of the *falciferum* zone grade into high bituminous shale of the *bifrons* zone and are intercalated by five carbonate beds, two of them ("Oberer Stein", "Unterer Stein") are used as stratigraphic marker beds (Figs.2-14, 2-15) (Riegraf, 1985; Littke *et al*.,1991).

The thickness of the Posidonia Shale varies, depending on the area where it was deposited. The maximum thickness was observed in the Langenbrücken Syncline with an average of 35–40 m. In a south-westerly direction, the thickness gradually decreases to 2–5 m (Geyer *et al*., 2011). The basal contact of the Posidonia Shale with the underlying rocks is transitional, whereas that in northern Germany is erosional (Littke *et al.,* 1991).

Lithologically, the Posidonia Shale consists of fine-grained calcareous bituminous shales, marls and marly limestones, yielding a low diversity of foraminifera (McCann, 2008). The bituminous calcareous shales have a dark colour and are finely laminated. According to some workers, bacterial mats and bacterial colonies generally play an important role in the fine lamination structure in bituminous shaless, as well as in the formation of amorphous organic matter (Geyer *et al*., 2011). Apart from the bituminous section of the Lower Toarcian succession, several lighter coloured beds and a bioturbated unit near the top and the bottom of the Posidonia Shale have been encountered as well (Littke *et al*., 1991).

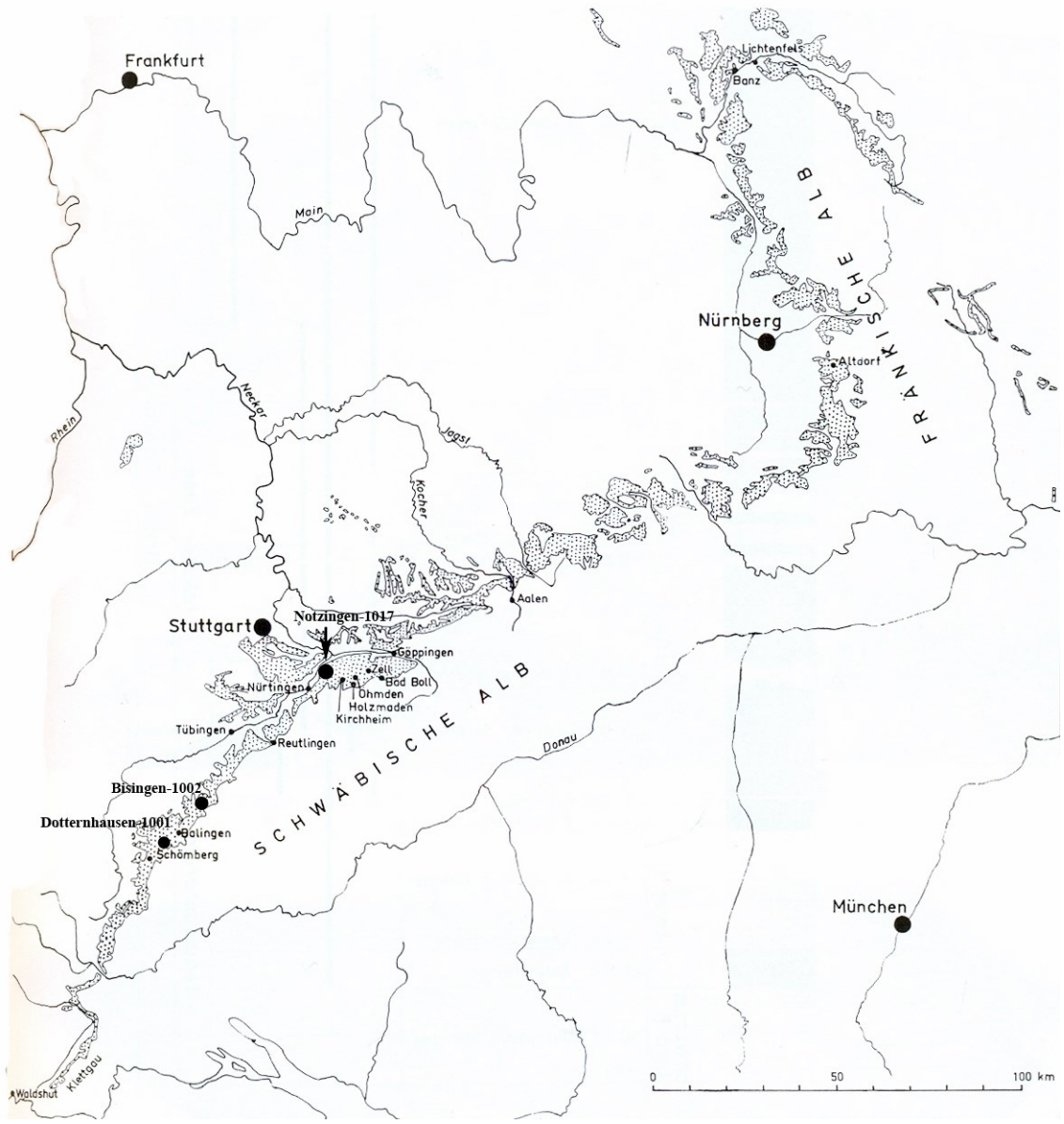

Fig. 2-11: Map showing the outcrop of Lower Toarcian sediments along the Swabian/Frankian Alps and the location of the investigated wells (Modified after Ulrichs et al., 1979; Riegraf, 1985; Prauss *et al*., 1991).

SW NE

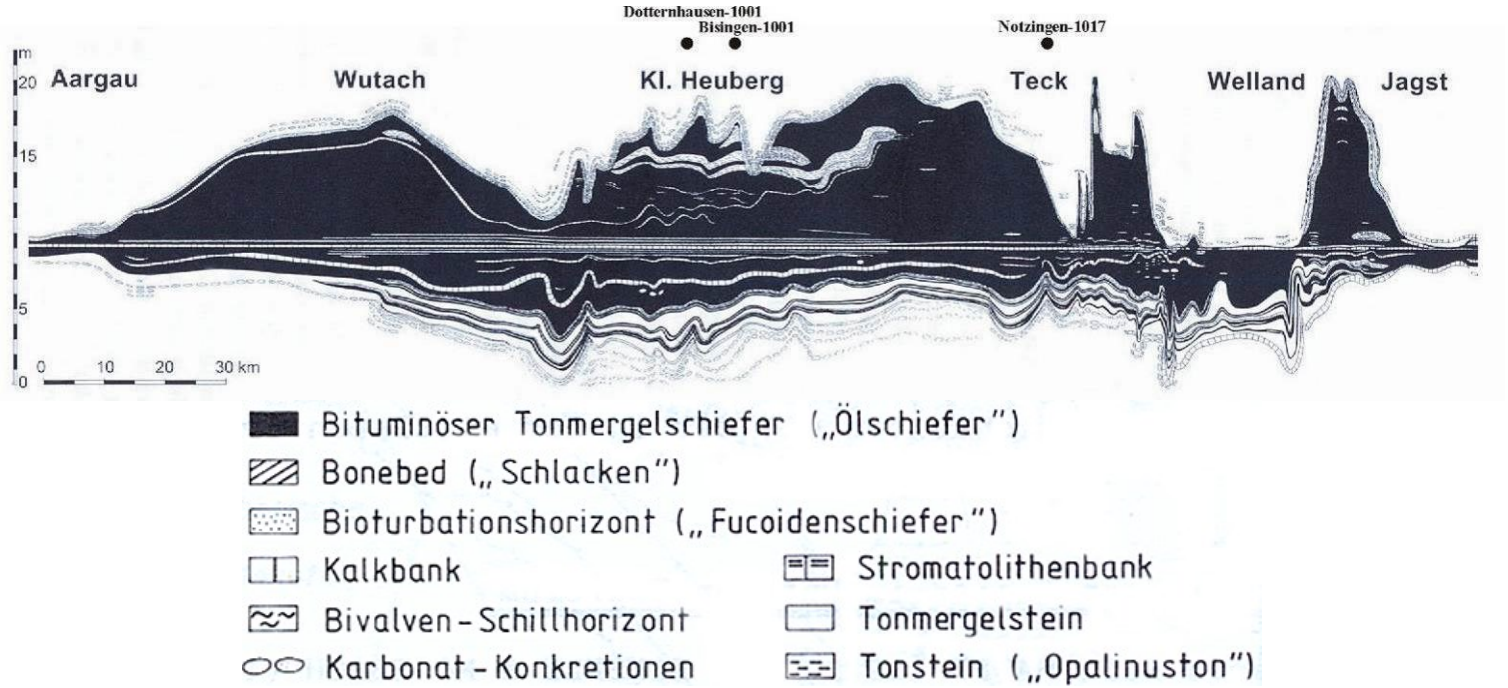

Fig. 2-12: Sedimentological cross-section of the Posidonia Shale Formation across the Swabian Albs (Modified after Riegraf, 1985; Geyer *et al.*, 2011).
Legend: Bituminöser Tonmergelschiefer ("Ölschiefer") – Bituminous silty marls (bituminous shaless); Bonebed ("Schlacken") – Bonebed; Biotubationshorizont ("Fucoidenschiefer") – Bioturbated horizon; Kalkbank - Limestone bed; Bivalven-Schillhorizont – Bivalvia-shell horizon; Karbonat-Konkretionen – Carbonate concretions; Stromatolithenbank – Stromatolite bed; Tonmergelstein-silty marls; Tonstein ("Opalinuston") – mudstones.

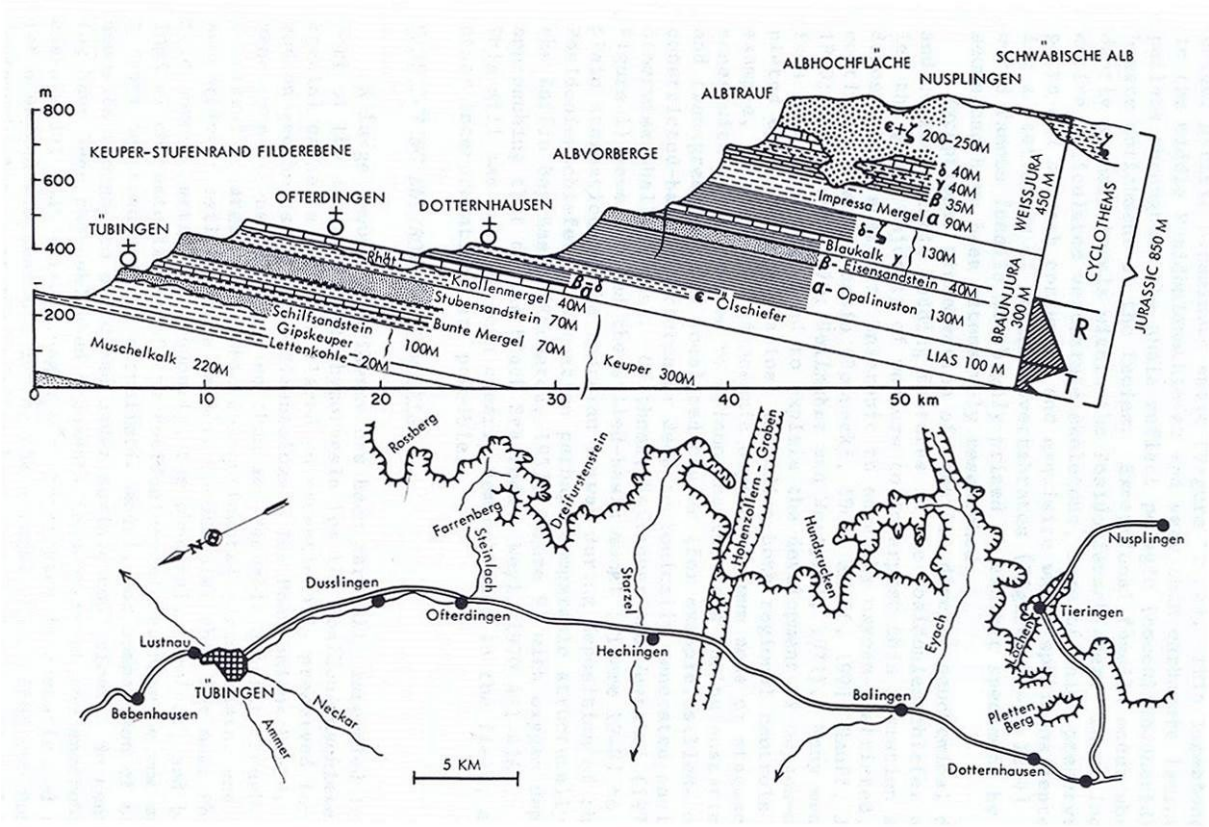

Fig. 2-13: Generalised stratigraphic section through Triassic and Jurassic rocks of southern Germany (top) and areas of principal outcrops: quarries at Dotternhausen (lower right) (Modified after Kauffman, 1981).

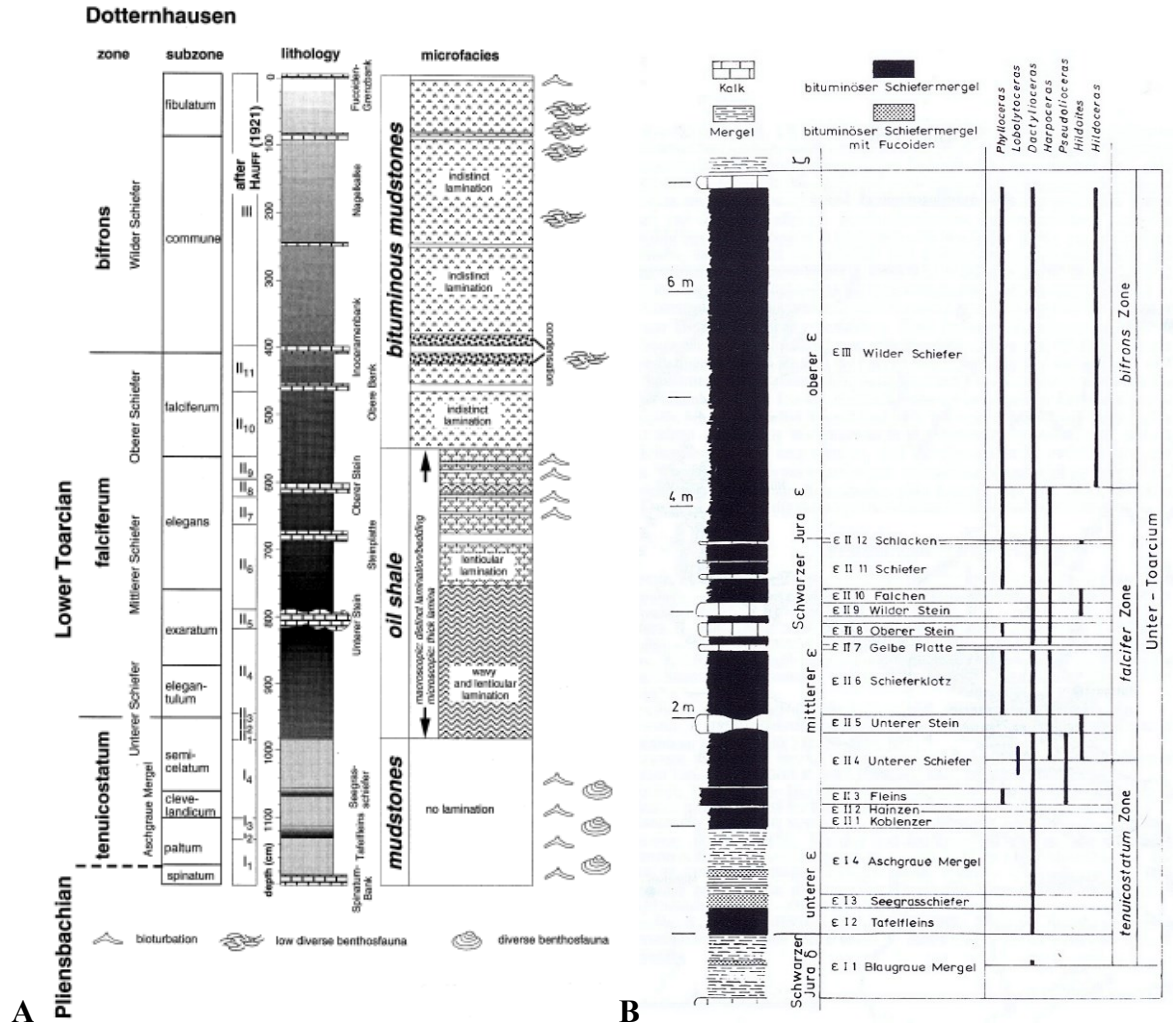

Fig. 2-14: Stratigraphic cross-section of the Posidonia Shale showing the distribution of Ammonite Zones in Dotternhausen (A) and Holzmaden (B) quarries (Modified after Urlichs *et al*., 1979; Röhl et al., 2001).

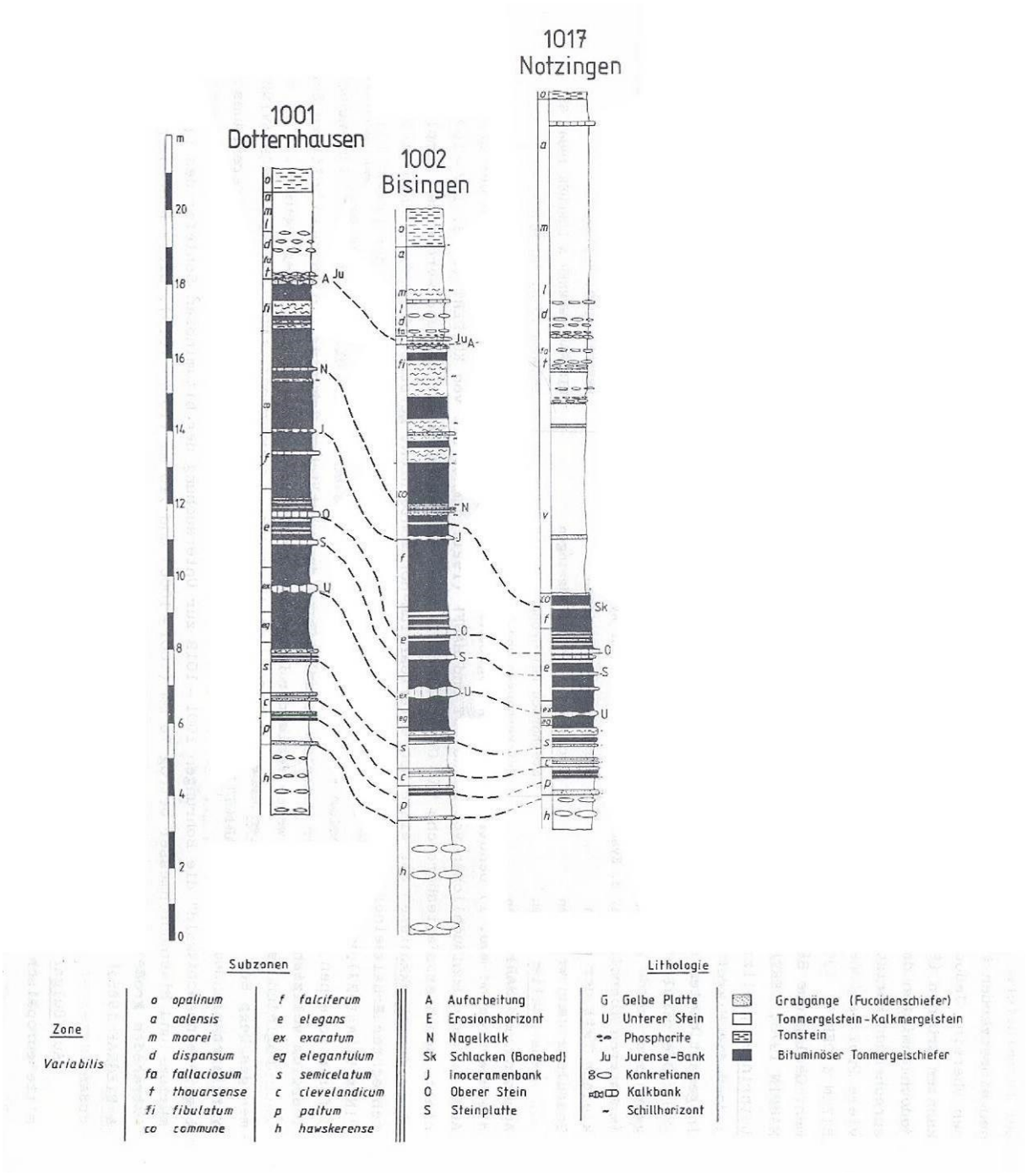

Fig. 2-15: Lithological log with distribution of the Ammonite Zones and Subzones for Dotternhausen-1001 well, Bisingen-1002 well and Notzingen-1017 well (Modified after Riegraf, 1985).
Lithology: Grabgänge (Fucoidenschiefer) – Burrows; Tonmergelstein - clayey marlstone; Kalkmergelstein – calcareous marlstone; Tonstein – mudstones; Bituminöse Tonmergelstein - bituminous clayey marlstone.

CHAPTER 3. METHODOLOGY OF THE RESEARCH WORK

Contents

3.1. Introduction

The methodology used in this study can be subdivided into 4 stages (Fig. 3-1). The first step is the lithological description of cores followed by sampling, which provides the original object of the investigations. Once samples are selected, the rock samples are prepared for investigation using the bulk of optical and geochemical analytical methods (Fig. 3-1).

Organic petrology in conjunction with geochemical analyses in the third stage provide insight into the thermal maturity of organic matter (OM), provide its quantitative and qualitative assessment, molecular composition, information on the condition of sedimentation, degree of preservation of OM and marine productivity. In other words, it provides comprehensive characteristics of the organic matter obtained by analytical methods in the second step (Fig. 3-1).

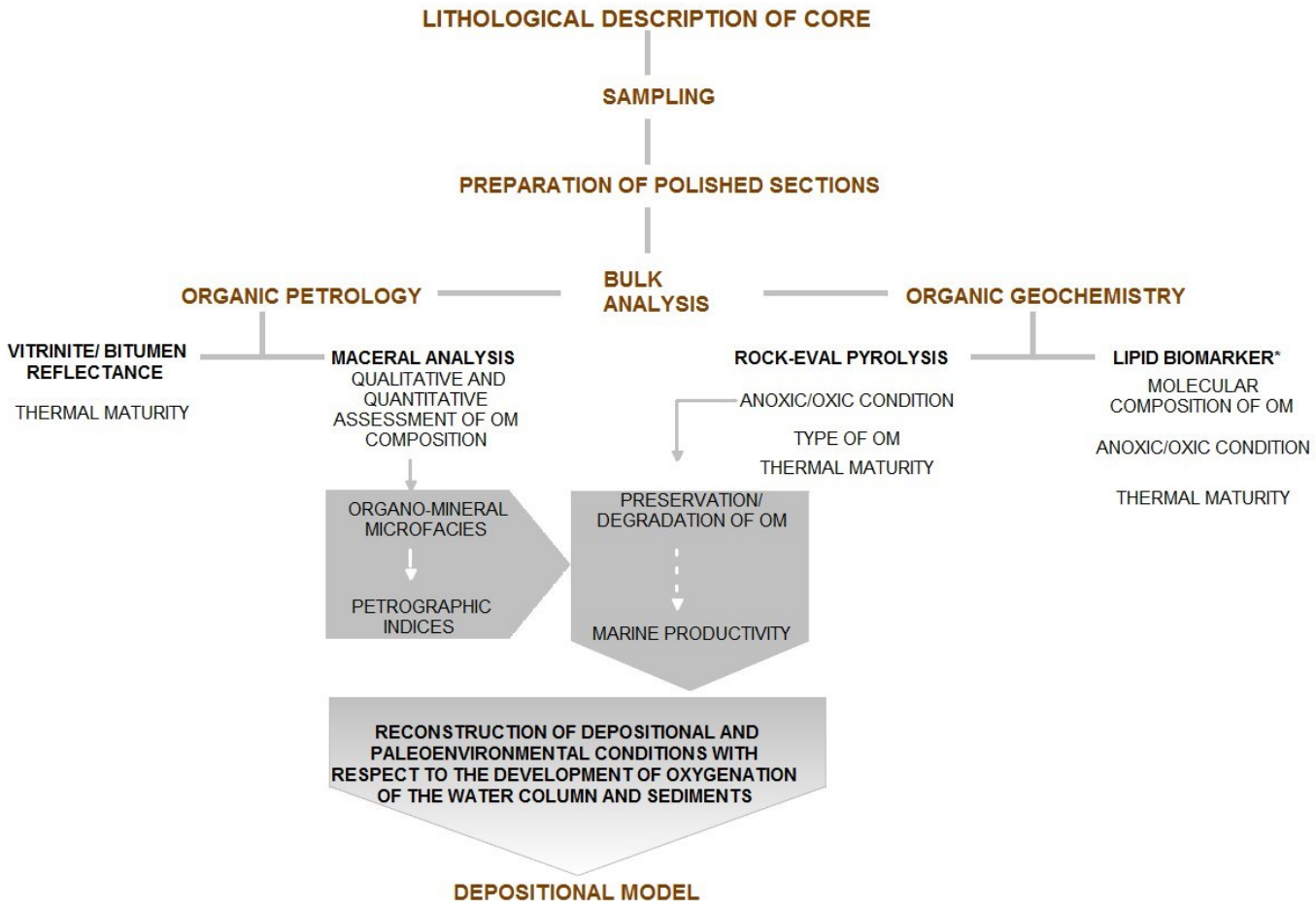

Fig. 3-1: Schematic flow chart describing the methodology of the current research.* not performed in this study.

The previous steps enable the final, fourth stage to be reached — investigation of the deposition and paleoenvironmental conditions of sedimentation, which, in turn, helps to construct the final depositional models of the Posidonia Shale (Fig. 3-1).

3.2. Sampling procedures and sample preparation

Analytical work was obtained from a total of 256 samples from wells, including both collected and incorporated data from three sedimentary basins of Western and Central Europe (Table 3-1). Investigated bituminous shaless from lithological successions of Lower Toarcian were selected by the author in two wells (E, M) from the Netherlands and three wells (A, D, B) from northwestern Germany, at the core storage in NAM Assen in the Netherlands (E, M wells) and in ExxonMobil Production GmbH Hannover, Germany (A, D, B wells). These wells were drilled between the years 1952 and 1981. All these core sections contain coring gaps in between, except the core of well D. Samples were taken at approximately equal intervals of approx. 2 m for samples from western Netherlands and each approx. 30 cm for samples from northwestern Germany. At the core storage, first the macroscopic description and testing with HCl of the core samples were performed to determine the carbonated character of the rock samples.

Table 3-1: Sample numbers and type of performed analyses.

No	Well name	Sedimentary basin	Number of samples	Type of analyses						
				Organic petrology			Organic geochemistry			
				maceral analysis	vitrinite reflectance	bitumen reflectance	Rock-Eval	TOC	lipid biomarker	isotope geochemistry
1	E	the West Netherlands	20	20		-	20	20	-	-
2	M		21	21		-	21	21	-	-
3	A	Lower Saxony Basin	38	38	5	-	38	38	-	-
4	D		39	39	5	-	39	39	-	-
5	B		39	39	5	2/5**	39	39	-	-
6	Dotternhausen-1001	South German Basin	24	24	4	-	24	-	-	-
7	Bisingen/Zimmern-1002*		41	41	15	0/15	41	Küspert (1983)	-	Küspert (1983)
8	Notzingen-1017		34	34	34	25		Küspert (1983)	-	Küspert (1983)

* Incorporated data

** Bitumen reflectance on homogeneous (first number) and heterogenous (second number) types

Samples from the South German well include 24 rock pieces from the Dotternhausen-1001 well which were provided by Dr. Ligouis. Maceral analysis on samples from the Dotternhausen-1001 well was performed by the author. Sampling procedure and the bulk of organic petrological analyses, including microphotographs on the Bisingen-1002 and Notzingen-1017 wells, were carried out by Dr. B. Ligouis in previous studies. Rock-Eval pyrolysis of the Bisingen-1002 well was undertaken by Exxon Production Research –

European Laboratories, Bégles, France, in 1986. Geochemical results on samples from the Notzingen-1017 well were obtained by BEB Erdgas and Erdöl GmbH in Hannover, Germany in 1989. Results of isotope geochemistry for the Dotternhausen-1001 and Bisingen-1002 wells were previously published by Küspert (1983).

3.3. Organo-petrological methods

3.3.1. Maceral analysis

The complex of organo-petrographical analyses, which includes maceral analysis and vitrinite/bituminite reflectance, were performed by the author at the Laboratories for Applied Organic Petrology (LAOP), University of Tübingen, Germany. Qualitative and quantitative analyses were carried out using a Leica DMRX – MPVSP microscope photometer. Quantitative investigations were undertaken using the point-count method (Pelcon automatic point counter attached to the microscope stage) based on 1000 individual determinations of maceral per sample. The polished blocks (~2.5x1.5 cm in size) prepared perpendicular to the bedding and dry polished, were analysed in both reflected white light and fluorescent illumination under oil immersion at 500x magnification.

Optical identification of various macerals other than alginite and bituminite is based on the internationally accepted nomenclature described in ICCP (International Committee for Coal Petrology) Handbooks (ICCP, 1971; ICCP, 1975; ICCP, 1993), Stach *et al*., 1982 and Taylor *et al*., 1998. Alginite macerals were classified according to Hutton and Cook (1980), Cook *et al*. (1981) and Hutton (1987). These authors have developed the most widely accepted nomenclature for liptinite macerals in bituminous shaless.

The identification of bituminite I, bituminite II and bituminite III is based on the definitions of Teichmüller and Ottenjann (1977). Any other types of bituminite recognised in this study were identified and classified according to Gorbanenko and Ligouis (2014).

3.3.1.1. Classification of organic matter in marine bituminous shales

3.3.1.1.1. Vitrinite group

Vitrinite is composed of macerals derived primarily from plant tissues (e.g. stem, root, bark, leaf). Depending on the structure of vitrinite particles, two types of submacerals – homogeneous and fine heterogeneous (telinite) – are distinguished. Originally, in low mature and mature bituminous shales, vitrinite can be subdivided into two types: indigenous vitrinite

and oxidised vitrinite (Appendix A). The first type has a grey colour and sometimes a dark brown fluorescence that can only be observed on relatively large particles (Fig. 3-2A). Morphologically, indigenous vitrinite is characterised by angular forms and its generally large size, which excludes a strong fragmentation due to long transportation from the terrestrial domains (more than 50 µm; Lo, 1992; Nzoussi-Mbassani *et al*., 2005). This type of vitrinite particle is non-rounded and has a high length-to-width ratio with a wispy appearance, often containing pyrite framboids (Malinconico, 2000). However, indigenous vitrinite may have a variety of curving and rounded shapes. In contrast, oxidised vitrinite has a light grey to whitish colour and no fluorescence (Fig.3-2B). The particles are smaller in size, more equidimensional in form, commonly well-rounded and often show oxidation rims, which is attributable to the long transport prior to burial in sediments (Lo, 1992; Nzoussi-Mbassani *et al.,* 2005).

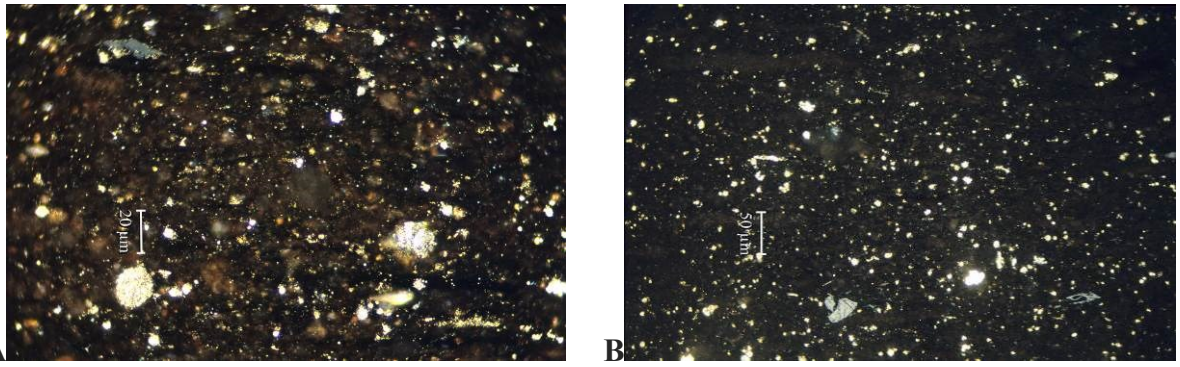

Fig. 3-2: Photomicrographs showing examples of indigenous (A: dark grey particles) and oxidised vitrinite (B: light grey particles) in well A. Reflected white light, oil immersion.

3.3.1.1.2. Liptinite group

Alginite and liptodetrinite

In mature Lower Toarcian shales, alginite macerals which are derived from algae vary considerably with respect to size, morphology, internal structure and fluorescence intensity. According to their morphology and size, and the alginite classification of Hutton and Cook (1980), Cook *et al*. (1981), two alginite macerals have been distinguished: telalginite and lamalginite.

Telalginite consists of marine-derived algae as well as brackish algae (*Botryococcus*). Telalginite exhibits either a flattened disc-shaped (thick-walled algae: *Tasmanites, Pterosphaeridia* or a spindle-shaped thin-walled large algae: (*Leiosphaeridia, Pleurozonaria, Campenia and/or Lancettopsis;* see Mädler, 1963; Prauss *et al*., 1991). It may show a corroded outline or be broken, indicating high energy paleoenvironments (Fig. 3-3 A, B). The

length of *Tasmanite*-derived telalginite ranges between 60 and 120 μm and its width is about 4–12 μm, while those derived from *Campenia* and/or *Lancettopsis* have a size of from 210 to 300 μm. *Leiosphaeridia*-derived telalginite has an average size of 180 μm. In reflected white light, telalginite exhibits a brown to dark brown colour, and has a yellow and brown-yellow fluorescence of variable intensity (Fig. 3-3 C-E; 3-4 A, B).

In the investigated wells, *Botryococcus*-derived telalginite appears in two forms. One is probably related to *Botryococcus braunii* and the larger form to *Botryococcus reinschia*. The size of *Botryococcus braunii* is 60 μm, whereas that of the other form is 90 μm. Both telalginite exhibit an orange or light brown colour in reflected white light and have a yellow fluorescence of middle to high intensity (Fig. 3-4 B, C).

Lamalginite occurs from a variety of precursors such as algae, dynocysts and acritarchs. In the investigated bituminous shale, dynocysts were not encountered, while acritarchs were present in some samples. Acritarchs, which are considered by most palynologists to have algal affinities, are small spiny cysts. They have a yellow-green or green intense fluorescence and variable size (Fig. 3-3 F). In the Early Jurassic, most genera are regarded as indicating nearshore, estuarian to shallow lagoon and/or slightly brackish water environments (Prauss *et al.,* 1991). Lamalginites are classified as discrete, filamentous and layered, according to Hutton and Cook (1980), Cook *et al*. (1981), and each category was counted separately (Fig. 3-3 B, E).

Discrete lamalginite is more common compared to filamentous lamalginite. It occurs as a short filament and has an average size of 4 μm. Filamentous lamalginite occurs as a thin filament, with no or little recognisable structure in the polished sections prepared perpendicular to the bedding. Layered lamalginite occurs as a lamellar lamalginite with an average size of 100 μm. Lamalginite exhibits a yellow fluorescence of moderate intensity (Fig. 3-3 B, E).

Liptodetrinite, which is defined as tiny fragments of liptinite macerals, occurs in variable concentrations scattered in the mineral groundmass and in association with bituminite I (Taylor et al., 1998). In the Posidonia Shale, it appears in two forms. The first form occurs as very short rods or filaments and is of a minute size, whereas the other form occurs as rounded bodies with a diameter of 4 μm. The content of liptodetrinite can be overestimated due to the difficulty of distinguishing it from the small spherical *Nostocopsis* algae (Mädler, 1963) which is usually classified in discrete lamalginite. Liptodetrinite is barely visible in reflected white light and shows yellow fluorescence of middle to high intensity (Fig. 3-4 D).

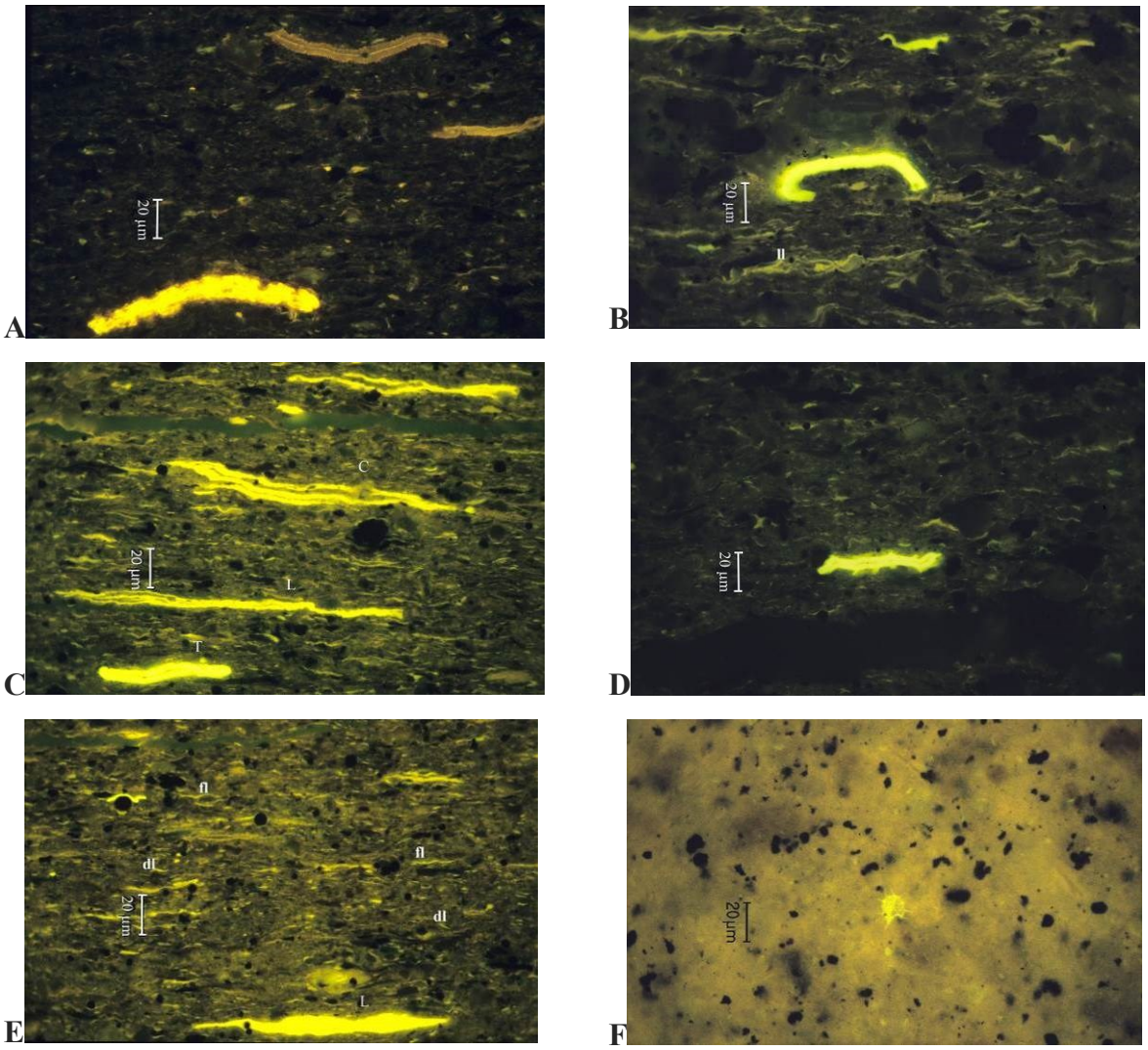

Fig. 3-3: Examples of different macerals of the liptinite group.
A), Strong fluorescing "corroded" telalginite derived from Tasmanites; B), Strong fluorescing Tasmanite-derived telalginite with broken outline; yellow fluorescing layered lamalginite (ll); C), Tasmanite-(T), Campenia-(C), Leiosphaeridia (L)-derived telalginite; D), Pterosphaeridia-derived telalginite; E), Lancettopsis (L)-derived telalginite; discrete lamalginite (dl); filamentous lamalginite (fl); F), Acritarch exhibits a green-yellow fluorescence of high intensity;. Fluorescence mode, oil immersion.

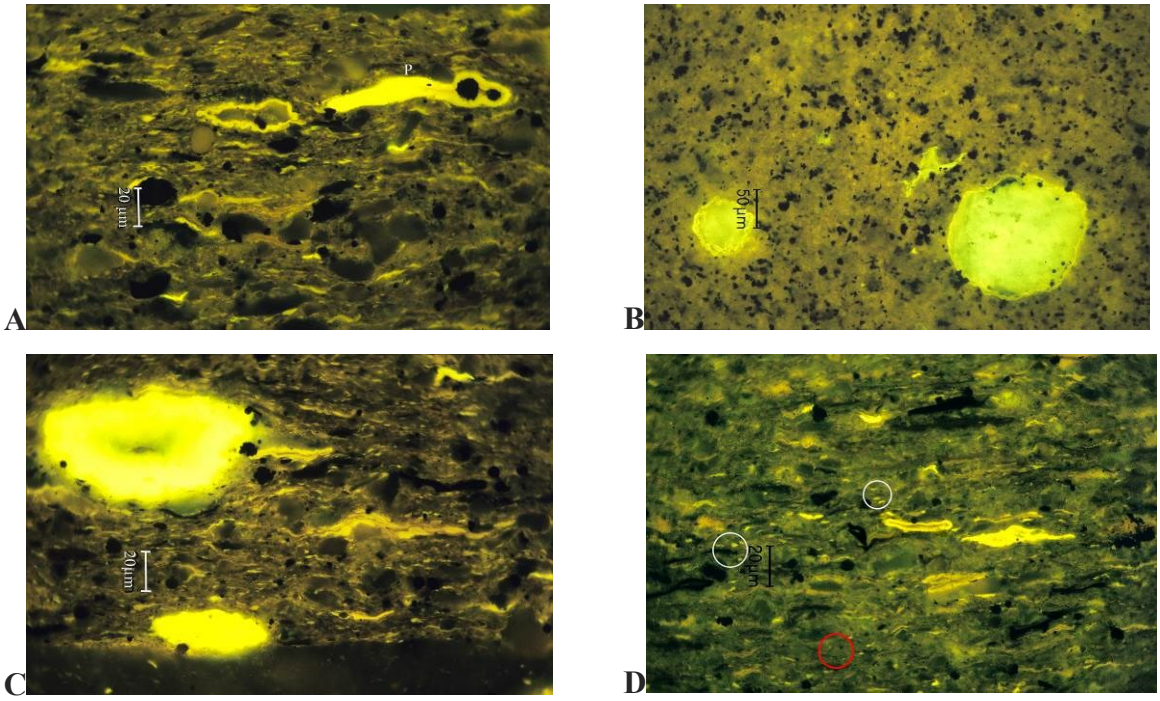

Fig. 3-4: Photomicrographs showing different maceral examples of liptinite group.
A), Pleurozonaria-derived telalginite (P); B), Leiosphaeridia-derived telalginite; C), *Botryococcus reinschia* (top left) and *Botryococcus braunii* (oval-shaped algae, bottom); D), different types of liptodetrinite: massive (white circles) and "classic" types (red circle). Fluorescence mode, oil immersion.

Bituminite

Bituminite, defined by organic petrologists as structureless organic matter (ICCP, 1993; Taylor et al., 1998), is commonly the major organic component in most potential source rocks (Teerman *et al*., 1995). Palynologists, who studied isolated kerogen in transmitted light, use the terms "amorphous", "sapropelic" or "amorphogen" to qualify the structureless organic matter in sediments (Tyson, 1995; Taylor *et al*., 1998). It may be lenticular in shape, when observed in white reflected light, in a polished section perpendicular to the bedding plane, and has variable reflectance and fluorescence properties, depending on its origin and the maturity of the rock sample. In mature bituminous shales, bituminite is generally wispy, and is elongated to lens-shaped, with a granular to pitted or moderately homogeneous surface. Bituminite is associated with fine occurrences like liptodetrinite, micrinite and faunal relics (Teerman *et al*., 1995). The origin of bituminite is still uncertain and there is no widely accepted nomenclature for this maceral (Teerman *et al*., 1995).

Bituminite (amorphous organic matter) originates from a variety of precursors, which, in turn, provide information on paleoenvironments. Therefore it is important to take into account the precursors of amorphous organic matter in studies of sedimentary organic matter. Structureless organic matter is not only a product of bacterial degradation of terrestrial

material, algae, faecal pellets or bacterial mass itself, but instead it also seems to be formed from dissolved organic matter, which is later absorbed by mineral matrix (Stasiuk and Goodarzi, 1988; Rullkötter *et al*., 1992; Tyson, 1995; Hutton and Rob, 1994; Taylor *et al.,* 1998).

Three types of bituminite macerals were introduced by Teichmüller and Ottenjann (1977) namely bituminite I, bituminite II and bituminite III, in the Toarcian Posidonia Shale of Germany. Later the ICCP approved their definition for rocks other than coals (ICCP, 1993). In addition to the "classic" bituminite types, other bituminites, called bituminite IV, bituminite V and bituminite VI, have been encountered in the investigated samples of Posidonia Shale (Gorbanenko and Ligouis, 2014). These new types of bituminite have been described and defined on the basis of their optical properties, which are closely linked to different paleoenvironmental conditions.

The following definitions of the three types of bituminite are based on the observations made in this study in early mature and mature bituminous shales.

Bituminite I has an indistinct lens shape (streaks) with a length of up to 60 μm. It is characterised by a mid to dark grey colour in reflected white light, a very low reflectance and a light brown to dark brown fluorescence of weak to moderate intensity (Fig.3-5 A, B). It often contains yellow fluorescent liptodetrinite inclusions.

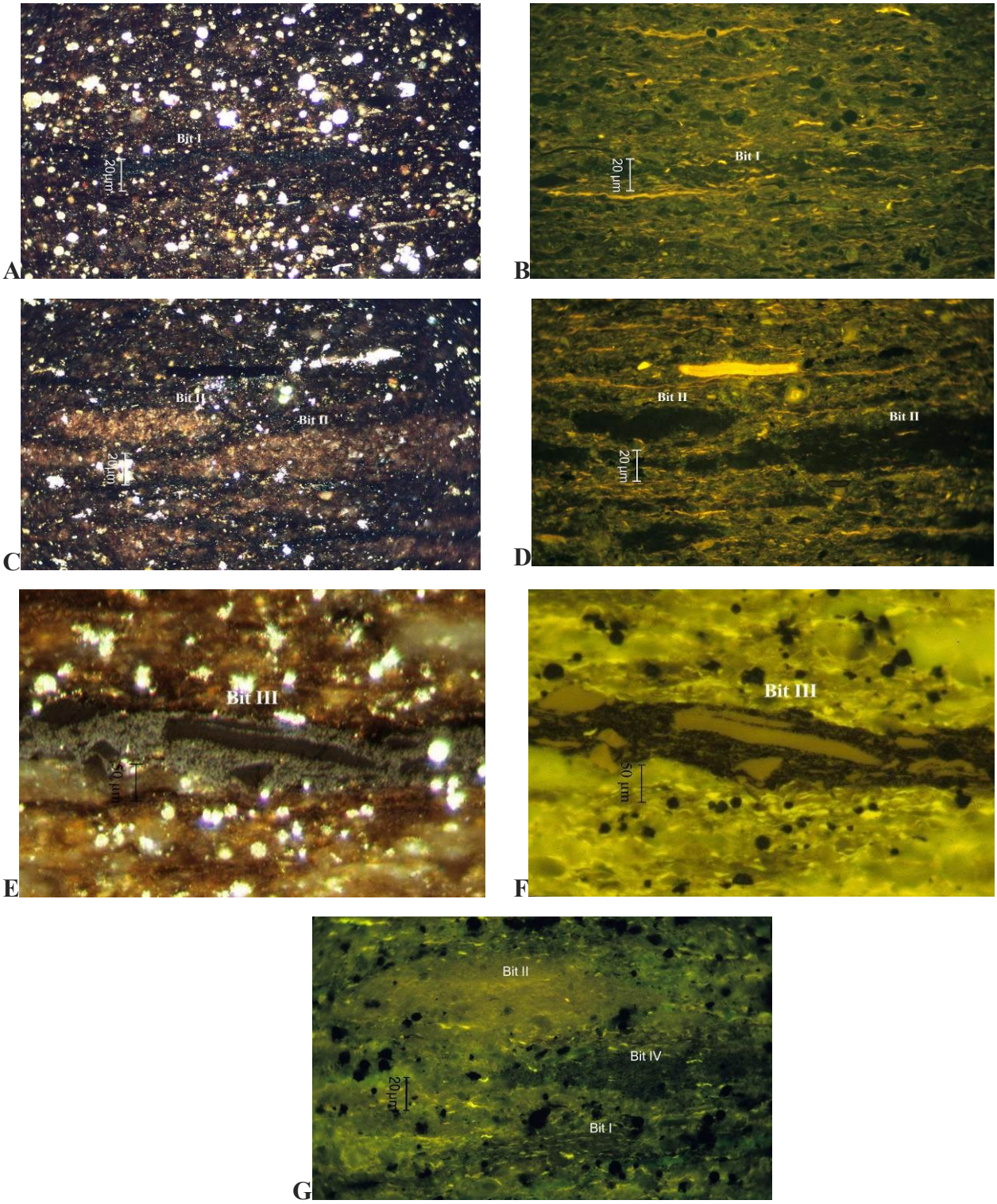

Fig. 3-5: Examples of the different types of bituminite in mature Posidonia Shale.
A), Bituminite I (Bit I) in the mineral bituminous groundmass rich in framboidal pyrite. Reflected white light, oil immersion; B), The same field of view in fluorescence mode, oil immersion. Note the bright fluorescing liptodetrinite inclusions in the bituminite I (Bit I). The greenish-brown fluorescing mineral bituminous groundmass contains liptodetrinite and lamalginite. C), D), Bituminite II (Bit II) lenses in the mineral bituminous groundmass with telalginite probably derived from Pleurozonaria in reflected white light, oil immersion (C) and fluorescence mode, oil immersion (D); E), Bituminite III (Bit III) with inclusions of zooclasts (dark brown) and light grey micrinite. Reflected white light, oil immersion; F), The same field of view in fluorescence mode, oil immersion. Note orange fluorescing zooclast inclusions; G), Bituminite IV (Bit IV) in the mineral bituminous groundmass together with bituminite I (Bit I) and bituminite II (Bit II). Fluorescence mode, oil immersion.

Bituminite II occurs as thick elongated lenses associated with small carbonate crystals. It exhibits a brown colour in reflected white light and a yellowish-brown to reddish-brown fluorescence, often with greenish fluorescing oil expulsions (droplets) (Fig. 3-5 C, D).

Bituminite III is defined as thick elongated bodies often associated with fluorescent

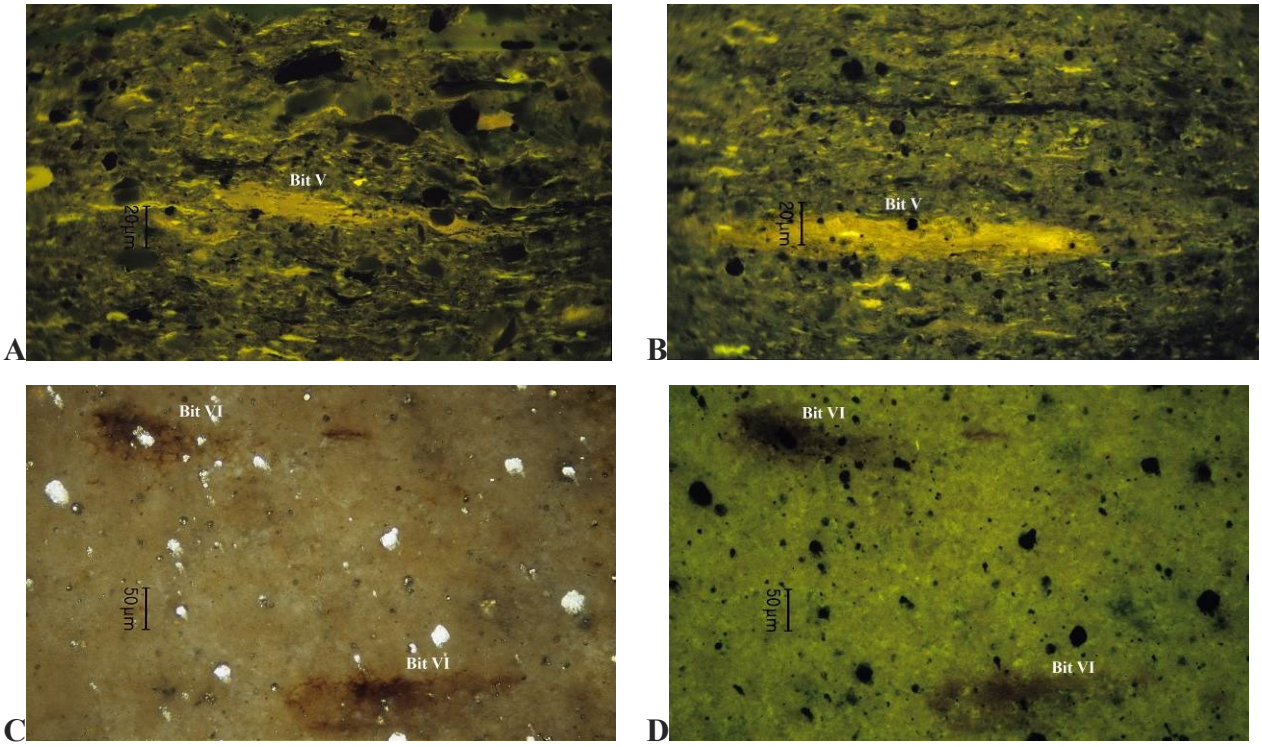

Fig. 3-6: Examples of bituminite V and bituminite VI in mature Posidonia Shale.
A), B), Bituminite V (Bit V) fluorescence mode, oil immersion. Note the bright fluorescing liptodetrinite inclusions in parts of the bituminite V; C), D), Bituminite VI dense network in the carbonate bituminous groundmass. Reflected white light, oil immersion (left) and fluorescence mode, oil immersion (right).

phosphate faunal remains (Fig.3-5 E, F) (Prauss *et al*., 1991; Teichmüller and Ottenjann, 1977). In Fig. 3-5 E, bituminite III is filled with micrinite and contains dark brown fishbones. In fluorescence mode it exhibits dark brown fluorescence.

Bituminite IV has a few similarities to bituminite I (Fig. 3-5 G). This unstructured material occurs as thick lenses of irregular outline. Similarly to bituminite I, it has micrinite inclusions, but contains no liptodetrinite and shows green fluorescence.

Bituminite V has optical properties very close to the bituminite encountered in the bituminous shales of the Kimmeridge Clay Formation in Dorset, England (unpublished Vogler, 2014) and has not previously been described in Posidonia Shale (Fig. 3-6 A, B). It

exhibits a dark grey to grey-brown colour in reflected white light and an orange-brown or greenish-brown fluorescence of moderate intensity. Its size is variable and its length ranges from 20 to 200 µm.

Bituminite VI has already been defined by Creaney (1980) as a "matrix-bituminite" (Fig. 3-6 C, D). It consists of amorphous organic matter, which occurs as a "network" between the carbonate crystals of calcareous groundmass and calcareous concretions. It has an orange-brown or brown colour in reflected white light and an orange fluorescence.

Sporinite and cutinite

Sporinite and cutinite are terrestrial-derived liptinite macerals (Taylor *et al*., 1998). Sporinite, which corresponds to microspores and pollen grains released by terrestrial plants, is rare in the investigated Posidonia Shale. In mature samples, it has a very low reflectance (brownish or greyish coloured) and an orange-brown fluorescence of variable intensity. Morphologically, two different types of sporinite have been identified. One has a smooth outline, whereas the other shows ornamentation (Fig. 3-7 A). Both types are of a size which does not exceed 30 µm. In addition, cutinite which corresponds to the cuticles of leaves, is identified by its typical morphology (Fig. 3-7 B). Optical properties of this maceral are similar to those of sporinite.

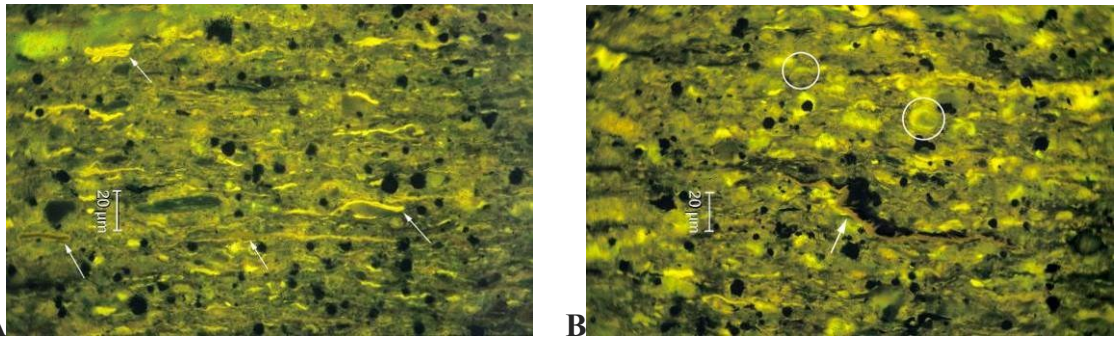

Fig. 3-7: Examples of sporinite and cutinite in the investigated Posidonia Shale.
A), Sporinite showing ornamentation (white arrows) and variable fluorescent colour; B), Cutinite (white arrow); in white circles showing greeny-yellow fluorescent coatings on coccoliths;

Secondary macerals: migrabitumen, exudates and oil

Migrabitumen or solid bitumen, which are secondary organic products generated from fossil organic matter during diagenesis and catagenesis (see Alpern *et al*., 1994; ICCP, 1993), are relatively rare in the investigated shales. Their shape is inherited from the form of the cavities they occupy, because it is a non-crystalline material (Schoenherr *et al*., 2007). The size of migrabitumen "particles" can be classified as intergranular pore fillings and reach

more than 200 µm in some samples of the investigated Posidonia Shale. Although microorganisms, for instance, algae, are the possible source material for migrabitumen, sporinite and bituminite might be also considered as a precursor of migrabitumen (Jacob, 1989; ICCP, 1993). However, in addition, it may also have been formed by biodegradation of oil or from de-asphalting (Petersen *et al*., 2013). Migrabitumen may indicate oil migration of any distance from a micron to tens of miles (Landis and Castaño, 1995).

The earliest classification of bitumen originated from the materials industry (Abraham, 1938). This primarily descriptive scheme distinguishes between bitumen by differing solubility in CS_2. Subsequent studies related to the petroleum industry recognised the importance of the solubility of migrabitumen for potential geochemical applications ("pyrobitumen" Landis and Castaño, 1995). The term "solid bitumen" was invented by (Hunt, 1979), signifying secondary solid bitumen (secondary macerals) generated from fossil organic material during diagenesis and catagenesis. Curiale (1986) classified solid hydrocarbons with respect to the relative timing of oil generation based upon comprehensive biomarkers and bulk geochemical data. Based on petrographic techniques, the first genetic classification of solid bitumen was made by Abraham (1938). This has since been revised by Jacob (1989), who classified "migrabitumen" into 8 groups. He characterised and described them from an organic petrographical and geochemical point of view (Fig. 3-8 A, B). Klubov (1993) broadly classified solid hydrocarbons based upon the type of thermal regime and dominant hydrocarbon assemblages.

The formation of bitumen or migrabitumen (for more details, see Jacob (1989) begins with a vitrinite reflectance of about 0.35 – 0.60 %Rr. During processes of maturation of the migrabitumen, their reflectance increases and, in some cases, an increase in the intensity of optical anisotropy. Based on vitrinite reflectance measurements, Jacob (1989) subdivided the reflecting bitumen into epi-impsonite (VRr 0.7 – 2.0 %), meso-impsonite (VRr 2.0 – 3.5 %) and cata-impsonite (VRr 3.5 – ca. 10 %) (Fig. 3-8 B). The impsonites may be optically isotropic and anisotropic.

A)

Maceral group	Maceral subgroup	Maceral
Migrabitumen		ozocerite
	asphaltite	asphalt
		gilsonite
		glance pitch
		grahamite
	impsonite	wurtzillite
		albertite
		epi-impsonite
		meso-impsonite
		cata-impsonite

B)

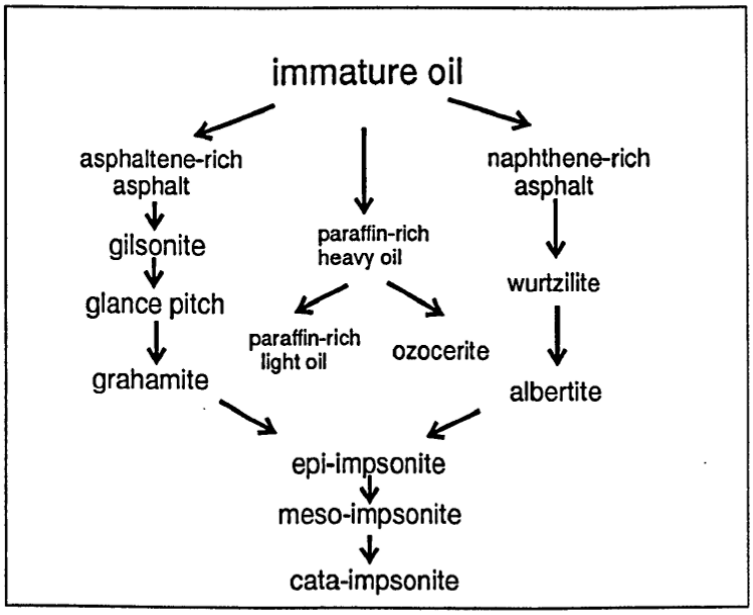

Fig. 3-8: Classification of migrabitumen **A)** petrographical, **B)** geochemical (Modified after Jacob, 1989).

With temperature increase, the migrabitumen might appear in one or two "generations". One is a heterogeneous bitumen, the other, a homogeneous bitumen (Fig. 3-9 A, B). The homogeneous type represents the "dead" carbon (Taylor *et al*., 1998) and loses its capability to generate petroleum, compared to the heterogeneous type, which can produce natural gas or condensate (Jacob, 1989). Landis and Castaño (1995) define the portion (< 0.7 %Bro – Bro=bitumen reflectance in oil immersion) of the series that yields some "bitumen", known in modern petroleum geochemistry as "solid bitumen". The migrabitumen (Bro > 0.7 %) is characterised by a minor extractable fraction.

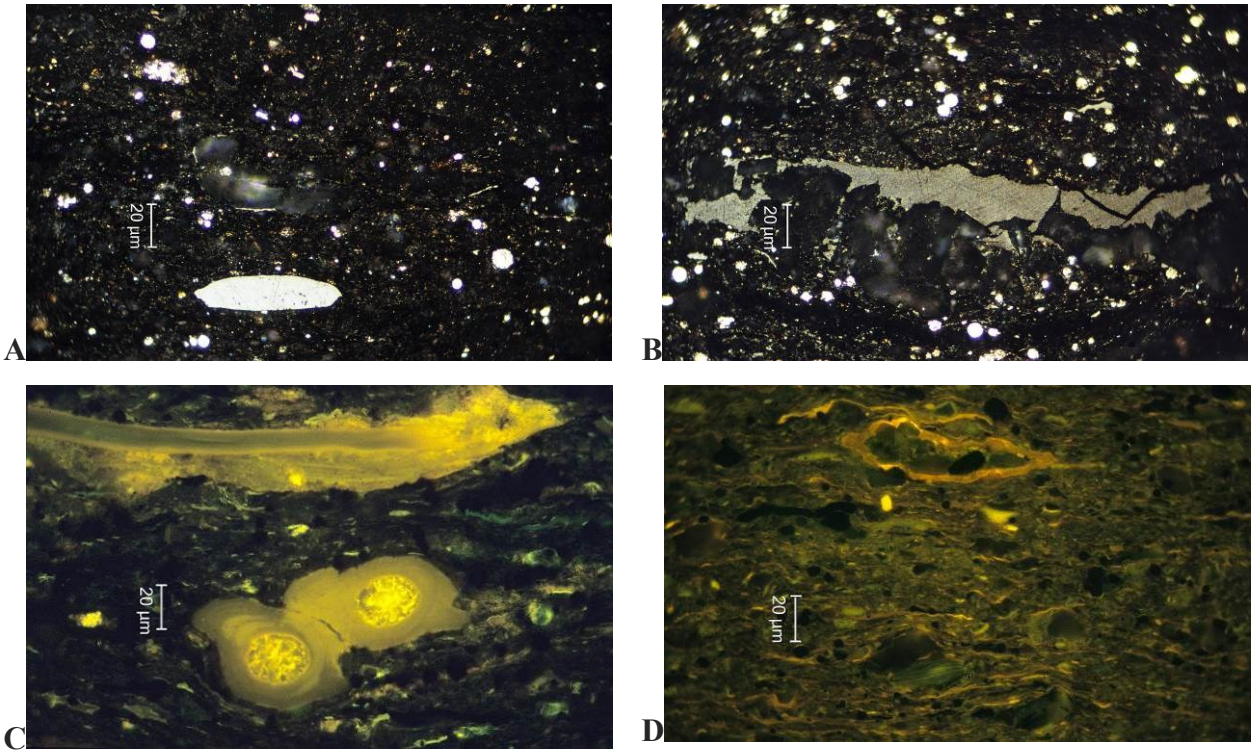

Fig. 3-9: Photomicrographs illustrating the different types of secondary macerals.
A), Post-mature telalginite consisting of high reflecting homogeneous migrabitumen; B), Low reflecting heterogeneous migrabitumen associated with a recrystallised calcareous bioclasts; C), Phosphatic fishbones showing yellow fluorescing oil exudates; D), Spindle-shaped telalginite filled by calcareous and framboidal pyrite, showing bright yellow fluorescing oil droplets. Reflected white light (upper row), fluorescence mode (lower row), oil immersion.

Another secondary maceral exudatinite appears in the Posidonia Shale as an infilling in the interspace of fishbones. This maceral might be considered as an asphaltic migrabitumen (Taylor *et al.,* 1998). It is barely recognisable in reflected white light. However, in fluorescence mode it has an orange colour of high intensity (Teichmüller, 1974) (Fig. 3-9 C).

Oil is quite a common secondary maceral in the investigated bituminous shales of the mature stage. It appears as inclusions in single carbonate grains and as droplets in bituminous mineral groundmass or associated to alginite and bituminite II and III. Oil has a green patchy fluorescence of high intensity (Fig. 3-9 C, D).

3.3.1.1.3. Inertinite group

The inertinite group in the Posidonia Shale samples is represented by the primary macerals, fusinite, semifusinite, secretinite, inertodetrinite, natural char and the secondary maceral, micrinite. Fusinite and semifusinite are strongly fragmented wood tissues (structured particles, isolated cell walls) and are distinguished by their variable degree of oxidation. Fusinite has a light grey to whitish colour in reflected white light, while semifusinite has a

darker colour, but is still lighter than indigenous vitrinite (Fig. 3-10 A). These macerals might be produced by different processes, such as forest fires, bacterial oxidation or sub-surface oxidation in terrestrial domains (Taylor *et al.,* 1998).

Secretinite has distinct morphological (non-cellular) properties. It is composed of commonly round, vesicled to non-vesicled, and equant to elongate bodies without obvious plant structure (ICCP, 2001). It originated from secretionary canals or sacs in vascular plants (Taylor *et al.,* 1998). In the Posidonia Shale, this maceral is rare. It has a light grey colour in reflected white light and no fluorescence.

Inertodetrinite consists of redeposited debris of fusinite, semifusinite, sclerotinite, and other small (<10 µm in size) fusinitised plant remains (Taylor *et al*., 1998). Many small fragments are probably formed through river transportation. However, small organisms might also contribute to the formation of this maceral.

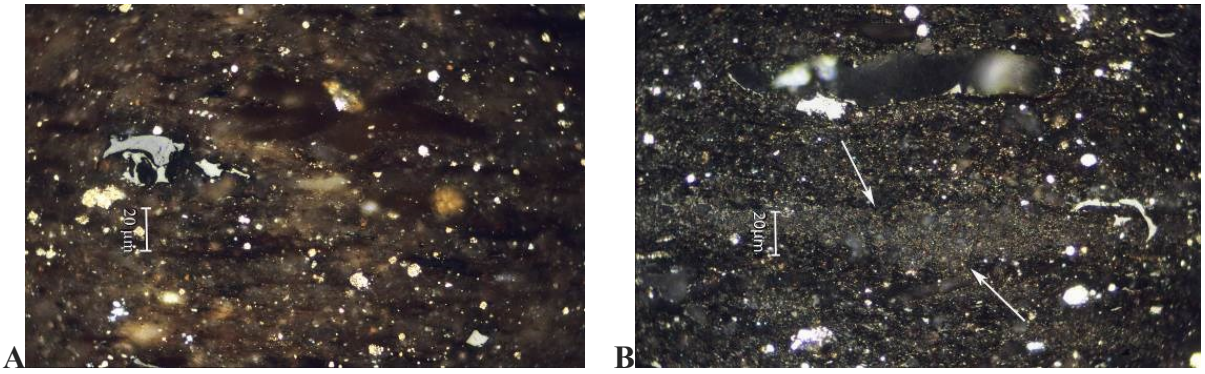

Fig. 3-10: Photomicrographs showing different macerals of the inertinite group.
A), Remains of semifusinite (grey colour) and inertodetrinite (light grey colour) in calcareous bituminous groundmass; B), Micrinite network (white arrows) replacing bituminite II in post-mature Posidonia Shale. Note the association of micrinite with small calcareous crystals. Reflected white light, oil immersion.

Natural char occurs in conditions of oxygen deficiency, where fire has taken place (Kwiecińska and Petersen, 2004). It is characterised by a random distribution of pores and a varying porosity. In well D, the Posidonia Shale contains char in a minute amount. It appears as particles with porous structures and a light grey colour in reflected white light and has a size of approximately 30x20 µm (Fig.3-11).

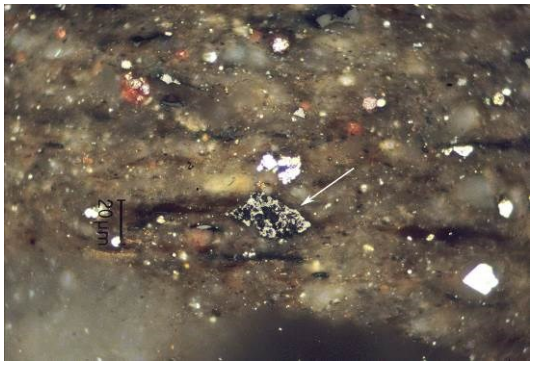

Fig. 3-11: Photomicrographs illustrating example of char in well D.
Note the light grey colour of char particles (white arrow). Reflected white light, oil immersion.

Micrinite is a finely particulate secondary maceral, occurring as whitish rounded grains apparently about 1 μm in diameter, commonly accumulated in aggregates (Taylor and Liu, 1989). It has a relatively high reflectance and no fluorescence (Fig. 3-10 B). Teichmüller and Ottenjann (1977) described micrinite as a maturation product of bituminite in bituminous shales. Alpern and Cheymol (1978) stated that the micrinite percentage increases when the fluorescence of liptinite begins to diminish, suggesting that it occurs during maturation from lipoid substances. Thus, micrinite represents "dead carbon", left over as hydrocarbon generation took place in organic-rich sediments and is considered to be a secondary maceral or a product of thermal maturation from certain vitrinite, liptinite macerals or bituminites (Teichmüller, 1974; Mukhopadhyay *et al*., 1985; Stach *et al*., 1982; Taylor and Liu, 1989; Taylor *et al*., 1998; Faraj and Mackinnon, 1993).

3.3.1.2. Mineral matter in the investigated Posidonia Shale

Apart from the organic components in the Posidonia Shale, mineral matter was also identified and taken into account in the maceral analysis. Mineral matter includes detrital minerals (quartz and micas), glauconite, gypsum, pyrite, peloids, carbonate minerals (isolated carbonate crystals, dolomite), zooclasts (fishbones, shell remains and coccoliths) and different types of mineral groundmasses (calcareous, clayey and their transitional forms). The classification of the mineral matter will not be developed in this chapter, as it is not the main subject of the study. However, a detailed description of the mineral matter will be given in Chapter 4. For more details regarding zooclast nomenclature, the author advises the reader to consult Tyson (1995), and Boggs (2009) for mineral matter classification.

3.3.1.3. Limitation of the maceral analysis

Organic petrography, particularly, maceral analysis, is widely used in the coal and petroleum industries for its rapid results and a technique that does not have specific requirements. Although some scientists were sceptical about the resolution of organic petrography, this method of optical investigation of organic matter has many applications in different branches of science, including the petroleum industry. Nevertheless, during the maceral analysis procedure, the worker needs to pay attention to the evaluation of the results:

(1) Although maceral analysis has become more accurate today compared to that of past decades, the risk of overestimating or/and underestimating the concentration of different organic components still exists and depends on the experience of the worker.

(2) Resolution of maceral analysis is equal to the minimal scale resolution and makes up 2μm by using a magnification of 500x (international standard). In this case, the risk of overestimation of fine-dispersed particles increases rapidly. In particular, the micrinite definition is close to or less than, 1μm in grain size (Taylor and Liu, 1989). It is difficult or impossible to observe and count precisely many grains of that size.

(3) Fluorescent organic matter is predominant in many known oil-source rocks. To obtain accurate and relevant results, maceral analysis, both in reflected white light and in fluorescent mode, is required. However, some of the macerals have no fluorescence and their recognition is possible only in reflected light or by use of polarised light. This evidence requires time resources and the extreme attention of the operator.

(4) Oil in mature bituminous shales is quite a common component. On the one hand, it indicates oil expulsion and the good quality of the source rocks. However, on the other hand, it results in a problem of the identification of macerals and/or their description. Increased immersion caused by the expulsed oil exhibits a green fluorescence. This complicates the maceral analysis in fluorescence mode and reduces the accuracy of the obtained results. To avoid errors and in order to obtain appropriate results, the regular exchange of oil is required.

(5) Gaps and/or lack of classification is another problem in maceral analysis. The nature and origin of the structured organic matter is well understood, whereas that of bituminite macerals or, in other words, amorphous organic matter, is still debated. Currently, there is no accepted classification of bituminites. Therefore, this complicates the evaluation of organo-petrographic results.

(6) Macerals and zooclasts showing similar optical properties. Together with the point previously described, there is still the actual problem of the recognition of some macerals. In bituminous shale, some zooclasts show optical properties similar to vitrinite particles or to bitumen. In some cases, this identification, based on morphological recognition and differences existing between zooclasts, vitrinite and bitumen, becomes an intractable issue. This is related to the experience of the analyst. In any event, these cases are so rare that they have no influence on the results.

3.3.2. Vitrinite reflectance and bitumen reflectance as indicators of organic matter maturity

3.3.2.1. Vitrinite reflectance

3.3.2.1.1. Instrumentation and operating conditions

Vitrinite reflectance is used as a maturation parameter in coals and other sedimentary rocks (Littke *et al*., 2012). Apart from developing technologies and problems encountered due to measuring procedures of vitrinite reflectance, this parameter is still considered as the most sensitive thermometer and widely used for basin modelling and maturity assessment of source rocks.

Generally, two main approaches are used to determine the reflectance of vitrinite in sediments and, consequently, to distinguish indigenous and oxidise vitrinite in immature, mature and post-mature oil shales. The first approach consists of measuring the random reflectance of about 50–100 particles, which is intended to represent the indigenous vitrinite in the studied sample. Usually vitrinite particles with the lowest reflectance are assumed to reveal the values of indigenous vitrinite. The second approach is to use the morphology of recycled and indigenous vitrinite as an identification parameter (Nzoussi-Mbassani *et al.,* 2005). In post-mature oil shales only the morphological criteria described before can be used to distinguish indigeneous vitrinite from recycled. It must be taken into account that vitrinite at high maturation level has a light colour in reflected white light, similar to fusinite. In addition, anisotropy of fusinite and vitrinite particles increases with temperature and becomes striking, as previously described. Hence, all the criteria mentioned above, especially size and shape, are not specific to one type of vitrinite and might depend on the particular depositional environment and the local maturation history (Nzoussi-Mbassani *et al.,* 2005).

Measurement of vitrinite reflectance in investigated bituminous shales was carried out under standard conditions (at 500x magnification, under oil immersion, using monochromatic light at wavelength of 546 nm and at 23°C; Taylor *et al.,* 1998) on 5 selected samples having appropriate vitrinite particles of good quality (Borrego *et al*., 2006) from different beds of Posidonia Shale for each well from northwestern Germany and the western Netherlands. For calibration procedure, different standards were used: the higher standards (0.589 %Rr – "sapphire glass" for early mature bituminous shale; 1.24 %Rr – "glass prism" for mature bituminous shales; 3.112 %Rr – "cubic zirconia" for post-mature oil shales) to adjust the measuring system, whereas the lower standards (0.529 %Rr – "glass" standard for early mature bituminous shale; 0.589 %Rr – "sapphire glass" for mature bituminous shale; 1.689 %Rr – "gadolinium-gallium-granat" for post-mature oil shales) to prove the quality of the calibration.

3.3.2.1.2. Limitation of vitrinite reflectance method

Although this method of maturity assessment is considered as the most powerful tool, the vitrinite reflectance technique has several problems and limitations which might be encountered by petrographers due to the measurement procedure. The most common are viewed below.

(1) Polishing quality of samples. The poor quality of preparation can significantly lower the result of vitrinite reflectance (Schegg, 1993). A clean, uniformly flat and scratch-free surface enables high-quality values of vitrinite reflectance to be obtained (Littke *et al*., 2012).

(2) Identification of "good" vitrinite particles. Oxidised vitrinite, which reflects previous burial history (Nzoussi-Mbassani *et al.,* 2005, Borrego *et al*., 2006), cavings and mud additives (in cuttings) and migrabitumens (in cuttings), are the cause of most of the problems (Lo, 1992) related to the recognition of the indigenous vitrinite population in mature and post-mature sediments. To distinguish vitrinite from other particles with similar morphology considerable care, interpretative skills and experience are required (Lo, 1992).

(3) Size of particles, quality and quantity of measurements. Taking into account the vitrinite in sedimentary rocks (generally smaller than or about 10 μm in size), there is difficulty in recognising its morphology and identifying its type (Mukhopadhyay, 1992). Moreover, it has been found that at least 20 measurements on indigenous vitrinite are needed to accurately calculate the mean reflectance (Barker and Pawlewicz, 1993). However, it is well recognised that some organic facies are poor in indigenous vitrinite and it is difficult to

obtain even 20 measurements (Malinconico, 2000). For this reason, it is better to focus the measurements on good quality vitrinite particles.

(4) Different population of the vitrinite in investigated samples. In the investigated samples of Posidonia shale, the existence of different populations of vitrinite particles has been clearly observed: vitrinite with different content of hydrogen (weathering); vitrinite-like particles; vitrinite impregnated with bitumen (Fang and Jianyu, 1992; Schegg, 1993).

(5) Vitrinite reflectance at high level of maturation. Organic petrographers can encounter problems measuring vitrinite reflectance in sediments with dispersed organic matter, especially in post-mature source rocks. As previously mentioned, with temperature increases, the chemical reorganisation of vitrinite begins. With a vitrinite reflectance value below 0.7 %, the reflectance increases slowly as a result of the limited formation of polycyclic aromatic molecules compared to those of 0.7 – 3.0 %VRr. For vitrinite with reflectance of more than 3.0 %Rr, the change in relation of aromatisation to Rr is due to the growth of aromatic sheets that occurs in such vitrinites of high maturity, and appears to produce a rapid increase in the anisotropy of the vitrinite (Carr and Williamson, 1990). According to *Zilm et al*. (1981) and Pugmire *et al*. (1982), in the meta-anthracite stage, the reflectance of inertinite is surpassed by the maximum reflectance of vitrinite. This is due to the higher hydrogen content and the tendency towards early pre-graphitisation (Durand et al., 1986; Taylor *et al.,* 1998).

(6) Variation of vitrinite reflectance values caused by the presence of liptinite macerals. Many authors mentioned in their work the phenomenon of lower vitrinite reflectance values than expected in samples with a high content of liptinite macerals (Hutton and Cook, 1980; Kalkreuth, 1982; Newman and Newman, 1982; Durand *et al*., 1986; Prauss *et al*., 1991; Fang and Jianyu, 1992). Some workers believe that bitumens or hydrocarbons impregnated into vitrinite particles can meet lower values than expected (Hutton and Cook, 1980). This is an accepted fact by the majority of authors.

(7) Mineral groundmass and pyrite. The influence on vitrinite reflectance values of different types of mineral groundmass and pyrite framboids has been debated for a long time. Many scientists have stated in particular that vitrinite exhibits lower values in sandstones than in mudstone. This phenomenon is probably related to oxidation caused by the porosity of sandstones which is somewhat higher than that of argillaceous rocks (Teichmüller and Teichmüller, 1968).

Pyrite is another important problem during the measurement procedure. This strong reflecting mineral increases the real values of vitrinite reflectance and complicates the interpretation of the data (Littke *et al*., 2012).

(8) Different tectonic history might be a cause of the variation in vitrinite reflectance values. Pressure may influence the Rmax and increase the anisotropy of the vitrinite particles and, as a consequence, its measured reflectance values (Stach *et al*., 1982; Littke *et al*., 2012).

3.3.2.2. Bitumen reflectance

3.3.2.2.1. General remarks and definition

The idea of alculating the equivalent of vitrinite reflectance arose to assess maturity in the sediments where vitrinite particles are of poor quality, too rare or absent, for instance, for carbonate and pre-Devonian rocks (Jacob, 1989; Bertrand, 1993; Schoenherr *et al*., 2007; Prauss *et al.,* 1991). Jacob (1989) determined the stochastic relationship between the vitrinite reflectance and the reflectance of migrabitumen (%BRr). However, the linear relationship between vitrinite and migrabitumen reflectance has been verified only to a migrabitumen reflectance of about 3.0 %. The following formula was proposed by Jacob (1989) for the calculation of an equivalent of vitrinite reflectance:

$$\mathbf{VRr=0.618*BRr+0.40} \qquad \text{(Eq. 1)}$$

VRr – calculated equivalent of vitrinite reflectance;
BRr – measured migrabitumen reflectance.

The idea to use migrabitumen reflectance as a thermal indicator was developed by Jacob (1989). Landis and Castaño (1985) continued to develop the principle established by Jacob (1989). They measured a large number of samples containing particles of vitrinite and migrabitumen. Their results show a linear correlation between migrabitumen reflectance and vitrinite reflectance. The correlation equation is:

$$\mathbf{VRr=(BRr+0.41)/1.09} \qquad \text{(Eq. 2)}$$

Schoenherr *et al*., (2007) combined the two formulas (1) and (2) in order to approach the best-fit regression equation, which can be applied to maturity studies, if migrabitumen is present and vitrinite is absent:

$$\mathbf{VRr=(BRr+0.2443)/\ 1.0495} \qquad \text{(Eq. 3)}$$

Despite these aforementioned studies, no universal calibration formula between reflectance of migrabitumen and vitrinite can be proposed (Bertrand, 1993). Values obtained from reflectance of migrabitumen vary from basin to basin and are dependent on lithology and the bituminous character of the lithofacies (Prauss *et al*.,1991). It must therefore be kept in mind that vitrinite equivalent must be calculated individually for each sedimentary basin and/or can be considered as approximate values (Bertrand, 1993).

3.3.2.2.2. Measuring procedures

The reflectance measurements of migrabitumen were obtained only on polished blocks of samples collected from post-mature well B. This constraint is related to the relatively high bitumen concentration of different types presented only in this well.

Measurement of migrabitumen reflectance was conducted on homogeneous migrabitumen in 2 samples and on heterogeneous migrabitumen in 5 selected samples. The number of the measurements ranges between 10 and 21, according to the abundance of suitable particles (with size more than 2x2 μm, with surface free from scratches and irregularities) for reflectance measurements. The measurement procedure was carried out under standard conditions similar to those used for reflectance measurements of vitrinite (at 500x magnification, under oil immersion, under monochromatic light at a wavelength of 546 nm and at 23 °C).

The calibration procedures were undertaken using different sets of standards with known reflectance values. With regard to the vitrinite reflectance calibration procedure, the first standard, which has a slightly higher value than the estimated reflectance of bitumen particle, was used for calibration procedure, and the other, which has lower reflectance than the first standard, to check the quality of the adjustment (for the name and values of standards see Paragraph 3.3.3.1.).

There are two most important considerations that must be kept in mind:

- assurance that the migrabitumen originated from indigenous organic matter like algae (see Gorbanenko and Ligouis 2014);
- absence of indicators of a secondary origin (pore, veins, etc.) (Bertrand, 1993).

3.3.2.2.3. Limitation of bitumen reflectance method

In mature and post-mature pre-Devonian source rocks and carbonate source rocks where there is a lack of vitrinite particles, migrabitumen forms an important part of the dispersed organic matter. In all these cited cases, migrabitumen becomes the best parameter to evaluate thermal maturation. The problems related to the technical procedure of bitumen measurement are similar to those cited in the paragraph: "Limitation of vitrinite reflectance method". However, the author would like to point out that the specific relationship that exists between the reflectance of migrabitumen and that of vitrinite is a function of lithology, basin origin and/or the age of the sequences that contain migrabitumen (Bertrand, 1993). This evidence requires the establishment of an individual formula to calculate the equivalent of vitrinite reflectance in those sediments where both particles are available. Otherwise, using existing formulas to calculate the equivalent of vitrinite reflectance may only show approximate values of thermal maturity level (Bertrand, 1993).

3.4. Bulk of organic geochemical analyses

3.4.1. Rock-Eval Pyrolysis and Total Organic Carbon

3.4.1.1. General remarks

In order to assess the quality and maturity of the kerogen, the IFP (Institut Français du Pétrole) developed a pyrolysis analyser instrument, the Rock Eval, which has become an industry standard in source rock assessment (Espitalié *et al*., 1977). This method enables researchers to estimate the petroleum potential of the rock sample by measuring the difference between its current total organic carbon and its residual organic carbon after pyrolysis and to obtain results of analysis, which would have taken millions of years in a sedimentary basin (Bordenave *et al*., 1993; McCarthy et al., 2011).

3.4.1.2. Instrumentation and operating conditions

The core samples selected for this study were analysed using a Rock-Eval 6 Analyser equipped with a Total Organic Carbon (TOC) module at Oxford University, Department of Earth Science. During Rock-Eval pyrolysis, samples are heated under an inert atmosphere of helium and a series of peaks are delivered on the pyrogram which are expressed in mg HC/g

rock: 1) S_1 is vaporised gaseous and liquid hydrocarbons from the rock samples without cracking the kerogen at approx. 300 °C (Fig. 3-12); 2) the second peak (S_2) are the hydrocarbon results from cracking of heavy hydrocarbons and from thermal breakdown of the kerogen at temperatures between 300 and 600 °C; 3) S_3 peak results from CO_2 that is evolved from thermal cracking of the kerogen during pyrolysis at 600 °C. The first two peaks are determined by a flame ionisation detector (FID) and the third one by sensitive infrared detector (IR). The organic carbon remaining (S_4) is measured by oxidation under air (or oxygen) atmosphere at 600 °C. The total organic carbon (TOC) is calculated from peaks S_1, S_2 and S_4: $\%TOC=k(S_1+S_2)/10+S_4/10$ (Bordenave *et al.*, 1993). Pyrolysis temperature at which maximum hydrocarbon generation (temperature of S_2 peak) occurs is the Tmax, which is used as a thermal indicator of the kerogen type II and type III (Fig. 3-12) (Espitalié, 1986; Espitalié, 1986b).

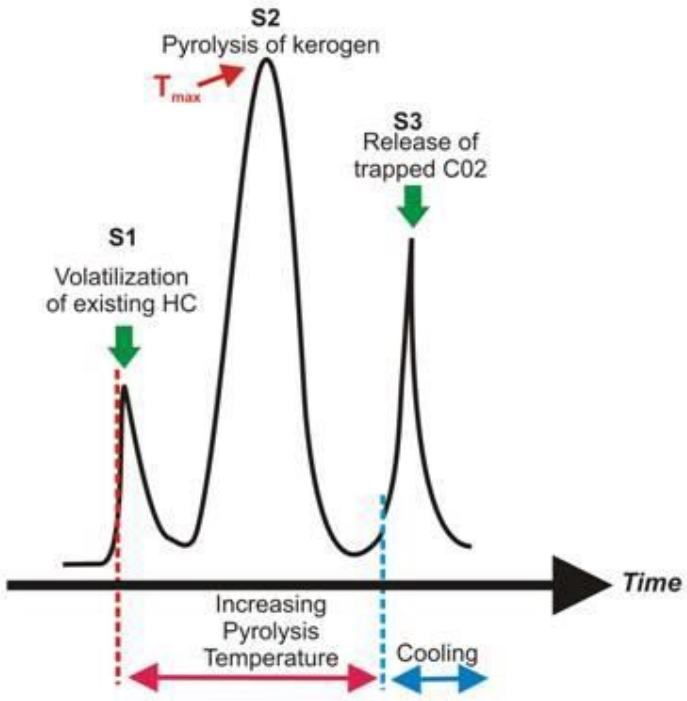

Fig. 3-12: Schematic Rock-Eval pyrogram showing the distribution of peaks S_1, S_2 and S_3 (Modified after Tissot and Welte, 1978).

3.4.1.3. Rock-Eval indices

The relationship between the measured compounds forms the basis of the indices used in the interpretation of the evaluated results (McCarthy et al., 2011). These indices are used

for the determination of the kerogen type, the petroleum potential and the organic matter maturity.

- The Hydrogen Index (HI) is calculated as S_2/TOC*100. High HI indicates a greater potential to generate oil.
- The Oxygen Index (OI) is derived from the ratio of CO_2 to TOC. Consequently, it is defined as S_3*TOC/100. This index shows the amount of oxygen contained in the kerogen.
- The Production Index (PI) is calculated from the relationship between hydrocarbon generated during the first and second pyrolysis stages and is defined as $(S_1+S_2)/S_1$. This index is used to characterise the evolution of the organic matter. It tends to increase prior to hydrocarbon expulsion.
- The petroleum potential parameter is defined as the sum of S_1 and S_2 peaks and shows the maximum quantity of hydrocarbons that the investigated source rock might generate (McCarthy *et al.,* 2011).

3.4.1.4. Limitation in evaluation of Rock-Eval pyrolysis results

Despite the indefeasible advantages of Rock-Eval pyrolysis, which include the evaluation of the petroleum potential and maturity of numerous source rocks in a short period of time and the relatively low costs of this method, this technique has a sufficient number of complexities to limit its efficiency and to complicate an interpretation of the results (Katz, 1983).

(1) One of the existing problems is the alteration degree of the altered samples due to their oxidation. Oxidised organic-rich samples tend to show lower HI and higher OI. These samples exhibit on a pyrogram overestimated Tmax values or are characterised by the absence of S2 peak (Peters, 1986).

(2) The complicity of pyrogram interpretation due to the similarities of some chemical compounds is another limitation parameter of this technique. Leventhal (1982) suggested that the S2 peak, obtained by FID and giving response to carbon-hydrogen bonds, carbon electrons and carbon mass, may show similar values for several organic chemical compounds such as benzene, hexane and six molecules of methane.

(3) Averaging of the chemical composition of the investigated kerogen. As we know, kerogen in investigated organic-rich sediments is composed of different types of organic constituents (mixture of different types of kerogen), which, in turn, have their specific

chemical and generation properties. Pyrolysis of powdered samples exhibits averaging results of HI and OI indices that complicate the identification of the type of kerogen and the interpretation of obtained values.

(4) Pyrolysis of resins and asphaltens might substantially lower the Tmax values (Schegg, 1993). Migrated oil is a likely explanation for immature source rocks with a high IP index. This problem increases with the investigation of coarse-grained or fractured organic lean rocks.

(5) Type of mineral groundmass and the contamination of samples by borehole lubricant may affect S_1, S_2 and Tmax values (Katz, 1983). The very low content of organic constituents (amorphous organic matter), as well as the presence of heavy hydrocarbons absorbed into the mineral matrix, where they are "cooked" during the heating, affect S2 and lead to overestimation of Tmax values (Espitalié, 1986a; Espitalié, 1986b; Peters, 1986). The retention will have two main effects: a decrease of S_1 and S_2 peaks and increase of Tmax of 5–6 °C for type II kerogen and 10–12 °C for type III (Schegg, 1993). However, in order to eliminate the effect of mineral matrix on pyrolysis results, Clementz (1979) offered to wash the mineral matrix with an organic solvent prior to pyrolysis.

(6) Concentrated organic matter (coals) does not respond to pyrolysis as dispersed organic matter samples do (Peters, 1986). For reasons not fully understood, some types of coal show type II/III kerogen, whereas, according to elemental analysis and microscopy, coals tend to be type III (Schegg, 1993).

(7) Low correlation between the results of organic geochemical analysis and of maceral analysis. Some workers have stated in their studies that there is a low correlation between geochemical and organic petrographic results (Powell *et al*., 1982). This discrepancy may relate to the resolution of both mentioned methods.

High-resolution organic petrography is a very detailed quantitative investigation of organic matter under microscopic level, based on the consistent counting of macerals on the given grid. In contrast, Rock-Eval provides average values on whole samples without evaluation of the generation potential quality of individual organic components. Hence, this method does not have such a high sensitivity compared to the high-resolution organic petrography technique.

3.4.2. Rock-Eval parameters as indicators of organic matter maturity

3.4.2.1. General remarks and definition

As was mentioned before, parameters obtained from Rock-Eval pyrolysis are closely linked with increasing temperature. This evidence enables the use of these parameters and ratios as maturation indicators. Pyrolysis parameters indicating different maturity levels of source rocks are presented in Table 3-2.

Table 3-2: Different Rock-Eval parameters indicating various maturation levels (Peters and Cassa, 1994).

Rock-Eval parameter	Maturity (products)		
	Immature	Mature	Post-mature
Tmax °C	<435	435-465	>465
S1/S2	<2.0	2.0-6.0	>6.0
S2/S3	>5.0	5.0-2.5	2.5-0.0
Production Index	<1.0	0.1-0.4	>0.5

It is well-known that Tmax is widely used to determine the maturity level because this parameter increases linearly with the maturation degree of the organic matter (Barker, 1974; Espitalié *et al*., 1977). In addition, it is dependent on the cracking kinetics of the different types of organic matter and, as a result, is in good agreement with HI and OI indices (Dellisanti *et al*., 2010). In other words, Tmax can show various values for the same maturity level for different types of organic matter (Type I, Type II, Type III). However, Type III kerogen, which corresponds to terrestrial organic matter, is the most reliable in estimating the maturation degree (Espitalié, 1986a; Espitalié, 1986b).

Teichmüller and Durand (1983), Espitalié *et al*. (1984) stated good relationships between Tmax and vitrinite reflectance values. Specifically, for kerogen Type III, the beginning of the oil window is characterised by Tmax in the range of 430–435 °C, whereas the values for the onset in the gas window correspond to a fixed value at VRr of 1.34 % and a Tmax of 465 °C (Espitalié, 1986a; Espitalié, 1986b).

As was mentioned before, parameters such as S_1, S_2 and S_3, more precisely, their ratios S_1/S_2 and S_2/S_3, can also be used in assessing the maturity level, because these parameters are closely linked to the type of organic matter and temperature changes (Table 3-2).

The Production Index is a measure of the relative proportion of S_1 and S_2 pyrolysis peaks ($S_1/(S_1+S_2)$) (Peters and Cassa, 1994). Low ratios show immature or extreme post-mature organic matter, whereas high ratios indicate either a mature level or contamination by migrated hydrocarbons or drilling additives (Table 3-2).

3.4.2.2. Limitation of the method

Unlike vitrinite reflectance, parameters obtained from Rock–Eval pyrolysis can provide information on thermal maturity of source rock older than Devonian or of those sediments where there are no appropriate migrabitumen particles for reflectance measurement. However, this method has a certain number of limitations and data interpretation problems.

Most of these difficulties encountered by workers due to this analysis have already been cited in the paragraph devoted to Rock-Eval pyrolysis. Nevertheless, it is important to note that this method is inferior to vitrinite reflectance in accuracy. Tmax is not very sensitive to variation in thermal maturity between 440 °C and 450 °C and hence estimates of VRr based on Tmax values are not recommended (Riediger, 1993). Moreover, values of parameters obtained from Rock-Eval pyrolysis vary, depending not only on the type of organic matter, but on its quantity as well.

CHAPTER 4. ORGANIC COMPOSITION AND ORGANO-MINERAL MICROFACIES VARIATIONS OF THE POSIDONIA SHALE FROM THE WEST NETHERLANDS BASIN, THE LOWER SAXONY BASIN AND THE SOUTH GERMAN BASIN

CONTENTS

4.1. Maceral and mineral composition of the Posidonia Shale

4.1.1. Lateral and vertical variations of organic matter in the Posidonia Shale

The proportion of previously identified organic components or macerals differs not only laterally from basin to basin, or from well to well, but also vertically within one well. Figs. 4-1 and 4-2 show variations of organic matter together with zooclasts. This relationship shows fairly different paleoenvironments allowing/preventing the existence of nekton and plankton. Using these diagrams, it is possible to define the assemblage of macerals indicating strong anoxic conditions, leading to the mass mortality of the fauna. Together with minerals, these assemblages form organo-mineral microfacies.

In the West Netherlands Basin, organo-mineral microfacies show a resemblance. However, there are some differences in maceral composition. Among the terrestrial organic matter, the association of sporinite-vitrinite-inertinite appears more often in well E than in well M. This association, together with the increasing content of zooclasts, according to Prauss (1996), indicates temporary oxygenation of the water column, resulting from storm (induced water masses' circulation) or water evaporation. Moreover, the vitrinite/inertinite ratio enables the reconstruction of more specific conditions. When the ratio is equal to 1 or more, this probably indicates those paleoenvironmental conditions in which surface water is oxygenated and bottom water is oxygen-depleted. Frequently, bituminite II is observed together with this terrestrial maceral assemblage. Evidently, oxygenation of the water column coincides with an algal-bloom event. In these paleoenvironments, not only the quantity, but also the diversity of the alginite increases. This event is clearly demonstrated in well A of the Lower Saxony Basin.

Liptodetrinite in the West Netherlands Basin appears in two different forms. It occurs in well M in a greater quantity than in well E. Moreover, the diversity among the lamalginite group is also higher in well M. The content of amorphous organic matter is greater in well E, among which bituminite I and bituminite V are predominant. In well M, amorphous organic matter is mostly represented by bituminite II, which is predominant in the microfacies of the upper part of the well section, whereas, in the lower part, bituminite II is replaced by bituminite I and bituminite V. This coincides with oxygen–exhausted paleoenvironments.

In the investigated Posidonia Shale, the specific association of organic microfacies and mineral matrix hosting it was not observed. However, bituminite V appeared to be formed more often in organic microfacies associated with marly limestone or limestone with a high content of dolomite crystals.

In the Lower Saxony Basin, bituminite II-enriched organo-mineral microfacies are well-represented in well A. In this well, and also in well D, not the quantity, but the diversity of algae is high. Particularly in well D, a higher diversity of lamalginite is observed than in well A, but a lower content of amorphous organic matter.

In the South German wells, variations in organo-mineral microfacies are higher than in the West Netherlands Basin and the Lower Saxony Basin. This indicates frequent changes in paleoenvironmental conditions. These organo-mineral microfacies from the Dotternhausen-1001 well, Notzingen-1017 well and Bisingen-1002 well are poorly correlated. The Posidonia Shale from southern Germany contains a higher quantity of bituminite III than from the other investigated sedimentary basins. It occurs after rapid changes in paleoenvironments from oxygenated to oxygen-depleted, leading to mass mortality of the nekton and zooplankton which had suffered from oxygen-exhausted conditions. In all these wells, a high content of bituminite I was observed, while bituminite II is suppressed and bituminite V was not observed at all.

In addition, the dynamic of the water is reflected in the quantity of the preserved organic matter in the investigated areas. The results of maceral analysis reveal that, in the wells from the West Netherlands Basin and the Lower Saxony Basin, the Posidonia Shale contains a high quantity of organic matter. In wells E and M, it reaches 43.5 vol.% and 40.4 vol.% respectively; in well A, Lias delta contains 1.6–7.8 vol.% organic matter, while Lias epsilon comprises 53.7 vol.%. Lias epsilon in well D reaches 43.7 vol.%.

In comparison, in southern Germany, the content of organic matter is lower. In Lias epsilon it ranges between 4.0 and 21.5 vol.%. It decreases in the low bituminous Lias zeta section to a low of 1.3 vol.%.

In the Notzingen-1017 well, the Lias delta section makes up a maximum of 6.5 vol.%. In Lias epsilon, the Posidonia Shale containing organic matter reaches 32.7 vol.%. In Lias zeta, organic matter content ranges from 5.6 to 13.8 vol.%.

In the Bisingen-1002 well, Lias delta organic matter ranges from 0.7 to 9.3 vol.%. In Lias epsilon, it reaches a high of 42.2 vol.%. However, in one sample it rapidly falls to a low

of 0.0 %. In Lias zeta, the amount of organic matter varies from 4.0 to 16.0 vol.%, while in Dogger alpha, the content of organic matter varies from 4.4 to 7.0 vol%.

The thickness of the Posidonia Shale section differs from one sedimentary basin to another. While the thickness of the Lias epsilon comprises 29.9 m in well E, 31.3 m in well M, 34.15 m in well A, that of the Lias epsilon in well D dropped to a low of 7 m. The thickness of the Lias epsilon in southern Germany is generally lower. The greatest thickness of the Lias epsilon succession is recorded in the Bisingen-1002 well, reaching 17.7 m. In the Dotternhausen-1001 well, it is decreased to 13.6 m and falls to 4.9 m in the Notzingen-1017 well (APPENDIX B).

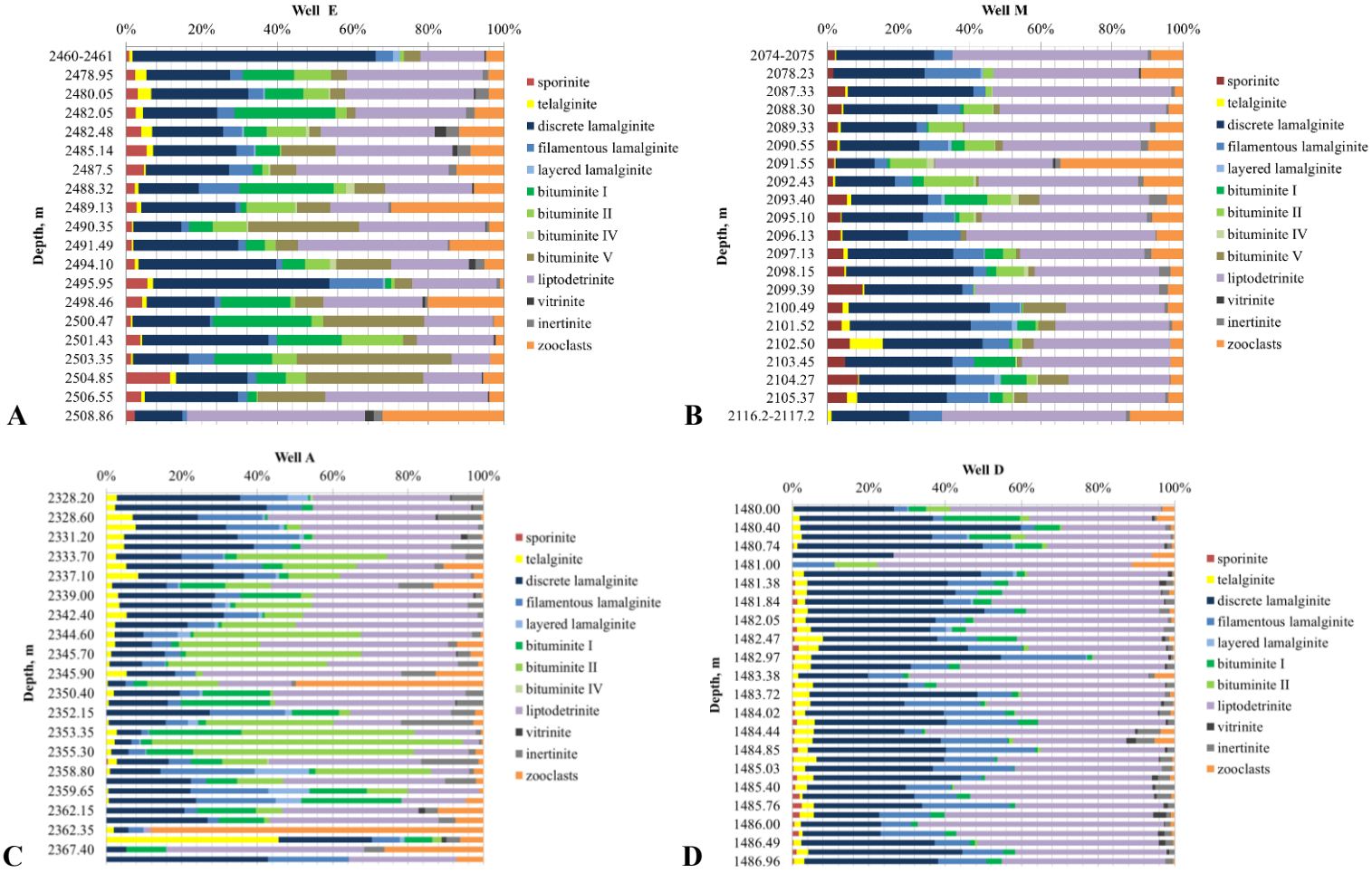

Fig. 4-1: Distribution of the different macerals and zooclasts in the wells from the West Netherlands Basin and the Lower Saxony Basin.
A), B), The West Netherlands Basin; C), D), The Lower Saxony Basin. Note that the sum of organic matter and zooclasts is 100 %. The macerals were grouped with zooclasts in order to show the oxygenation of the water column in the investigated sedimentary basins.

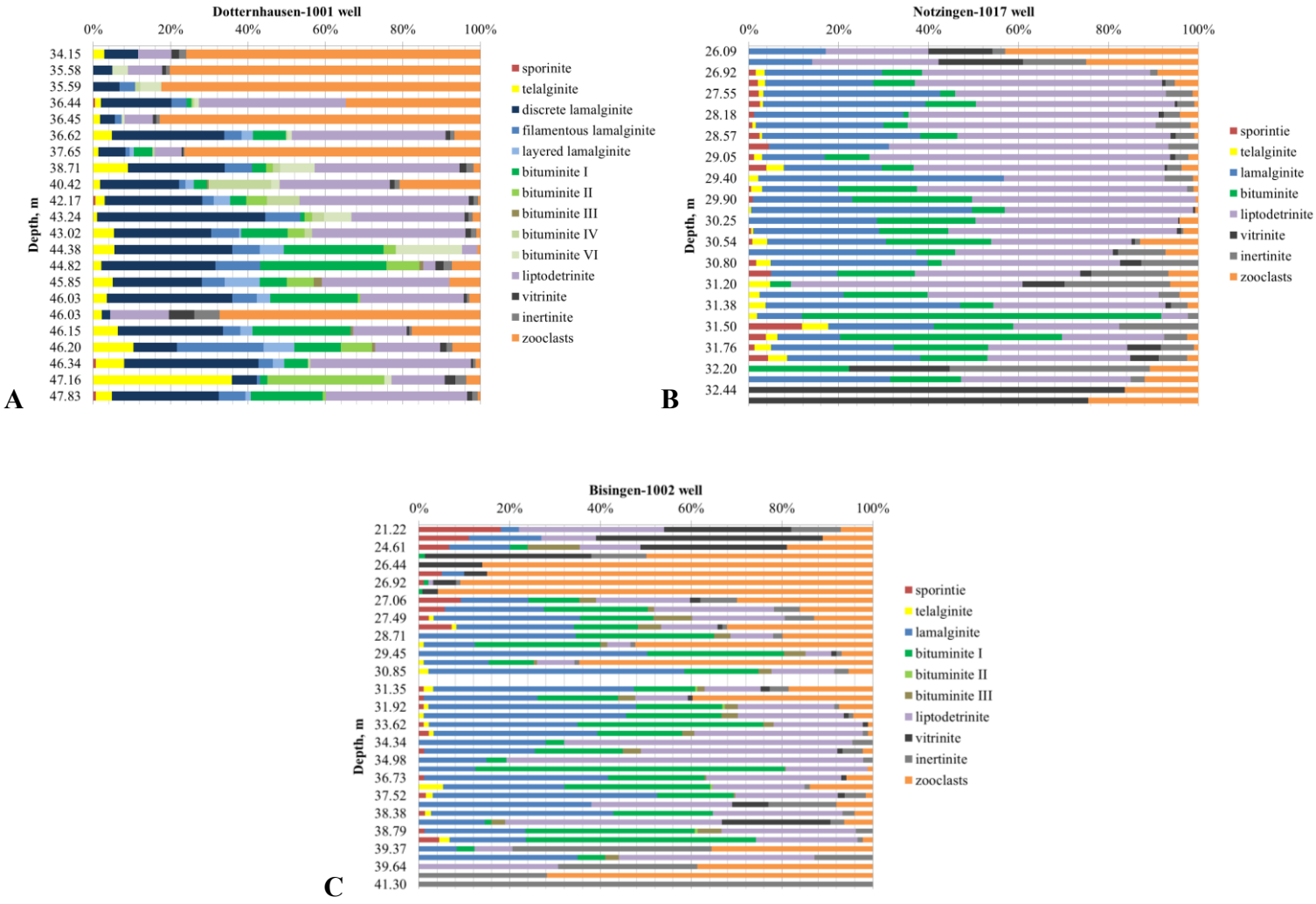

Fig. 4-2: Distribution of the different macerals and zooclasts in the South German wells.
Note that the sum of organic matter and zooclasts is 100 %. This association was taken to show oxygenation of the water column in the sedimentary basin.

4.1.2. Organic matter composition

4.1.2.1. Vitrinite group

A minute amount of vitrinite macerals occurs in all the investigated samples of the Posidonia Shale (APPENDIX A). Vitrinite appears as indigenous and oxidised vitrinite. In polished blocks from the West Netherlands Basin (well E and well M), the content of indigenous vitrinite does not exceed 0.1–0.3 vol.% (APPENDIX A). This vitrinite comprises small elongated (5–8 μm) homogeneous grey non-fluorescent particles. Oxidised vitrinite is more abundant and reaches 0.4 vol.%. It is identified by a light grey colour in reflected white light, absence of fluorescence, rounded shape and small size (4–10 μm). In addition, in well E in one sample (No 2498.46), trimaceral (vitrinite+sporinite+fusinite) recycled coal particles were observed. They reach the size of 500 to 600 μm.

The content of vitrinite macerals from the Lower Saxony Basin varies from well to well. In well D, the quantity of indigenous vitrinite reaches 0.4 vol.%. It is found as equidimensional angular and/or elongated thin forms, in size ranging from 4x4 to 90x12 μm. Moreover, fluorescent vitrinite was recorded. Such particles, which are impregnated with bituminous substances during diagenesis, can be classified as a jet. These particles do not exceed 20 μm in size. The content of recycled vitrinite reaches 0.7 vol.%. On the contrary, in well A, vitrinite particles are rare. Their quantity ranges from 0.1 to 0.2 vol.% for both types of vitrinite.

In southern Germany, vitrinite is more frequent than in the other investigated areas (Dotternhausen-1001, Bisingen- 1002, Notzingen-1017 wells). However, in the Dotternhausen-1001 well, it does not exceed 0.2 vol.%. This maceral was observed mostly in a rounded form of recycled vitrinite, rather than in the indigenous form. In the Bisingen-1002 well, vitrinite in Lias Ɛ was also poor represented. Indigenous vitrinite has an elongated size ranging from 10–250 μm and variable thickness of 5–50 μm. Oxidised vitrinite has a small size from 5 to 20 μm and no fluorescence. In the Notzingen-1017 well, the content of all vitrinites varies regarding the local biostratigraphic subdivisions. It increases in Lias delta (0.2–1.4 vol.%), falls in Lias epsilon (0.0–0.7 vol.%) and again increases in Lias zeta (1.4–3.4 vol.%).

4.1.2.2. Liptinite group

4.1.2.2.1. Alginite: telalginite and lamalginite

Telalginite

In the studied samples, alginite is represented by telalginite and lamalginite (Fig. 4-1A). Telalginite is observed in all samples, but in different concentrations. Contrary to Posidonia Shale from the Netherlands, in the Lower Saxony Basin, particularly, in well D it reveals a high diversity. Telalginite occurs in the form of thick-walled algae (*Tasmanites, Pterosphaeridia*) and thin-walled algae (*Leiosphaeridia, Campenia and/or Lancettopsis;* see Mädler, 1963) (Fig. 4-1A, for more examples see Chapter 3). *Botryococcus*-derived telalginite was encountered mostly in well D.

The content of telalginite in well D as well as in wells E and M does not exceed 1.9 vol.%, whereas that in well A can reach 3.7 vol.% in Lias Delta, while in Lias epsilon, the content of telalginite does not exceed 1.6 vol.%. The size of these algae varies from 10 μm to 80 μm for thick-walled algae and may reach 300 μm for some thin-walled species (APPENDIX A).

The diversity of the telalginite in southern Germany is lower than in northern Germany. In the Dotternhausen-1001 well, telalginite occurs in the form of *Leiosphaeridia* (100-130 μm), which has thin cell walls (1-2 μm), and *Tasmanites* (120-130μm, with cell walls of 2-3 μm). Telalginite is well preserved in some samples and in some of them is partly degraded. It has a dark-brown colour in reflected light and yellow in fluorescence mode with high intensity. The Posidonia Shale from the Dotternhausen-1001 well contains telalginite reaching 3.9 vol.% (APPENDIX A). In the Bisingen-1002 well, telalginite is comprised of *Tasmanales* and *Botryococcus*. *Botryococcus*-derived telalginite is identified in most of the samples of the *spinatum* zone and the *tenuicostatum* zone. Its content dips in the *falciferum* zone and increases again from the middle part of the *bifrons* zone into the Dogger alpha (Prauss *et al*., 1991). Telalginite exhibits a brown colour with reddish-brown internal reflections and green to yellow fluorescence of high intensity (Prauss *et al.,* 1991). In the Notzingen-1017 well, telalginite maceral was not observed in some samples. In Lias delta, telalginite was not encountered, whereas in Lias epsilon, the percentage of this maceral reaches 1.2 vol.%. In Lias zeta, telalginite content drops to a low of 0.0 vol.%.

Lamalginite

The percentage of lamalginite varies from well to well. This maceral mainly consists of discrete and filamentous lamalginite in all the investigated wells, but layered lamalginite was also encountered in the samples from the Lower Saxony Basin. Discrete and filamentous lamalginite could be related to *Nostocopsi*s algae (4–10 μm in size) and *Halosphaeropsis* algae (20–35 μm in size) respectively (Mädler, 1963). Furthermore, Prauss *et al*. (1991) pointed out the existence of a good correlation between the distribution of lamalginite and spheroidal palynomorphs. In the investigated bituminous shaless, acritarchs were observed in a minute quantity in some samples of well E (the West Netherlands Basin), well D (the Lower Saxony Basin) and the Dotternhausen-1001 well (the South German Basin).

The amount of discrete lamalginite is higher in well E, ranging between 1.1 and 11.1 vol.% in Lias epsilon and reaching 22.4 vol.% in Lias zeta, wells M (4.5–14.8 vol.% in Lias epsilon) and D (0.0–19.4 vol.% in Lias epsilon). However, in well A, it comprises a maximum of 10.3 vol.%. It frequently appears enclosed in the mineral-bituminous groundmass. Percentages of filamentous lamalginite are low (0.1–2.8 vol.%) in wells E, M and A, but high (up to 11.3 vol.%) in well D. The quantity of layered lamalginite is relatively low (0.1–0.6 vol.%) in the samples of wells E, M and D, whereas it reaches 12.6 vol.% in well A. Layered lamalginite appears as lamellar alginite with a length of 100 μm and variable diameter (around 4μm). Lamalginite exhibits a yellow fluorescence of moderate intensity.

In the Dotternhausen-1001 well, lamalginite occurs as thin filaments with no or little recognisable structure in the polished sections, which exhibit a high fluorescence. Discrete lamalginite is more common, compared to the less frequent filamentous lamalginite. The content of both these types reaches 7.8 vol.% and 2.8 vol.% respectively. The content of layered lamalginite is low and reaches only 1.0 vol.%. In the Bisingen-1002 well, the percentages of lamalginite increase gradually in the *tenuicostatum* zone (Lias delta–Lias epsilon), reaching 3.3 vol.%, and reach a high of 12.2 vol.% in the *falciferum* and *bifrons* zones (Lias epsilon). Lamalginite appears as lamellar alginite, ranging in size from a few μm to about 100 μm. In some samples, it occurs as coatings on mineral grains or enclosed in the mineral matrix (Prauss *et al*., 1991). Lamalginite shows a moderately intense to intense green to yellow fluorescence.

According to Prauss *et al.* (1991), who carried out palynological investigations on samples from the Bisingen-1002 well, the acritarch assemblage is represented by only two genera *Micrhystridium* and *Veryhachium*. Their percentage does not exceed 7.0 vol.%. They

are commonly distributed outside the more bituminous intervals (Prauss *et al.,* 1991), but unlike dinocysts, the latter were found in the strongly bituminous lowermost interval of the *falciferum* zone. In addition, a minute quantity of dinocysts is present in the Bisingen-1002 well at the top of the *bifrons* zone and at the top of the *tenuicostatum* zone. However, it is not found within the highly bituminous *falciferum* zone (middle part of the Posidonia Shale section).

In the Notzingen-1017 well, in Lias delta, lamalginite was counted only in one sample and its content does not exceed 2.3 vol.%. In Lias epsilon, it was observed in almost all samples. Its content ranges from 0.0 to 12.8 vol.%. In Lias zeta, lamalginite reaches 4.1 vol.%.

4.1.2.2.2. Liptodetrinite

Liptodetrinite occurs in variable concentrations (0.4–28.7 vol.%) scattered in the mineral-bituminous groundmass and in association with bituminite I. However, the content of this maceral can be overestimated due to the difficulty of distinguishing liptodetrinite from discrete lamalginite. Liptodetrinite in wells E and A reaches 15.2 vol.% and 14.1 vol.% respectively, whereas that in wells M and D increases and comprises 18.8 vol.% and 28.8 vol.% respectively. Liptodetrinite consists of two forms. The first form is of a minute size, whereas the other occurs as rounded bodies with a diameter of 4 μm size. The latter are possibly related to *Nostocopsis* algae (Mädler, 1963). Both types show a yellow colour in fluorescence mode of high intensity (Fig. 3-4D).

The content of liptodetrinite in the Dotternhausen-1001 well ranges between 0.3 and 10.7 vol.% in Lias epsilon and between 0.0 and 9.6 vol.% in Lias zeta. On the contrary, in the Notzingen-1017 well, the percentage of liptodetrinite is higher. In Lias delta, it ranges from 0.0 to 2.8 vol.% and reaches 17.0 vol.% in Lias epsilon. In Lias zeta, the content of liptodetrinite varies from 2.1 to 5.5 vol.%. In the Bissingen-1002 well, liptodetrinite is found mainly in the Lias epsilon and the Dogger alpha. In a bituminous bed close to the "Steinplatte", it reaches a high of 30.3 vol.%. However, it gradually decreases in the upper part of the *falciferum* zone and in the *bifrons* zone.

4.1.2.2.3. Bituminites

Bituminite comprises bituminite I, bituminite II, bituminite III, bituminite IV, bituminite V and bituminite VI (Fig.4-3B, E, F; for more examples see Chapter 3 and Gorbanenko and Ligouis, 2014). All these types were identified in all the studied samples, except bituminite V, which was not observed in well D.

Bituminite I

Bituminite I (up to 10.6 vol.% in wells E and A, but decreases to 1.0–3.0 vol.% in the other wells) shows the optical properties described by Teichmüller and Ottenjann (1977). Nevertheless, in wells E and M, it was observed with inclusions of sporinite and without fluorescence, with inclusions of short lamalginite and telalginite (Fig. 4-3A-C). In the Dotternhausen-1001 well, the content of bituminite I reaches 4.0 vol.%, while in the Bisingen-1002 well it reaches a high of 28.5 vol.%.

Bituminite II

The lowest content of bituminite II was recorded in well D (0.0–0.4 vol.%). It increases in well E (max. 5.3 vol.%) and well M (max. 5.3 vol.%) and reaches 59.0 vol.% in well A. In the Dotternhasuen-1001 well, bituminite II does not exceed 3.3 vol.%, while in Bisingen-1002 its quantity ranges from 0.0 to 0.1 vol.%.

Bituminite III

Bituminite III was only counted in the Dotternhausen-1001 and Bisingen-1002 wells in the South German Basin. Nevertheless, its content does not exceed 0.2 vol.%.

Bituminite IV

The quantity of bituminite IV is low in all the investigated wells in the West Netherlands Basin and the Lower Saxony Basin. Its content does not exceed 0.5 vol.%. On the contrary, in the Dotternhausen-1001 well, bituminite IV may reach 3.8 vol.% (APPENDIX A).

Bituminite V

The percentage of bituminite V is low in wells A, D, M and in the wells of the South German Basin, while in well E it reaches 13.2 vol.%.

Bituminite VI

Bituminite VI is well represented only in well A, reaching 18.9 vol.%. However, in well D, its content can reach 1.2 vol.%.

In the Notzingen-1017 well, the content of all bituminites is low. It reaches 1.1 vol.% in Lias delta. In Lias epsilon, the percentage ranges from 0.0 to 26.1 vol.%.

In addition, the relationships between different types of bituminites and alginite macerals were encountered due to maceral analysis. In samples enriched in telalginite, the content of the bituminites is low. Simultaneously, the Posidonia Shale enriched in bituminites contains a low quantity of alginite, as shown in Fig.4-3 C, D.

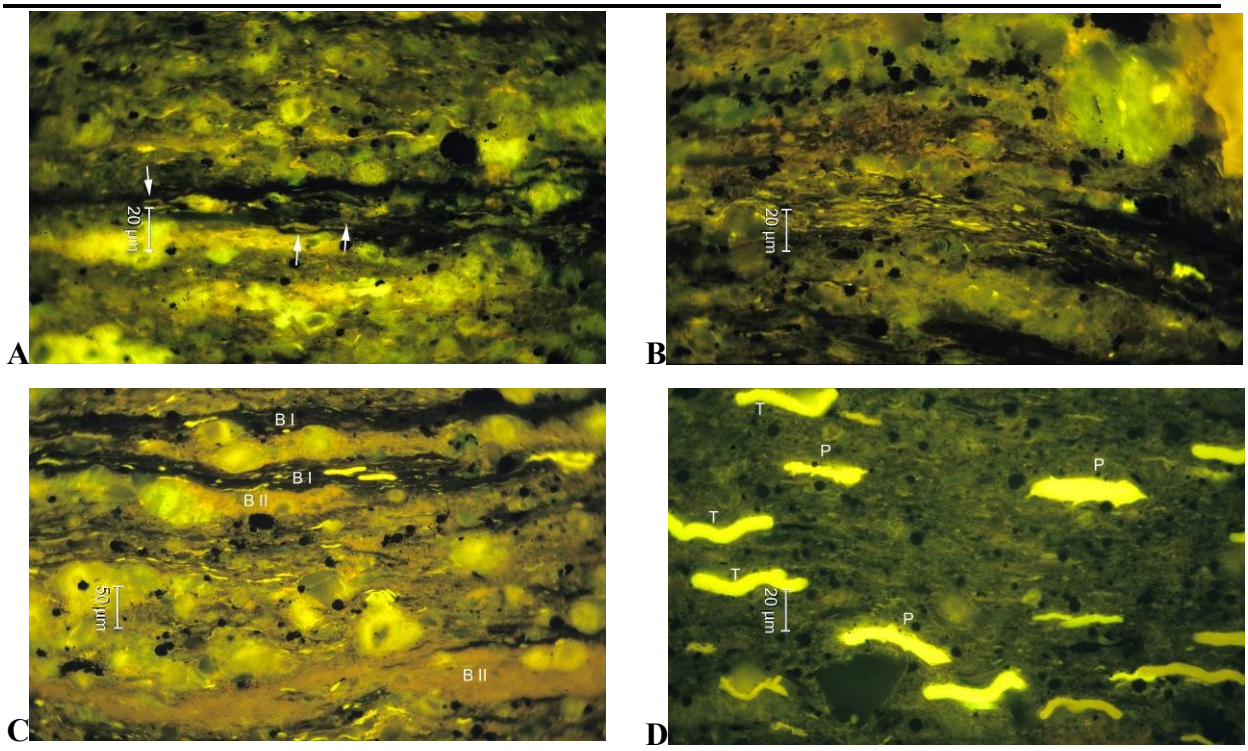

Fig. 4-3: Photomicrographs illustrating different macerals of the liptinite group.
A), Bituminite I with sporinite inclusions; B), Bituminite I with telalginite, liptodetrinite, lamalginite and sporinite inclusions; C), Telalginite-dominated samples: mostly *Tasmanite*- (T) and *Pterosphaeridia*-derived algae (P); D), Bituminite-dominated samples: bituminite I (B I) and bituminite II (B II). Fluorescence mode, oil immersion.

4.1.2.2.4. Sporinite

Macerals of the liptinite group are predominant in almost all the investigated samples. Their content varies according to the organo-mineral microfacies from 6.0 to 46.7 vol.% and with a maximum of 71.0 vol.% in well A. Macerals of this group are represented by sporinite, alginite, liptodetrinite, different types of bituminites. Oil droplets were counted in addition in the liptinite group. In wells E and M, sporinite is well-represented (0.3–4.5 vol.%) and appears in two different types (APPENDIX A). One has a smooth outline, whereas the other shows ornamentations (Fig. 3-7 A). Both types are of a size not exceeding 30 µm. Sporinite was seldom found in sporangia of variable size exceeding 200 µm. Sporinite is well-recognised by its orange fluorescence of moderate intensity. In addition, Posidonia Shale from the Netherlands contains cutinite, which was identified by its typical morphology (Fig. 3-7 B). The optical properties of this maceral are similar to those of sporinite.

In the Lower Saxony Basin, sporinite was only found in well D. Its content does not exceed 0.5 vol.% and decreases at the top of the Lias epsilon (Fig. 4-4).

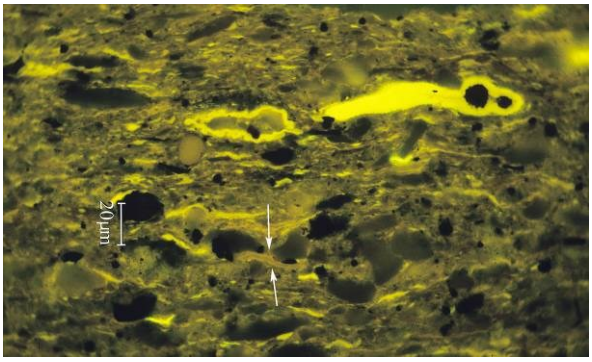

Fig. 4-4: Photomicrograph showing sporinite (white arrows) in well D. Fluorescence mode, oil immersion.

The Posidonia Shale from the Dotternhausen-1001 well contains 0.1 vol.% sporinite. It is characterised by a dark brown colour in reflected white light and shows a brown colour in fluorescence mode of weak intensity. In the Bisingen-1002 well, sporinite is rust-brown in reflected white light. It shows yellow, orange-brown and brown fluorescent colours of weak intensity. In this well, sporinite mainly occurs in the non-bituminous claystones of the Dogger alpha, reaching 1.3 vol.% (Prauss *et al.,* 1991). In the Notzingen-1017 well, sporinite is more frequent than in the Dotternhausen-1001 well. While sporinite has not been observed in samples from Lias delta, in Lias epsilon, it was encountered in most of the investigated samples, ranging between 0.0 and 0.8 vol.%. In Lias zeta, the quantity of this maceral dips to a low of 0.0 vol.%.

4.1.2.2.5. Migrabitumen and oil droplets

Migrabitumens in all the investigated samples occur as minor constituents mainly in Lias epsilon in a few samples in well A, Dotternhausen-1001 well, Notzingen-1017 well and Bisingen-1002 well. However, it is more frequent in post-mature well B (for more details see Chapter 5). Migrabitumen in mature bituminous shaless shows a dark grey colour in reflected white light and dark brown fluorescence.

Oil droplets, indicating an initial phase of oil generation, occur as inclusions in telalginite bodies and calcareous grains. They were identified by a green-yellow fluorescence of high intensity. The content of oil droplets is higher in northern Germany and the Netherlands than in southern Germany.

4.1.2.3. Inertinite group

In all the studied wells, the content of inertinite macerals (inclusive of secondary maceral micrinite) ranges between 0.1 and 5.6 vol.%. Macerals of the inertinite group are represented in almost all investigated samples (APPENDIX A) and comprise fusinite, semifusinite, secretinite, inertodetrinite and the secondary maceral–micrinite, which is a dehydrated residue from oil and gas generation (Teichmüller and Ottenjann, 1977).

In the Dotternhausen-1001 well, macerals of the inertinite group occur primarily as fusinite and semifusinite, which are very rare in the Posidonia Shale, reaching only 0.1 vol.% and 0.3 vol.% respectively. The more widespread maceral is inertodetrinite (0.3 vol.%). The secondary maceral-micrinite reaches a maximum of 0.7 vol.%. All inertinite macerals are characterised by a homogeneous structure, light grey colour in reflected light and no fluorescence. In the Bisingen-1002 well, the inertinite is represented by inertodetrinite and less by fusinite. Its content is higher in the *spinatum z*one, but lower in the *tenuicostatum* zone. It dips in the *falciferum* and *bifron*s zones as well as in the Lias zeta and lower Dogger (Prauss *et al*., 1991). In the Notzingen-1017 well, in Lias delta the percentage of the inertinite group reaches 1.6 vol.%, in Lias epsilon it ranges from 0.0 to 1.9 vol.%. In Lias zeta, the content of macerals in the inertinite group decreases to a low of 1.0 vol.%. Among all the investigated wells, the increasing content of macerals of the vitrinite and inertinite groups correlates well with a rising percentage of faunal remains, indicating, probably, dry climatic conditions.

Among all the investigated mature Posidonia Shale samples, micrinite content is highest in well A and makes up a maximum of 4.6 vol.%. Moreover, relationships between micrinite and oil droplets show a positive trend in that well. In wells M and D, percentages of this material diminish to 0.0–0.4 vol.% and 0.0–0.9 vol.% respectively (APPENDIX A). The reflectance of these macerals is high and their morphologies are distinctive (see Taylor *et al.,* 1998).

4.1.2.4. Summary

4.1.2.4.1. Macerals of vitrinite group

The Posidonia Shale contains a low percentage of macerals of the vitrinite group in the West Netherlands Basin and the Lower Saxony Basin. In the South German Basin, the vitrinite content varies from well to well. While in the Dotternhausen-1001 well, the amount of macerals of the vitrinite group is low, reaching only 0.1 vol.%, in the Notzingen-1017 well,

it increases to 5.1 vol.% in Lias delta, makes up 0.7 vol.% in Lias epsilon and 3.0 vol.% in Lias Zeta. In the Bisingen-1002 well, macerals of the vitrinite group were not observed in Lias delta. In Lias epsilon, the vitrinite content increased marginally to 1.8 vol.% and reached 2.0 vol.% in Dogger alpha.

4.1.2.4.2. Macerals of liptinite group

Each investigated sedimentary basin is characterised by a specific assemblage of macerals of the liptinite group. Among all the investigated wells, the sporinite content is higher in wells E and M, reaching 4.5 and 3.0 vol.% respectively. The content of telalginite does not vary significantly. However, its diversity increases in wells A and D. The quantity of liptodetrinite varies, depending on the paleoenvironmental conditions. It reaches a high when the dynamic of the water column masses increases.

The Posidonia Shale from the West Netherlands Basin, the Lower Saxony Basin and the South German Basin is characterised by the occurrence of specific types of bituminite. In the West Netherlands Basin, the Posidonia Shale contains high quantities of bituminite V reaching 13.2 and 4.4 vol.% in wells E and M respectively. Investigated samples from well A contain the greatest quantity of bituminite II making up 59.0 vol.%. Well D is characterised by a relatively low content of bituminites.

Bituminous shales from the South German Basin contain bituminite III which is a particularity of this sedimentary basin. However, its content does not exceed 1.0 vol.%

4.1.2.4.3. Macerals of inertinite group

Primary macerals of the inertinite groups are rare in Posidonia Shale from the West Netherlands and the Lower Saxony Basin. In wells E, M and D, fusinite is the most frequent inertinite maceral. In those wells, it does not exceed 1.0 vol.%. In well A, the content of inertodetrinite is slightly higher than that of fusinite and it reaches 1.4 vol.%.

Among the wells from the South German Basin, the Dotternhausen-1001 well has the lowest content of primary macerals of the inertinite group, which does not exceed 1.0 vol.%. In the Bisingen-1002 well, Posidonia Shale of the Lias delta contains the highest amount of inertinite macerals, reaching 1.9 vol.%. In the Lias epsilon, its content decreases to 1.4 vol.% and reaches only 0.8 vol.% in Dogger alpha. In the Notzingen-1017 well, the quantity of primary macerals of the inertinite group is highest in Lias epsilon, reaching 2.0 vol.%.

In wells M, D and the wells from the South German Basin, the content of secondary maceral micrinite does not exceed 1.0 vol.%. However, in wells E and A, it increases to 2.2 and 4.6 vol.% respectively.

4.1.3. Features of the Posidonia Shale lithology

4.1.3.1. Mineral groundmass

Generally, the mineral groundmass of wells E and M has a lower bituminous character compared to that of wells A and D. This is due to a higher amount of bituminous substances scattered in the mineral groundmass of the wells in the Lower Saxony Basin (APPENDIX A).

The mineral groundmass of non- or low-bituminous and bituminous samples is represented by clayey-calcareous and calcareous-clayey groundmasses. The calcareous groundmass of non-bituminous samples exhibits a light beige colour in reflected white light and has green diffuse fluorescence of weak intensity. The clayey groundmass of non-bituminous microfacies reveals a grey colour in reflected white light and a pale green fluorescence. The calcareous and clayey groundmasses of bituminous shales show a brown to dark brown colour in reflected white light and have a yellow-brown to brown fluorescence of moderate intensity.

4.1.3.1.1. The West Netherlands Basin

In the West Netherlands Basin in well E, Posidonia Shale contains a maximum of 44.6 vol.% of calcareous bituminous groundmass, but the clayey bituminous fraction reaches a maximum of 39.3 vol.%. One sample comprises 78.1 vol.% of non-bituminous groundmass. On the contrary, in well M, the content of carbonate increases up to a maximum of 57.7 vol.%, while clayey bituminous is only 11.0 vol.%. Low bituminous groundmass may contain 67.7 vol.% of calcareous fraction, but in non-bituminous samples it reaches 79.9 vol.%.

4.1.3.1.2. The Lower Saxony Basin

In the Lower Saxony Basin in well A, the content of bituminous groundmass increases among all wells up to a high of 68.8 vol.%, but the clayey bituminous fraction reaches 35.4 vol.%. In non-bituminous samples, the content of calcareous fraction increases to a high of 75.2 vol.%. In well D, the percentage of calcareous bituminous groundmass slightly decreases to a value of 51.8 vol.%, however, the content of bituminous clay increases up to a

high of 39.0 vol.%. The non-bituminous calcareous fraction can reach a maximum of 91.3 vol.%.

4.1.3.1.3. The South German Basin

In the Dotternhausen-1001 well, the non-bituminous groundmass has no lamination and consists of mostly crystallised calcareous mineral matter, showing a beige to light brown colour in reflected white light and with green fluorescence of weak or moderate intensity (APPENDIX A).

Bituminous groundmass has a brown-grey colour in reflected white light with moderate to intense brown fluorescence.

Clayey groundmass (bituminous and non-bituminous) is found as thin laminae and occurs in alternation with calcareous groundmass. Clayey bituminous groundmass has a brown to dark brown colour in reflected white light and dark brown fluorescence of weak intensity. It can reach a maximum of 65.7 vol.%. Non-bituminous clayey groundmass has a grey colour in reflected light and green fluorescence. It reaches 32.9 vol.%.

In bioturbated bituminous beds in the Dotternhausen-1001 well, and also in the Bisingen-1002 well, mineral matrices have different optical properties within and outside the burrows (Prauss *et al*., 1991). The mineral matrix outside the burrow is similar to that of the other part of the bituminous shales, while that within the burrow shows a striking resemblance to non-bituminous groundmass. These differences are caused by biochemical oxidation catalysed by burrowing organisms (Prauss *et al.,* 1991).

The total percentage of mineral groundmass in the Notzingen-1017 well varies from 93.4–96.7 vol.% in Lias delta, 67.1 to 96.5 vol.% in Lias epsilon and from 86.1 and 94.3 vol.% in Lias zeta. In the Bisingen-1002 well, clayey groundmass is predominant in Lias delta, reaching 91.7 vol.%. In Lias epsilon, the proportion of clayey and calcareous fraction varies, indicating unstable paleoenvironments. In Lias zeta in almost all samples, the content of calcareous groundmass increases to a high of 97.3 vol.%, while later in Dogger alpha, the content of clayey groundmass reaches a high of 96.7 vol.% (APPENDIX A).

In the mineral groundmass of bituminous, non-bituminous, low-bituminous shales, scattered faunal zooclasts, faecal pellets, coccoliths, detrital minerals (quartz and micas), and syngenetic as well as epigenetic pyrite (framboids and isolated microcrystals) were recorded. Their content varies regarding the organo-mineral microfacies. Each of these components,

which have been incorporated in the sediment, might act as an indicator for specific depositional events (Taylor *et al.,* 1998).

4.1.3.2. Minerals

4.1.3.2.1. Detrital minerals

The predominant detrital constituents of the Posidonia Shale are quartz and micas, which could provide information on the distance between the investigated areas and the landmasses (Fig. 4-5 A, B). It is particularly important to pay attention to the size of the grains and their morphology (Dias *et al*., 1984). These minerals can be transported from the land by wind or by water prior to their incorporation in the sediments (Taylor *et al*., 1998). For instance, the size of the mica flakes are the hydraulic equivalent of clay-sized material (Dias *et al.,* 1984). The rate of mica settling takes place more slowly than that of quartz grain. Therefore it might be transported for a longer distance.

In the investigated samples, the quantity and size of detrital minerals increase in the West Netherlands Basin compared to the Lower Saxony Basin. However, the content of quartz in well D can reach 8.1 vol.% (APPENDIX A).

In well E, the Posidonia Shale contains a maximum of 2.8 vol.% of quartz, but in well M it reaches only 1.6 vol.%. The content of the mica flakes in wells A and D is 0.1 vol.% and 0.4 vol.% respectively. In wells E and M it is 0.7 vol.% and 1.6 vol.% respectively. The broken outline of the mica flakes and their smaller size in well M than in well E indicate transportation over a longer distance.

In the Dotternhausen-1001 well, Posidonia Shale contains a higher quantity of quartz than of mica. The content of quartz reaches 5.8 vol.%, while the percentage of mica does not exceed 0.8 vol.%.

Dolomite

Dolomite deposits occur in restricted environments where evaporation has produced saline brines, for instance, in lagoons where water circulation is restricted or in the pore waters of deposits on broad mud flats (Williams *et al*., 1982). Posidonia Shale from the West Netherlands Basin contains the highest percentage of dolomite crystals among all the investigated wells. Its content reaches a significant 55.5 vol.% in well E and 22.3 vol.% in well M. This indicates specific paleoenvironments which favour the occurrence of bituminites (APPENDIX A).

In the Lower Saxony Basin in well A, dolomite generally occurs in microfacies where calcareous groundmass is predominant and can make up a maximum of 9.4 vol.%. It is easily recognisable in fluorescent light, where dolomite has a milky colour with a characteristic zonated appearance (Fig. 4-5 B). In well D, dolomite crystals are rare. The amount of dolomite reaches only 0.2 vol.%. In fluorescent mode, dolomite crystals have a greenish-yellow colour with a characteristic zonation.

In southern Germany, dolomite crystals have only been counted in the Dotternhausen-1001 well. Its occurrence is limited to specific samples and reaches 7.9 vol.%.

Gypsum

Gypsum is of a strictly chemical origin. It is formed as a result of evaporation (Williams, 1982). Gypsum was only encountered in the wells of the Lower Saxony Basin (APPENDIX A). In well A, gypsum can reach about 2.9 vol.% and has a round form. In reflected white light, it has a beige colour and a milky colour in fluorescence mode. However, in well D it is relatively abundant in the investigated samples. It occurs as a filling of the cavities and cracks in the mineral groundmass and has a secondary origin. The content of secondary gypsum reaches 6.8 %. In reflected white light, it has a whitish colour and a milky-white colour in fluorescence mode (Fig. 4-5 C, D, E).

Glauconite

Glauconite is a hydrous potassium aluminium silicate containing both ferrous and ferric iron and some magnesium. It is a typical sedimentary mineral, formed by marine authigenesis (Williams *et al*., 1982). In reflected light, glauconite is found as green sand-size pellets which have a green fluorescence of moderate intensity. This mineral was only observed in well D and the Dotternhausen-1001 well (Fig. 4-6 A, B).

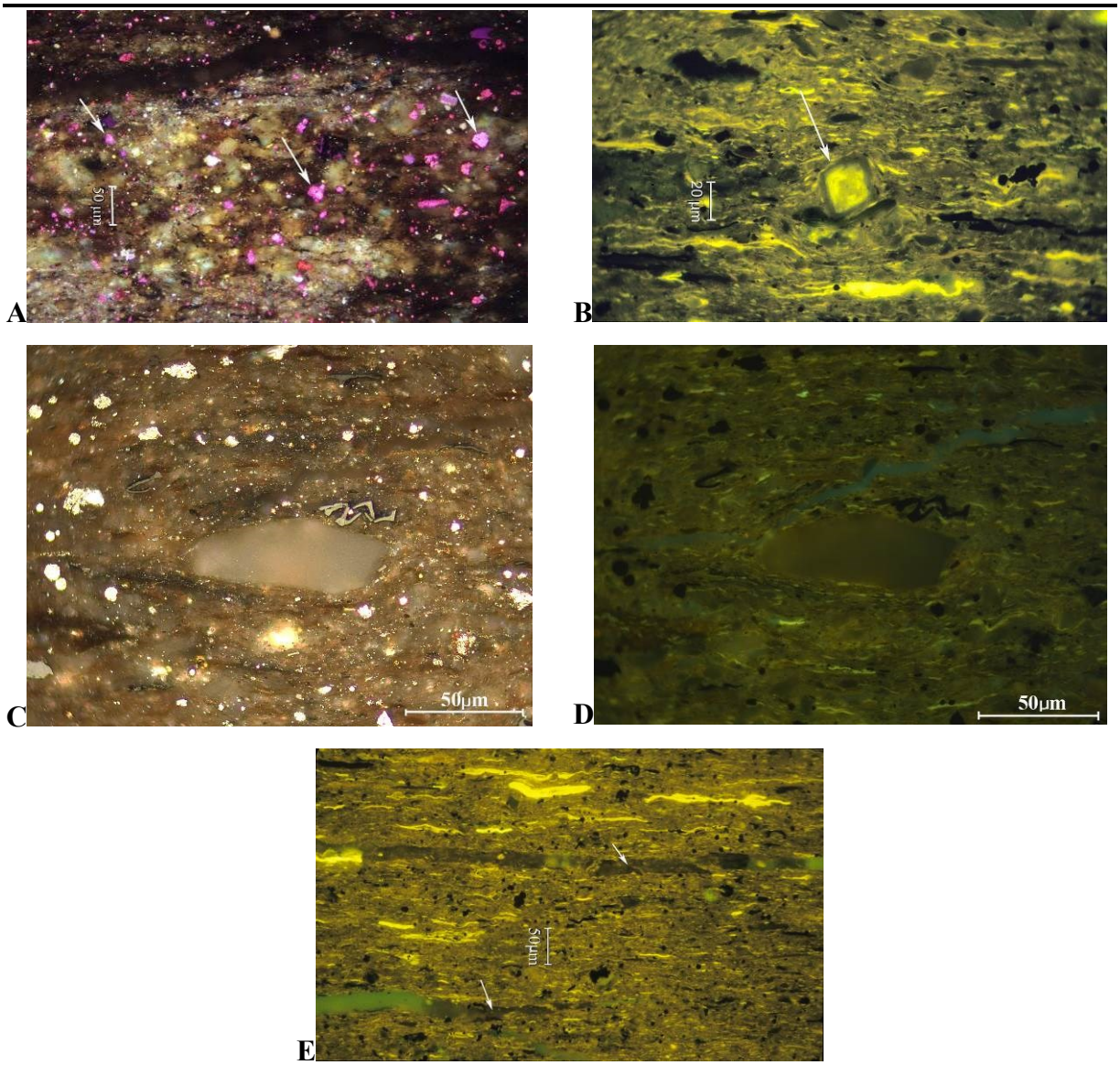

Fig. 4-5: Photomicrographs showing examples of quartz, dolomite grains, gypsum (in the center) and glauconite (Gl) grains in the Posidonia Shale.
A), A medium to coarse-grained carbonate-clay lens rich in quartz (white arrows show examples of quartz). Reflected white light, cross polars, lambda plate, oil immersion; B), Dark green to black micas (top) and deformed by a crystal of dolomite (white arrow). Fluorescence mode, oil immersion. C), Gypsum grain showing milky colour in reflected white light, oil immersion; D), Same view in fluorescence mode, oil immersion; E), Secondary gypsum filling the cavities (white arrows). Fluorescence mode, oil immersion

Pyrite

Pyrite generally forms in sedimentary deposits in relatively stagnant oxygen-depleted water, where the bacterial decay of organic matter prevails (Williams *et al.,* 1982). It is common in organic-rich bituminous limestone and bituminous shales. It occurs as single crystals, with their agglomeration into spheroidal masses — framboids or epigenetic recrystallised forms (Fig. 4-6 C, D). Sometimes, in some investigated samples, pyrite replaces skeletal parts of faunal remains (Fig. 4-6 D). All types of pyrites have the same optical

properties such as a bright yellowish colour in reflected light and dark red colour in fluorescence mode intensity.

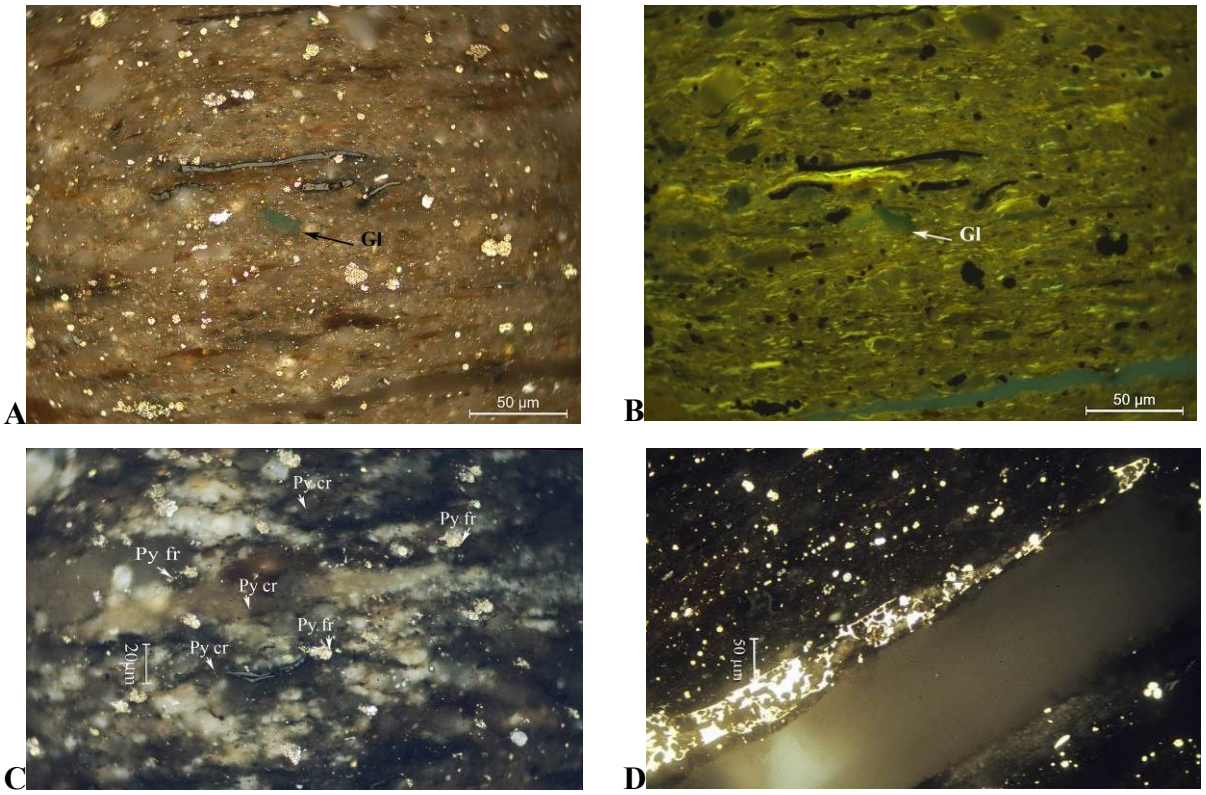

Fig. 4-6: Photomicrographs showing a glauconite grain and different forms of pyrite in the Posidonia Shale. A), Showing the green glauconite grain in reflected white light, oil immersion; B), Same view in fluorescence mode, oil immersion; C), Examples of pyrite crystals (Py cr) and framboidal pyrite (Py fr). Reflected white light,oil immersion. D), Faunal remain partly replaced by epigenetic pyrite. Reflected white light, oil immersion.

In the West Netherlands Basin, the content of framboidal pyrite reaches 11.0 vol.% in well E. In well M, it is marginally decreased and does not exceed 9.9 vol.%. In the Lower Saxony Basin, the content of framboidal pyrite is highest among all the investigated wells. Its content climbs to 16.5 vol.%, but in well D it decreases and ranges between 0.0 and 1.9 vol.%.

In the Dotternhausen-1001 well, the percentage of framboidal pyrite reaches 7.8 vol.%. In the Notzingen-1017 well, the total amount of pyrite ranges from 1.4 to 6.8 vol.%. However, in one sample, it reaches a high of 15.9 vol.%. In the Bisingen-1002 well, the content of pyrite does not exceed 11.0 vol.%.

4.1.3.2.2. Radioactive minerals

Radioactive minerals occur in variable amounts in bituminous shales (Swanson, 1961; Wolf, 1966). In the investigated Posidonia Shale, a few radioactive minerals were encountered in wells E (West Netherlands Basin) and in wells B and D (the Lower Saxony Basin). They have a mid-grey colour in reflected white light and are surrounded by a diffuse

lighting ring (Fig.4-7). This halo, which is caused by radiation damage, is particularly visible in fluorescence mode (Fig. 4-7 B). In fluorescent mode, the colour and intensity of the organic matter are typically altered.

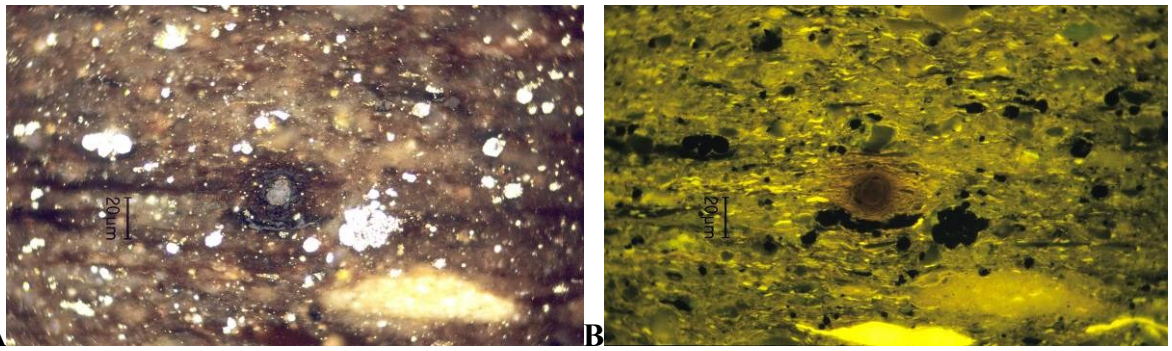

Fig. 4-7: Photomicrographs of a radioactive mineral in the Posidonia Shale from well D.
A), Reflected white light; B), Fluorescence mode, oil immersion.

4.1.3.3. Nektonic and planktonic remains

4.1.3.3.1. Zooclasts

The West Netherlands Basin

In the West Netherlands Basin, the content of shell remains shows a resemblance between the wells and ranges from 0.0 to 0.8 vol.%. However, the percentage of fish remains is marginally higher in well E than in well M, revealing a maximum of 1.9 vol.%. The content of unidentified faunal remains in well M reaches 9.8 vol.%. In addition, some zooclasts show oil exudates of intense yellow fluorescence (Fig. 3-9C).

The Lower Saxony Basin

In the Lower Saxony Basin, Posidonia Shale in well A contains a maximum of 1.6 vol.% of zooclasts. The content of fish remains ranges from 0.0 to 1.1 vol.%, but in one sample its percentage reaches a high of 12.0 vol.%. By contrast, in well D, the percentage of zooclasts and fish remains is significantly low, but the amount of unidentified faunal remains shows a resemblance to that in well A (APPENDIX A). In addition, in a few samples of well D, cephalopod hooks (belemnites) were observed. These have a dark grey colour in reflected white light and no fluorescence. According to the cutting angle, several morphological types were recorded (Fig. 4-8).

Shell fragments in both wells from the Netherlands and in northern Germany show a brownish colour in reflected white light and greenish fluorescence of mineral origin. Fish

remains exhibit a light brown to dark brown colour in reflected white light with orange fluorescence (Fig. 4-9). Unidentified faunal remains, probably, related to recrystallised foraminifera chambers, have optical properties in reflected white light and fluorescence mode similar to those of calcareous minerals.

The South German Basin

In the Dotternhausen-1001 well, faunal remains are represented by recrystallised foraminifera fragments of irregular form and phosphate fish remains such as scales, teeth and bones. In reflected white light, they show a brownish colour. Certain fragments are non-fluorescent and others show an orange fluorescence of moderate intensity. Some faunal remains are found as inclusions in bituminite III. The amount of faunal remains in the Dotternhausen-1001 well in some samples reaches a maximum of 14.1 vol.% (APPENDIX A). In the Bisingen-1002 well, zooclasts are encountered in a medium to high percentage in the *spinatum* and *bifrons z*ones. They are mainly represented by foraminifera, fragments of calcareous shells of microfossils, and fish fragments (scales, teeth, bones), which are common in the Lias epsilon. Oil exudates of intense yellow fluorescence were observed in some fish remains from the "Schlacken". In the Notzingen-1017 well, the content of faunal remains is very low. In Lias delta, it drops to values ranging from 0.4 to 1.3 vol.%. In Lias epsilon, the percentage of faunal remains ranges from 0.0 to 4.7 vol.%. However, in Lias zeta it reaches 10.4 vol.%.

4.1.3.3.2. Faecal pellets (Peloids)

Faecal pellets (Boggs, 2009) are represented in all the wells (APPENDIX). They are of a variable size (up to more than 300 μm) and their concentration differs according to the organo-mineral microfacies (Fig. 4-10). The highest content was encountered in well A, reaching 76.2 vol.%, while in well E and well M, the content is lower and does not exceed 15.7 vol.% and 6.6 vol.% respectively. Finally, the content of faecal pellets in well D shows a resemblance to that of well M. The presence of peloids of faecal origin is a further indication of anoxic conditions (Cuomo and Bartholomew, 1991).

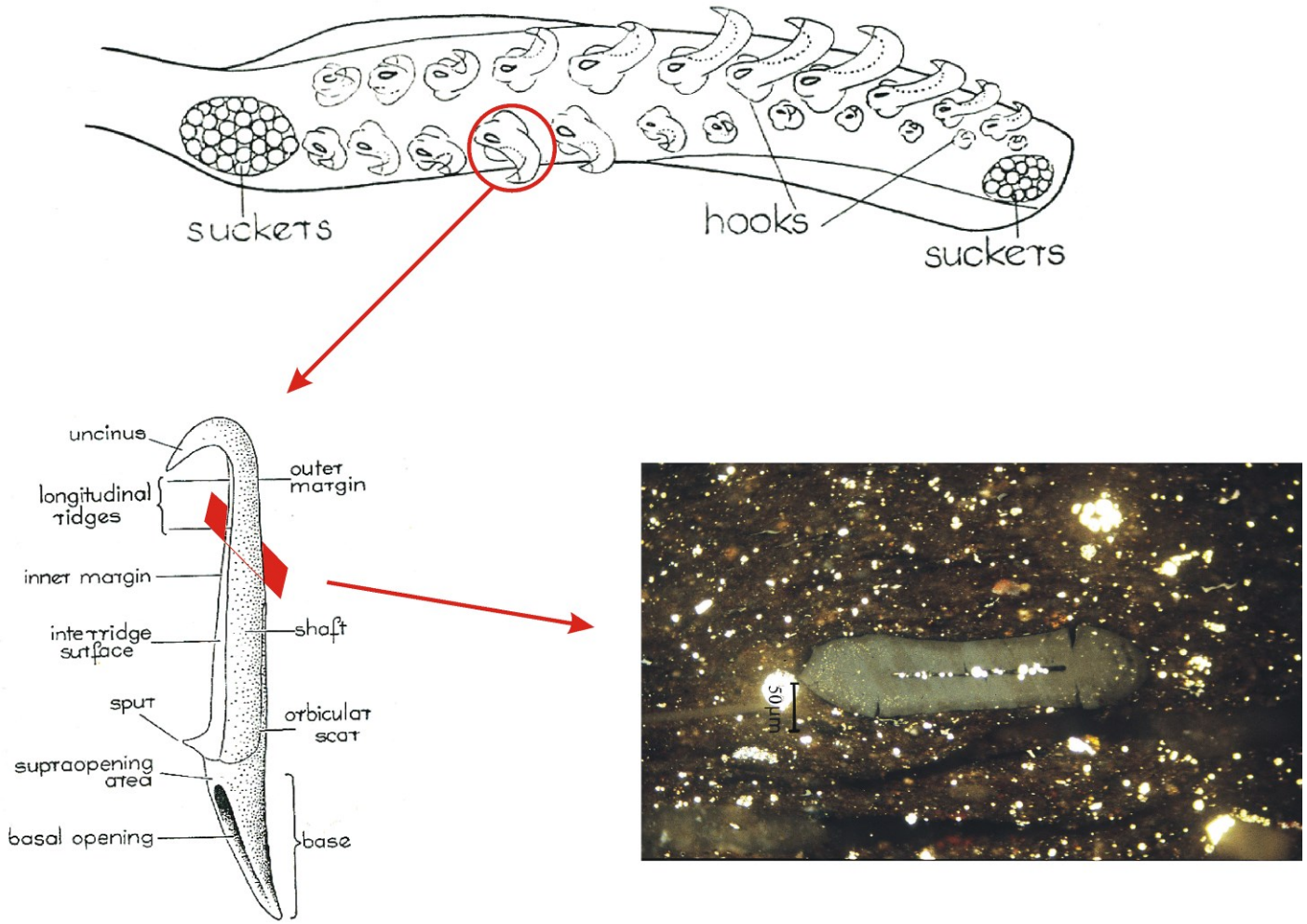

Fig. 4-8: The main elements of the hooks and suckers of the tentacle of Onychoteuthis banksi (belemnites) (Modified after Kulicki and Szaniawski, 1972). Oblique section of chitinous hook (from belemnite) in the samples of well D. Reflected white light, oil immersion.

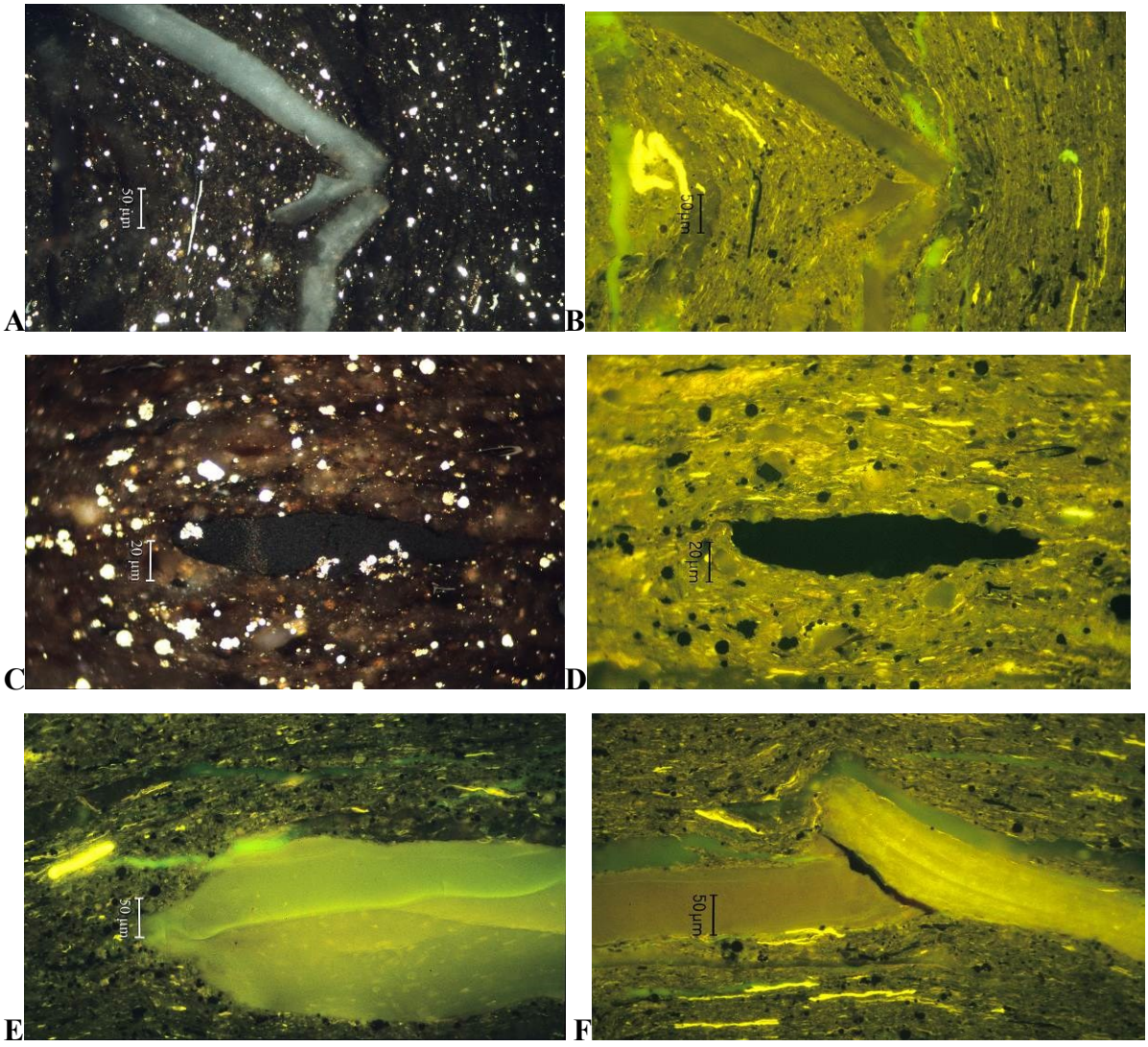

Fig. 4-9: Photomicrographs showing different types of faunal relics.
A), Shell fragments disturbing the texture of the bituminous shales, probably, indicating a storm event; B), The same view in fluorescence mode; C), D), "Vitrinite–like" zooclasts in reflected and fluorescence mode; E), F), Phosphate zooclasts. A), C), Reflected white light, B), D), E), F), Fluorescence mode, oil immersion.

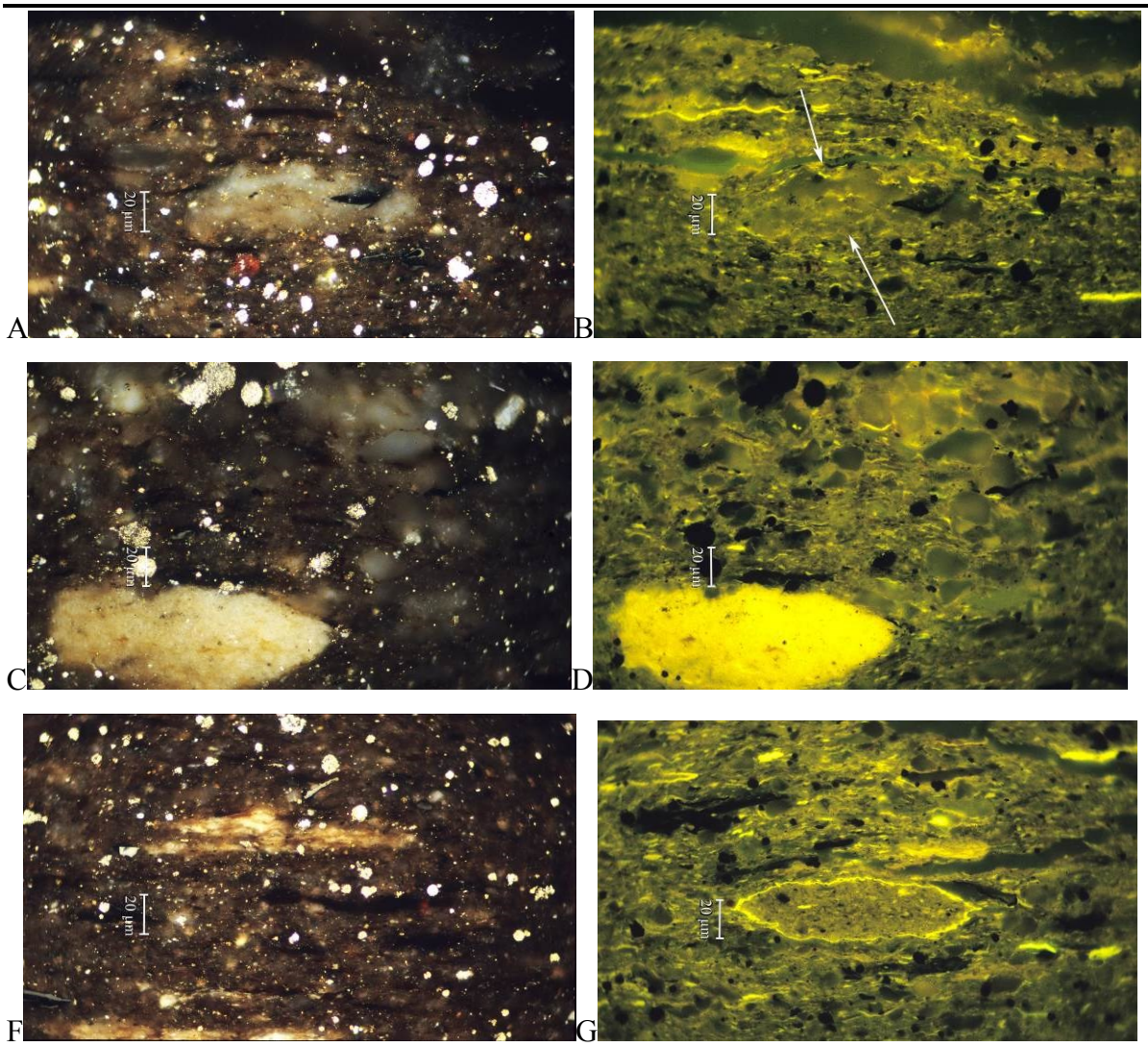

Fig. 4-10: Photomicrographs showing some examples of peloids encountered in the Posidonia Shale.
A), B), Peloids poor in organic matter containing rare liptodetrinite and rare lipidic substances; C), D), Bright peloids containing rare lamalginite and rich in oil; F), G), Peloids similar to A), B), but with yellow fluorescing outer rim (well-preserved faecal pellet). A), C), F), Reflected white light, oil immersion; B), D), G), Fluorescence mode, oil immersion.

In the Dotternhausen-1001 well, faecal pellets occur as elongated bodies having a beige colour in reflected white light and a green or brownish fluorescence of weak intensity. The size of these peloids can reach more than 200 µm and their quantity makes up 9.0 vol.% (APPENDIX A). In other southern German wells, faecal pellets were not taken into consideration in the maceral analysis.

Many workers mentioned the contribution of faecal pellets in oil generation as they may contain a significant amount of organic matter (Cuomo and Bartholomew, 1991; Rullkötter *et al*., 1992; Boggs, 2009; Gonçalves Sá da Silva, 2014). The planktonically-produced faecal pellets generally consist of an assortment of organic debris, skeletal material, bacteria. Their content may vary, depending on the different food sources (Cuomo and Bartholomew, 1991). Moreover, Rullkotter *et al.,* (1992) claimed that there is a relationship between faecal pellet and bituminite II. However, from the paleoenvironmental point of view, faecal pellets indicate high biomass productivity and can exist when oxygen is available. However, dysoxic-anoxic conditions favour the preservation of organic matter. Therefore, a high content of faecal pellets enriched in organic matter possibly indicates environments with a stratified water column (Cuomo and Bartholomew, 1991; Tyson, 1995).

Apart from pellets of faecal origin, Flügel (2004) distinguished peloids of algal and microbial origin. These peloids also contain a high quantity of organic matter and indicate dysoxic-anoxic paleoenvironments with restricted circulation of the water column.

4.1.3.3.3. Coccoliths

The occurrence of coccoliths is frequently attributed to the sedimentation of organic-rich sediments and provides evidence of their affinity to amorphous organic matter (Batten, 1985). The identification of these fossils is difficult, due to their bad state of preservation, resulting from microbial activity and fungal attack. Therefore, some workers have not paid much attention to their identification and they have seldom been recognised (Batten, 1995).

Ecologically, some coccolithophores are largely planktonic organisms which inhabit oceanic, littoral, lagoonal and estuarine realms. However, some were found in fresh-water environments (Batten, 1985). The identification of these microfossils can provide valuable information on paleoenvironments. Batten (1985) claimed that the presence of coccoliths in sediments may suggest the marine origin of the amorphous organic matter sedimented in anoxic conditions.

In some samples of wells E and M, numerous coccoliths were encountered (APPENDIX A). It is common that a high number of these calcareous nannofossils is related to specific organo-mineral microfacies, which will be described later (Fig.3-7 B). Among these calcareous nannofossils, abundant *Schizosphaerella* showing a thin bright-yellow fluorescing coating of organic origin were recognised (Fg.3-7 B). Similar organic surface coatings have been described and studied by Godoi *et al*. (2009) on a modern

coccolithophore. These authors demonstrate the association of bacteria with the coccosphere. This suggests that the coating provides a physical substrate for bacterial assemblages. Therefore, the fluorescence observed on the surface of the coccoliths in some of the studied samples could be considered in part as being of bacterial origin. This suggests the development of strong anoxic conditions to ensure the preservation of the organic coatings described above. In northern and southern Germany, coccoliths were found and described in some samples. However, they were not counted (APPENDIX A). In addition, coccolithophorids can be transported to the sea bottom via faecal pellets of zooplanktonic and nektonic animals (Flügel, 2004).

4.1.3.4. Summary

The mineral groundmass in almost all the investigated samples is bituminous, except for the samples which have a low content of organic matter and burrows. The ratio of clayey and calcareous fraction varies not only from one sedimentary basin to another, but from well to well.

Posidonia Shale from well D shows the highest values of detrital mineral content reaching 8.5 vol.%. Bituminous shales from the Dotternhausen-1001 well contain quartz and mica grains, together reaching 6.6 vol.%. By comparison, in wells E and M, the content of detrital minerals is lower, making up a maximum of 4.1 and 5.2 vol.% respectively.

The highest percentage of dolomite crystals is attained in wells E and M, reaching 55.5 and 22.3 vol.% respectively. Gypsum is well-represented only in the Lower Saxony Basin. It is represented by a primary and a secondary form. The primary form occurs in well A, reaching 2.9 vol.%, while in well D, the bituminous shales contain a basically secondary form comprising a maximum of 6.8 vol.%.

The content of pyrite varies. In wells E, M and A, it is higher than in the other investigated wells. The content of framboidal pyrite in these wells reaches 11.0, 9.9 and 16.5 vol.% respectively.

The type of zooclasts and their quantities differ from one sedimentary basin to another. While in wells E and M of the West Netherlands Basin, calcareous zooclasts are more frequent, reaching 7.8 and 9.3 vol.% respectively, in wells A and D of the Lower Saxony Basin, the content of zooclasts is lower with a slight predominance of bioclasts as well, comprising a maximum of 4.2 and 2.4 vol.% respectively. In the Dotternhausen-1001 well,

the zooclasts are basically represented by shell fragments, whose content in one sample reaches a high of 40.6 vol.%.

Coccoliths are represented in almost all the wells. However, in some wells they are poorly preserved (A and D wells). In wells E and M, coccoliths show a yellow-green fluorescing coating, probably, of bacterial origin.

4.2. Identified organo-mineral microfacies

4.2.1. The West Netherlands Basin

4.2.1.1. OMFN 1: Low bituminous limestone with low content of bituminites (AOM)

Maceral composition of OMFN 1

Well E

This organic microfacies is characterised by a low content of bituminites (Fig. 4-11 A, B). Among the bituminites, bituminite I and bituminite V have the highest contents, reaching 1.0 and 1.5 vol.% respectively. The telalginite content is low (0.1–0.3 vol.%). However, that of discrete lamalginite reaches a high of 22.4 vol.%, The content of filamentous lamalginite does not exceed 2.8 vol.% and the content of layered lamalginite dips to a low of 0.6 vol.%. The liptodetrinite percentage attains a maximum of 8.0 vol.%. Among the terrestrial organic matter, sporinite and inertinite were recorded. Sporinite shows values ranging from 0.3–1.1 vol.%, but inertinite does not exceed 0.4 vol.% (APPENDIX B).

Well M

In well M, a similar organic microfacies was identified (Fig.4-12 A, B). However, there are some slight differences in the maceral composition. The content of bituminites is low. However, that of bituminite I, bituminite II and bituminite V can reach a maximum of 4.2 vol.%, 1.6 vol.% and 1.4 vol.% respectively. The quantity of telalginite and filamentous lamalginite shows a resemblance to well E and well M, but that of discrete lamalginite does not exceed 11.0 vol.%. In comparison to well E, the content of liptodetrinite in well M is two times higher than in well E. It rises to a maximum of 18.8 vol.% (APPENDIX B).

Mineral composition of OMFN 1

The organic microfacies OMFN1 is associated with low bituminous limestones containing dolomite crystals. The content of clayey groundmass in wells E and M ranges from 10.2 to 38.9 vol.% and from 0.2 to 10.7 vol.% respectively. The quantity of calcareous groundmass varies from 22.1 to 56.0 vol.% in well E and from 35.9 to 74.2 vol.% in well M. The content of coccoliths might be underestimated. It is similar in both wells and reaches about 4.0 vol.%. Dolomite crystals show variable percentages. The highest content reaches 22.3 vol.% in well M. The content of quartz is higher in well E, ranging from 0.2 to 2.1 vol.%; in well M it reaches only 0.9 vol.%. However, in well M, the content of mica is four times higher than in well E and reaches 4.4 vol.%. The content of pyrite framboids is predominant among other forms. It ranges between 2.4 and 6.4 vol.% in well E and 0.6 and 9.9 vol.% in well M.

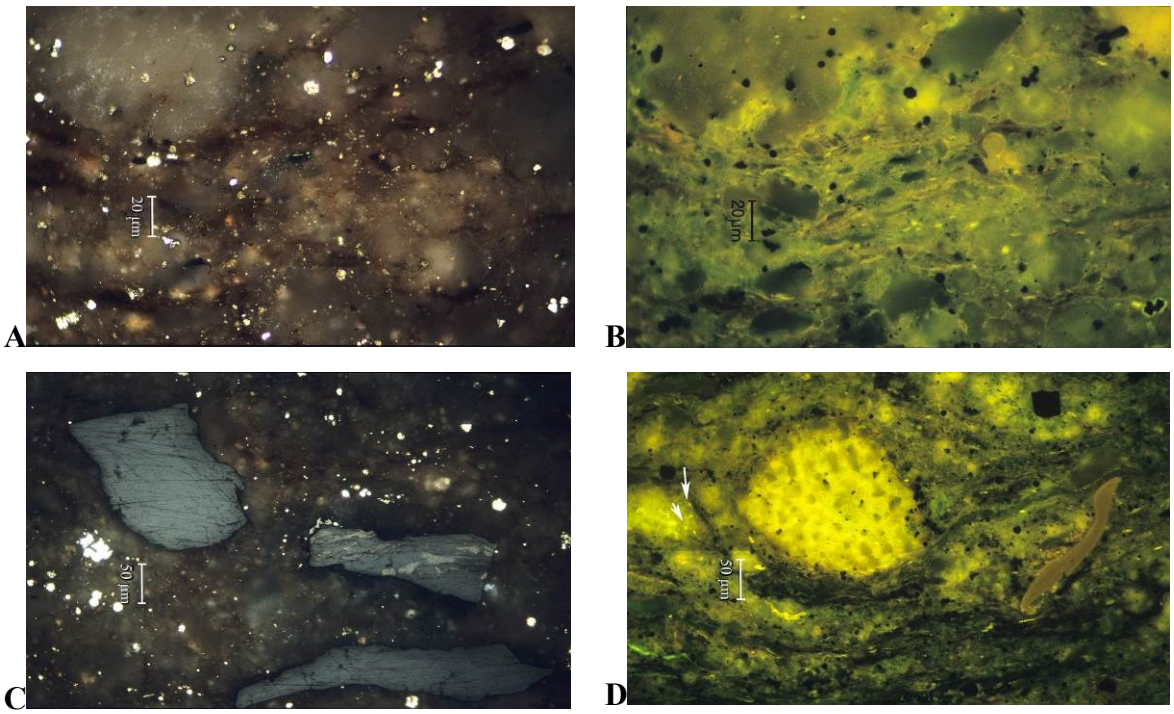

Fig. 4-11: Microphotographs illustrating the OMFN1 in well E and some related particularities indicating specific events during its deposition.
A), B), General view of OMFN1 in well E in reflected white light (A) and in fluorescence mode (B), oil immersion; C), Tri-maceral coal particles, transported from landmasses by wind or by water flux. Note: the good preservation of the particles indicates the deposition in an oxygen-depleted environment. Reflected white light, oil immersion; D), Zooclast, probably from Echinoderm, indicating a short-term oxygenation of the water column; fluorescence mode, oil immersion.

The content of zooclasts in both wells shows a resemblance of about 3.0 vol.%. Zooclasts are irregularly distributed and often depict a wavy particular texture, indicating a

short-term storm event (Fig.4-12 C). This coincides with the input of terrestrial organic particles such as recycled particles of carboniferous coal (Fig. 4-11C), Echinoderm (Fig. 4-11 D), fresh-water derived algae (*Botryococcus*-derived algae) and a blooming event of *Tasmanite*-derived algae (Fig.4-12 D).

4.2.1.2. OMFN 2: Bituminous marly limestone enriched in bituminite I

Maceral composition of OMFN 2

Well E

In well E, bituminite I is predominant among other bituminites, ranging from 3.0 to 7.2 vol.% (Fig. 4-13 A, B). Other types of bituminite are present in low concentrations and do not exceed 0.8 vol.%. The percentage of liptodetrinite ranges between 4.3 and 7.9 vol.%. The contents of telalginite and filamentous lamalginite show similarities to those of OMFN1, whereas the amount of discrete lamalginite drops to a low of 5.3 vol.% (APPENDIX B). Among the terrestrial organic matter, vitrinite and inertinite percentages are similar, ranging from 0.0 to 0.6 vol.%. The sporinite content varies between 0.5 and 0.7 vol.%.

Well M

In well M, the content of bituminite I reaches 4.2 vol.% (Fig. 4-13 C). The percentage of bituminite II and bituminite V is higher than in well E, and varies from 0.2 to 1.6 vol.% and from 0.5 to 1.4 vol.% respectively. While the content of telalginite and filamentous lamalginite does not show significant discrepancy compared to well E, the content of discrete lamalginite is higher, ranging from 5.2 to 11.0 vol.%. The liptodetrinite quantity is two times higher than that in well E, reaching 15.2 vol.%. Among the terrestrial organic matter, only vitrinite and sporinite are represented. Vitrinite ranges from 0.0 to 1.2 vol.% and sporinite reaches 3.0 vol.%.

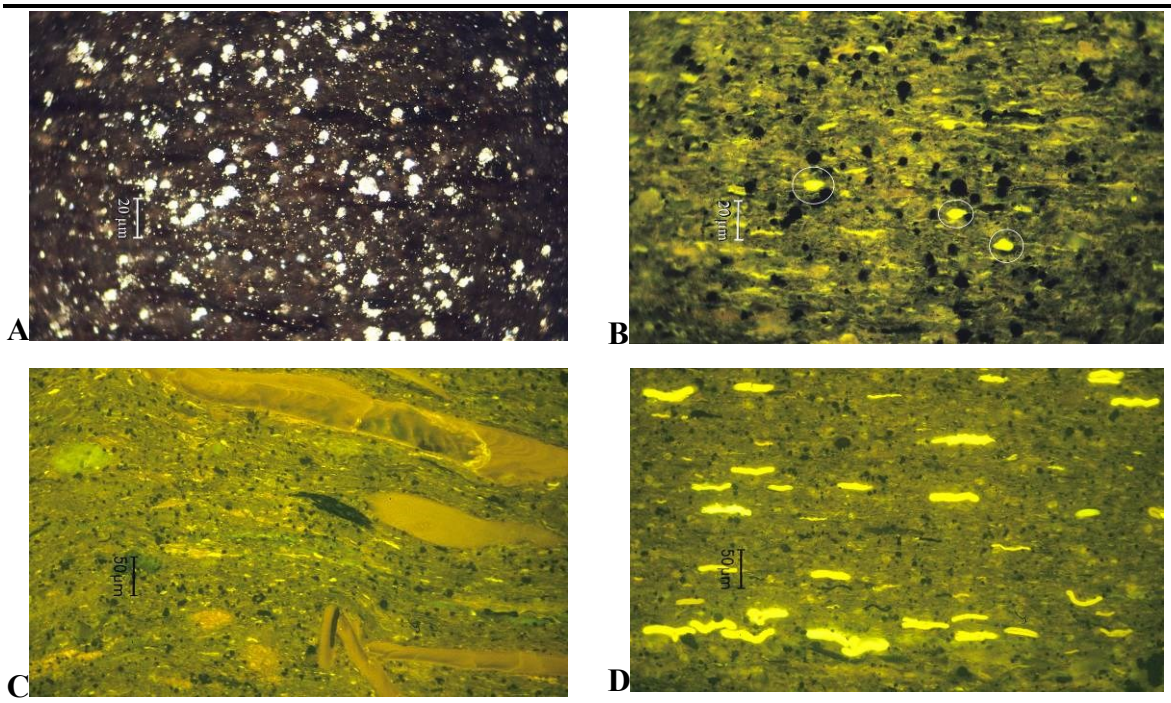

Fig. 4-12: Microphotographs showing general views and different particularities of OMFN1 in well M.
A), B), General view of the OMFN1 in well M in reflected white light (A) and fluorescence mode (B), oil immersion; C), Chaotically distributed fish bones, indicating short-term storm event. Fluorescence mode, oil immersion; D), *Tasmanite*-derived telalginite, indicating algal-bloom event. Fluorescence mode, oil immersion.

Mineral composition of OMFN 2

This organic microfacies is associated with bituminous marly limestones. The quantity of clayey groundmass varies between 1.1 and 39.3 vol.% in well E and between 0.9 and 5.2 vol.% in well M. The percentages of calcareous groundmass in well E range from 17.0 to 29.8 vol.%, and in well M from 31.9 to 50.1 vol.%. The content of dolomite crystals is greater in well E and reaches 53.8 vol.%. The content of coccoliths is high but does not exceed 26.2 and 21.8 vol.% in wells E and M respectively. The content of quartz grains is similar in both wells; however, the quantity of micas is higher in well M and reaches 1.9 vol.%. The percentage of pyrite framboids is in a range between 3.2 and 9.7 vol.% in well E and 4.2 and 7.6 vol.% in well M. The content of zooclasts in both wells is similar, ranging from 2.9 to 3.3 vol.%.

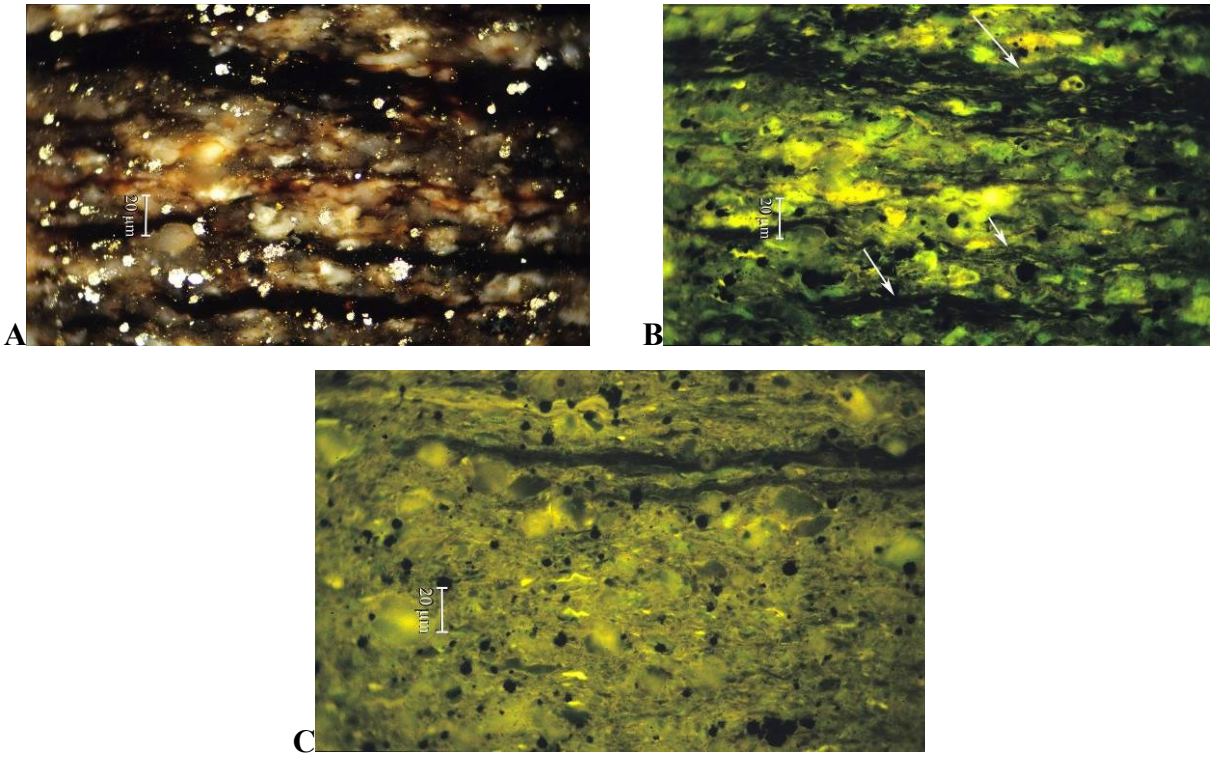

Fig. 4-13: Microphotographs showing general views of OMFN2 in well E (A, B) and in well M (C).
A), Reflected white light, oil immersion; B), Same field of view as A) in fluorescence mode; C), Fluorescence mode, oil immersion.

4.2.1.3. OMFN 3: Bituminous calcareous mudstone and marly limestone enriched in bituminite V

Maceral composition of OMFN 3

Well E

The maceral assemblage of this microfacies is represented by a great quantity of bituminite V, varying from 3.4 to 13.2 vol.% (Fig. 4-14). While the content of bituminite I and bituminite II reaches 10.5 and 4.1 vol.% respectively, that of the bituminite IV does not exceed 0.5 vol.%. Among the alginite group, telalginite reaches 0.6 vol.%, the content of discrete and filamentous lamalginite ranges from 3.2 to 11.1 vol.% and from 0.3 to 1.5 vol.% respectively. The content of liptodetrinite ranges between 2.2 and 15.2 vol.%.

Terrestrial organic matter is represented by a minute amount of vitrinite and inertinite, with the sporinite quantity reaching 1.3 vol.%.

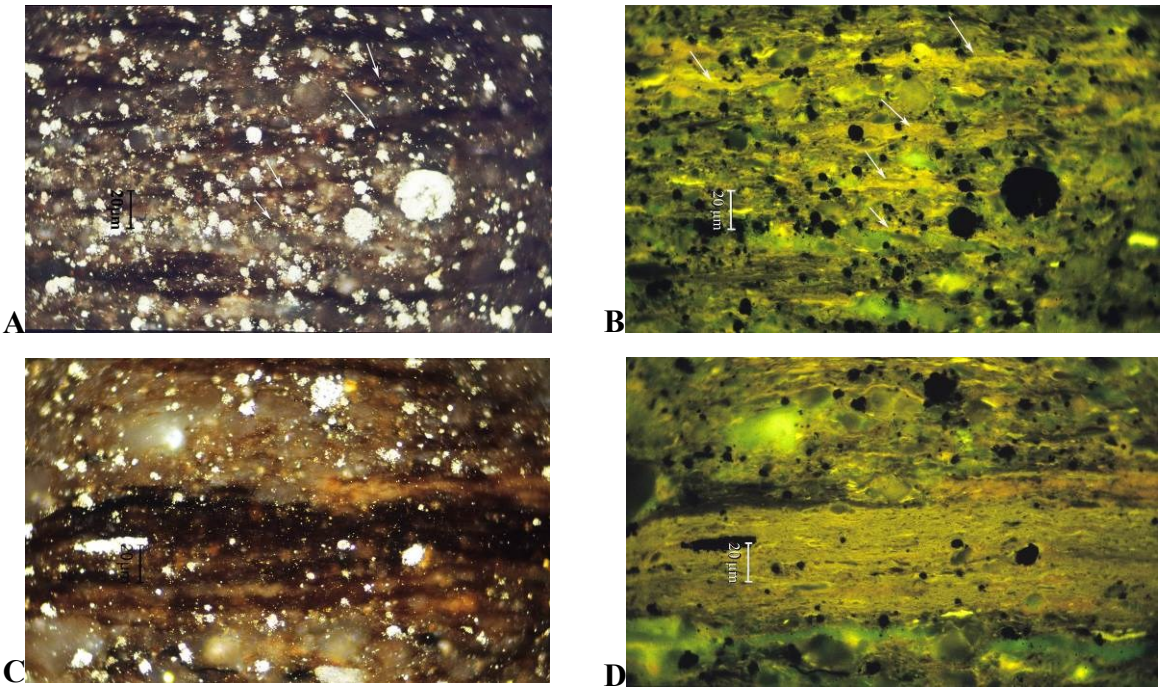

Fig. 4-14: Microphotographs illustrating OMFN3 in well E.
A, B), General view of OMFN3 in reflected white light (left) and in fluorescence mode (right). Bituminite V (white arrows). Oil immersion; C, D), Bituminite V in reflected white light (left) and fluorescence mode (right), oil immersion.

Well M

By comparison, in well M bituminite V reaches only 4.4 vol.% (Fig. 4-15). The content of bituminite I ranges between 0.1 and 2.3 vol.%, whereas the percentage of other bituminites is very low. Although the contents of telalginite in wells E and well M show a resemblance, that of discrete and filamentous lamalginite is higher. Discrete and filamentous lamalginite attain a maximum of 14.8 vol.% and 3.4 vol.% respectively. The liptodetrinite content is in a range between 9.0 and 10.4 vol.%.

Terrestrial organic matter is represented by inertinite and sporinite. Inertinite content reaches only 0.3 vol.%, however, that of sporinite ranges between 1.6 and 2.7 vol.%.

Mineral composition of OMFN 3

The organic microfacies OMFN3 occurs in association with bituminous calcareous mudstone and marly limestone. The amount of clayey groundmass ranges from 1.9 to 29.3 vol.% and 2.5 to 11.0 vol.% in wells E and M respectively, while that of calcareous groundmass ranges from 0.9 to 36.9 vol.% and 32.3 to 52.0 vol.% in wells E and M respectively. The content of dolomite crystals reaches a high of 55.6 vol.% in well E. In well M, the dolomite crystals are represented in lower quantities. Coccoliths are better expressed in

well E than in well M and their percentage reaches 7.6 vol.%. While the content of quartz shows a resemblance in both wells, reaching about 1.6–1.9 vol.%, that of micas is higher in well M and reaches 1.5 vol.%. The content of framboidal pyrite is high in both wells. It ranges from 4.1 and 11.0 vol.% in well E and from 8.6 to 9.2 vol.% in well M.

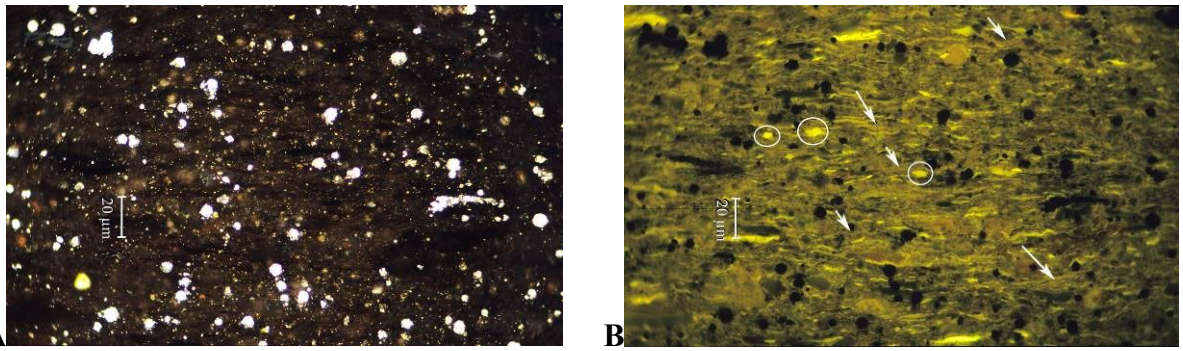

Fig. 4-15: Microphotographs illustrating OMFN3 in well M.
A), Reflected white light, oil immersion; B), Fluorescence mode, oil immersion. Note the white arrows show numerous sporinite examples; white circles enclose the massive liptodetrinite.

The content of zooclasts is low in both wells, ranging between 0.8 and 2.1 vol.% and 1.1 and 1.6 vol.% in wells E and M respectively.

4.2.1.4. OMFN 4: Low bituminous limestone rich in liptodetrinite and discrete lamalginite

Maceral and mineral composition of OMFN 4

It is poor in organic matter and characterised by a relatively low liptodetrinite content (around 4.1 vol.%), discrete lamalginite (1.1 vol.%) and a few sporinites in both wells. It is associated with non-laminated low bituminous limestone (Fig. 4-16, 4-17). The percentage of clayey groundmass reaches 0.2 and 0.0 vol.% in wells E and M respectively, while calcareous groundmass makes up 84.2 vol.% in well E and 83.0 vol.% in well M. The content of detrital minerals is higher in well E than in well M. The quantity of quartz and micas ranges between 2.0 and 4.2 vol.% respectively, whereas that in well M is 0.8 and 2.7 vol.% respectively. The content of pyrite framboids is low and does not exceed 0.8 vol.% in both wells.

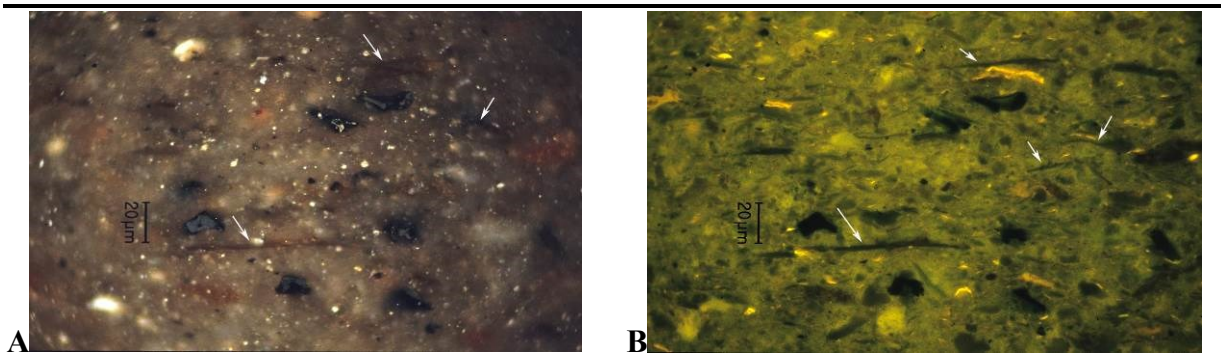

Fig. 4-16: Microphotographs illustrating OMFN4 in well E.
A), Reflected white light, oil immersion; B), Fluorescence mode, oil immersion. Note the relatively high content of vitrinite (grey particles (A)) and zooclasts (white arrows).

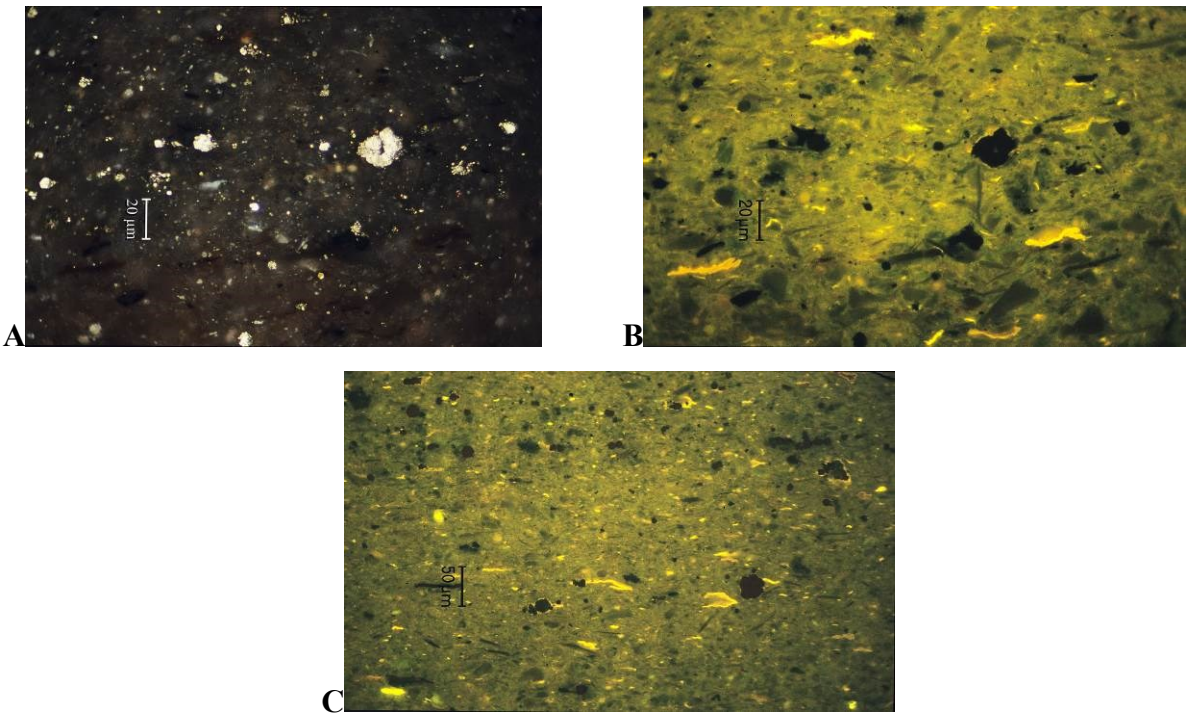

Fig. 4-17: Microphotographs showing OMFN4 in well M.
A), Reflected white light, oil immersion. B), C), Fluorescence mode, oil immersion.

4.2.1.5. OMFN 5: Bituminous calcareous mudstone and limestone enriched in bituminite II

Maceral composition of OMFN 5

Well E

Organic matter is represented by a high content of bituminite II. In well E it reaches 5.3 vol.% (Fig. 4-18). However, in one sample from the lower part of the core profile, bituminite I is slightly predominant and makes up 5.6 vol.%. This lower part of the Posidonia Shale section indicates oxygen-depleted conditions, where bituminite I and bituminite V are

predominant. However, in this section, the increasing content of bituminite II, which reaches a percentage equal to that of bituminite I, indicates temporary oxygenation of the water column. The percentage of bituminite V ranges from 0.6 to 3.4 vol.%.

The quantity of telalginite is high, ranging from 0.8 to 1.2 vol.%. The content of discrete and filamentous lamalginite reaches 10.9 and 1.1 vol.% respectively. The liptodetrinite content ranges from 6.1 to 6.6 vol.%. The sporinite and inertinite contents show a resemblance and reach about 0.6 vol.%.

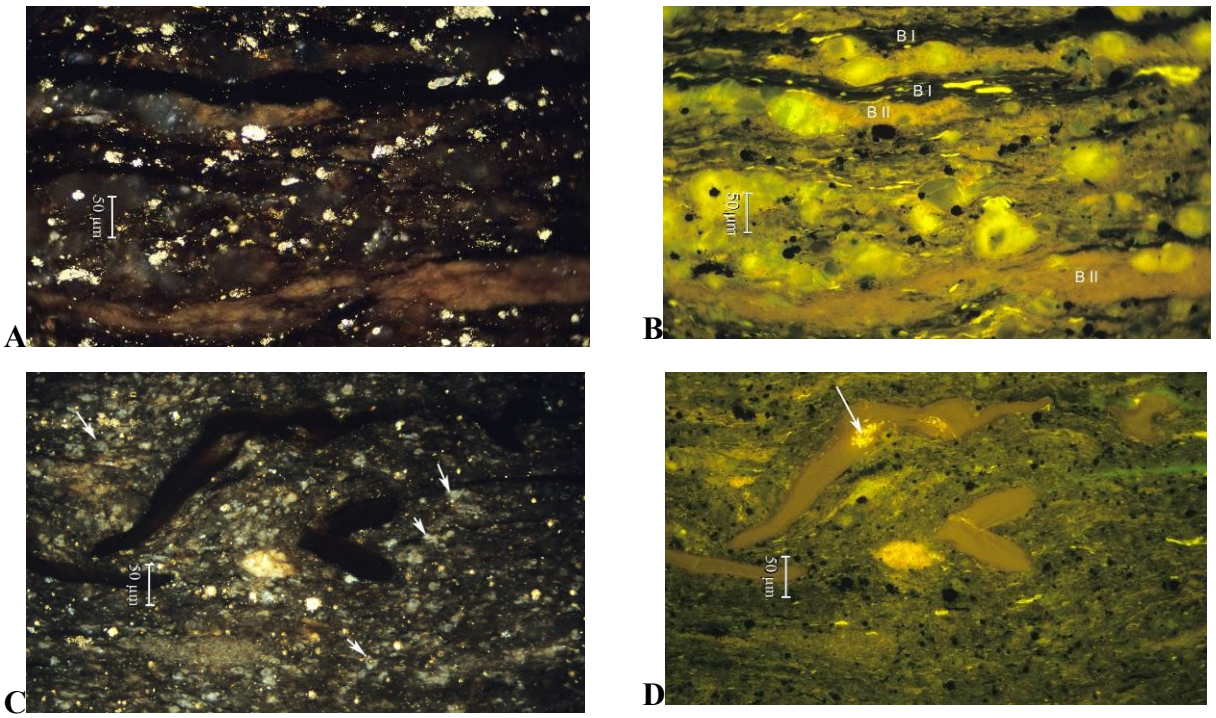

Fig. 4-18: Microphotographs illustrating OMFN5 in well E and a few of its different particularities.
A), B), General view of the organic microfacies in reflected white light (left) and fluorescence mode (right); C), D) Zooclasts showing oil exudates and obliquely oriented in the bedding plane, indicating a flux resulting from a storm event.

Well M

In well M, the content of bituminite II ranges between 2.0 and 4.4 vol.%, bituminite I content reaches 1.3 vol.% (Fig.4-19). Telalginite in this organic microfacies constitutes a minute percentage, while the content of discrete and filamentous lamalginite reaches 13.9 and 2.8 vol.%. The percentage of liptodetrinite does not exceed 14.0 vol.%. Terrestrial macerals are represented by sporinite and inertinite, reaching 1.9 and 1.2 vol.% respectively.

Mineral composition of OMFN 5

The organic microfacies OMNF5 is associated with bituminous calcareous mudstone and limestone. The content of clayey groundmass ranges from 11.6 to 29.4 vol.% in well E and 0.3 to 9.4 vol.% in well M, while that of calcareous groundmass varies between 13.5 and 42.6 vol.% in well E and between 19.8 and 64.2 vol.% in well M. The percentage of dolomite crystals climbs to 28.5 vol.% in well E. While the content of quartz is higher in well E and reaches 2.8 vol.%, the content of micas is two times lower compared to well M, ranging from 0.4 to 1.3 vol.%. The amount of pyrite framboids reaches 9.3–9.9 vol.% in both wells. The content of coccoliths is greater in well M and reaches 5.4 vol.%.

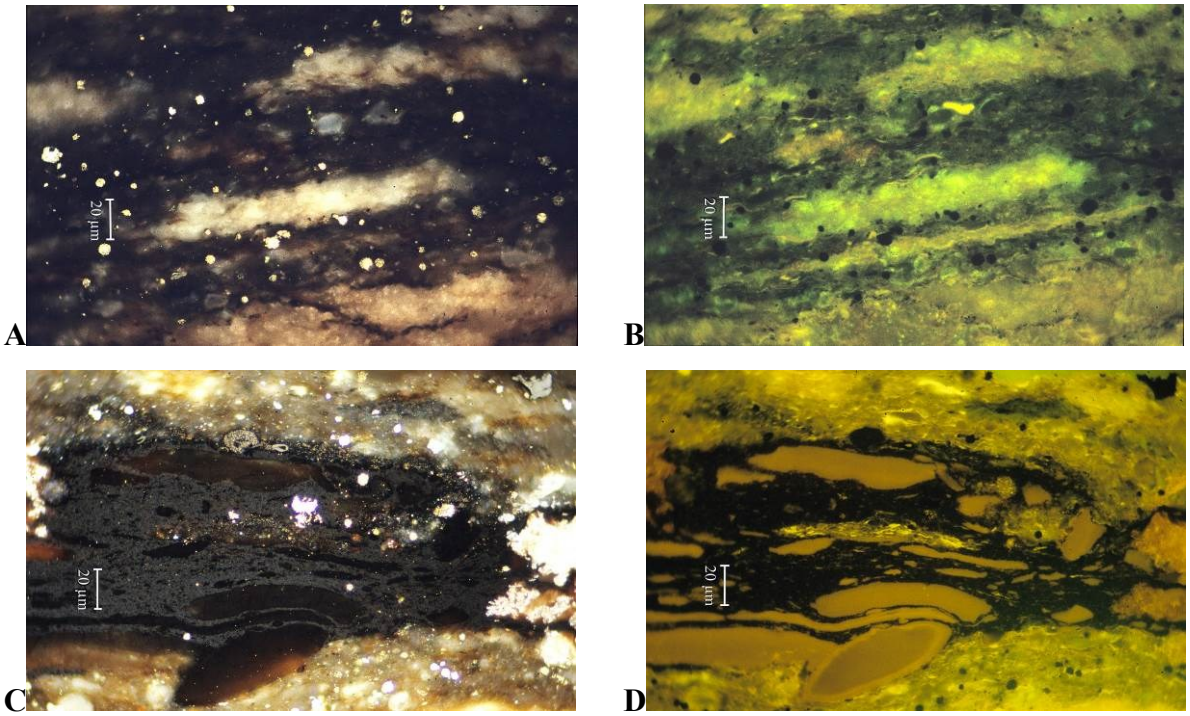

Fig. 4-19: Microphotographs showing examples of OMFN5 in well M.
A), B), View of OMFN5 in reflected white light (left) and fluorescence mode (right); oil immersion; C), D), zooclasts of variable size but obviously having the same origin, embedded in bituminite III in reflected white light (left) and fluorescence mode (right), oil immersion.

4.2.2. The Lower Saxony Basin

4.2.2.1. Well A

4.2.2.1.1. OMFLa1: Bituminous calcareous mudstone enriched in terrestrial macerals with low content of bituminites

Maceral composition of OMFLa 1

Oxidised terrestrial macerals are more abundant in this microfacies than in the others. The inertinite content reaches 2.6 vol.%, whereas that of vitrinite does not exceed 0.4 vol.%. This coincides with the increased content of telalginite reaching 1.1 vol.% (Fig. 4-20, APPENDIX B). The percentage of discrete lamalginite in this organic microfacies reaches the highest values, ranging between 2.7 to 10.3 vol.%. The amount of filamentous and layered lamalginite is in a range between 4.0 and 1.7 vol.% respectively. Liptodetrinite varies from 6.7 to 11.5 vol.%.

Amorphous organic matter is represented by bituminite I and bituminite II. OMFLa1 contains bituminite I in a range between 0.1 and 0.6 vol.%. The bituminite content II reaches 1.7 vol.%.

Mineral composition of OMFLa 1

This organic microfacies is associated with bituminous calcareous mudstone, with a low percentage of coarse faecal pellets, ranging from 0.1 to 1.0 vol.%. The content of clayey groundmass ranges from 30.8 to 35.4 vol.%, while that of calcareous groundmass is from 4.2 to 14.6 vol.%. The content of detrital minerals is low. The quartz quantity does not exceed 1.3 vol.% and that of micas reaches 0.4 vol.%. The percentage of framboidal pyrite is high and reaches 16.5 vol.%.

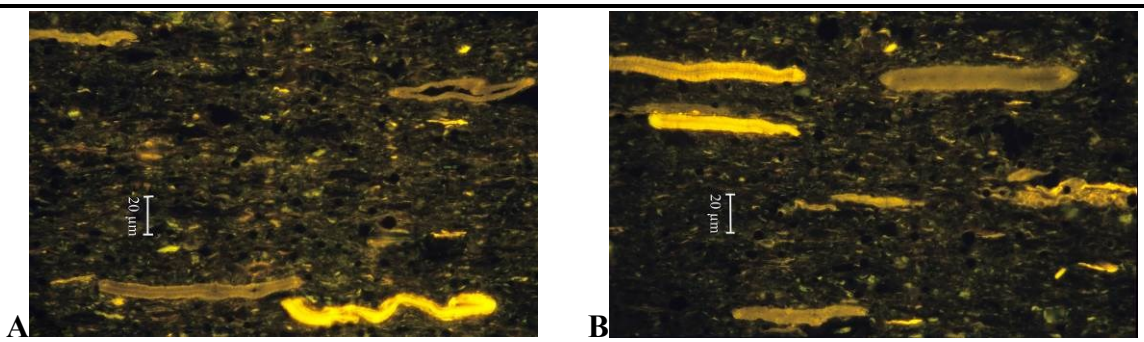

Fig. 4-20: Photomicrographs illustrating OMFLa1.
Fluorescence mode, oil immersion. Note the high content of the telalginite of different fluorescence intensity. This evidence indicates increasing water masses' circulation leading to the spreading of the oxygen-minimum zone.

4.2.2.1.2. OMFLa 2: Bituminous limestone enriched in bituminite II

Maceral composition of OMFLa 2

In comparison with OMFLa1, the assemblage of liptinite macerals is more diverse, but the content of terrestrial macerals and its variations decrease (Fig. 4-21). Among alginite, telalginite marginally increases to a high of 1.6 vol.%. However, that of discrete lamalginite drops to a low of 5.6 vol.%. The quantity of layered lamalginite is in a range between 0.3 and 10.4 vol.% and the content of layered lamalginite reaches 6.0 vol.%. Liptodetrinite, compared to OMFLa1, slightly increases to 12.7 vol.%. While the bituminite I quantity does not exceed 4.7 vol.%, that of bituminite II climbs to a high of 38.8 vol.%.

Mineral composition of OMFLa 2

From a lithological point of view, this organic microfacies is associated with bituminous limestones, in which coarse peloids, reaching 18.5 vol.%, telalginite and bituminite I emphasise the indistinct microlamination. The clayey groundmass reaches 13.2 vol.%, while calcareous groundmass makes up 69.3 vol.%. The content of dolomite crystals does not exceed 4.0 vol.%. The amount of detrital minerals is low. The percentage of pyrite framboids ranges from 2.9 to 15.6 vol.%.

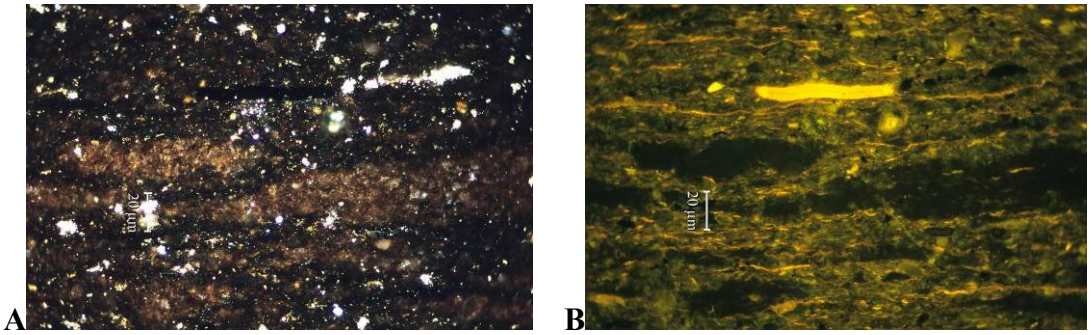

Fig. 4-21: Photomicrographs showing examples of OMFLa2.
A), Reflected white light oil immersion; B) Same field of view, fluorescence mode, oil immersion. Note the dark fluorescence of the bituminite II, probably indicating thermal transformation.

4.2.2.1.3. OMFLa 3: Bituminous limestone enriched in bituminite I

Maceral composition of OMFLa 3

The high content of bituminite I, ranging from 3.0 to 10.6 vol.%, is characteristic of this organic microfacies. The amount of bituminite II yields a maximum of 4.2 vol.%. The telalginite content shows a resemblance to the previous organic microfacies and reaches 1.2 vol.%. The content of lamalginite decreases. Discrete lamalginite content comprises values ranging from 2.8 to 4.8 vol.%, filamentous lamalginite content reaches 1.3 vol.% and the amount of layered lamalginite dips to a low of 0.2 vol.%. The percentage of liptodetrinite increases to a high of 14.1 vol.%.

Mineral composition of OMFLa 3

This organic microfacies is hosted by bituminous limestone with a low content of detrital minerals. The content of clayey groundmass reaches 15.1 vol.%, while calcareous groundmass ranges from 28.7 to 78.9 vol.%. Shell remains are chaotically distributed, possibly indicating a storm event (Fig. 4-22). The percentage of coarse peloids increases to 22.4 vol.%. The quantity of pyrite framboids is high and reaches 12.4 vol.%.

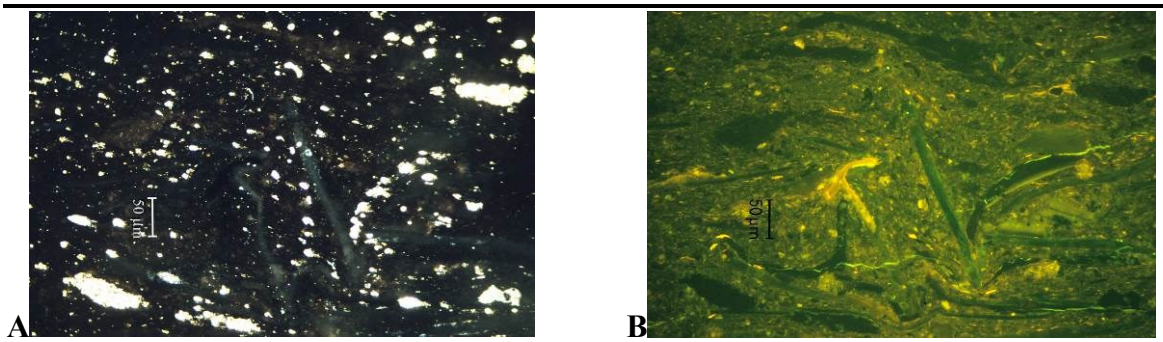

Fig. 4-22: Photomicrographs illustrating examples of OMFLa3.
A), Reflected white light, oil immersion; B), Same field of view, fluorescence mode, oil immersion. Note the wavy microfabrics, probably indicating a short-term storm event. The dark fluorescing bituminite I emphasises the microfabric.

4.2.2.1.4. OMFLa 4: Low bituminous limestone with low content of lamalginite

Maceral composition of OMFLa 4

This microfacies is represented by a low content of lamalginite (Fig. 4-23). The quantity of discrete, filamentous lamalginite reaches 1.8 and 0.6 vol.% respectively. The telalginite content ranges between 0.0 and 3.7 vol.%. The percentage of liptodetrinite decreases to a low of 5.3 vol.%. The content of bituminite I and bituminite II comprises a maximum of 1.0 and 4.0 vol.% respectively.

Mineral composition of OMFLa 4

This organic microfacies is hosted by low bituminous limestones. The content of clayey groundmass reaches 0.9 vol.%, while the percentage of calcareous groundmass ranges between 64.8 and 97.6 vol.%. The content of coarse faecal pellets reaches a high of 76.2 vol.%. The percentage of dolomite crystals reaches 9.4 vol.%. The content of detrital minerals does not exceed 0.8 vol.%. The low content of organic constituents in this organo-mineral microfacies coincides with the decreasing quantity of pyrite framboids, which reaches only 2.6 vol.%.

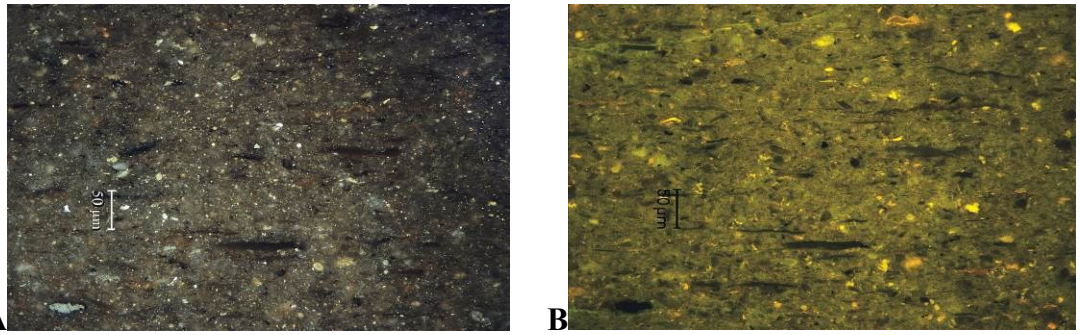

Fig. 4-23: Photomicrographs illustrating OMFLa4 in well A.
A), Reflected white light, oil immersion; B), Same field of view, fluorescence mode, oil immersion. Note the numerous yellow fluorescing liptodetrinite and discrete lamalginite (B).

.

4.2.2.2. Well D

4.2.2.2.1. OMFLd 1: Bituminous limestone enriched in bituminite II

Maceral composition of OMFLd 1

The predominance of bituminite II is characteristic of this organic microfacies (Fig. 4-24). Its content reaches 2.0 vol.%. The percentage of bituminite I is marginally lower and comprises 1.4 vol.%. The alginite content is generally low, except that of discrete lamalginite, which reaches 8.2 vol.%. The percentage of liptodetrinite is high, yielding a maximum of 17.2 vol.%.

Mineral composition of OMFLd 1

The maceral assemblage of this microfacies is associated with bituminous limestone with a low content of faecal pellets and zooclasts. The amount of clayey groundmass reaches 5.0 vol.%, while that of calcareous groundmass reaches a high of 55.2 vol.%.The content of gypsum reaches 3.9 vol.%. The percentage of pyrite — both framboid and epeginetic form — does not exceed 2.0 vol.%.

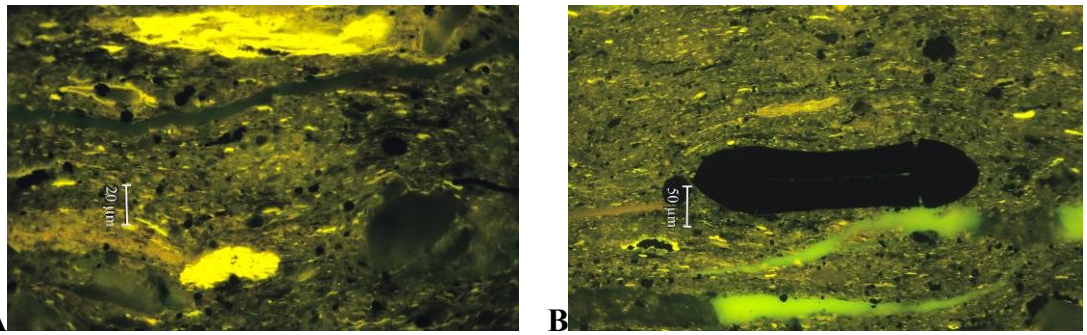

Fig. 4-24:. Photomicrographs illustrating OMFLd1.
A), Example of bituminite II showing a yellow-orange fluorescence (close to the scale bar). The wavy microfabric indicates an environment with a relatively high water dynamic; B), The occurrence of the belemnite hook cross-section demonstrates the oxygen availability in the water column. Fluorescence mode, oil immersion.

4.2.2.2.2. OMFLd 2: Bituminous limestone enriched in bituminite I

Maceral composition of OMFLd 2

By comparison, OMFLd 2 is characterised by an increasing content of bituminite I, ranging from 0.6 to 6.5 vol.% (Fig. 4-25). The percentage of bituminite II reaches 1.1 vol.%. Among the alginite group, the amount of telalginite varies between 0.3 and 1.6 vol.%. The content of discrete, filamentous and layered lamalginite increases, ranging from 6.3 to 19.4 vol.%, from 0.9 to 4.2 vol.% and from 0.0 to 0.4 vol.% respectively. The quantity of

liptodetrinite reaches a high of 28.7 vol.%. The input of terrestrial organic matter is low, the percentages reaching 0.4 vol.% and 0.9 vol.% for vitrinite and inertinite respectively.

Mineral composition of OMFLd 2

This organic microfacies is hosted by bituminous limestones with faecal pellets and zooclasts, reaching 3.2 and 2.4 vol.% respectively. The content of clayey groundmass increases and ranges from 6.0 to 35.8 vol.%, while that of calcareous groundmass varies from 22.0 to 58.3 vol.%. The content of gypsum reaches 5.6 vol.%. The input of detrital minerals is still low. It does not exceed 0.8 vol.% for both quartz and mica. The content of framboids decreases to 1.0 vol.%, whereas that of epigenetic pyrite slightly increases to 2.9 vol.%.

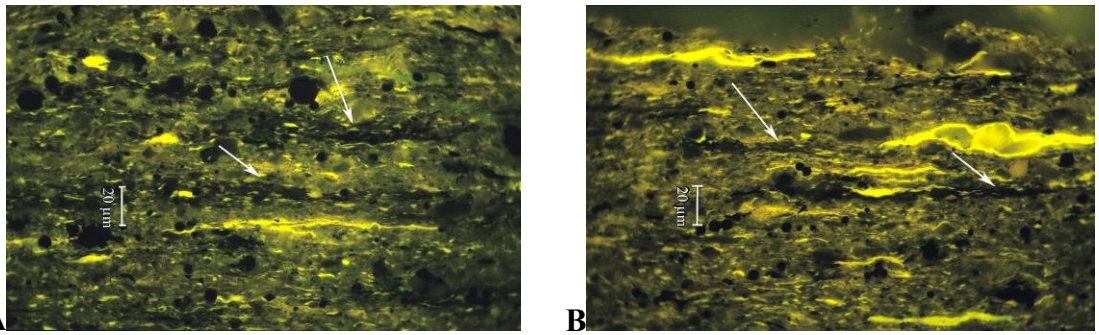

Fig. 4-25: Photomicrographs illustrating OMFLd2.
Note the high content of bituminite I (white arrows). Fluorescence mode, oil immersion.

4.2.2.2.3. OMFLd 3: Bituminous limestone with high content of filamentous lamalginite and decreased content of bituminites

Maceral composition of OMFLd 3

This organic microfacies is characterised by the highest content of filamentous lamalginite among all the identified organic microfacies in well D. Its content ranges from 2.9 to 7.0 vol.% (Fig. 4-26). That of discrete lamalginite is high as well, reaching 15.7 vol.%. However, layered lamalginite was not observed in this microfacies. The content of telalginite and liptodetrinite is also high, reaching 1.9 and 17.5 vol.% respectively. Among the amorphous organic matter, the content of bituminite I does not exceed 1.2 vol.%. The content of bituminite II dips to a low of 0.3 vol.%. In comparison to other microfacies, the input of terrestrial macerals is relatively high. It reaches 0.4, 1.1 and 1.3 vol.% for sporinite, vitrinite and inertinite respectively.

Mineral composition of OMFLd 3

The lithologies associated with this organic microfacies are bituminous limestones and mudstones with scattered faecal pellets and zooclasts, comprising 4.7 and 0.4 vol.% respectively. The percentages of clayey and calcareous groundmass range from 19.7 to 38.1 vol.% and from 18.5 to 49.4 vol.% respectively. The content of quartz reaches 8.1 vol.% and micas make up 1.1 vol.%. The percentages of pyrite — framboids and epigenetic form — are 1.8 and 2.9 vol.% respectively.

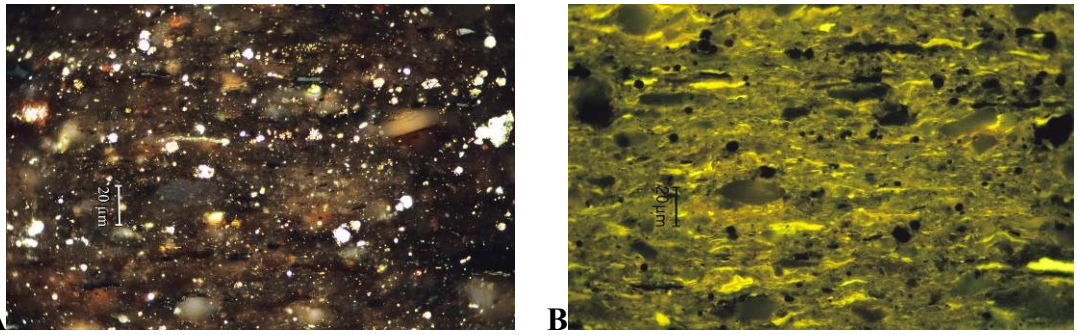

Fig. 4-26: Photomicrographs illustrating OMFLd 3.
A), Reflected white light, oil immersion; B), Same field of view, fluorescence mode, oil immersion. Note the high content of the yellow fluorescing filamentous lamalginite in B.

4.2.2.2.4. OMFLd 4: Low bituminous limestone with low diversity of the macerals

Maceral and mineral composition of OMFLd 4

This organic microfacies is characterised by a content of discrete lamalginite and liptodetrinite reaching 0.9 and 2.3 vol.% respectively. This microfacies is associated with low bituminous limestones with scattered epigenetic pyrite, whose content climbs to a high of 6.3 vol.%. The content of calcareous groundmass reaches 91.4 vol.% (Fig. 4-27).

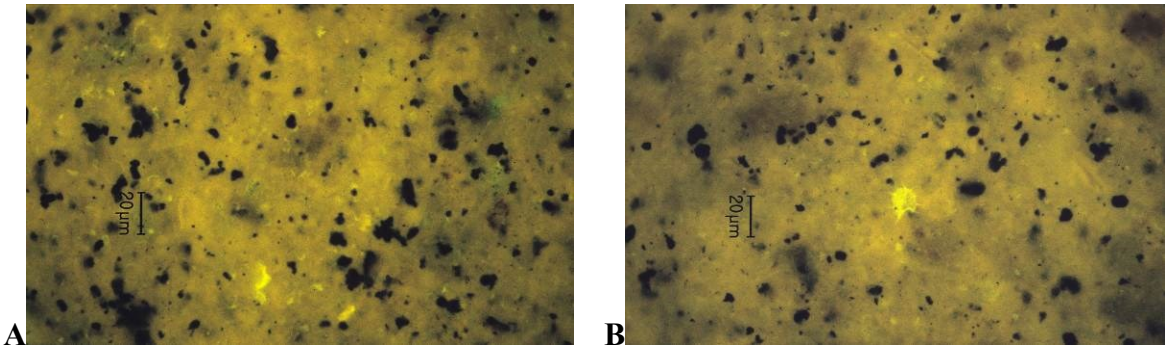

Fig. 4-27: Photomicrographs illustrating OMFLd 4.
A), Brownish fluorescence halos in the middle consist of bituminite VI. B), Acritarch exhibits a yellow-green fluorescence of high intensity surrounded by bituminite VI. Fluorescence mode, oil immersion.

4.2.2.2.5. OMFLd 5: Bituminous limestone with low content of discrete, filamentous lamalginite and bituminites

Maceral composition of OMFLd 5

This organic microfacies is similar to OMFLd3, but the content of filamentous lamalginite dips to a low of 2.9 vol.% (Fig. 4-28). The content of discrete lamalginite is decreased as well, ranging from 7.1 to 9.8 vol.%. However, telalginite is present in a greater quantity, reaching 1.5 vol.%. Liptodetrinite percentages comprise 11.1 to 23.6 vol.%. The input of terrestrial macerals is relatively high. The amount of sporinite, vitrinite and inertinite ranges between 0.2 and 0.3 vol.%, 0.1 and 0.2 vol.% and 0.5 and 1.8 vol.%.

Mineral composition of OMFLd 5

This organic microfacies is hosted by bituminous limestone and calcareous mudstone. The amount of clayey and calcareous groundmass ranges from 29.1 to 39.0 vol.% and 25.1 to 33.4 vol.% respectively. The content of faecal pellets and zooclasts reaches 2.5 and 1.1 vol.% respectively. The amount of gypsum increases to 3.1 vol.%. The input of quartz grains reaches 6.1 vol.%. The percentage of framboids and epigenetic pyrite ranges from 0.6 to 0.8 vol.% and from 0.6 to 2.5 vol.% respectively.

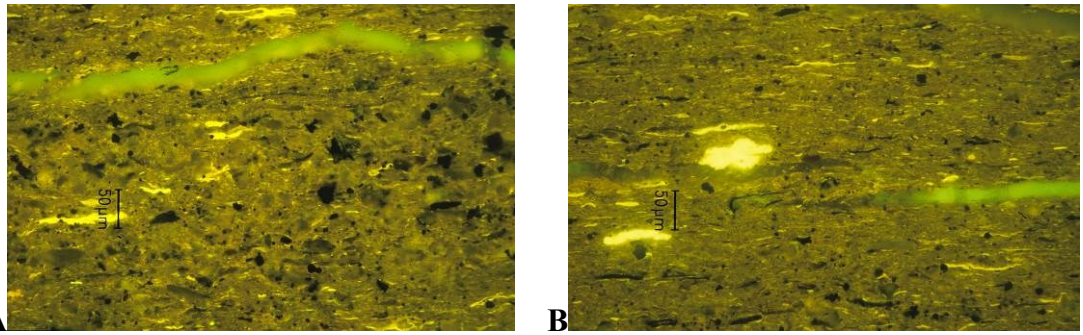

Fig. 4-28: Photomicrographs of OMFLd 5.
Fluorescence mode, oil immersion. Note the presence of a bright yellow fluorescing Botryococcus-derived algae in B.

4.2.3. The South German Basin

4.2.3.1. Dotternhausen-1001 well

4.2.3.1.1. OMFDot 1: Non-bituminous silty marls enriched in zooclasts

Maceral composition of OMFDot 1

This organic microfacies is characterised by a low content of organic constituents. The input of terrestrial macerals is low and their quantity reaches a maximum of 0.3 vol.% for each of vitrinite, inertinite and sporinite. Among the alginite macerals, the telalginite content only reaches 0.7 vol.%. However, that of discrete lamalginite ranges from 2.1 to 18.1 vol.%. The quantity of filamentous lamalginite comprises a maximum of 1.0 vol.% (APPENDIX A, B).

Mineral composition of OMFDot 1

Lithologically, the organic microfacies of OMFDot1 is associated with non-laminated and non-bituminous silty marls and marly shales, which are locally bioturbated. The content of clayey groundmass ranges from 0.7 to 14.5 vol.%, while that of calcareous groundmass varies from 25.3 to 85.0 vol.%. The content of scattered framboidal pyrite is low, whereas that of epigenetic pyrite reaches 5.2 vol.%. Among detrital minerals, micas predominate, with a percentage reaching 3.0 vol.%, whereas the content of quartz comprises a maximum of 1.4 vol.%. The quantity of dolomite crystals ranges between 0.3 and 6.0 vol.%.

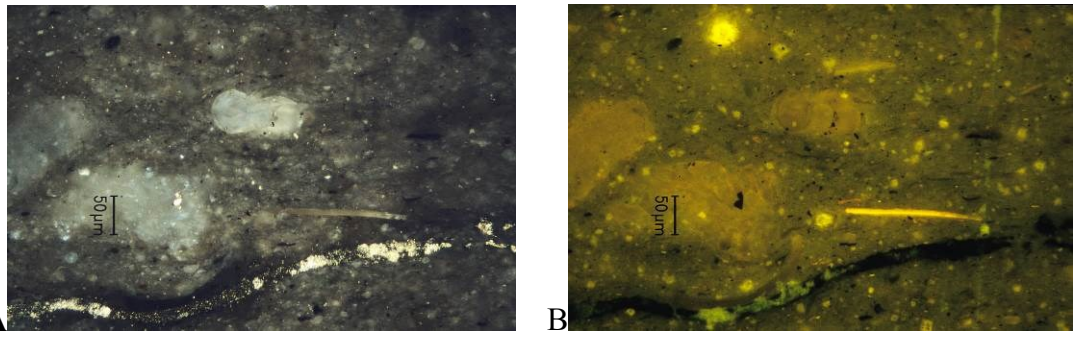

Fig. 4-29: Photomicrographs illustrating examples of OMFDot 1.
A), Reflected white light, oil immersion; B), Same field of view, fluorescence mode, oil immersion. Note the high amount of the different types of the zooclasts, which are well recognisable in fluorescence mode by a yellow-orange and a yellow colour.

This organic microfacies is associated with an extremely high content of phosphatic and recrystallised calcareous zooclasts. They are represented by recrystallised remains of foraminifera and coccoliths, fishbones and teeth, and other faunal remains of uncertain affinity, whose content reaches a high of 41.5 vol.% (Fig. 4-29). Shell fragments are irregularly oriented. Non-bituminous peloids are also observed.

4.2.3.1.2. OMFDot 2: Bituminous silty marls, limestone and mudstone enriched in bituminite I

Maceral composition of OMFDot 2

The increased content of bituminite I is characteristic of this organic microfacies (4-30). Similar to OMFDot1, the content of vitrinite, inertinite, sporinite is low. However, the amount of telalginite (0.2–1.3 vol.%) increases, together with that of bituminite I (1.0–4.0 vol.%). The percentage of discrete lamalginite marginally declines to a value of 7.8 vol.%. The content of filamentous lamalginite ranges from 0.6 to 1.2 %. The liptodetrinite content varies from 0.3 to 10.7 vol.%.

Maceral composition of OMFDot 2

Lithologies associated with this organic microfacies are bituminous silty marls, limestones and mudstones. The content of clayey and calcareous groundmass ranges from 1.2 to 53.9 vol.% and from 17.1 to 79.4 vol.% respectively. The amount of framboidal and epigenetic pyrite reaches 7.8 and 10.2 vol.% respectively. The percentage of micas does not exceed 0.4 vol.%, whereas that of quartz climbs to a high of 6.2 vol.%.

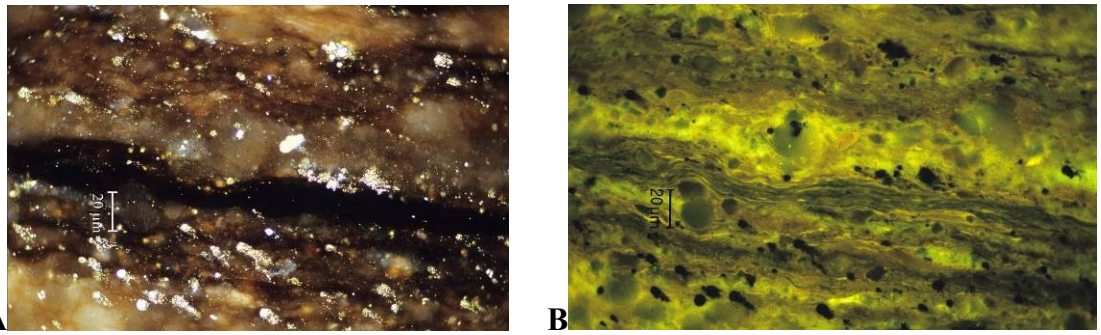

Fig. 4-30: Photomicrographs showing examples of bituminite I in OMFDot 2.
A), Reflected white light, oil immersion; B), Same field of view, fluorescence mode, oil immersion. Note the richness of the bituminite I in lamalginite.

4.2.3.1.3. OMFDot 3: Bituminous silty marls and limestone enriched in bituminite I and bituminite VI

Maceral composition of OMFDot 3

This organic microfacies is represented by an increased content of bituminite I (3.3 vol.%) and bituminite VI (2.2 vol.%) (Fig.4-31). Among alginite, the content of discrete lamalginite is the highest (5.2 vol.%).

Mineral composition of OMFDot 3

This organic microfacies is hosted by bituminous silty marls and limestones with burrows (Fig. 4-30). The amount of clayey groundmass ranges from 3.0 to 27.4 vol.%, while that of calcareous groundmass varies from 38.0 to 89.1 vol.%. The content of framboidal pyrite ranges from 0.5 to 2.6 vol.%, whereas that of epigenetic pyrite comprises from 1.9 to 7.5 vol.%. The percentage of quartz and micas shows a resemblance, reaching 0.3 vol.%.

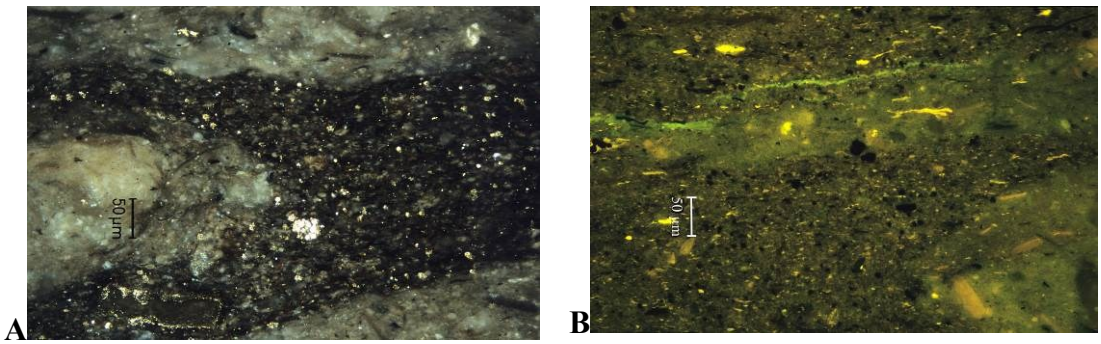

Fig. 4-31: Photomicrographs illustrating burrows in OMFDot 3.
A), The burrows appear light grey and light brown in comparison to the dark grey mineral bituminous groundmass (right). Reflected white light, oil immersion; B), Fluorescence mode, oil immersion. Note the light fluorescence colour of the burrows and their low content in liptinite. Optical properties of the burrows are similar to those of the non-bituminous calcareous groundmass, poor in organic matter.

4.2.3.1.4. OMFDot 4: Bituminous silty marls and limestone enriched in bituminite IV

Maceral composition of OMFDot 4

The predominance of bituminite IV among other amorphous organic matter is characteristic of this organic microfacies (Fig. 4-32). Similar to the previously described microfacies, the content of telalginite and terrestrial organic matter reaches 0.3 vol.%. The discrete lamalginite content ranges from 4.2 to 4.8 vol.%, while the content of filamentous lamalginite reaches 0.5 vol.%. Among the amorphous organic matter, the amount of

bituminite I and bituminite II is low, while that of bituminite IV climbs to a high of 3.8 vol.%. The percentage of liptodetrinite varies from 6.7 to 7.3 vol.%. The zooclast content increases to a value of 4.9 vol.%.

Mineral composition of OMFDot 4

This organic microfacies is associated with bituminous limestones and silty marls. The content of clayey and calcareous groundmass ranges from 10.8 to 22.6 vol.% and from 52.8 to 69.0 vol.%. The percentage of framboidal pyrite ranges from 0.7 to 1.1 vol.%, but that of epigenetic pyrite reaches 3.0 vol.%. Among the detrital minerals, quartz is predominant and its percentage reaches 1.9 vol.%, whereas that of micas is suppressed. The content of zooclasts increases to a value of 4.9 vol.%.

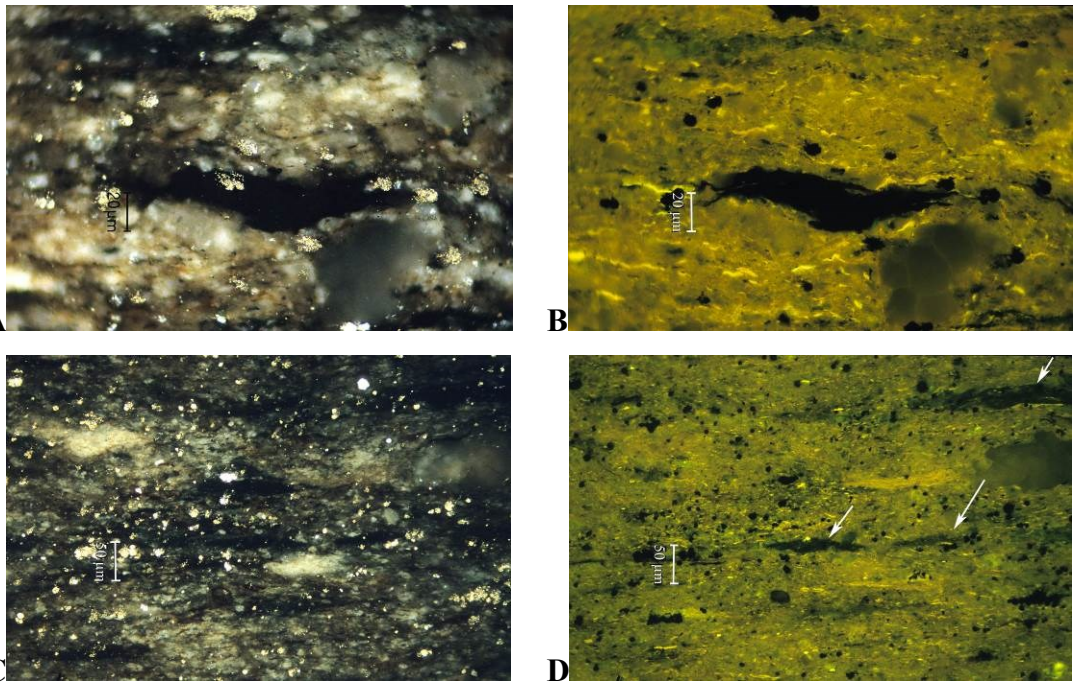

Fig. 4-32: Photomicrographs illustrating the particularities of OMFDot 4.
A) Bituminite IV in reflected white light, oil immersion; B), The same view in fluorescence mode, oil immersion; C), General view of OMFDot4, showing the widely distributed bituminite IV in the mineral bituminous groundmass; D), The same view in fluorescence mode (white arrows show bituminite IV), oil immersion.

4.2.3.1.5. OMFDot 5: Bituminous mudstone with even quantity of bituminite I and bituminite II

Maceral composition of OMFDot 5

The OMFDot5 is composed of increasing contents of sporinite and telalginite, which attain 1.6 vol.% and 1.3 vol.% respectively. The content of discrete lamalginite ranges from 1.4 to 2.3 vol.%, while the content of filamentous and layered lamalginite increases to a high

of 2.8 and 1.0 vol.% respectively. The amount of liptodetrinite in this organic microfacies dips to a low of 3.3 vol.%. Among the amorphous organic matter, the content of bituminite I (0.7–1.5 vol.%) and bituminite II (0.7–1.0 vol.%) shows a resemblance. The bituminite III quantity marginally increases to 0.2 vol.%.

Mineral composition of OMFDot 5

This organic microfacies is hosted by bituminous mudstone. The content of clayey groundmass varies from 63.7 to 70.7 vol.%, while that of calcareous groundmass ranges from 7.0 to 13.3 vol.%. Framboidal pyrite comprises 6.4–6.8 vol.%. The content of quartz reaches 4.5 vol.% (Fig.4-33).

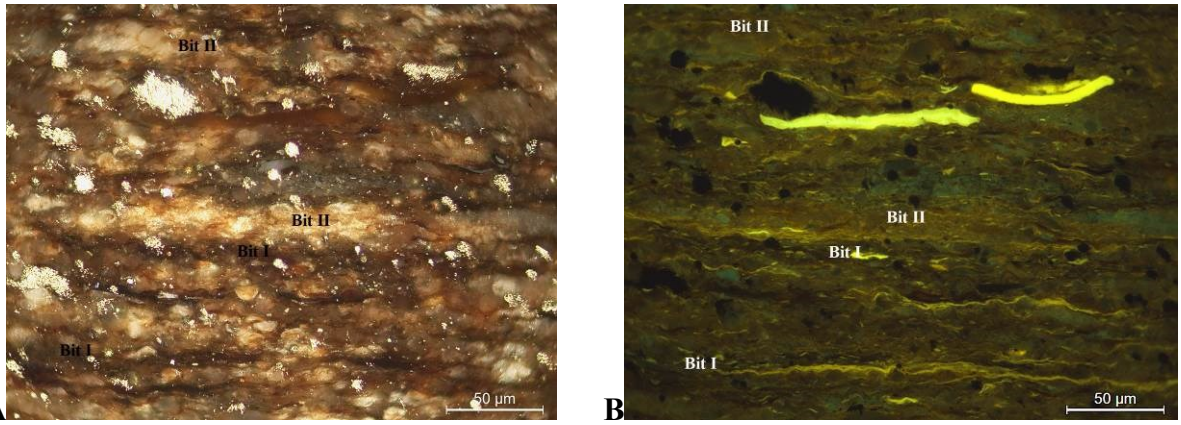

Fig. 4-33: Photomicrographs illustrating the particularities of the OMFDot 5.
A) Bituminite I (Bit I) and bituminite II (Bit II) in reflected white light, oil immersion. B), Same view in fluorescence mode, oil immersion.

4.2.3.2. Notzingen – 1017 well

4.2.3.2.1. OMFNot 1: Calcareous shales with high input of terrestrial organic matter

Maceral composition of OMFNot 1

This organic microfacies is characterised by a high input of inertinite and vitrinite macerals and an increased content of zooclasts (Figs. 4-34; APPENDIX B). Among the terrestrial organic matter, vitrinite macerals prevail, ranging from 1.4 to 3.4 vol.%, whereas inertinite quantity varies from 0.6 to 1.0 vol.%. Among the liptinite macerals, liptodetrinite is marginally predominant with percentages ranging from 2.1 to 5.5 vol.%, while the lamalginite content reaches 4.1 vol.%.

Mineral composition of OMFNot 1

This organic microfacies is hosted by calcareous shale with scattered pyrite, whose content is in a range between 1.4 and 2.2 vol.%. The groundmass content reaches 90.2 vol.%. The percentage of zooclasts reaches 10.0 vol.%.

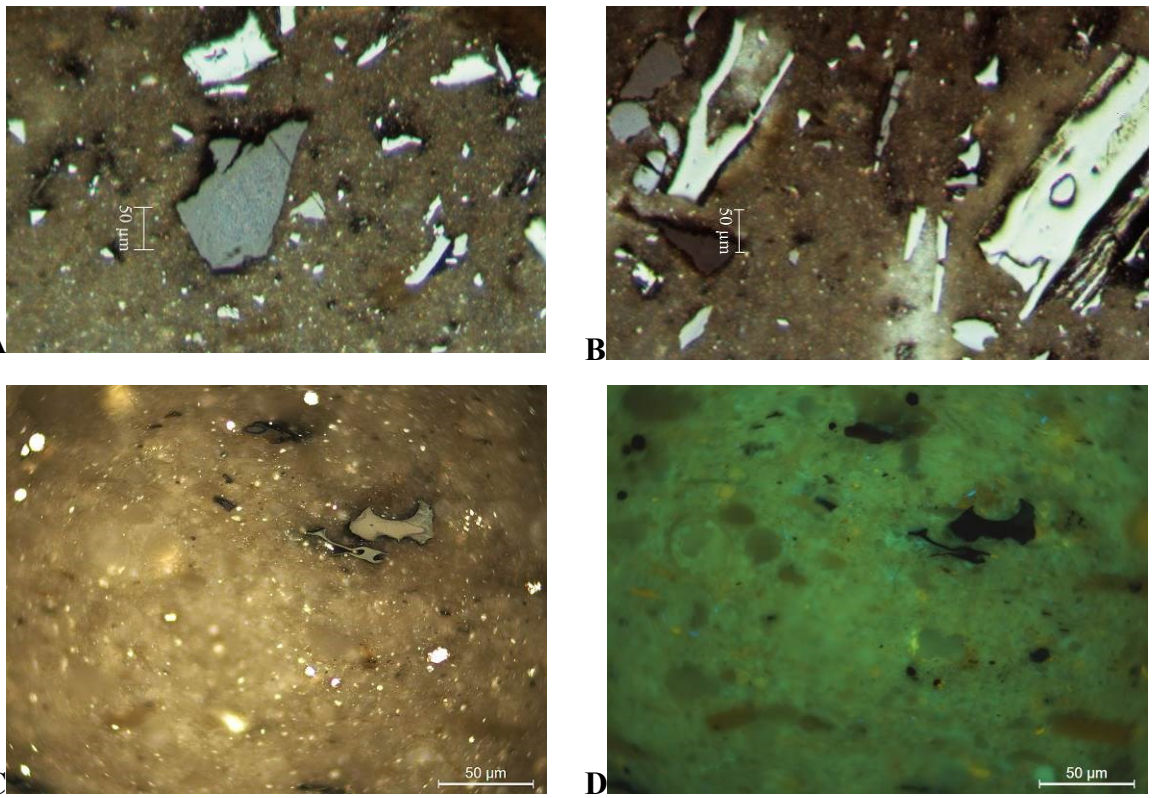

Fig. 4-34: Photomicrographs illustrating the OMFNot 1in an organic concentrate prepared by density separation (A, B) and cross-section perpendicular to the bedding plane (C, D).
A), Indigenous vitrinite (grey) and oxidised vitrinite (light grey) surrounded by inertodetrinite (white); B), Different examples of fusinite (white), and dark grey and light grey vitrinite particles. Reflected white light, oil immersion; C), OMFNot1 in cross-section, reflected white light oil immersion. Note grey reflecting vitrinite particles and light grey reflecting fusinite partciles; D), Same view in fluorescence mode, oil immersion.

4.2.3.2.2. OMFNot 2: Bituminous limestone and bituminous calcareous shales with low content of zooclasts and increased content of sporinite and telalginite

Maceral composition of OMFNot 2

The increased content of sporinite, telalginite and zooclasts is the principal characteristic of this organic microfacies (Fig. 4-35). The content of sporinite and telalginite is more or less equal and may reach 0.8 vol.%. The content of zooclasts drops to a low of 3.0 vol.%. The percentage of liptodetrinite is higher than that of lamalginite. It reaches a maximum of 17.0 vol.%, while lamalginite is 8.9 vol.%. In contrast to the previously described organic microfacies, the content of bituminite increases and reaches 2.9 vol.%. Inertinite macerals predominate among the terrestrial organic matter and reach 1.3 vol.%, while vitrinite makes up only 0.2 vol.%.

Mineral composition of OMFNot 2

This organic microfacies is associated with bituminous limestones and bituminous calcareous shales, locally bioturbated. The content of groundmass varies from 66.4 to 84.9 vol.%. The amount of pyrite reaches 6.9 vol.% (Fig.4-35).

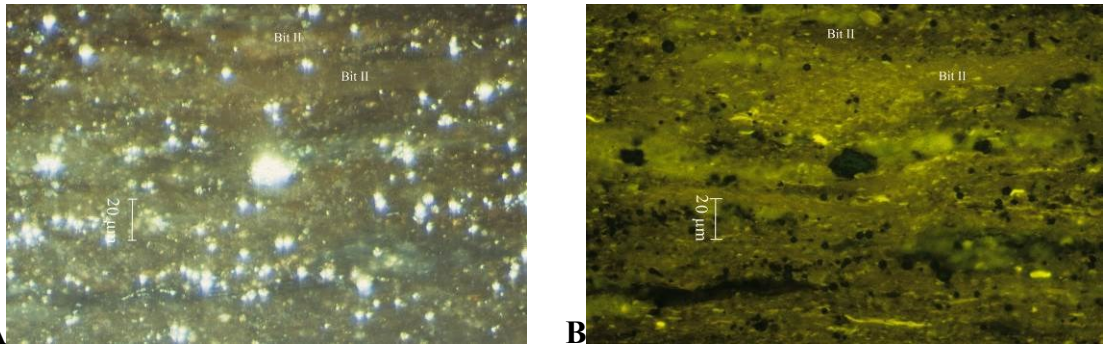

Fig. 4-35: Example of bituminite II in OMFNot 2.
A), Reflected white light, oil immersion; B), Same field of view, fluorescence mode, oil immersion. Note the yellow-orange fluorescence colour of the bituminite II (Bit II) with numerous liptodetrinite inclusions of a yellow fluorescence of high intensity.

4.2.3.2.3. OMFNot 3: Bituminous shales and limestone with increased content of liptodetrinite and bituminite

Maceral composition of OMFNot 3

This organic microfacies is characterised by a decreased content of sporinite, telalginite and zooclasts, while that of liptodetrinite, lamalginite and bituminite increases. Compared to OMFNot2, the content of bituminite reaches a high of 8.0 vol.%. Liptodetrinite is still predominant with percentages ranging from 2.9 to 16.4 vol.%, but the quantity of lamalginite slightly increases to a high of 12.8 vol.%. (Fig. 4-36).

Mineral composition of OMFNot 3

This microfacies occurs in association with bituminous shales and limestones with a low content of zooclasts, dipping to a low of 0.1 vol.%. The content of groundmass varies between 63.5 and 88.1 vol.%. The percentage of pyrite varies from 3.9 to 5.5 vol.%.

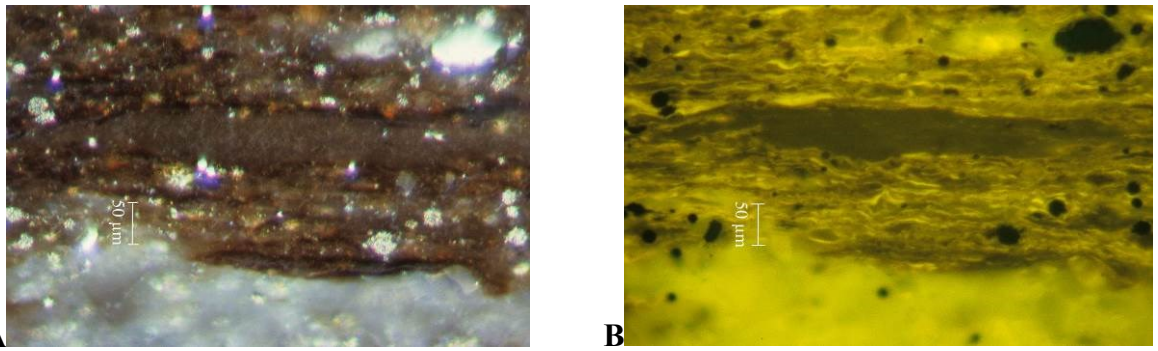

Fig. 4-36: General microscopic view of OMFNot 3.
A) Reflected white light, oil immersion; B), Same field of view, fluorescence mode, oil immersion. Note the high content of the lamalginite well illustrated in B.

4.2.3.2.4. OMFNot 4: Bituminous shales and calcareous shales characterised by increased content of telalginite together with inertinite

Maceral composition of OMFNot 4

Organic matter is represented by an increased content of telalginite and inertinite, probably indicating a dry climate, leading to temporary oxygenation of the water column. The amount of telalginite reaches 0.4 vol.%, while the inertinite percentage rises to a high of 1.9 vol.%. The content of lamalginite and liptodetrinite is high, ranging from 0.0 to 9.7 vol.% and from 2.7 to 11.5 vol.% respectively. The percentage of bituminite is variable, ranging from 0.3 to 8.6 vol.% (Fig. 4-37).

Mineral composition of OMFNot 4

This microfacies is hosted by bituminous calcareous shales, locally bioturbated. The content of groundmass ranges from 60.6 to 88.1 vol.%. The percentage of pyrite ranges between 2.9 and 5.4 vol.%.

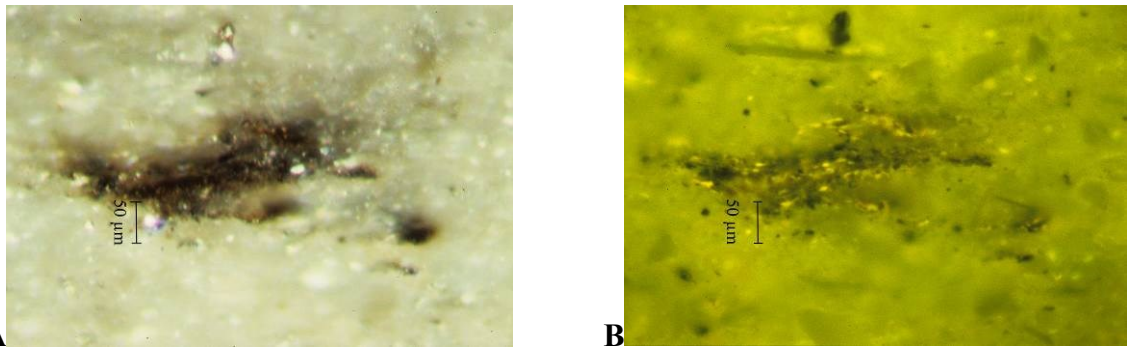

Fig. 4-37: Photomicrographs illustrating example of the bituminite I in OMFNot 4.
A), Reflected white light, oil immersion; B), Same field of view, fluorescence mode, oil immersion.

4.2.3.2.5. OMFNot 5: Bituminous shales and calcareous shales enriched in telalginite, bituminite and sporinite

Maceral composition of OMFNot 5

An increased content of telalginite, bituminite and sporinite is characteristic of this microfacies. The sporinite and telalginite content reaches 0.4 and 0.5 vol.% respectively. Simultaneously, the percentage of inertinite increases to a high of 3.1vol.% %. The contents of lamalginite and liptodetrinite are equally high and reach 3.1 vol.%. Bituminite values climb to a high of 26.1 vol.%.

Mineral composition of OMFNot 5

This organic microfacies is hosted by calcareous shales and bituminous shales, in part bioturbated (Fig. 4-38). The percentage of groundmass ranges from 66.2 to 88.7 vol.%. The content of pyrite ranges between 1.8 and 3.5 vol.%. However, in one sample its quantity reaches a high of 15.9 vol.%.

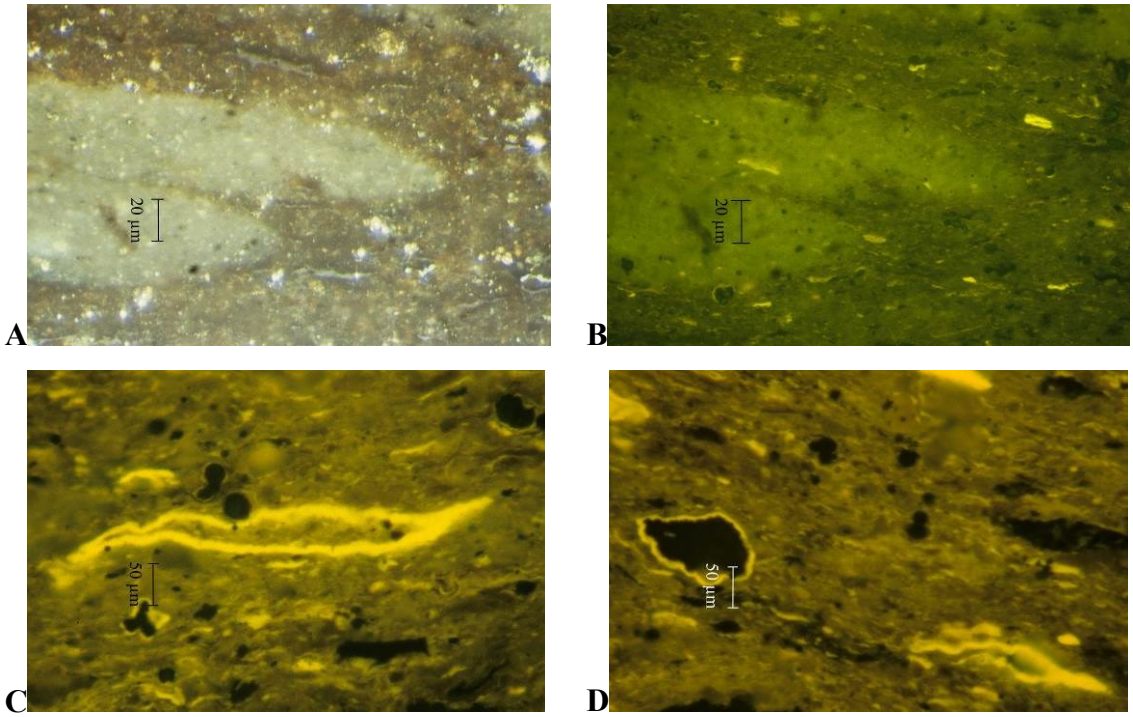

Fig. 4-38: Photomicrographs showing the particularities of OMFNot 5.
A), Examples of burrows. Reflected white light, oil immersion (left); B) same field of view, fluorescence mode, oil immersion (right); C), Telalginite showing a yellow fluorescence of high intensity; D), Telalginite and bituminite I (under the scale bar) with yellow fluorescing liptodetrinite inclusions.

4.2.3.2.6. OMFNot 6: Calcareous shales enriched in inertinite

Maceral composition of OMFNot 6

In this organic microfacies, the terrestrial organic matter prevails (Fig.4-39). Inertinite content reaches 1.6 vol.%, while vitrinite content attains only 0.8 vol.%. The percentage of zooclasts makes up 0.4 vol.%. Amorphous organic matter reaches only 0.8 vol.%.

This microfacies is hosted by calcareous shales. The content of groundmass reaches 93.8 vol.%. Its pyrite content reaches 2.5 vol.%.

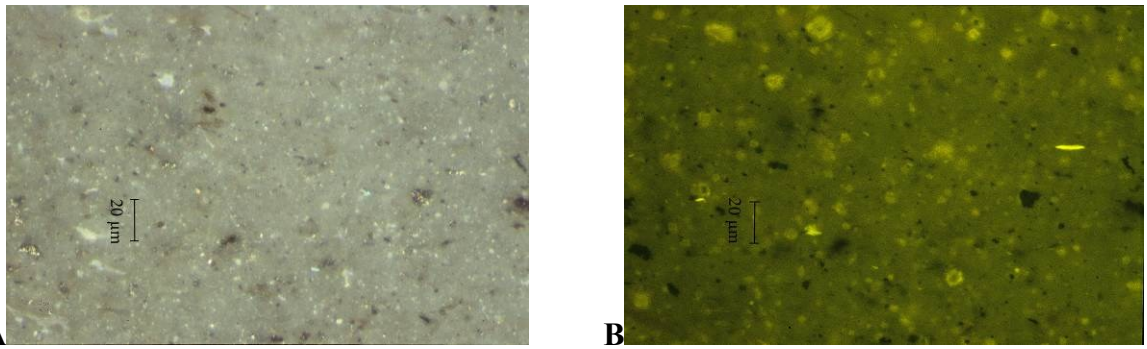

Fig. 4-39: Photomicrographs showing the organic poor calcareous groundmass of OMFNot 6 with scattered numerous particles of inertodetrinite.
A), Reflected white light, oil immersion; B), Same field of view, fluorescence mode, oil immersion.

4.2.3.2.7. OMFNot 7: Bituminous calcareous shales enriched in vitrinite

Maceral and mineral composition of OMFNot 7

This microfacies is similar to OMFNot 6, however, vitrinite is the sole organic component which constitutes this microfacies. Its content ranges from 4.0 to 5.1 vol.%. The amount of zooclasts increases to 1.3 vol.%. The organic microfacies OMFNot7 is associated with calcareous bituminous shales locally burrowed. The content of groundmass reaches 92.1 vol.%. The pyrite percentage is in a range between 2.5 and 4.0 vol.% (Fig.4-40).

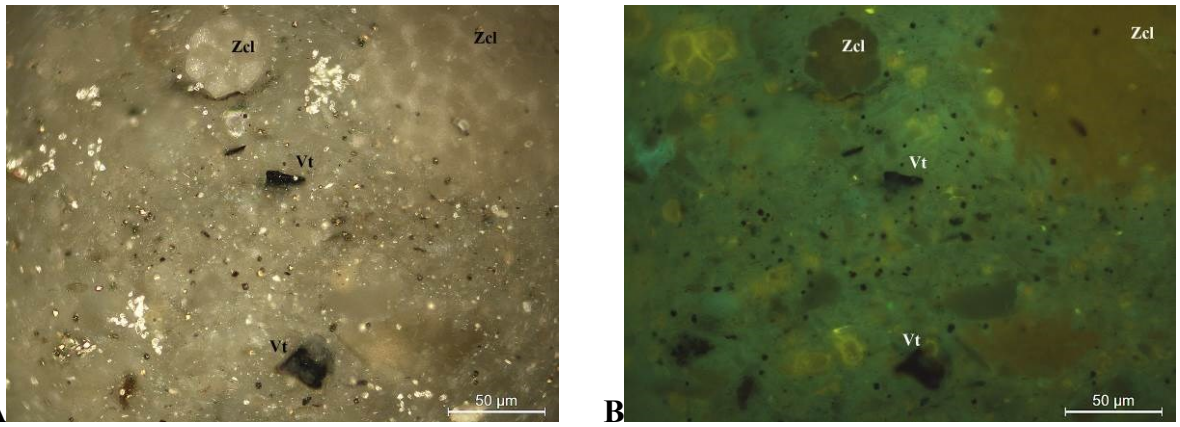

Fig. 4-40: Photomicrographs showing the organic poor calcareous groundmass of the OMFNot 7 with scattered numerous particles of vitrinite (Vt). Note Echinoderms (Zcl) in the top - centre and top - right.
A), Reflected white light, oil immersion. B), Same field of view, fluorescence mode, oil immersion.

4.2.3.3. Bisingen-1002 well

4.2.3.3.1. OMFBis 1: Claystones and calcareous shales with high input of vitrinite maceral and suppressed content of zooclasts

Maceral composition of OMFBis 1

This organic microfacies is characterised by a high content of terrestrial organic matter associated with a low zooclast quantity, which does not exceed 0.7 vol.% (Fig.4-41 A, B; APPENDIX B). Among all the organic matter, vitrinite prevails. Its content varies from 1.4 to 2.5 vol.%. The percentage of sporinite ranges from 0.3 to 1.2 vol.%, while that of other macerals of marine origin such as lamalginite, liptodetrinite, bituminite I and bituminite III, is suppressed.

Mineral composition of OMFBis 1

The organic microfacies OMFBis 1 is associated with claystones and calcareous shales. The content of clayey groundmass reaches 96.7 vol.%. The content of pyrite reaches only 2.0 vol.%.

4.2.3.3.2. OMFBis 2: Calcareous shales and limestone enriched in vitrinite and with a high content of zooclasts

Maceral composition of OMFBis 2

This organic microfacies is represented by a high content of zooclasts ranging from 2.2 to 14.5 vol.% (Fig.4-41 C, D). Among all the organic matter, vitrinite macerals are predominant and reach 1.6 vol.%. The percentage of other macerals is low. In OMFBis 2 sporinite, liptodetrinite and bituminites are also represented, but in low quantities.

Mineral composition of OMFBis 2

This organic microfacies occurs in calcareous shales and limestones. The content of clayey groundmass varies from 4.4 to 58.5 vol.%, while that of calcareous groundmass varies from 35.7 to 97.3 vol.%. The percentage of pyrite is marginally higher than in OMFBis 1 and reaches 4.0 vol.%.

4.2.3.3.3. OMFBis 3: Bituminous shales enriched in bituminite I with moderate content of zooclasts

Maceral composition of OMFBis 3

Lamalginite, liptodetrinite, bituminite I and bituminite III are common constituents of this organic microfacies (Fig 4-42 A, B). Among the amorphous organic matter, bituminite I is predominant with percentages ranging from 0.9 to 4.3 vol.%, whereas the content of bituminite III only reaches a high of 0.9 vol.%. Among the terrestrial organic matter, inertinite is slightly dominant with percentages ranging from 0.0 to 0.8 vol.%, but the content of vitrinite makes up 0.4 vol.%. The sporinite quantity is relatively low, but in one sample reaches a high of 1.1 vol.%.

Mineral composition of OMFBis 3

This organic microfacies is associated with bituminous shales. The content of clayey groundmass varies between 19.4 to 77.3 vol.%, that of calcareous groundmass ranges from

16.0 to 57.9 vol.%. The content of pyrite ranges from 2.0 to 3.0 vol.%. The percentage of zooclasts decreases to 9.8 vol.%.

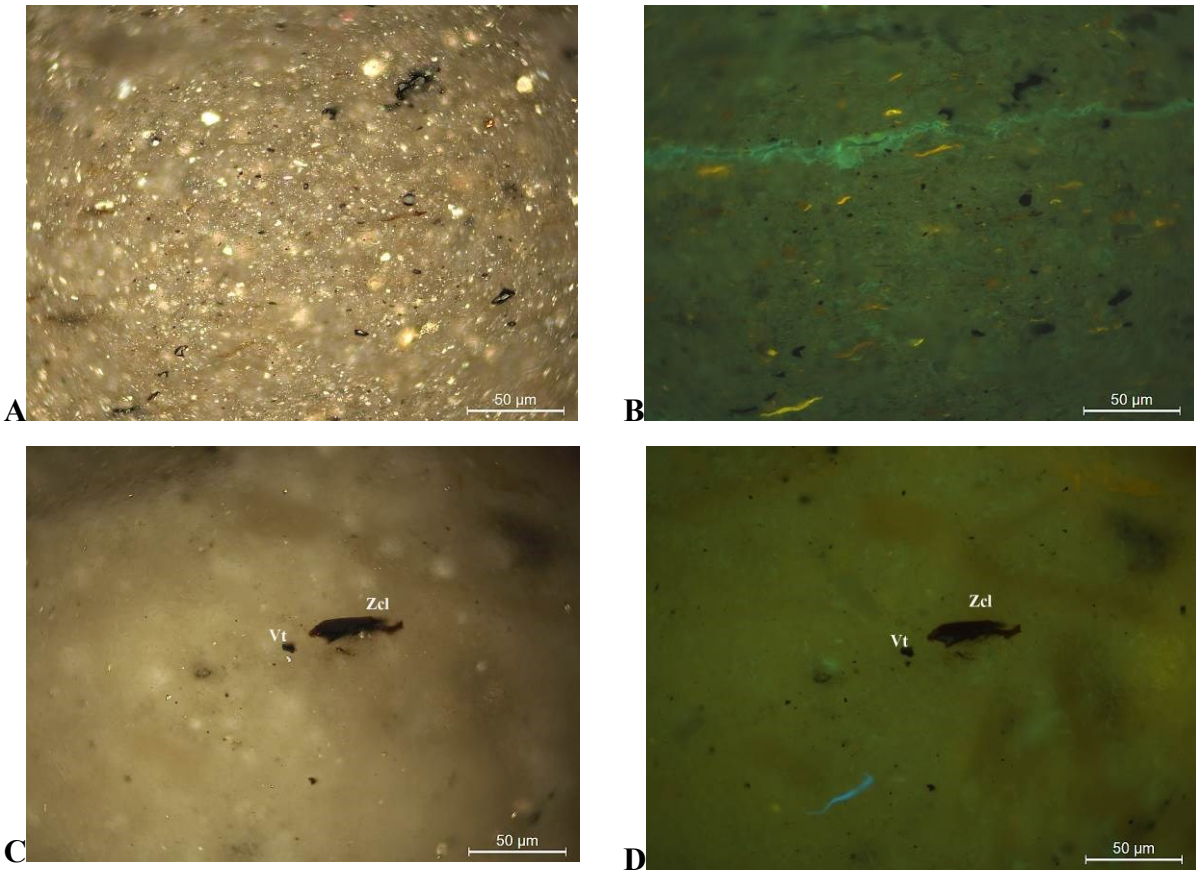

Fig. 4-41: Photomicrographs showing the organic poor calcareous groundmass of the OMFBis 1 and OMFBis 2. A), View of OMFBis 1 in reflected white light, oil immersion. Note small particles of recycled vitrinite; B), Same view in fluorescence mode, oil immersion; C), View of OMFBis 2 in reflected white light, oil immersion. Note the grey particle of indigenous vitrinite (Vt) and zooclasts (Zcl); D), Same view in fluorescence mode, oil immersion.

4.2.3.3.4. OMFBis 4: Bituminous shales with high content of zooclasts

Maceral and mineral composition of OMFBis 4

The percentage of zooclasts ranges between 17.6 and 18.3 vol.%, the content of telalginite marginally rises to 0.3 vol.% (Fig. 4-42 C,D). This organic microfacies occurs in association with bituminous shales. The content of clayey groundmass ranges from 32.7 to 34.9 vol.%, and that of calcareous groundmass varies from 31.3 to 42.5 vol.%. The content of pyrite reaches 3.0 vol.%.

4.2.3.3.5. OMFBis 5: Bituminous limestone poor in organic matter

Maceral and mineral composition of OMFBis 5

This organic microfacies has a low content of any type of organic matter and was identified only in one sample. The organic microfacies OMFBis5 was identified in a bituminous limestone bed. The percentage of calcareous groundmass reaches 96.0 vol.%, while the content of clayey groundmass reaches 3.0 vol.%. The content of pyrite is low, reaching 1.0 vol.% (Fig.4-43 A, B).

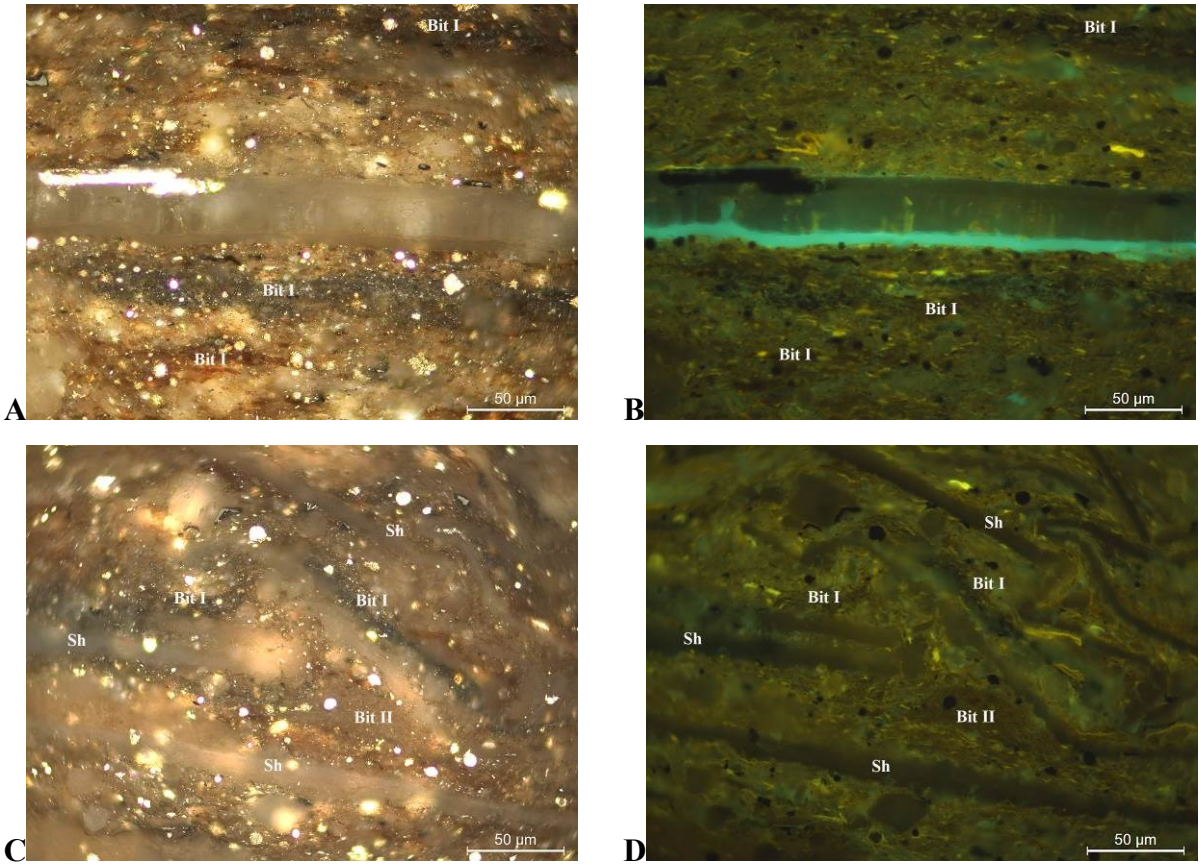

Fig. 4-42: Photomicrographs showing the organic poor calcareous groundmass of the OMFBis 3 and OMFBis 4. A), View of OMFBis 3 in reflected white light, oil immersion. Note numerous bituminite I (Bit I); B), Same view in fluorescence mode, oil immersion; C), View of OMFBis 4 in reflected white light, oil immersion. Note the high content of shells (Sh) and bituminite I (Bit I); D), Same view in fluorescence mode, oil immersion.

4.2.3.3.6. OMFBis 6: Bituminous shales enriched in bituminite I with low content of zooclasts

Maceral and mineral composition of OMFBis 6

This marine organic matter-dominated organic microfacies is similar to that described as OMFBis3. However, the content of zooclasts decreases to 1.4 vol.%. The quantities of liptodetrinite and lamalginite are similar and reach a maximum of 9.2 vol.%. The telalginite content makes up only 0.2 vol.%. Among the amorphous organic matter, bituminite I prevails with percentages ranging between 2.9 and 9.0 vol.%, whereas the content of bituminite III

reaches only 0.8 vol.%. This organic microfacies is hosted by bituminous shales. The content of clayey groundmass ranges from 16.4 to 51.8 vol.%, while calcareous groundmass ranges from 29.2 to 62.0 vol.%. The percentage of pyrite comprises from 3.0 to 5.0 vol.% (Fig. 4-43 C, D).

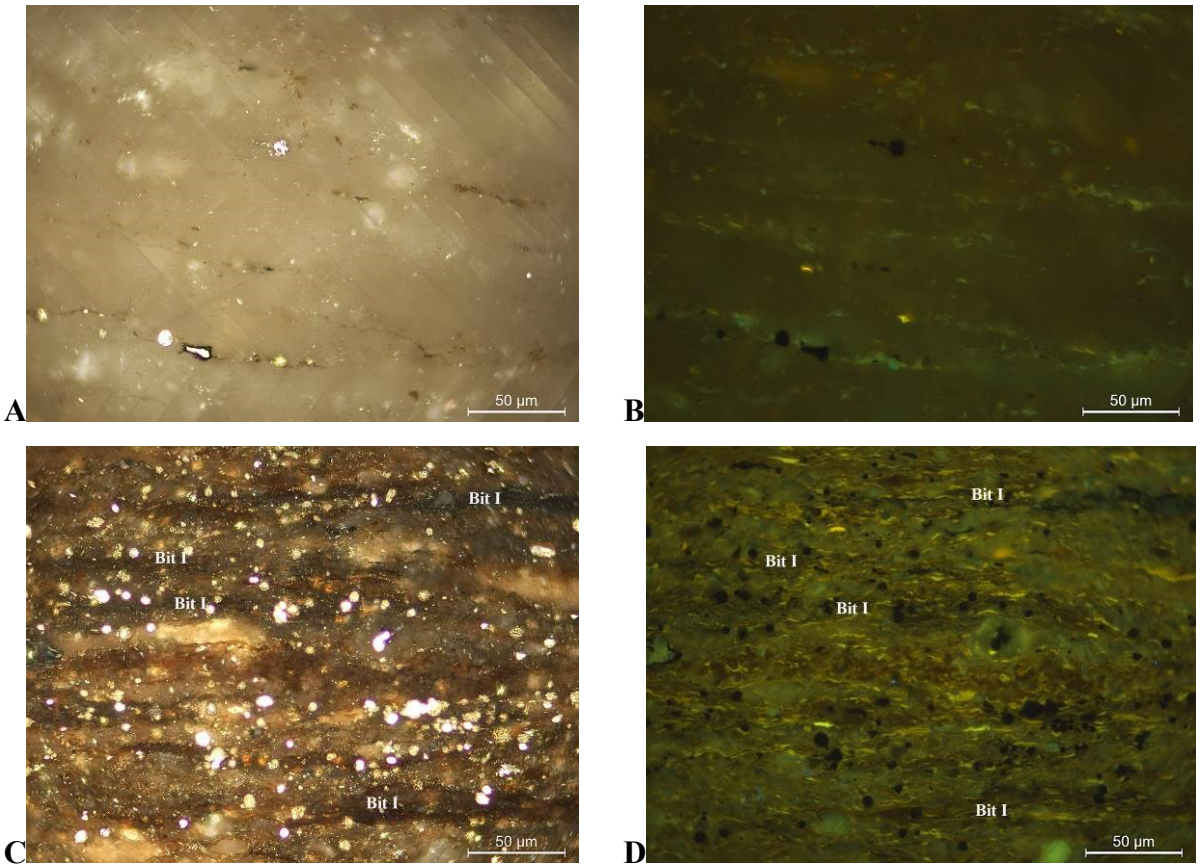

Fig. 4-43: Photomicrographs showing the organic poor calcareous groundmass of the OMFBis 5 (Nagelkalk) and OMFBis 6.
A), View of OMFBis 5 in reflected white light, oil immersion; B), Same view in fluorescence mode, oil immersion; C), View of OMFBis 6 in reflected white light, oil immersion. Note the high content of bituminite I (Bit I); D), Same view in fluorescence mode, oil immersion.

4.2.3.3.7. OMFBis 7: Bituminous limestone with high content of lamalginite and liptodetrinite

Maceral composition of OMFBis 7

Lamalginite and liptodetrinite characterise this microfacies. The lamalginite content ranges from 1.8 to 2.5 vol.%, whereas that of liptodetrinite varies from 5.7 to 9.6 vol.%. Among the terrestrial organic matter, only the inertinite maceral is represented, the content of which dips to a low of 0.4 vol.%. Among the amorphous organic matter, only bituminite I is represented, with percentages reaching 0.5 vol.% (Fig. 4-44 A, B).

Mineral composition of OMFBis 7

Zooclasts are absent. This organic microfacies is associated with bituminous limestones, in which the percentage of pyrite reaches 4.0 vol.%. The content of clayey groundmass varies from 0.2 to 0.6 vol.%, that of calcareous groundmass ranges from 90.7 to 93.1 vol.%

4.2.3.3.8. OMFBis 8: Bituminous shales with high content of lamalginite, bituminite I and liptodetrinite

Maceral composition of OMFBis 8

A relatively high content of lamalginite, bituminite I and liptodetrinite are the principal characteristics of this organic microfacies (Fig. 4-44 C, D). The lamalginite content reaches 12.2 vol.%, liptodetrinite 7.8 vol.% and the percentage of bituminite I ranges from 3.7 to 28.4 vol.%. Bituminite I prevails among the amorphous organic matter. The content of terrestrial organic matter is low. It is dominated by inertinite, whose quantity reaches 1.1 vol.%. The percentage of telalginite and sporinite is equally low and reaches a maximum of 1.1 vol.%. The amount of zooclasts ranges from 0.3 to 2.9 vol.%.

Mineral composition of OMFBis 8

This organic microfacies is commonly found in bituminous shales. The content of clayey groundmass ranges from 41.9 to 73.1 vol.%, while calcareous groundmass varies from 6.2 to 28.1 vol.%. The content of pyrite ranges from 3.0 to 11.0 vol.%.

4.2.3.3.9. OMFBis 9: Calcareous shales with high content of inertinite and zooclasts

Maceral composition of OMFBis 9

The content of liptodetrinite falls to a low of 1.5 vol.%. The percentage of inertinite ranges from 0.7 to 1.5 vol.% and the amount of zooclasts reaches a maximum of 4.7 vol.% (Fig. 4-44 E, F).

Mineral composition of OMFBis 9

This organic microfacies is associated with calcareous shales. The amount of clayey groundmass ranges from 67.7 vol.% to 91.7 vol.%, while calcareous groundmass varies from

6.0 to 21.6 vol.%. The content of pyrite reaches only 2.0 vol.%. Zooclasts and inertinite are the common constituents of this organic microfacies.

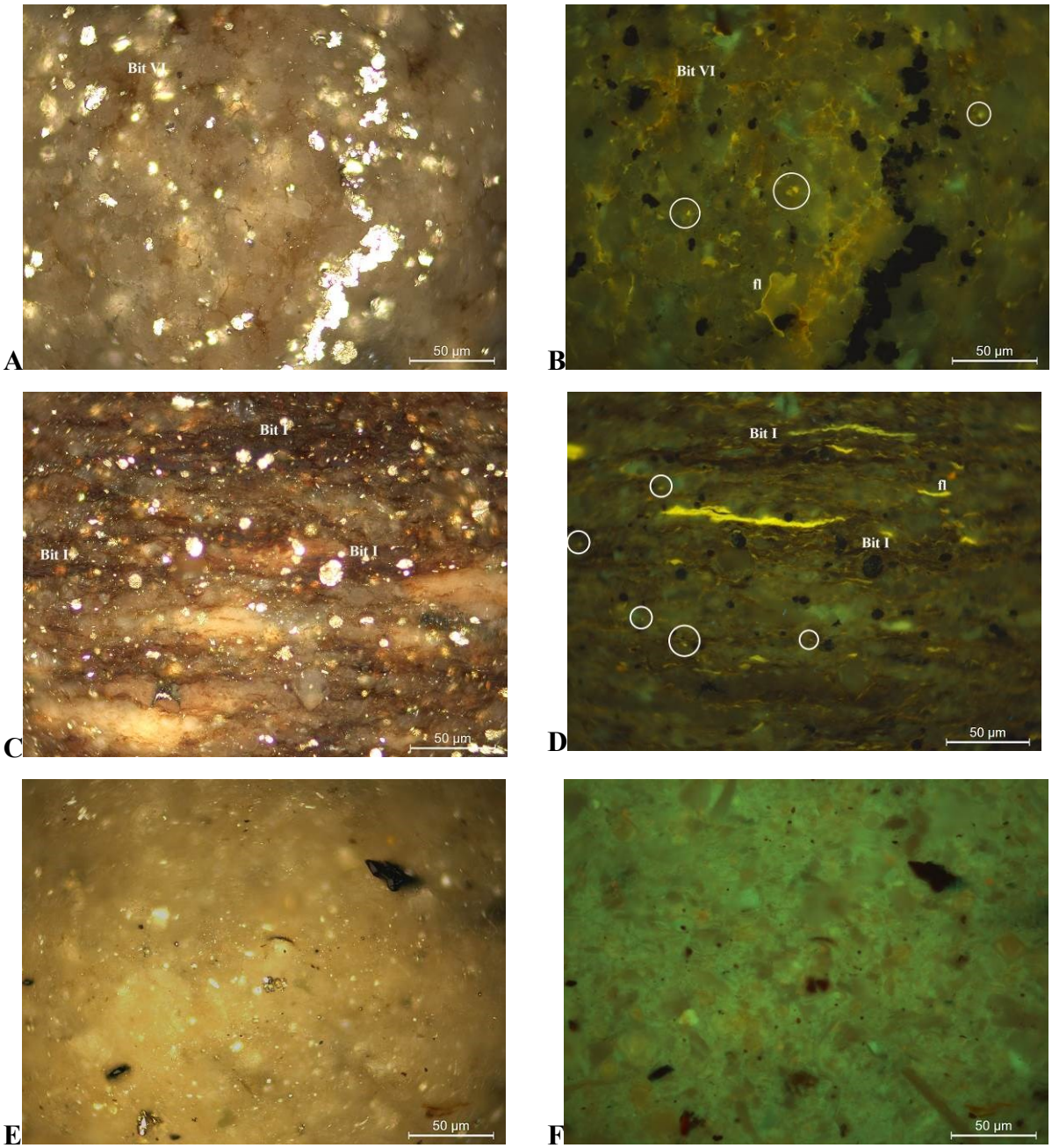

Fig. 4-44: Photomicrographs showing the OMFBis 7, OMFBis 8 and OMFBis 9.
A), View of OMFBis 7 in reflected white light, oil immersion; B), Same view in fluorescence mode, oil immersion. Note yellow fluorescing liptodetrinite, enclosed in white circles, filamentous lamalginite (fl) and bituminite VI (Bit VI); C), View of OMFBis 8 in reflected white light, oil immersion. Note the high content of bituminite I (Bit I). D), Same view in fluorescence mode, oil immersion. Note bituminite I (Bit I), yellow fluorescing liptodetrinite, enclosed in white circles, and filamentous lamalginite (fl) E), View of OMFBis 9 in reflected white light, oil immersion. F), Same view in fluorescence mode, oil immersion. Note numerous zooclasts, oil immersion.

4.2.4. Summary

In the West Netherlands Basin, in wells E and M, 5 organo-mineral microfacies were identified. In both wells, these organo-mineral microfacies show a resemblance. However, those in well M contain a higher amount of liptodetrinite than in well E. A variable quantity of bituminite V is a particularity of the identified microfacies from this sedimentary basin.

In the Lower Saxony Basin, 4 and 5 organo-mineral microfacies were identified in wells A and D respectively. These microfacies differ from well to well and show no similarities. In well D, similarly to well M, Posidonia Shale samples contain a high percentage of liptodetrinite. In organo-mineral microfacies from well A, a high content of bituminite II was encountered.

The highest number of organo-mineral microfacies was identified in wells in the South German Basin. There are 5, 7 and 9 organo-mineral microfacies from the Dotternhausen-1001 well, Notzingen-1017 well and Bisingen-1002 well respectively. These microfacies are poorly correlated between these wells. In addition, particularities of the organo-mineral microfacies are a repetition of microfacies containing burrows, the high content of specific types of bituminite or their enrichment in zooclasts, indicating rapid changes of paleoenvironmental conditions.

4.3. Geochemical features of the defined organo-mineral microfacies

4.3.1. General remarks

It is self-evident that petroleum generation results from the transformation of the kerogen buried in the sediments under the influence of temperature and pressure (Huc, 1990). The quality and the quantity of the generated petroleum products are controlled by different types of kerogen, which, in turn, are composed of variable assemblages of organic constituents insoluble in organic solvents (Huc, 1990). These organic constituents are formed under distinct environmental conditions. The properties of the kerogen within the same formation can significantly vary, not only from one sedimentary basin to another, but also within one formation itself. All these features are well-established and must be taken into account during the evaluation of the different source rocks (Huc, 1990).

As can be seen in Fig. 4-45, the HI and OI values of Posidonia Shale which derived from Rock Eval, plotted in a HI-OI diagram show a significant scatter. This scatter is determined by distinct paleoenvironmental conditions controlling the quality and quantity of

the preserved organic matter. Even the kerogen of one distinct type of organic matter may have a much higher generation potential than that of an assemblage of other different types.

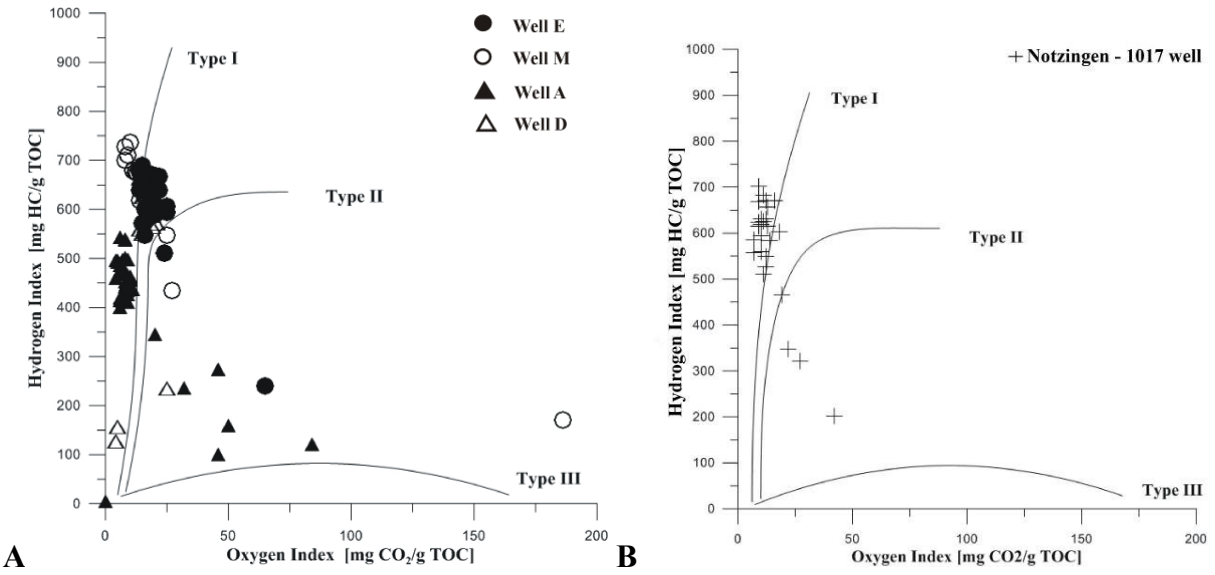

Fig. 4-45: Hydrogen Index (HI) versus Oxygen Index (OI) for the Posidonia Shale samples from the investigated wells.
A) The West Netherlands Basin (Well E and Well M) and the Lower Saxony Basin (Well A and Well D); B) The South German Basin, Notzingen-1017 well (Data from a previous unpublished study by B. Ligouis see Chapter 3).

The TOC of the Posidonia Shale Formation from the West Netherlands Basin and the Lower Saxony Basin shows a resemblance (Table 4-1; 4-2). TOC values are slightly lower in the Posidonia Shale in the Notzingen-1017 well in southern Germany. While the TOC values of Posidonia Shale do not show significant variations, the HI values differ notably (Table 4-1, 4-2, 4-3).

The highest values of HI are exhibited by bituminous shales from the West Netherlands Basin, while those of the Lower Saxony Basin are located lower in the diagram (Fig.4-45). Posidonia Shale from southern Germany contains higher values of HI than that from the Lower Saxony Basin, but lower than from the West Netherlands. Thus, the type of kerogen of Posidonia Formation from the West Netherlands and the South German Basin is type I/II, whereas that from the Lower Saxony Basin is type II. Nevertheless, some of the investigated samples fall within the area of type II/III kerogen. This indicates considerable oxygenation of the water column and an increasing number of scavengers (Table 4-1, 4-2, 4-3). The OI values of the Posidonia Shale in well A are lowest among all investigated wells. It

increases in sediments poor in organic matter from all the investigated wells (Table 4-1, 4-2, 4-3).

4.3.2. The West Netherlands Basin

In the West Netherlands Basin, results of the Rock-Eval pyrolysis revealed that TOC values are in the range of 0.9 to 16.6 % with an average of 9.0 %. HI for most of samples from well E shows values of more than 300 mg HC/g TOC with an average of 588 mg HC/g TOC, indicating good oil source rock. Only one sample yields HI of 239 mg HC/g TOC. OI does not show high variations, however, in the microfacies poor in organic matter, it climbs to a high of 65 mg CO_2/g TOC.

In well M, almost all samples show TOC values higher than 5 %, with an average of 9.2 %. HI is higher than in well E. It reaches values of between 434 and 737 mg of HC/g TOC with an average of 624 mg HC/g TOC. OI in well M is marginally lower, than in well E. However, OI in samples poor in organic matter attain a maximum of 186 mg CO_2/g TOC. Although organo-mineral microfacies in both wells from the West Netherlands Basin show a resemblance in organic matter composition, the values of geochemical indices exhibit a variation, indicating differences in the paleoenvironmental conditions in which these identified organo-mineral microfacies were deposited.

In well E, OMFN1 shows TOC values ranging from 3.4 to 13.3 % with an average of about 8.0 % . The HI is in a range between 548 and 676 mg HC/g TOC, averaging about 625 mg HC/g TOC. OI values show a variation of between 14 and 25 mg CO_2/g TOC. In OMFN 1 and OMFN 2, average TOC values show a resemblance, whereas OMFN 2 exhibits lower values of HI, probably indicating oxidation of the organic matter. This is in agreement with the greater OI in OMFN 2 than OMFN 1, which reaches 24 mg CO_2/g TOC.

In well M, OMFN 1 has TOC values ranging from 3.3 to 14.1 %. HI reaches a maximum of 728 mg HC/g TOC. OI varies between 8 and 27 mg CO_2/g TOC, with an average of about 17 mg CO_2/g TOC. OMFN 2 is characterised by higher TOC than OMFN 1. It reaches an average of 10.5 %. HI is in a range between 619 and 700 mg HC/g TOC, that is in agreement with the OI values ranging from 8 to 17 mg CO_2/g TOC, averaging about 13 mg CO_2/g TOC.

Thus, the event responsible for the high concentration of bituminite I in OMFN 2 in both wells coincides with the oxygenation of the water column in well E, whereas in well M

oxygen-depleted paleoenvironments were preserved. This explains the lower values of HI in well E than in well M.

Table 4-1: Relationships between the defined organo-mineral microfacies from the West Netherlands Basin and the results of Rock-Eval.

Well	Organo-mineral microfacies	TOC [%] range of values		TOC [%] average	HI [mg HC/g TOC] range of values		HI [mg HC/g TOC] average	OI [mg CO2/g TOC] range of values		OI [mg CO2/g TOC] average
Well E	OMFN 1	3.4	13.3	8.0	548	676	625	14	25	18
	OMFN 2	2.7	11.0	7.8	510	640	583	16	24	20
	OMFN 3	5.2	16.6	10.5	432	689	605	9	25	17
	OMFN 4	0.9		-	239		-	65		-
	OMFN 5	7.7	13.4	9.4	583	640	610	14	22	17
Well M	OMFN 1	3.3	14.1	8.3	434	728	607	8	27	17
	OMFN 2	0.5	12.4	10.5	619	700	663	8	17	13
	OMFN 3	11.4	16.8	14.7	674	710	692	9	13	11
	OMFN 4	0.9		-	170		-	186		-
	OMFN 5	6.2	13.1	9.1	604	737	660	10	20	15

OMFN 1: Low bituminous limestone with low content of bituminites; OMFN 2: Bituminous marly limestone enriched in bituminite I; OMFN 3: Bituminous calcareous mudstone and marly limestone enriched in bituminite V; OMFN 4: Low bituminous limestone rich in liptodetrinite and discrete lamalginite; OMFN 5: Bituminous calcareous mudstone and limestone enriched in bituminite II.

The OMFN 3 microfacies shows lower values of TOC in well E than in well M. In well E, it reaches a maximum of 10.5 % compared to 14.7 % in well M. HI in well M is also greater than in well E (Table 4-1). This is in agreement with the lower values of OI in well M than in well E, showing an average of about 17 and 13 mg CO_2/g TOC respectively.

OMFN 4 in both wells shows equal values of TOC, which reaches 0.9 %. HI in well E is four times lower than in well M (Table 4-1). The poor preservation of the organic matter is in agreement with the high values of OI, reaching 65 and 186 mg CO_2/g TOC in well E and M respectively.

OMFN5 shows the same values of TOC in both wells, reaching an average about 9.4 and 9.1 % in wells E and M respectively. However, HI values are greater in well M than in well E. They are in a range between 583 and 640, and 604 and 737 mg HC/g TOC respectively. This inconsistency is in agreement with the OI, which shows more oxidised conditions in well E than in well M (Table 4-1).

4.3.3. The Lower Saxony Basin

In the Lower Saxony Basin, TOC values of most samples in well A are more than 5.0 %, with an average of 7.4 %, except for some samples poor in organic matter. In these

samples, the TOC varies from 0.6 to 2.4 %. Organic-rich shales have HI greater than 300 mg HC/g TOC, varying between 340 and 539 mg HC/g TOC and averaging about 416 mg HC/g TOC. Sediments poor in organic matter have HI values ranging from 96 to 240 mg HC/g TOC. OI values are high in the organo-mineral microfacies poor in organic matter. They range between 20 and 84 mg CO2/g TOC.

In well D, TOC ranges from 7.9 and 11.3 %, with an average of 8.7 %. However, in one sample, the TOC decreases dramatically to values of 1.5 %. In well D, HI yields values higher than in well A. It varies from 401 to 663 mg HC/g TOC, with an average of 599 mg HC/g TOC. Only one sample in well D yields 235 mg HC/g TOC. The OI, for other organo-mineral microfacies than those poor in organic matter, is slightly higher and reaches values from 14 to 20 mg CO_2/g TOC, with an average of 17 mg CO_2/g TOC.

The OMFLa 1 in well A shows the highest average values of TOC and HI, which are 10.4 % and 479 mg HC/g TOC respectively. This coincides with the low OI, which shows a minimum of 4 mg CO_2/g TOC, indicating strong anoxic conditions. In comparison, OMFLa 2 shows lower values of TOC, averaging about 8.2 %. HI is marginally lower, averaging about 457 mg HC/g TOC and OI indicates a marginal increase to a maximum of 11 mg CO_2/g TOC.

The OMFLa 3 shows an average of TOC of about 7.9 %. HI shows values ranging from 296 to 535 mg HC/g TOC. The OI is similar to that of OMFLa 2.

The OMFLa 4 represents an organically poor microfacies. It coincides with the lowest TOC values among all microfacies, ranging from 0.7 to 2.5 %. The HI reaches only 340 mg HC/g TOC. The OI values indicate oxygenated paleoenvironments. They reach 86 mg CO_2/g TOC.

In well D, OMFLd 2, OMFLd 3 and OMFLd 5 show marginal variations in TOC, HI and OI values. The highest values of TOC, reaching 11.3 %, were recorded in OMFLd2. HI yields the highest values as well, ranging from 550 to 663 mg HC/g TOC. OI reaches 17 mg CO_2/g TOC. Similarly, TOC, HI and OI of OMFLd3 show averages of about 8.8 %, 616 mg HC/g TOC and 18 mg CO_2/g TOC respectively.

OMFLd 1 and OMFLd 5 also show a resemblance in their geochemical parameters. In OMFLd 1, TOC reaches 8.3 %, HI, 599 mg HC/g TOC and OI, 19 mg CO_2/g TOC. By comparison, the OMFLd5 is characterised by a TOC average of about 8.6 %, an HI of 593 mg HC/ g TOC and an OI of 17mg CO_2/g TOC.

OMFLd 4 shows the lowest values of TOC, averaging 5.0 %. HI reaches an average value of about 420 mg HC/g TOC, and OI increases compared to the other microfacies, reaching 25 mg CO2/g TOC.

Table 4-2: Relationships between the organo-mineral microfacies defined in the Lower Saxony Basin and the results of Rock-Eval.

Well	Organo-mineral microfacies	TOC [%] range of values		TOC [%] average	HI [mg HC/g TOC] range of values		HI [mg HC/g TOC] average	OI [mg CO2/g TOC] range of values		OI [mg CO2/g TOC] average
Well A	OMFLa 1	8.1	11.2	10.4	456	492	479	4	6	5
	OMFLa 2	5.5	14.4	8.2	406	539	454	6	11	8
	OMFLa 3	5.5	9.6	7.9	396	535	449	6	10	8
	OMFLa 4	0.7	2.5	1.6	95	340	201	20	84	46
Well D	OMFLd 1	8.3		-	599		-	19		-
	OMFLd 2	7.2	11.3	9.3	550	663	617	14	21	17
	OMFLd 3	7.7	9.5	8.8	565	654	616	16	20	18
	OMFLd 4	1.5	8.4	5	235	606	420	22	25	23
	OMFLd 5	7.8	9.3	8.6	559	627	593	14	20	17

Well A. OMFLa 1: Bituminous calcareous mudstone enriched in terrestrial macerals with low content of bituminites; OMFLa 2: Bituminous limestone enriched in bituminite II; OMFLa 3: Bituminous limestone enriched in bituminite I; OMFLa 4: Bituminous limestone with low content of lamalginite.**Well B**. OMFLd1: Bituminous limestone enriched in bituminite II; OMFLd2: Bituminous limestone enriched in bituminite I; OMFLd3: Bituminous limestone with high content of filamentous lamalginite and decreased content of bituminites; OFLd4: Low bituminous limestone with low diversity of macerals; OMFLd5: Bituminous limestone with low content of discrete, filamentous lamalginite and bituminites.

The post-mature oil shales in well B from the Lower Saxony Basin have TOC ranging from 4.8 to 7.2 % and averaging about 6.1 %. HI dips to a low of 0 to 14 with an average of about 5.2 mg HC/g TOC, and OI shows values of 0 to 31 mg CO_2/g TOC. The results of organic petrological and organic geochemical investigations are discussed in more detail in Chapter 5.

4.3.4. The South German Basin

Posidonia Shale samples in the Notzingen-1017 well have TOC values which do not exceed 12 % (Table 4-3). HI ranges from 201 to 701 mg HC/g TOC. OI comprises values ranging from 9 to 27 mg CO_2/g TOC. In this well, 7 different organo-mineral microfacies were identified. All organo-mineral microfacies contain a similar average of TOC reaching about 5.3–5.8 %. However, for these microfacies, HI shows an average in a range between 535 and 635 mg HC/g TOC, indicating a different quality of the organic constituents. OMFNot4 and OMFNot5 have the highest average HI, reaching 634 and 635 mg HC/g TOC respectively. This coincides with the lowest values of OI, yielding 11 and 15 mg CO2/g TOC in OMFNot 4 and OMFNot 5 respectively.

OMFNot7, which is located at the bottom of the investigated Lias delta, shows the lowest values of TOC and HI, and the highest OI. The TOC dips to a low of 0.7 %. It coincides with the low amount of HI, reaching 201 mg HC/g TOC. OI in this organo-mineral microfacies reaches a high of 42 mg CO_2/g TOC.

Table 4-3: Relationships between the defined organo-mineral microfacies in Notzingen-1017 and Bisingen-1002 wells and the results of Rock-Eval.

Well	Organo-mineral microfacies	TOC [%]			HI [mg HC/g TOC]			OI [mg CO2/g TOC]		
		range of values		average	range of values		average	range of values		average
Notzingen-1017 well	OMFNot 1	-	-	-	-	-	-	-	-	-
	OMFNot 2	2.8	7.3	5.8	466	618	537	7	19	14
	OMFNot 3	6.3	11.2	8.5	559	701	615	7	13	9.8
	OMFNot 4	1.8	8.8	5.5	583	682	634	9	16	11
	OMFNot 5	3.2	7.2	5.3	603	671	635	10	18	13
	OMFNot 6	10.0		-	624		-	9		-
	OMFNot 7	0.7		-	201		-	42		-
Bisingen-1002 well	OMFBis 1	0.7	0.9	0.8	88	108	95	-	-	-
	OMFBis 2	0.1	0.5	0.3	75	211	120	-	-	-
	OMFBis 3	1.9	7.0	4.9	365	580	496	-	-	-
	OMFBis 4	4.0	5.6	4.8	567	597	582	-	-	-
	OMFBis 5	0.4		-	200		-	-	-	-
	OMFBis 6	1.7	7.8	5.4	251	548	490	-	-	-
	OMFBis 7	1.3	6.5	3.9	557	569	563	-	-	-
	OMFBis 8	4.0	8.5	6.3	408	586	522	-	-	-
	OMFBis 9	0.2	0.6	0.4	60	164	74.8	-	-	-

Notzingen-1017 well: OMFNot 1: Calcareous shales with high input of terrestrial organic matter; OMFNot 2: Bituminous limestone and bituminous calcareous shales with low content of zooclasts and increased content of sporinite and telalginite; OMFNot 3: Bituminous shales and limestone with increased content of liptodetrinite and bituminites; OMFNot 4: Bituminous shales and calcareous shales characterized by increased content of telalginite together with inertinite; OMFNot 5: Bituminous shales and calcareous shales enriched in telalginite, bituminite and sporintie; OMFNot 6: Calcareous shales enriched in inertinite;OMFNot 7: Bituminous calcareous shales enriched in vitrinite.
Bisingen-1002 well: OMFBis 1: Claystones and calcareous shales with high input of vitrinite maceral and suppressed content of zooclasts; OMFBis 2: Calcareous shales and limestone enriched in vitrinite and with a high content of zooclasts; OMFBis 3: Bituminous shales enriched in bituminite I with moderate content of zooclasts; OMFBis 4: Bituminous shales with high content of zooclasts; OMFBis 5: Bituminous limestone poor in organic matter; OMFBis 6: Bituminous shales enriched in bituminite I with low content of zooclasts; OMFBis 7: Bituminous limestone with high content of lamalginite and liptodetrinite; OMFBis 8: Bituminous shales with high content of lamalginite, bituminite I and liptodetrinite; OMFBis 9: Calcareous shales with high content of inertinite and zooclasts.

In the Bisingen-1002 well, the lowest TOC is recorded in the Lias delta, the Lias zeta and Dogger alpha. In these organo-mineral microfacies, the highest value of TOC does not exceed 0.9 % and HI is in the range between 60 and 211 mg HC/g TOC (Table 4-3). The highest HI among all identified organo-mineral microfacies was documented in OMFBis 4. However, TOC values range from 4.0 to 5.6 %. The highest TOC values were recorded in OMFBis 8. However, HI was lower than that measured in OMFBis4.

CHAPTER 5. MATURITY OF THE INVESTIGATED AREAS AND THERMAL EVOLUTION OF THE SELECTED LIPTINITE MACERALS

CONTENTS

5.1. Maturity of the Posidonia Shale from the West Netherlands, the Lower Saxony Basin and the South German Basin.

5.1.1. Vitrinite reflectance and Tmax

The relationship between vitrinite reflectance and Tmax values has been stated by many workers (Teichmüller and Durand, 1983; Barker *et al*., 1986; Espitalié, 1986a). In their work, they claim that there is a fairly linear correlation between vitrinite reflectance (VRr%) and Tmax values obtained on coal samples. Teichmüller and Durand (1983) stated that this correlation, however, is noticeable only within an interval which includes the oil window (from 0.5 %VRr correlated to a Tmax of 425 °C and 1.5 %VRr correlated to a Tmax of 475 °C) and that, below and above this interval, the absence of this correlation has been demonstrated. This inconsistency is related to the particularity of methodology for both these methods. While in vitrinite reflectance, measurements are obtained only on individual indigenous vitrinite particles, Tmax is obtained from the organic matter of a whole sample (Teichmüller and Durand, 1983). In organic-rich sediments, other than coals, the scattering of the data will be more significant due to the presence of different types of kerogen, the small size of the vitrinite particles and the influence of the groundmass and liptinite macerals on the Rock-Eval results (for more details see Chapter 3. Methodology of the research work.).

The Posidonia Shale from the West Netherlands Basin shows values of VRr ranging from 0.44 to 0.46 %Rr in well E and averaging about 0.44 %Rr. These values are in agreement with average Tmax values of 430 °C. In well M, however, the vitrinite reflectance was not measured as appropriate particles of indigenous vitrinite were not encountered. The Tmax of bituminous shaless in well M reaches 437 °C, with an average of 429 °C (APPENDIX A). These data enable the classification of the Posidonia Shale from the West Netherlands Basin as a source rock reaching the beginning of the oil window.

Vitrinite reflectance values of bituminous shaless from the Lower Saxony Basin were obtained in all investigated wells. However, Tmax data were only registered in wells A and D. Vitrinite reflectance of the Posidonia Shale from well A shows values varying from 0.54 to 0.60 %Rr and averaging about 0.55 %Rr (APPENDIX A). In well D, vitrinite reflectance reaches 0.55 %. These results are in agreement with the Tmax values averaging about 435 °C in well D and 446 °C in well A, indicating the beginning of the oil window (APPENDIX A).

In well B, vitrinite reflectance shows values ranging from 3.26 to 3.66 %Rr, with an average of 3.46 %Rr (APPENDIX A). The organic matter of this well is considered as post-mature and will be discussed below.

In the Dotternhausen-1001 well, vitrinite reflectance reaches 0.47 %Rr, with an average value of 0.43 %Rr (APPENDIX A). In the Notzingen-1017 well, vitrinite reflectance shows values ranging from 0.42 to 0.64 %Rr, with an average of 0.53 %Rr (APPENDIX A). Tmax of this well reaches 433 °C with an average of 430 °C (APPENDIX A). Accordingly, maturation of Posidonia Shale in the Dotternhausen-1001 well is close to the margin of the beginning of the oil window, whereas bituminous shaless in the Notzingen-1017 well fall in the oil window. Vitrinite reflectance of Posidonia Shale in the Bisingen-1002 well shows values from 0.45 to 0.59 % and corresponds to the beginning of the oil window (Prauss *et al.,* 1991).

5.1.2. Vitrinite and migrabitumen reflectance

Results of the migrabitumen reflectance were obtained on samples from well B and the Notzingen-1017 well. In post-mature well B, two generations of migrabitumen were distinguished — homogeneous and heterogeneous — whereas, in the Notzingen-1017 well, only heterogeneous migrabitumen was recorded. Heterogeneous migrabitumen has a dark grey colour in reflected white light and dark brown fluorescence. It occurs as a filling of the cracks and grain interspaces, as well as in association with zooclasts in post-mature well B. The migrabitumen content in well B ranges from 1.07 to 1.21 %, whereas in the mature Notzingen-1017 well, it varies from 0.22 to 0.32 %. Apart from heterogeneous migrabitumen, in the Notzingen-1017 well, reflectance of dark indigenous vitrinite particles was measured. These results reveal significant lowered reflectance values ranging from 0.34 to 0.47 %Rr, due to the impregnation of these vitrinites by lipoidal substances.

Homogeneous migrabitumen was only described in well B. It has a light grey colour in reflected white light and no fluorescence. In addition, this type shows a weak anisotropy. Homogeneous migrabitumen appears as replacement and/or coating of the post-mature telalginite, infilling of the fusinite cells or replacement of bituminite I. The origin of homogeneous migrabitumen is unknown, but it is presumed to be formed by exposure to relatively high temperatures. In well B, homogeneous migrabitumen reflectance was obtained only on two samples. Its reflectance values reach 3.43 and 3.53 %Rr.

The impact of the morphological type of migrabitumen on the reflectance data is significant. Typically, heterogeneous migrabitumen exhibits the lowest reflectance (Landis and Castaño, 1995). However, it should be taken into account that, for measurements, only migrabitumen occurring “in situ” is appropriated for providing valuable measurements.

Fig. 5-1 summarises the vitrinite reflectance values obtained in this study, as well as the calculated vitrinite-equivalent reflectance values from the migrabitumen reflectance, using the previously described formulas (Equation 1, Equation 2, Equation 3; for more details see Chapter 3. Methodology of the research work). Reflectance was measured either on vitrinite or migrabitumen because investigated samples do not contain both vitrinite and migrabitumen particles. Nevertheless, Fig. 5-1 A demonstrates the correlation trend between these two parameters. It is apparent that the reflectances obtained from Equation 2 and Equation 3 differ from those delivered by Equation 1. The difference can be explained by the regression equation of Jacob (1989) which includes only $\%BR_r$ values with a reflectance maximum of 2.7 %. Nevertheless, in well B, reflectance values measured on the homogeneous migrabitumen are very similar to those measured on vitrinite. This could be explained by the high maturity level, since the aromatisation degree of homogeneous bitumen and vitrinite is very close.

As can be seen in Fig. 5-1 B, in the Bisingen-1002 well, there is a good correlation between measured vitrinite reflectance and bituminite reflectance calculated according to Equation 3. Similarly, in the Notzingen-1017 well, the values of vitrinite equivalence calculated according to Equation 3 are in agreement with the measured vitrinite reflectance (5-1 C).

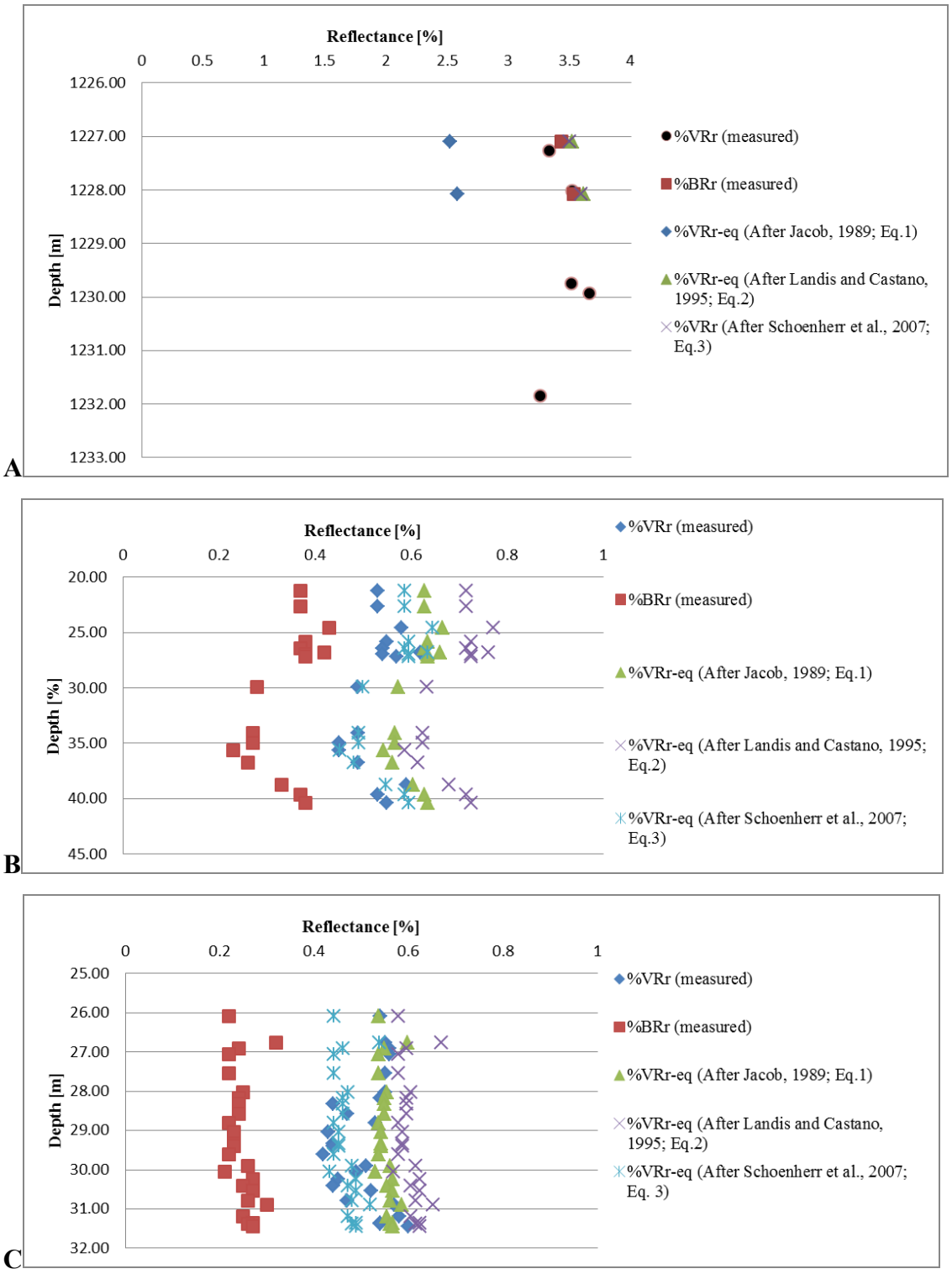

Fig. 5-1: Plot of measured vitrinite reflectance (VRr) and vitrinite-equivalent reflectance values calculated from the three different equations: formulas of Jacob (1989), Landis and Castaño (1995), Schoenherr *et al*. (2007). A), In well B. Note that the equivalent of the vitrinite reflectance has been calculated using values of homogeneous migrabitumen reflectance. On the contrary, in Bisingen-1002 well; (B), In the Notzingen-1017 well; (C), Values of heterogeneous migrabitumen reflectance have been used.
Reflectance data of vitrinite and migrabitumen in the Bisingen-1002 well, modified after Prauss *et al*., (1991). Reflectance data of vitrinite and migrabitumen in the Notzingen-1017 well, after B. Ligouis, (unpublished).

5.2. Changes in optical properties of selected liptinite macerals

Within this study, the optical properties of the macerals of the liptinite group in two wells A and B of different maturity located in northern Germany were characterised. The distance between the wells is about 44 km. The thickness of the investigated Posidonia Shale formation is about 35.15 m in well A and 5.2 m in well B. The bituminous shaless from the first well are composed of mudstone with indistinct or no lamination, marls, clayey marls and limestone, whereas the composition of the second well is more monotonous and composed of non-laminated mudstone. Our investigations show that the organic matter in well A is mature (Rr = 0.53 to 0.54 %), while in well B it is post-mature (Rr = 3.36 to 3.66 %).

The objective of this paragraph is not only to investigate the changes in the optical properties of liptinite macerals of mature and post-mature oil shale, but also processes leading to the formation of secondary macerals. In this work, the following terms: post-mature telalginite, post-mature bituminite I, post-mature bituminite II, and post-mature sporinite are used to describe the transformation “products” of these liptinite macerals at a high level of maturity.

5.2.1. Meta-telalginite

In the post-mature Posidonia Shale of well B, the optical properties of macerals have changed in response to the maturation process. In particular, the reflectance of all organic particles has increased considerably, whereas the brightness of the mineral groundmass decreased with simultaneous disappearance of the fluorescence of liptinite macerals, including the bituminous substances in the mineral groundmass. The fluorescence observed locally in the mineral groundmass of the post-mature samples is related to fluorescent minerals. These oil shales have undergone diagenetic, catagenetic and metagenetic processes. The abundance of secondary carbonate crystals and epigenetic pyrite, as well as micrinite, migrabitumen, and the occurrence of pyrolitic carbon (Fig. 5-2), shows the extent of the transformations which have affected the minerals and macerals. In addition, degassing pores and fissures have formed in vitrinite, which reflectance is characteristic of the metagenetic stage.

In the post-mature Posidonia Shale, relics of former telalginite, named post-mature telalginite, occur in three forms. These forms are identified on the basis of morphology.

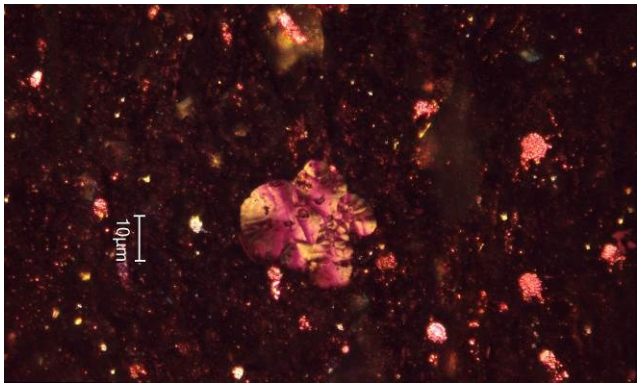

Fig. 5-2: Pyrolytic carbon in post-mature Posidonia Shale.
Reflected light, obliquely crossed polars, lambda plate, oil immersion.

Due to high temperature maturation, the transformed algal body left an empty space filled with secondary macerals or epigenetic minerals. Its shape is similar to that of the former alginite. Thus, we interpret these forms as a former alginite.

- The first form consists of migrabitumen associated with carbonate crystals as described before. However, the carbonate crystals are completely or partly recrystallised and have increased in size. Homogeneous (Rr: 1.0–1.2 %) or heterogeneous (Rr: 3.4–3.5 %) migrabitumen fills the interstices between the carbonate crystals and/or surrounds the carbonate fillings of the former algal bodies (Figs. 5-3 A; B). The recorded length of the transformed algal bodies ranges from 80 to 150 µm and their width varies from 15 to 30 µm. This form of post-mature telalginite occurs during diagenesis when telalginite expels oil and, as a consequence, a microporosity develops in the algal bodies. In these new interspaces, carbonate has started to grow. Botz *et al*. (2011) reported that the evolution of carbonates can already begin at 90 °C. Our observations seem to support this statement, since carbonate crystals can already occupy the alginite bodies of early mature bituminous shale (Fig. 5-4).

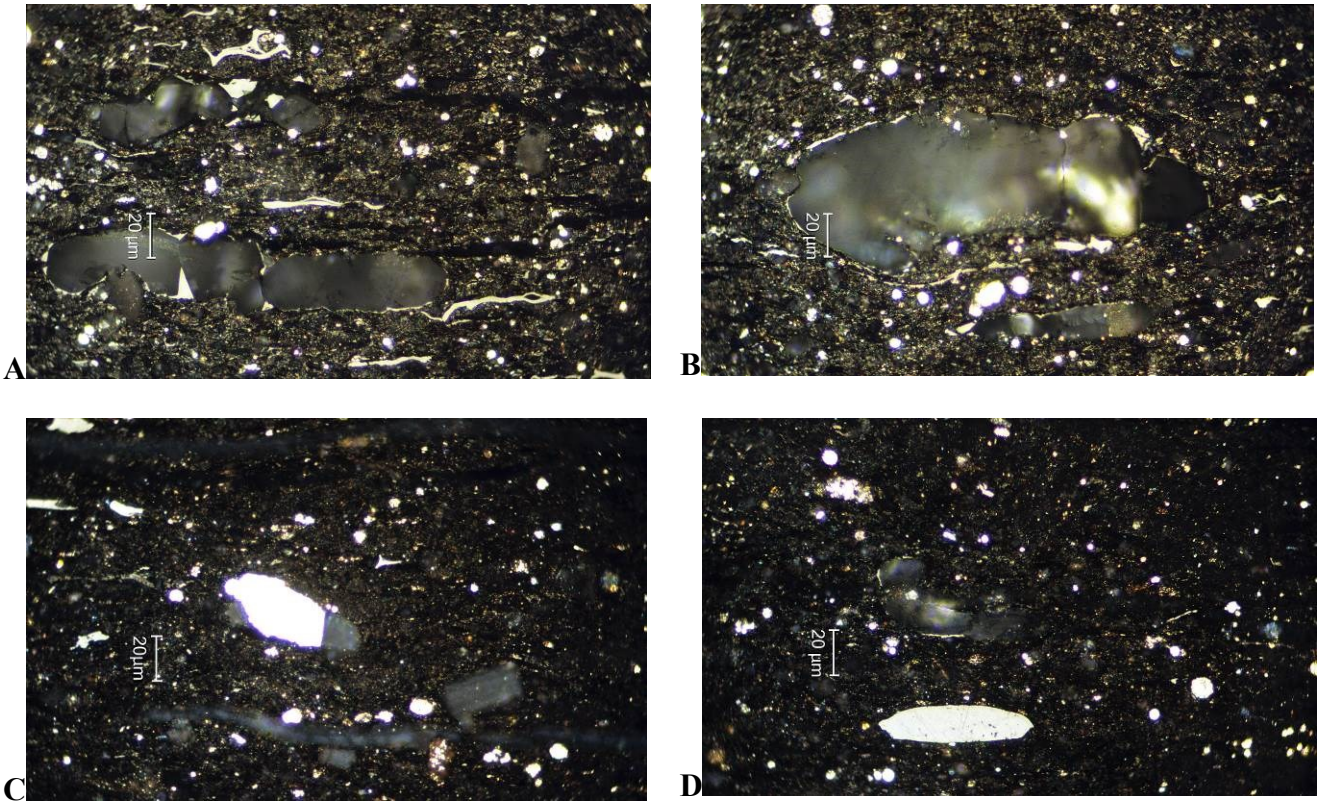

Fig. 5-3: Photomicrographs of post-mature telalginite in the samples of post-mature Posidonia Shale.
A), B), Post-mature telalginite bodies are filled with secondary carbonate crystals. Homogeneous migrabitumen fills the interstices between the crystals and surrounds the carbonate fillings. Note the dark colour of the micrinite (residual carbon) – rich mineral groundmass and the numerous pyrite framboids (bright spots); C), Post-mature telalginite body filled with calcareous crystals and epigenetic pyrite; D), Post-mature telalginite consisting of highly reflecting homogeneous migrabitumen (meta-telalginite). Reflected white light, oil immersion.

- The second post-mature telalginite form corresponds to algal bodies derived from telalginite, partially or completely replaced by epigenetic pyrite (Fig. 5-3 C). In the mature Posidonia Shale, pyrite occurs mostly as single crystals and framboids in the mineral bituminous groundmass and rarely as an infilling in lumens of telalginite. With maturation and temperature increase, pyrite recrystallises in the form of epigenetic pyrite (Berner, 1964; Berner, 1984), and its quantity and grain size expand. The presence of other sulphides usually allows the pyrite to recrystallise into euhedral grains (Berner, 1984). Hence, free sulphur and iron from silicates accompanied by high pressure and temperature lead to the formation of new modifications in pyrite (Berner, 1984; McClay and Ellis, 1983).

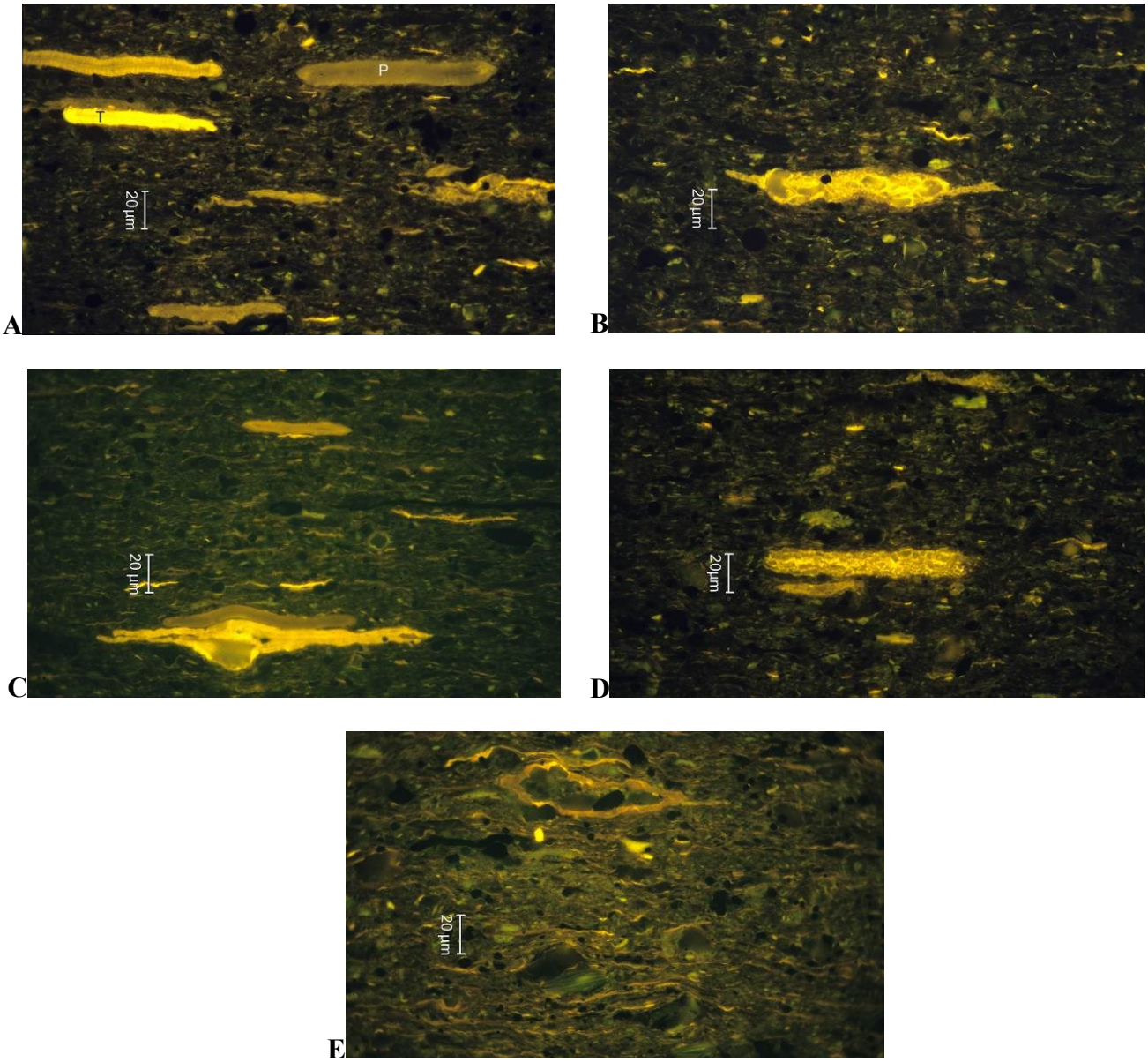

Fig. 5-4: Examples of telalginite in the samples of early mature Posidonia Shale.
A), Telalginite showing variable fluorescence colour and intensity derived from *Tasmanites* (T), *Pleurozonaria* (P); B),C), Spindle-shaped telalginite almost entirely filled by carbonate crystals showing bright yellow fluorescing oil droplets; D), telalginite derived from *Tasmanites* filled by very fine carbonate crystals and showing bright yellow fluorescing oil droplets. E), Spindle-shaped telalginite filled by calcareous crystals and framboidal pyrite, showing bright yellow fluorescing oil droplets. Fluorescence mode, oil immersion.

- The third form is rare and consists of alginite bodies partly or completely replaced by homogeneous migrabitumen (Fig. 5-3 D), identified as impsonite (Jacob, 1983, Jacob, 1989). In petroleum source rocks, migrabitumen is generated mostly from the liptinite macerals and redistributed by primary migration within the rock groundmass during late diagenesis and the early catagenetic stage (Mukhopadhyay, 1992). Post-mature telalginite, which consists of migrabitumen, corresponds to telalginite in which the processes of

calcification have not previously occurred. In this case, extreme increase of temperature increases the viscosity of the oil generated from telalginite kerogen. This evidence prevents fluid from migrating easily (Taylor *et al.,* 1998). Once the oil is generated, the migrabitumen starts to form and fills all the space in the former telalginite, completely replacing it.

The second and third forms of post-mature telalginite are smaller in size compared with the first one and their length does not exceed 60 µm. Moreover, the shape and size of the former algae are more or less well preserved.

In considering the content of post-mature telalginite in well B and the content of telalginite in mature well A, both contents show a resemblance (Fig. 5-5). Therefore, the identification and quantification of post-mature telalginite in post-mature oil shale provide genetic information (traceability of telalginite), which can be used to estimate the telalginite content of the bituminous shale before it reached the oil death line (~1.35 %VRr). This approach allows for the traceability of the telalginite maceral, which is an important oil-prone component throughout the catagenetic and metagenetic stages.

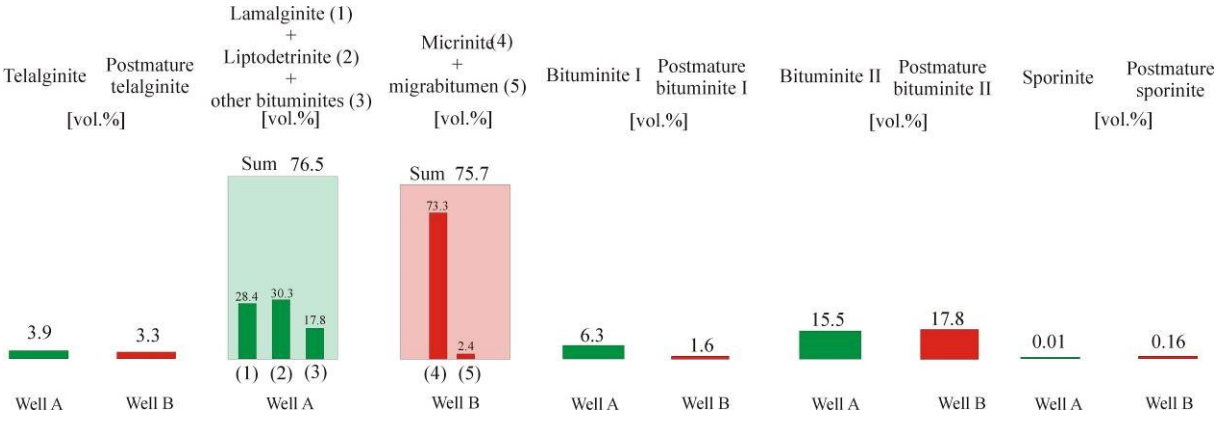

Fig. 5-5: Content of the selected liptinite macerals and their thermally altered analogies in well A and well B (mineral-free).
Comparison between the contents of liptinite macerals in well A and the contents of post-mature "liptinites" in well B (Liptinite = 100 %; mineral-free).

As can be seen in Fig.5-5, the abundance of telalginite in early mature Posidonia Shale (telalginite content = 3.9 vol.%) and the telalginite replacements in the post-mature Posidonia Shale (post-mature telalginite content = vol.3.3 %) are almost equivalent. The marginal difference observed in the percentage (Fig. 5-5) can be explained by lateral variations in the distribution of algae due to discrepancy in paleoenvironments.

5.2.2. Meta-lamalginite and meta-liptodetrinite

With increasing maturation, lamalginite as well as liptodetrinite lose their morphology due to the generation of petroleum-like substances, which are absorbed by the surrounding mineral groundmass. The residual products left after the hydrocarbon generation from lamalginite and liptodetrinite turn into fine granular micrinite (Taylor *et al.,* 1998, Teichmüller and Ottenjann, 1977). This evidence explains the difficulties encountered in relating the micrinite content to that of lamalginite and/or liptodetrinite. However, Fig.5-5 shows, as can be expected, a rather good correlation between the sum of the contents of lamalginite, liptodetrinite and "other bituminites" (76.5 vol.%; see the definition of "other bituminites" below) and the sum of the contents of micrinite and migrabitumen (75.7 vol.%). This proves that there is a clear genetic relationship between these two groups of components. Taking into account the labile character of bituminite and lamalginite, we assume that these macerals will strongly contribute to oil generation and expulsion (Bordenave et al., 1993; Stasiuk, 1994; Peters et al., 2005).

5.2.3. Meta-bituminites

Teichmüller (1974; 1990) studied the changes in the optical properties of bituminite in coals and oil shales of increasing maturity, and used the term "meta-bituminite" to classify the product of diagenetic transformation of bituminites, consisting of "a line of fine grain micrinite".

Based on the morphology, post-mature bituminite I (meta-bituminite I) in the investigated post-mature oil shales appears as light grey lenses, which consist of massive micrinite, or as homogeneous and non-fluorescing migrabitumen (Rr of migrabitumen: 1.0–1.2 %) (Fig.5-6 A). Relics of bituminite II, named post-mature bituminite II, appear as lens-shaped bodies which consist of a network of micrinite and small carbonate crystals (Fig.5-6 B). Moreover, the shape and size of the relics of bituminite I and bituminite II are preserved, which facilitates their identification.

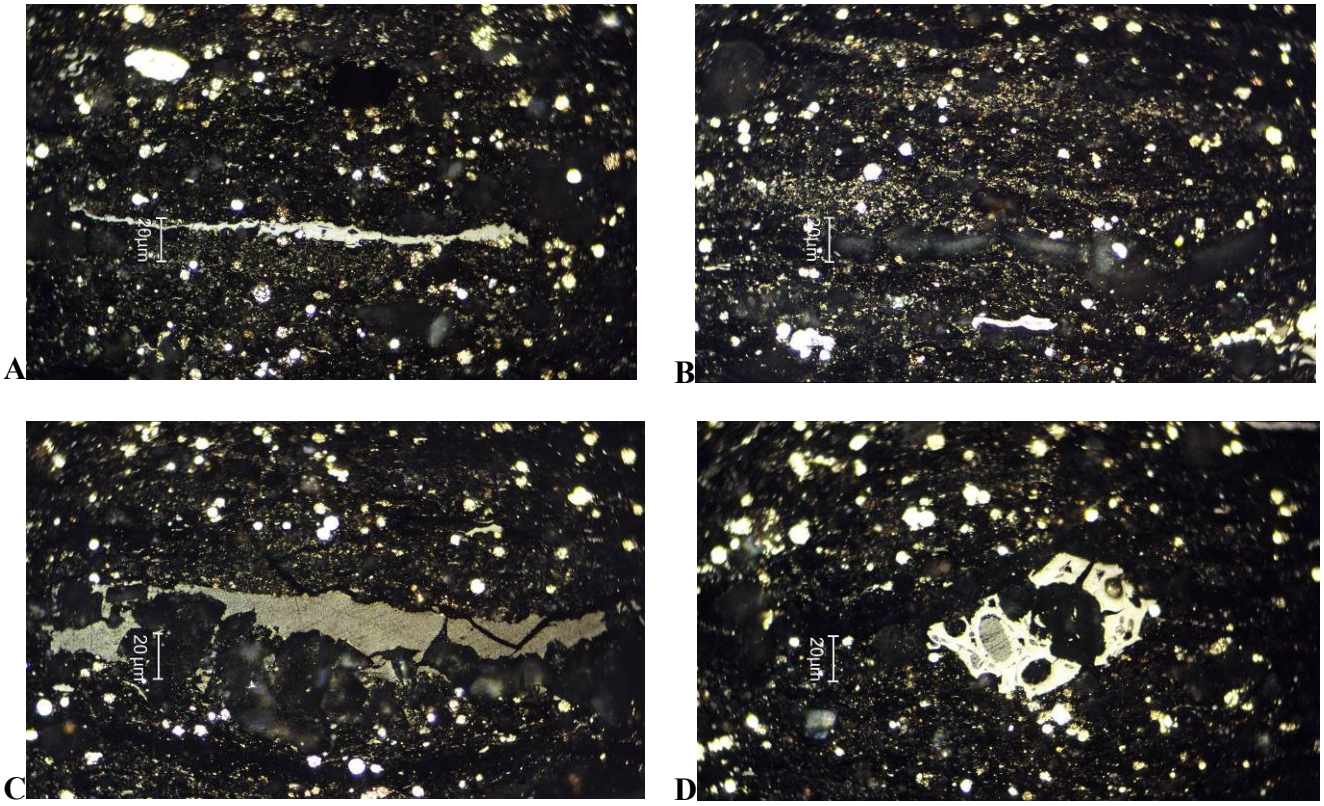

Fig. 5-6: Post-mature bituminites and examples of migrabitumen occurrences in post-mature Posidonia Shale. A) Post-mature bituminite I: homogeneous migrabitumen replacing bituminite I; B) post-mature bituminite II: micrinite network associated with small carbonate crystals forming lens-shaped bodies; C) heterogeneous migrabitumen associated with a recrystallised calcareous bioclasts; D) heterogeneous migrabitumen filling cell lumens in fusinite. Reflected white light, oil immersion.

In source rocks, oil generation from bituminite begins at lower maturity level than from telalginite (Taylor *et al*., 1998). Under extreme increase of temperature caused by an intrusive body after the generation and expulsion of oil, no residues or only very fine micrinite residues, which form single tabular masses of micrinite, and/or homogeneous non-fluorescing migrabitumen (Rr of migrabitumen: 1.0–1.2 %) are left by bituminite (Teichmüller and Ottenjann, 1977; Taylor *et al*., 1998) (Fig.5-6A, B).

The quantity of bituminite I is four times higher than that of post-mature bituminite I (Fig.5-5). This difference might be explained by the difficulties in recognising the morphology of post-mature bituminite I in post-mature oil shales, since it is replaced by micrinite. However, migrabitumen recorded in the mineral groundmass could also have been generated from bituminite I, as well as from the lipidic substances contained in the mineral bituminous groundmass of the mature Posidonia Shale. Migrabitumen was also found as a coating on isolated carbonate crystals in the micrinite-rich mineral groundmass, in association with faunal relics (Fig.5-6 C) and calcareous concretions, and as infillings of cell lumen of fusinite (Fig.5-6 D). The optical properties and the reflectance of the identified migrabitumen

indicate that the heterogeneous and homogeneous types can be assigned respectively to epi-impsonite and cata-impsonite (Jacob, 1983, 1989).

Taking into account the different origins of bituminite I and bituminite II, the latter is likely to be associated with oil exudates in mature Posidonia Shale (Teichmüller and Ottenjann, 1977). This oil, in turn, is absorbed by the minerals of the groundmass (Taylor *et al.,* 1998). At a high level of maturation, these petroleum-like substances are converted into fine-grained micrinite. This micrinite, in turn, is scattered as a network between the carbonate grains in the post-mature bituminite II (meta-bituminite II) lenses. The rather good correlation between the contents of bituminite II (15.5 vol.%) and post-mature bituminite II (17.8 vol.%) demonstrates that the morphology and the structure (fabric) of bituminite II remain preserved in post-mature Posidonia Shale. Moreover, the total content of the organic matter in early mature oil shales is equal to that in post-mature oil shales (Fig. 5-7).

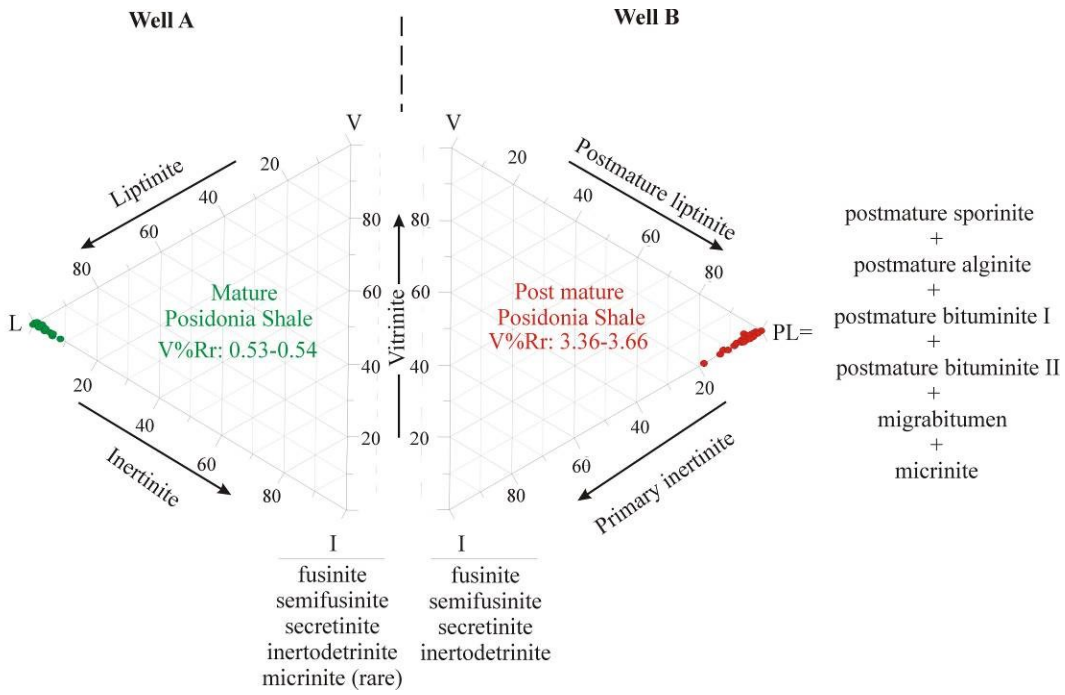

Fig. 5-7: Relationship between the maceral composition of the mature Posidonia Shale (well A) and the petrographic composition (including macerals as well as the mineral replacement of sporinite and alginite bodies; see the text) of post-mature Posidonia Shale (well B).

5.2.4. Meta-sporinite

In the investigated post-mature Posidonia Shale (well B), post-mature sporinite is filled with pyrite crystals, which emphasise the sporinite morphology. It is characterised by reddish orange internal reflections in reflected white light and is either non-fluorescent or

shows weak greenish fluorescence which results from the association of the pyrite with other minerals (Fig. 5-8). With regard to the secondary forms of replacement of alginite and bituminite (see above), bodies with contours which resemble sporinite morphologies are named post-mature sporinite (Gorbanenko and Ligouis, 2014).

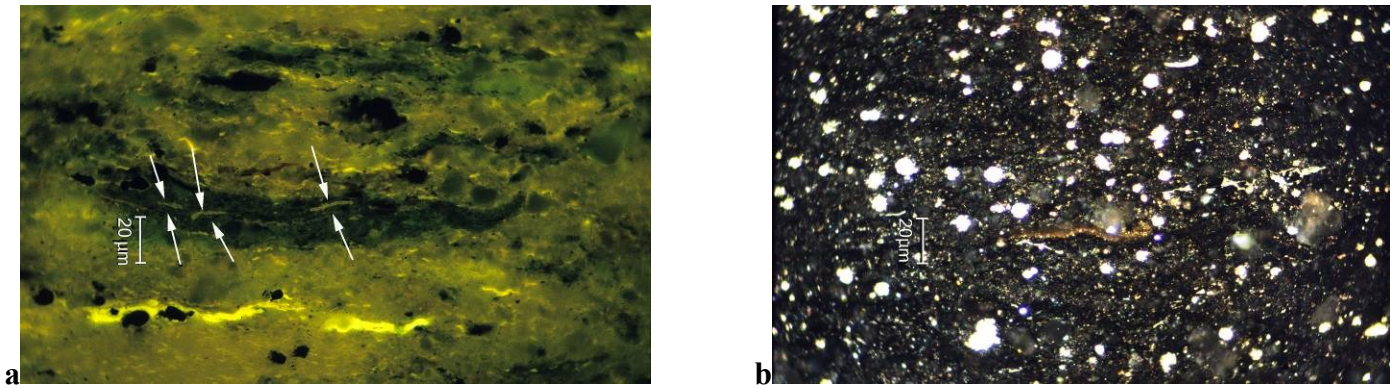

Fig. 5-8: Photomicrographs of sporinite and post-mature sporinite in Posidonia Shale.
A), Weak fluorescing sporinite (white arrows) in clayey lenses of early mature Posidonia Shale (fluorescence mode, oil immersion); B), Post-mature sporinite showing reddish internal reflections in the micrinite-rich mineral groundmass of the post-mature Posidonia Shale. Reflected white light, oil immersion.

CHAPTER 6. DISCUSSION: DEVELOPMENT OF THE ORGANO-MINERAL MICROFACIES AND THEIR PETROGRAPHIC AND GEOCHEMICAL PROPERTIES

CONTENTS

6.1. Maceral composition in the service of paleoenvironmental reconstruction

It is self-evident that, among all the identified constituents, liptinite macerals of marine origin are the inalienable and major components of Posidonia Shale. Each of these macerals acts as an indicator of specific paleoenvironments. While the precursors of structured organic matter are well known, those of bituminites (AOM) are still uncertain, as well as their paleoenvironmental conditions (Stasiuk, 1994; Teerman *et al*., 1995). Obviously, bituminite is still a focus of the particular interest of investigation in order to shed light on paleoenvironments' triggered deposition of organic-rich sediments of an excellent oil generation potential. Therefore the main relationships between macerals and paleoenvironments will be discussed with an attempt to define the origin of bituminites.

6.1.1. Terrestrial macerals (sporinite, macerals of vitrinite and inertinite groups)

A detailed overview of macerals of terrestrial origin, their concentration in the Posidonia Shale and the ways of their transportation were given in Chapter 3. For the interpretation of the results obtained by maceral analysis, it is important to take into account their content in the organic-rich sediments. The increasing input of these macerals may provide valuable information on the distance between sedimentary area and adjacent landmasses and climate, which was established at that time (for more details see Chapter 3).

Frequently, an increase in the content of allochthonous vitrinite indicates long transportation and, probably, a dry climate on the continent (Tyson, 1995; Traverse, 2005). When indigenous vitrinite is observed in the sediments as a single particle or together with other terrestrial macerals, it may represent nearshore location of the sedimentation area (Tyson, 1995; Traverse, 2005). Moreover, its presence demonstrates dysoxic-anoxic conditions which favour rapid burial of these particles and their good preservation.

6.1.2. Alginite (telalginite, lamalginite) and liptodetrinite

6.1.2.1. Telalginite

A detailed description of macerals of the alginite group was given in Chapter 3. Taking into account the variety of existing macerals of the alginite group, it becomes apparent that each of them has paleoenvironmental significance. Changes in the quantity of these

macerals, their diversity and preservation can be used in a stratigraphic and paleoenvironmental approach. Specifically, in the case of telalginite, the diversity, content of organic-walled phytoplankton assemblages and the level of their preservation are significantly affected by paleoenvironmental conditions. These changes give us particular information on salinity, sunlight availability, nutrient supply, temperature, stability of the water column and an expansion of the oxygen minimum zone (Palliani and Riding, 1999). Therefore, significant relationships between telalginite, particularly Prasinophyceae algae, and high values of geochemical parameters such as TOC and HI have been discerned by many workers (Stasiuk, 1994; Tyson, 1995; Taylor *et al*., 1998; Palliani and Riding, 1999; Palliani *et al*., 2002; Vigran *et al*., 2008).

In general, Posidonia Shale represents the last major Prasinophyte event (Prauss, 1996). This event has been related to changes of paleoenvironmental conditions from a more strictly marine environment, dominated by dinocysts and acritarchs, to environments of decreasing salinity with the prevalence of Prasinophyte genera (Loh *et al*., 1986; Riegel *et al*., 1986; Prauss, 1996; Prauss *et al*., 1991) (Table 6-1). Therefore, this reduced saline environment induced the density stratification of the water column, which led to the deposition of bituminous shales (Prauss *et al.,* 1991; Prauss, 1996). Moreover, within the investigated Posidonia Shale, several genera such as *Pterosphaeridia* or *Leiosphaeridia* were observed among the Prasinophytes. In well A, for instance, the number of genera is much higher, whereas in other wells in the West Netherlands Basin and the South German Basin, only the *Tasmanites* genera prevail.

Farrimond *et al*. (1988) suggested that the gradual replacement of other palynomorphs by *Tasmanites* is attributed to the decreasing salinity in the photic zone, which finally led to density stratification and the spread of the anoxic condition at least into the lower part of the water column. Moreover, the rising content of *Tasmanites* has been related by some authors to the competition of nutrients that occurred when the oxygen minimum zone extended into the lower photic zone and enriched it in reduced nitrates. *Tasmanites*, which use reduced nitrates more efficiently than other genera, became prevalent among them (Wilde *et al*., 1990; Prauss, 1996; Palliani and Riding, 1999; Palliani et al., 2002; Götz and Feist-Burkhardt, 2012).

Paleoecologically, Prasinophyceae, opposed to acritarchs, indicate deep basin paleoenvironments and represent cooling intervals close to the margin of climatic turnover (Prauss, 1996). Prauss (1996), who studied the Toarcian palynomorphs in the Posidonia Shale in Grimmen (North-East Germany), stated that, among all identified genera of Prasinophytes,

only a few may show relations to lithology. The *Pleurozonaria* genera mainly occur within sandy to silty horizons and outside the argillaceous horizons. *Campenia* has a somewhat stronger occurrence within the clays. In addition, Mudie (1992) indicated that *Leiosphaeridia* has its main distribution north of the 60° latitude in both neritic and estuarine environments. *Botryococcus sp*., which has been observed in a minute quantity in wells D and E, is considered as an indicator of a fresh-to-brackish water paleoenvironment (Hunt, 1979; Prauss *et al.,* 1991).

Besides salinity, temperature and nutrients' supply, which Prasinophyceae indicates, its size may provide insight into the distribution from inner shelf to deep basin in a black shale lithology (Stasiuk, 1994). For instance, the size of *Tasmanite*s is smaller in the West Netherlands Basin than in the Lower Saxony Basin. Stasiuk (1994) stated that the basinal carbonates of the Middle Devonian deep basin shale are characterised by large unicellular *Tasmanites* and *Leiosphaeridia* telalginite, ranging in size between 50 and 300 μm. However, oil shale, which has accumulated within the outer to inner shelf paleoenvironments, contains a smaller form of *Leiosphaeridia* and *Tasmanites* telalginite varying from 40-100 μm (Stasiuk, 1994) (Fig. 4-3A,B).

6.1.2.2. Lamalginite

Lamalginite (see the classification and definition of this maceral in Chapter 3) is widely distributed in Posidonia Shale. It occurs in a variety of environments and is derived from varied groups of precursors such as algae, acritarchs and/or dynocysts indicating freshwater, lacustrine and marine environments (Hutton, 1987). In addition, Golubic (1976) attributed filamentous alginite to *Nostocales* because of cellular morphological similarities to filamentous cyanophyte, which may tolerate a relatively high fluctuation in salinity and appear in environments with a (pycnocline) stratified water column (Table 6-1).

In the investigated wells, the vertical distribution of the discrete, filamentous and layered lamalginite varies. Golubic (1976) stated that species diversity is inversely proportional to the harshness of environmental conditions. This is in agreement with the current study: with an increasing oxygen content, the quantity of filamentous and layered lamalginite also rose. In oxygen-deficient environments, only the *Tasmanites* genera, which are probably more resistant to paleoenvironmental changes, were observed. However, *Tasmanites* appear in lower quantities in microfacies with a relatively high content of

Table 6-1: Precursors of macerals of the liptinite group and their paleoenvironmental significance in Posidonia Shale

Maceral				Organic petrology **Description** (in early mature Posidonia Shale of this study)
Telalginite		*Botryoccocus*		Irregular globular colonies with an average of 15-25 µm in diameter with a maximum of 100 µm (Stasiuk, 1994). It has a yellow colour of high intensity in fluorescence mode (Tyson, 1995).
	Prasinophytes	*thick-walled*	*Tasmanites* *Pterosphaeridia*	*Tasmanites*-derived telalginite is well distinguished by its relatively thick cell walls (up to 15 µm) (Stasiuk, 1994). *Pterosphaeridia*-derived telalginite consists of an agglomeration of very thin-walled(<1 µm), spheroidal chambers representing raised, regular reticulations (Teichmüller & Ottenjann, 1977; Prauss et al., 1991; Stasiuk, 1993). The particularity is the network structure of the cell wall.
		thin-walled	*Leiosphaeridia* *Campenia/* *Lancettopsis*	*Leiosphaeridia* is characterised by crumbled fold structures. It has a size from less than 10 to 70 µm in diameter (Stasiuk, 1994). *Campenia* and/or *Lancettopsis* appears as spindle-formed bodies of size varying from 210 to 300 µm.
Lamalginite, liptodetrinite (in part)		*Acritarchs*		Acritarchs (akritos= uncertain, mixed and arche=origin) are small spiny cysts of unknown botanical affinity (5 to 150 µm) (Prauss et al., 1991). They are characterised by a green-yellow fluorescence whose intensity is higher than that of dinocysts. The great majority are marine phytoplankton.
		Dinoflagellate cysts		The fossil record of dinocysts is almost entirely confined to forms that have a meroplanktonic life cycle. Major dinoflagellate cyst morphotypes: proximate, cavate and chorate (Tyson, 1995). It has a yellow-brown fluorescence of moderate intensity. Dinoflagellate-derived telalginite is difficult to identify in sections perpendicular to bedding. In the absence of data from palynomorphs study, sections parallel to bedding are more appropriate to prove the existence of dinoflagellates in bituminous shales.
	Nostocaceae (cyanobacteria)		*Nostocopsis (Mädler, 1968)* *Clorococcal algae (spaeroidal palynomorphs, Prauss et al., 1991)*	*Nostocales* is classified as a filamentous alginite. The alginite filaments vary in length from less than 20 to more than 100 µm and consist of cells with a diameter of 2-5 µm. The minute sized lamalginite occur as a simple, rounded to oval body with a single, central fold structure (Teichmüller & Ottenjann, 1977). Chlorococcal algae are tiny algae (1-2 µm) which occur in marine phytoplankton (van den Hoek et al., 1993) All these small algae may be assigned to discrete lamalginite as well as in part to liptodetrinite (Prauss et al., 1991).
Sporinite, cutinite				In Posidonia Shale sporinite appeared as thick-walled strongly ornamented or with a smooth outline (Tyson, 1995). Cutinite is rare in the Posidonia Shale. It originates from leaf- or twig-covering plant cuticle. Frequently, it exhibits a serrated edge in sections perpendicular to the bedding plane. It shows an orange-brown fluorescence of moderate intensity. Sporinite and cutinite have a dark brown colour in reflected white light and an orange brown fluorescence of moderate intensity.

	Palynological subgroups	Paleoenvironmental significance	Photomicro-graphs
Freshwater Microplankton	Chlorococcales algae (Stasiuk, 1994)	Botryoccocus-derived alginite is an indicator of **brackish** to **freshwater lacustrine, fluvial, lagoonal and deltaic facies** conditions. It is most abundant in coastal marine environments (Stasuik, 1994). **Unstable** salinity **regimes** characterised by periodic deposition of gypsiferous or other shallow water evaporitic facies (Hunt, 1987). Can be transported by river and deposited in marine prodelta and adjaecent shelf facies.	Fig. 3-4C
Marine Microplankton	Perpendicular to bedding plane these unicellular algae appear as very fine, curvaceous disk-like bodies resembling microspores (Stasiuk, 1994). In a section parallel to bedding, they occur as simple, rounded to oval bodies with a single, central fold structure (Mädler, 1963; Stasiuk, 1994).	Always characterise the most organic-rich and most uranium-rich intervals, which were formed under **starved marine** conditions (Tyson, 1995). Extremely high concentration of the Prasinophyceae indicate early highstand system track. Tracks with carbonate poor shaley lithology. The content of *Tasmanites* algae increasing to acritarchs indicate pelagic facies or **stratified water column**. Prasinophyceae related to cold water. Occur in the **lower part** of the **transgressive system** (Prauss, 1996). Predominance of the thin-walled algae (*Leiosphaeridia*) testify to a **nearshore**, **shallow-marine** to **brackish marine**, sometimes hypersaline environment (Jacobson, 1979). *Campenia* is frequently found in facies hosted by clayey-dominant groundmass (Prauss, 1996).	Figs. 3-3 A-F; Fig. 3-4 A, B
	Fossilised cysts, unicellular with organic wall. Acritarchs have no formal taxonomic status (Tyson, 1995). Cell produced during the sexual phase of the dinoflagellate life cycle. The fossilised cysts are composed of sporopollenin-like material (Tyson, 1995)	In the Early Jurassic, most genera indicate nearshore or **eustarine** to **shallow lagoon** and/or **slightly brackish-water** environments (Wall, 1965; Praus et al., 1991). High diversity and best preserved acritarchs characterized open marine facies, while sediments from marginal marine facies (barrier and tidal lagoon facies) are poorly preserved (Vecoli, 2000). Low diversity and low to moderately abundant assemblage with common Veryhachium and Micrhystidium indicate a **nearshore**; high diversity and moderate abundance without a single diminant taxon - **offshore**; low diversity and low to moderate abundance with a dominance of the spheromorph acritarchs - **deeper water assemblage** (Dorning, 1981). Relative to the pelagic background sediments, **deeper turbiditic** sediments may have significantly higher proportions of dinocysts. Facies deposited in high-stand sea level have high concentration of dinocysts, but lowest concentration of total palynomorphs (Palliani and Riding, 1999).	Fig. 3-3F
	unicellular "algae"	Relative to the pelagic background sediments, **deeper turbiditic** sediments may have significantly higher proportions of dinocysts. Facies deposited in high-stand sea level have high concentration of dinocysts, but lowest concentration of total palynomorphs (Palliani and Riding, 1999).	Fig. 3-3E
Sporomorphs	Terrestrial palynomorphs (spores, cuticula) produced by Pteridophyte, Briophyte and Fungi; Cuticula - resistant to degradation leaf epiderma of higher plants (Taylor et al., 1998)	In marine sediments shows the proximity of sedimentation area from the continent. Can be delivered to marine sediments by wind or by water fluxes (Tyson, 1995). Sporinite and cutinite with macerals of vitrinite and inertinite group may also indicate short-time storm events (Prauss, 1996).	Fig. 3-7

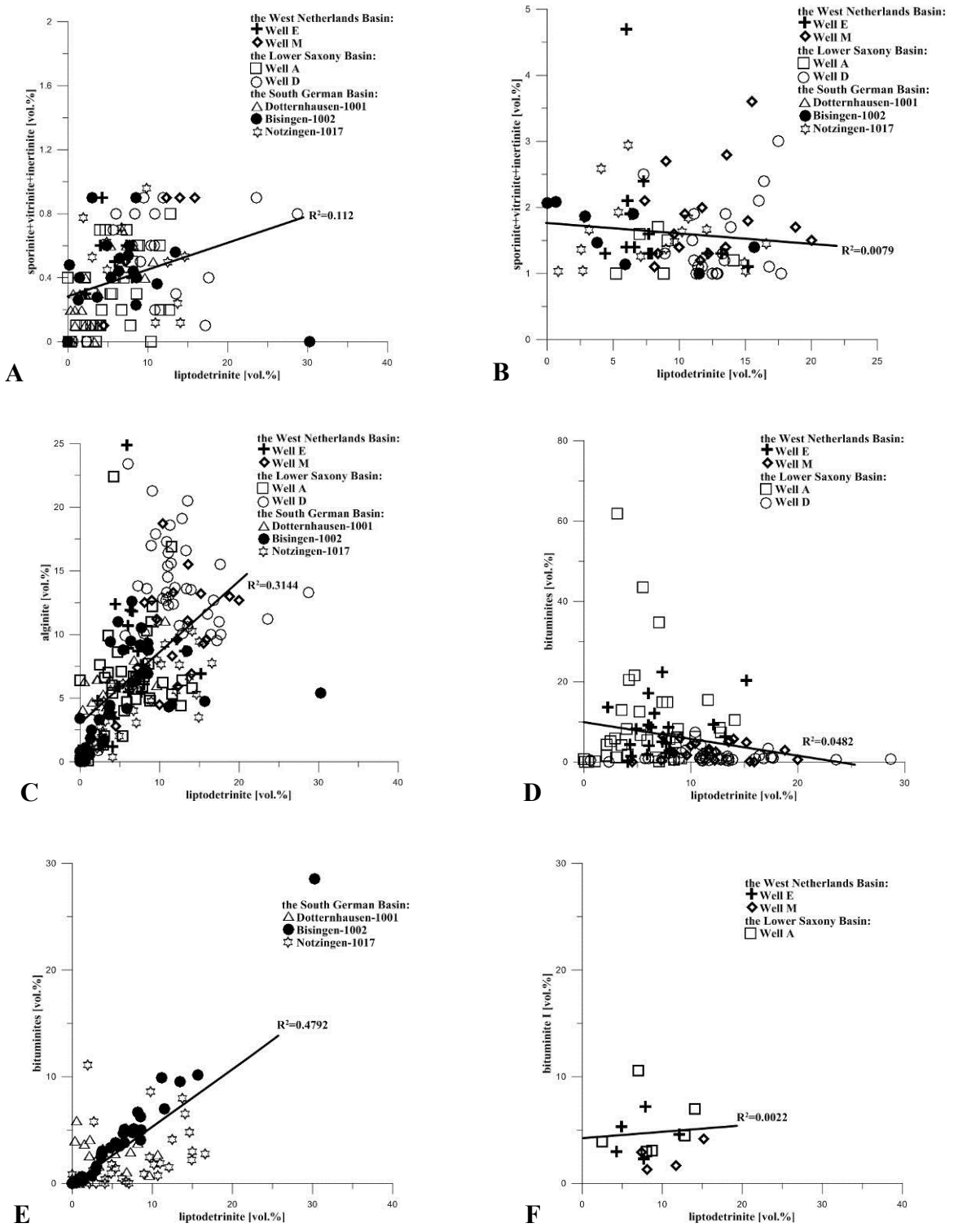

Fig. 6-1: Scatter plots indicating relationships between liptodetrinite and selected macerals.
A), Correlation between the sum of the amounts of sporinite, vitrinite and inertinite, and the content of liptodetrinite. Note that sporinite+vitrinite+inertinite<1.0 [vol.%]; B), The same relationships, but sporinite+vitrinite+inertinite>1.0 [vol.%]; C), Correlation between alginite and liptodetrinite; D), Relationships between bituminites and liptodetrinite (the West Netherlands Basin and the Lower Saxony Basin); E) relationships between bituminites and liptodetrinite (the South German Basin); F) Correlation between bituminite I and liptodetrinite (samples from the West Netherlands Basin and the Lower Saxony Basin). Note that V+L+I+Mineral Matter=100%.

bituminite I and bituminite V, which indicates anoxic environments (more details below in paragraph 6.1.2. Bituminites).

6.1.2.3. Liptodetrinite

Originally, Stach *et al.* (1982) defined liptodetrinite in coals as a maceral consisting of fragments and degradation remains of liptinite. However, Mädler (1963) and Teichmüller and Ottenjann (1977) assigned this maceral in the Posidonia Shale to the very small unicellular "algae" *Nostocopsis* (cyanobacteria) (Table 6-1).

Figures 6-1 A-F are the plotted data of maceral analysis, illustrating relationships between liptodetrinite and sporinite, macerals of vitrinite and inertinite groups, liptodetrinite and macerals of the alginite group, liptodetrinite and bituminites (AOM). As can be seen in Fig. 6-1 A, the content of liptodetrinite is in good agreement with the increasing content of sporinite, together with macerals of the inertinite and vitrinite groups, but only when the input of macerals of terrestrial origin does not exceed 1.0 vol.%. In addition, the observed positive correlation may also indicate that a part of the liptodetrinite is of terrestrial origin, having been generated by the mechanical fragmentation through the transport of the terrestrial liptinites. However, when the quantity of terrestrial macerals makes up more than 1.0 vol.%, it probably demonstrates the increasing availability of oxygen, preventing the preservation of the liptodetrinite, which content tends to decrease as illustrated in Fig. 6-1 B. The positive correlation trend between liptodetrinite and macerals of the alginite group evidences that either part of liptodetrinite is composed of detrital particles of algae, or it is a small algae as has been mentioned above (Fig. 6-1 C). Therefore, the formation of liptodetrinite is probably associated with oxygen availability and increased circulation of water masses.

Figure 6-1 D-F illustrates the correlation between bituminites and liptodetrinite contained in samples from the West Netherlands Basin, the Lower Saxony Basin and the South German Basin. This relationship between samples from the West Netherlands Basin and the Lower Saxony Basin illustrates the negative trend between bituminites and liptodetrinite (Fig. 6-1 D). However, Fig. 6-1 E shows positive relationships between these two macerals in samples from the South German Basin. These differences are probably related to the particularity of distribution of the different types of bituminites in the investigated sedimentary basins. In the Posidonia Shale of the South German Basin, bituminite I was more often observed than in the samples from the West Netherlands and the

Lower Saxony Basins. Moreover, it prevails among other types of bituminite in almost all organo-mineral microfacies enriched in amorphous organic matter. In order to confirm the positive trend between bituminite I and liptodetrinite, organo-mineral microfacies enriched in bituminite I from the West Netherlands and the Lower Saxony Basins were selected (Fig. 6-1 F). Fig. 6-1 F verifies the positive correlation between these two macerals in samples from the West Netherlands and the Lower Saxony Basins as well. This prompts suggestions that bituminite I as well as liptodetrinite are formed in the water column.

6.1.3. Bituminites

Bituminites (AOM) appear to have originated from a variety of precursors such as algae, faunal plankton, bacterial bodies and bodies of higher animals (fish, crayfish, etc.), which in turn may provide insights into different paleoenvironments (ICCP, 1993). It is important to take into account that bituminites originated not only by bacterial degradation of these precursors, but also seem to be formed from dissolved organic matter, which is later absorbed by mineral matrix (?). Hence, unstructured organic matter varies in petrographic, physical and chemical properties and can also vary between hydrogen-rich and hydrogen-poor (Teerman et al., 1995) (Table 6-2; 6-3; Fig.6-2).

Petrographic identification of different types of amorphous organic matter and its characterisation is important, because of its major contribution to the high petroleum potential of most hydrocarbon source rocks (Masran and Pocock, 1981; Gutjahr, 1983; Loh et al., 1986; Shewrood and Cook, 1986; Taylor *et al*., 1991). Many authors have stated that bituminite is well known to generate oil earlier than other liptinites, including telalginite (Masran and Pocock, 1981; Gutjahr, 1983; Taylor *et al*., 1991). Alpern (1980) discerned, for instance, that oil generation from bituminites already starts at a vitrinite reflectance of 0.5 %. However, Cook (1982) later determined a vitrinite reflectance range from 0.5 to 0.9 %.

However, in terms of paleoenvironments, Masran and Pocock (1981) suggested that bituminites may be derived either from marine or terrestrial precursors, but most of them were formed in marine environments in oxygen-depleted conditions.

6.1.3.1. Bituminite I

Bituminite I was observed in different concentrations in almost all the investigated samples. The origin of bituminite I is still debated. However, molecular studies have confirmed that originally bituminite I results from the selective preservation of resistant cell walls of green microalgae (Boussafir and Lallier-Vergès, 1997).

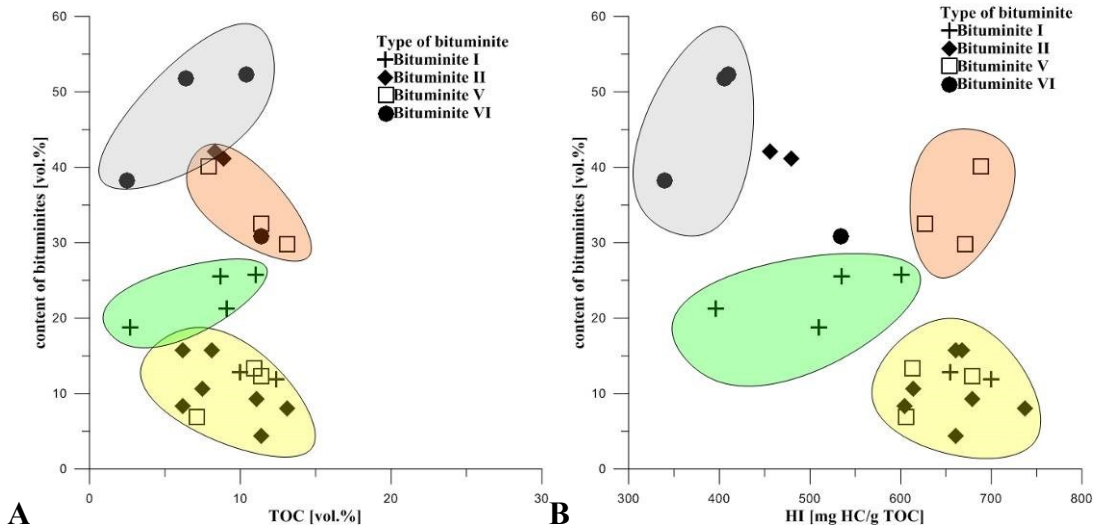

Fig. 6-2: Relationships between bituminites, the Total Organic Carbon and Hydrogen Index.
A), Correlation between bituminites and the total organic carbon (TOC). B), Correlation between bituminites and the Hydrogen Index (HI). The graphic is based on selected data shown in Table 6-3.

However, in Posidonia Shale, particularly in the investigated wells of the West Netherlands Basin, two types of bituminite I were observed: a "classic" type, defined by Teichmüller and Ottenjann (1977) and a non-fluorescent type with inclusions of sporinite. The latter type is probably a product of bacterial degradation of terrestrial organic matter and might already have been formed before its incorporation into the marine sediments (ICCP, 1993).

Table 6-2: Definition of the different types of bituminite and their paleoenvironmental significance.

	Bituminite types	References	Petrographic description (in early mature Posidonia Shale of this study)
Bituminites (AOM)	Bituminite I	Teichmüller and Ottenjann (1977)	It has indistinct lens shapes (streaks) with length up to 60 µm. Bituminite I is characterised by a very low reflectance and a light brown to dark brown fluorescence, frequently contains yellow fluorescent liptodetrinite, seldom sporinite and discrete lamalginite.
	Bituminite II		Bituminite II occurs as thick (around 40-100 µm) elongated lenses associated with small carbonate crystals. It exhibits a yellowish-brown to reddish-brown fluorescence, often with greenish fluorescing oil expulsions (droplets).
	Bituminite III		Bituminite III is defined as thick (60-150 µm) elongated bodies often associated with fluorescent phosphate faunal remains.
	Bituminite IV	Gorbanenko & Ligouis (2014)	Bituminite IV has a few similarities to bituminite I. This unstructured organic matter occurs as thick (60-120µm) lenses of irregular outline. Similar to the bituminite I, it has micrinite inclusions, but contains no liptodetrinite and shows green fluorescence.
	Bituminite V	Gorbanenko & Ligouis (2014); Vogel (2014, unpublished)	It forms rather uniformly and strongly fluorescent cohesive bodies, which show relatively sharp and distinct (sometimes quite angular) outlines. Dark-grey to grey brown colour in reflected white light and an orange-brown or greenish-brown fluorescence of moderate intensity. Size is variable and length ranges from 20 to 200 µm
	Bituminite VI	Creaney (1980)	Bituminite VI is very similar to bituminite frequently described as a "matrix-bituminite". It consists of amorphous organic matter, which occurs as a "network" between the carbonate crystals of calcareous groundmass and calcareous concretions. It has an orange-brown or brown colour in reflected white light and an orange fluorescence.

Precursors	Paleoenvironmental significance (based on the results of this study)	Photomicrographs
mixture of marine algae and terrestrial organic matter (sporinite)	shallow-water anoxic environments with restricted water circulation. It, probably, indicates sea-level rise (?).	Figs. 3-5 A, B
fecal pellets (Wehner and Hufnagel, 1986); Coccolithophoridaceae (Ramsden, 1983), algal and microbial peloids (Flügel, 2004)?	deep-water suboxic-anoxic environments with water column stratification; with lower water energy and circulation	Figs. 3-5 C, D
faunal relics, fish rests	shallow-marine anoxic environments, occurs when oxic conditions turn into oxygen-depleted, which triggers mass mortality of the fauna	Figs. 3-5 E,F
terrestrial amorphous organic matter or product of diagenetic transformation (?)	shallow-marine suboxic-anoxic environments, presumably occurs after strong oxic conditions, which later gradually changed to suboxic, triggered by sea-level decrease, or storm/rain event. This led to increasing input of terrestrial macerals	Fig. 3-5G
microbial or algal-fungal mats (Cook, 1982)	indicate shallow-marine anoxic harsh environment, probably, isolated sedimentation areas, when fluctuations of the sea level are caused by rain and evaporation; frequently associated with evaporites.	Figs.3-6 A, B
uncertain affinity (probable precursors: dissolved organic matter (?); Coccolithophoridaceae (Ramsden, 1983)	bituminite VI is poorly represented in Posidonia Shale, that makes the interpretation complicated; it is presumably composed of bacterially degraded dissolved organic matter (?) or formed from bacterially produced coating on coccoliths. It indicates strong anoxic environments with low water energy	Figs. 3-6 C, D

Table 6-3: The geochemical characterisation of the Posidonia Shale samples enriched in distinct types of bituminites (AOM). V+L+I=100 %

Basin	Well	Sample	Bit I	Bit II	Bit V	Bit VI	Dis. Lamalg.	Ltd.	TOC [%]	HI [mg HC/g TOC]
the West Netherlands	E	2482.05	**25.7**	2.9	2.1	-	18.9	28.2	11.0	601
		2485.14	5.9	0.4	**13.4**	-	20.5	28.7	10.9	613
		2487.50	2.6	1.6	**6.9**	-	22.2	40.7	7.1	606
		2490.35	6.3	9.3	**29.8**	-	12.9	34.3	13.1	671
		2498.46	**18.8**	1.3	7.5	-	18.1	26.9	2.7	510
		2503.35	14.9	6.3	**40.1**	-	14.4	9.9	7.9	689
		2504.85	8.1	5.7	**32.5**	-	20.1	16.3	11.4	627
	M	2088.30	0.8	8.4	1.7	-	27.6	48.5	6.2	604
		2089.33	0.5	**10.6**	0.5	-	23.1	56.9	7.5	614
		2090.55	4.2	9.3	2.3	-	25.1	43.4	11.1	679
		2091.55	1.0	**15.7**	0.5	-	16.8	50.8	6.2	661
		2092.43	3.6	**15.8**	0.7	-	18.6	50.2	8.1	668
		2093.40	**12.8**	7.1	6.2	-	23.0	32.7	10.0	655
		2095.10	1.4	**4.4**	1.6	-	25.5	51.5	11.4	661
		2098.15	3.0	**8.1**	1.9	-	37.4	36.6	13.1	737
		2100.49	0.3	0.3	**12.3**	-	41.3	29.1	11.4	679
		2103.45	**11.9**	0.3	1.4	-	31.2	43.1	12.4	700
Lower Saxony	A	2345.9	0.0	0.9	-	**51.8**	6.3	25.9	6.4	406
		2352.05	**21.3**	1.2	-	9.4	14.0	42.9	9.1	396
		2352.15	6.1	1.4	-	**52.4**	13.3	13.0	10.4	410
		2353.35	22.4	**42.1**	-	8.9	5.9	14.8	8.3	456
		2355.3	8.8	**41.2**	-	31.1	3.2	10.2	8.9	479
		2359.2	4.5	6.7	-	38.2	12.4	23.6	2.5	340
		2359.65	**10.5**	7.5	-	30.8	15.0	13.2	11.4	534
		2361.1	**25.5**	0.0	-	8.5	22.2	16.3	8.7	535

TOC-Total Organic Carbon; Bit. I - bituminite I; Bit. II - bituminite II; Bit. III - bituminite III; Bit. V - bituminite V; Bit. VI. - bituminite VI; Dis. Lamalg. - discrete lamalginite; Fil. Lamalg - filamentous lamalginite: Ltd. - liptodetrinite

The Posidonia Shale samples characterised by a high concentration of bituminite I, show high values of TOC and HI as illustrated in Figs. 6-2 A, B. Specifically, almost all samples enriched in bituminite I contain values of TOC of more than 5.0 % and HI of more than 500 mg HC/g TOC. However, it must be kept in mind that other macerals of the liptinite group can influence the geochemical results.

6.1.3.2. Bituminite II

Bituminite II, defined by Teichmüller and Ottenjann (1977), is a relatively common constituent of the investigated organo-mineral microfacies. This maceral was originally attributed to faecal pellets (Littke and Rullkötter, 1987; Rullkötter *et al*., 1992). Faecal pellets, in turn, are widely considered as a significant and potential source of amorphous organic matter (Tyson, 1995). Because the sedimentation rate of faecal pellets is higher than that of

other organic particles, their sinking time through the oxygenated upper part of the water column into the oxygen-depleted part is faster than other organic particles (Rullkötter *et al.,* 1992). Therefore, good preservation of bituminite II results from a water column stratification: on the one hand, it provides environments for zooplankton habitation, on the other hand, good preservation of the organic matter within the faecal pellets. However, some authors are sceptical regarding faecal pellets as a precursor of bituminite II. Porter and Robbins (1981) stated that faecal pellets of zooplankton contain only 1–4 % organic carbon and it is unlikely that they are precursors of bituminite II.

Organo-mineral microfacies enriched in faecal pellets contain a higher percentage of zooclasts. Vigran *et al*. (2008) discerned that faecal pellets are often associated with *Tasmanite*-derived telalginite and bivalve microcoquina. Moreover, the organo-mineral microfacies enriched in bituminite II may contain ichnofaunal remains, as was observed in well E, indicating a fluctuation between anoxic and dysoxic-oxic conditions. In these environments, the influx of oxygenated storm water enabled the rapid colonisation of ichnofauna within a dominantly anoxic environment (Mørk and Bromley, 2008). The latter enhanced anoxia led to mass mortality of the affected fauna by oxygen-depleted conditions (Vigran *et al*., 2008).

In terms of organic geochemistry, organo-mineral microfacies contains relatively high values of TOC and HI (Figs. 6-2A, B; Table 6-3). Samples chosen for the geochemical analysis contain the highest amount of bituminite II, which is well represented only in well A.

6.1.3.3. Bituminite III

Bituminite III was defined by Teichmüller and Ottenjann in 1977, as “unfigured bituminite”, fine granular, without fluorescence, occurring in association with fauna. This type of bituminite is characteristic of the organo-mineral microfacies of Posidonia Shale from southern Germany. In the Dotternhausen-1001 and Bisingen-1002 wells, it appears after the mass mortality of fauna, indicating significant changes in environments from oxygenated to dysoxic to anoxic conditions, in which the habitation of organisms becomes impossible. This may suggest a genetic relationship between faunal remains and bituminite III. In addition, in those samples in which bituminite III occurs, bituminite I is also very common. These two types of bituminite probably indicate anoxic bottom water conditions.

6.1.3.4. Bituminite IV

Bituminite IV is rare in the samples. It is relatively well-represented only in well M. Bituminite IV appears to be similar to bituminite I. However, it contains micrinite inclusions and shows no fluorescence (Gorbanenko and Ligouis, 2014). Due to the low concentration of this maceral in the investigated bituminous shales, it is difficult to assess the precursor of bituminite IV.

A minute amount of bituminite IV and the absence of fluorescence may suggest its genetic relation to bacterially degraded organic particles of terrestrial origin. However, the absence of fluorescence and the occurrence of micrinite inclusions in bituminite IV may suggest a diagenetic transformation of bituminite I.

6.1.3.5. Bituminite V

Bituminite V defined in this study of the Posidonia Shale was also encountered in the bituminous shales of the Kimmeridge Clay formation of the Dorset coast, where this type of bituminite is a part of the groundmass (Boussafir and Lallier-Vergés, 1997; unpublished Vogler, 2014). Originally, Loh *et al*. (1986) assumed that there is a genetic relationship between lamalginite and bituminite in Posidonia Shale. However, the suppressed content of other organic constituents in those sediments where bituminite V is abundant may indicate that this bituminite V is composed of bacterial mats itself (?). This is also confirmed by the fact that relatively high values of TOC and the HI (Figs.6-2 A, B) are shown in bituminite V-dominated organo-mineral microfacies.

In the investigated Posidonia Shale, some relationships between the different types of bituminite and telalginite were identified. For instance, while the content of bituminite V increases, that of telalginite diminishes. In these samples, telalginite appears as small disc-shaped bodies ranging in size between 6 and 10 μm. This evidence probably indicates specific environments which exclude habitation or even the permanent occurrence of algae (Oschmann, 2000). The probability of the preservation of microbial relics increases with the inhabitability of the depositional environment, because more highly evolved competitors are excluded, whereas certain bacteria are well-adapted to those harsh environments (Stasiuk, 1994; Oschmann, 2000). Organo-mineral microfacies in which bituminite V is predominant among other organic constituents indicates strong anoxic conditions. Moreover, this oxygen-depleted environment triggers the occurrence of certain toxic metals, such as uranium in well

E, which makes organic matter less susceptible to microbial attack and ensures its preservation (Degens and Mopper, 1976; Demaison and Moore, 1980).

6.1.3.6. Bituminite VI

Bituminite VI shows similarities to bituminite IV and is rare in the studied Posidonia Shale. It appears between the calcareous grains in the mineral groundmass and has a strong fluorescence (Gorbanenko and Ligouis, 2014). This maceral is close to the "matrix bituminite" defined by Creaney (1980) and later described by Stasiuk and Goodarzi (1988). It probably represents amorphous substances of unknown affinity adsorbed by the mineral matrix, described by Teichmüller and Ottenjan (1977) as a "bituminous matrix". In addition, the petroleum potential of bituminite VI is lower than other bituminites. It shows values of TOC, which usually do not exceed 10.0 %, and HI reaching 500 mg HC/g TOC, when its content is extremely high compared to other bituminites on the plot (Figs. 6-2A, B).

Bituminites (AOM) in the investigated Posidonia Shale can occur not only in limestones or marly limestones, but in mudstones as well. Although the generally accepted point of view that amorphous organic matter dominates other organic constituents deposited in carbonate environments (Tyson, 1995), the following examples challenge this statement and show the existence of correlations between distinct types of amorphous organic matter and hosted in mineral groundmass other than carbonate. This inconsistency is probably related to the different origin and variety of possible precursors of the amorphous organic matter.

Each individual type of bituminite can be used in a stratigraphic approach. Among all the defined amorphous organic matter, almost all types of bituminite show relationships between their type and the hosted mineral groundmass. Bituminite I and bituminite III, for instance, are more common bituminites in mudstones and calcareous shales, whereas the others are frequently found in limestones, marly limestones and marls. Among all the investigated wells, bituminite V is often observed in high concentration in calcareous-dominated groundmass with a high content of dolomite crystals, whereas the content of other constituents is suppressed. This possibly indicates extremely harsh paleoenvironments. These paleoenvironments are more appropriate for the habitation of cyanobacteria than for other organisms. Therefore bituminite V is probably composed of bacterial mats itself (?) (Table 6-2).

6.2. Depositional environments

Occurrence and preservation of the organic-rich sediments require oxygen-depleted conditions (Lipson-Benitah *et al*., 1990). These conditions appeared, for instance, in many sedimentary basins throughout Europe in the Toarcian time, triggered by the Oceanic Anoxic Event (OAE) (Jenkyns, 1980). High-resolution organic petrography demonstrates the differences appearing in the composition of individual organo-mineral microfacies. This indicates variations in paleoenvironmental conditions which triggered the formation of these organo-mineral microfacies. Indeed, the theory of globality of the Oceanic Anoxic Event is not a contradiction of this fact, but requires individual adjustment of the general scenario in each of the investigated areas (Lipson-Benitah *et al*., 1990).

To explain the occurrence of the organo-mineral microfacies, two models were introduced: the preservation model and the productivity model (Pratt, 1984; Zimmerman *et al*., 1987; Kauffman and Sageman, 1990; Pedersen and Calvert, 1990). The first model proposes that salinity stratification and stagnation enable the incorporation of organic matter in the sediments and its preservation, whereas the second model suggests that increased surface productivity and enhanced oxygen-minimum zone contributed to the deposition of the organic matter (Lipson-Benitah *et al.,* 1990). Both concepts, as well as the sea-bottom relief and the depth of the sedimentary basin, were taken into account by many authors, when they reconstructed the depositional history of the organic-rich sediments using sedimentological and/or geochemical methods. These models were introduced and described in the Introduction. In the current study, usage of high-resolution organic petrography enables the provision of more specific details of the accumulation and preservation of the Toarcian Posidonia Shale and facilitates the creation of depositional models for its formation.

6.2.1. The West Netherlands Basin

As was mentioned in Chapter 4, in the identified organo-mineral microfacies from the West Netherlands Basin, organo-mineral microfacies in well E resemble those in well M. This is probably caused by the existence of a communication between these two areas during sedimentation. However, the greater content of amorphous organic matter and contemporaneous suppressed amount of telalginite, lamalginite and liptodetrinite in well E indicate a higher isolation of this sedimentation area from others. It led to the restriction of the water column circulation and to the establishment of the stronger anoxic conditions with low

rate of organic matter sedimentation. It also confirms the thickness of the Lias epsilon in well E, reaching 29.9 m, whereas that in well M comprises 42.2 m.

Generally, a variation of the organo-mineral microfacies is caused by sea-level fluctuation. There is no significant difference in paleoenvironments compared to those from southern Germany. However, variations were recognised not only among organo-mineral microfacies within one well, but also between wells from the West Netherlands Basin. Distribution of the organo-mineral microfacies from the bottom to the top is illustrated in Appendix B.1. and Appendix B.2. The detailed scenarios of the deposition of the identified organo-mineral microfacies are represented in Fig. 6-3. It clearly appears that organo-mineral microfacies in well E echoes those in well M, however, with some delay. This is caused by the "isolation" of sedimentary sub-basins, as was previously mentioned. This also supports the higher diversity of macerals, the lower content of bituminites and the greater quantity of liptodetrinite, indicating a higher water dynamic in well M.

In particular, in well M, the Lias delta is composed of OMFN 4. The latter is overlaid by OMFN 1 and OMFN 3, indicating the sea-level fall and rise respectively. This resembles the developments of the sedimentation in well E, however with some delay. Precisely, early Lias epsilon sediments were comprised of OMFN 4 and then, directly overlaid by OMFN 3. At that time, these two sub-basins of well M and well E communicated. The continuing sea-level fluctuation is indicated by the sedimentation of OMFN 3-OMFN 2-OMFN 1 in both wells. This succession of organo-mineral microfacies is caused by gradual sea-level fall and the establishment of conditions with higher oxygen availability. The constantly increasing sea level led to the formation of the OMFN3 in well E. Unlike well M, strong anoxic conditions appeared in well E and were not influenced by short-term fluctuation in sea level. These changes were recorded only in well M (OMFN 2). Later the continuous sea level decreased and led to the formation of the OMFN 5 and OMFN 1 in both wells.

The results of Rock-Eval analysis are in agreement with the proposed depositional models (Chapter 4). They reveal, for instance, that organo-mineral microfacies enriched in bituminite V show lowest values of OI among all the investigated microfacies (Chapter 4). In well E and well M, these organo-mineral microfacies contain av. 17 and av. 11 [mg. CO2/g TOC] respectively. Organo-mineral microfacies indicating an oxygenated water column contain OI 65 and 186 [mg. CO2/g TOC] in wells E and M respectively

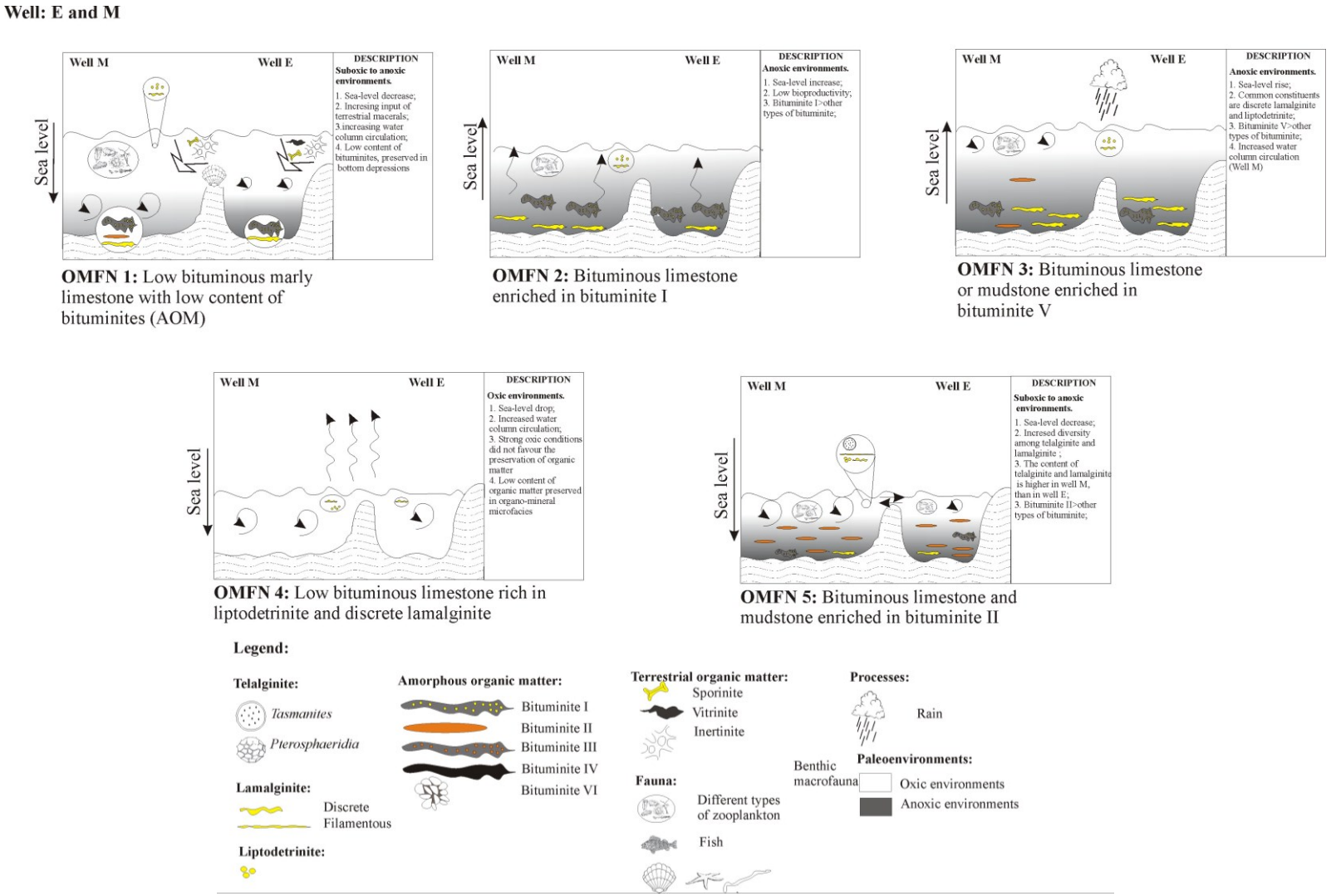

Fig. 6-3: Schematic illustration of different scenarios of organic matter sedimentation for each organo-mineral microfacies from well E and well M of the West Netherlands Basin.

6.2.2. The Lower Saxony Basin

Well A and well D represent two different paleoenvironments. The formation of the organo-mineral microfacies in the first well is characterised by a slow sedimentation rate, water column stratification and very warm marine environment. All organo-mineral microfacies resemble each other. However, they indicate slight sea-level fluctuations, probably caused by a short-term storm event/sea-level fluctuation. Organo-mineral microfacies in well A were probably deposited in deeper water environments than those in well D. Specifically, it is possible that well D was located closer to the landmasses than well A. This is indicated by a greater input of terrestrial organic matter in this well. The sea water was oxygenated with a good water column circulation which prevented expansion of the anoxia. The increased content and diversity of the telalginite and lamalginite and high liptodetrinite content indicate good oxygenation of the water column with a high water dynamic. However, in some deeper parts, the still existing anoxia enabled the preservation of some indigenous vitrinite and bituminites and prevented the appearance of macrofauna.

The distribution of the organo-mineral microfacies is presented in Appendix B.3 for well A and in Appendix B.4 for well D. All organo-mineral microfacies in well D resemble OMFLa 1 in well A. However, slight differences are encountered among the identified organo-mineral microfacies in well D, caused by sea-level fluctuation or by a short-term storm event.

Organo-mineral microfacies with an extremely high content of bituminite II (OMFLa 2) indicates low energetic suboxic-anoxic environments with oxygenated surface water and oxygen-exhausted bottom water, allowing both the habitation of algae and zooplankton and the preservation of the organic matter (Fig. 6-4). The increased content of bituminite I (OMFLa 3) represents more dynamic environments. Enhanced anoxia into the photic zone caused the low bioproductivity and, as a result, lower content of the organic matter buried in the sediments. The evaporation of the water or the rapid fall of the sea level led to the increased oxygen availability in the water column (OMFLa 4). This led to the low preservation of organic matter.

The described scenarios are in agreement with the low OI which ranges from 4 to 10 mg CO_2/g TOC for organo-mineral microfacies, indicating suboxic-anoxic environments, and with values of OI reaching 84 mg CO_2/g TOC in OMFLa4 (geochemical properties of identified organo-mineral microfacies described in Chapter 4).

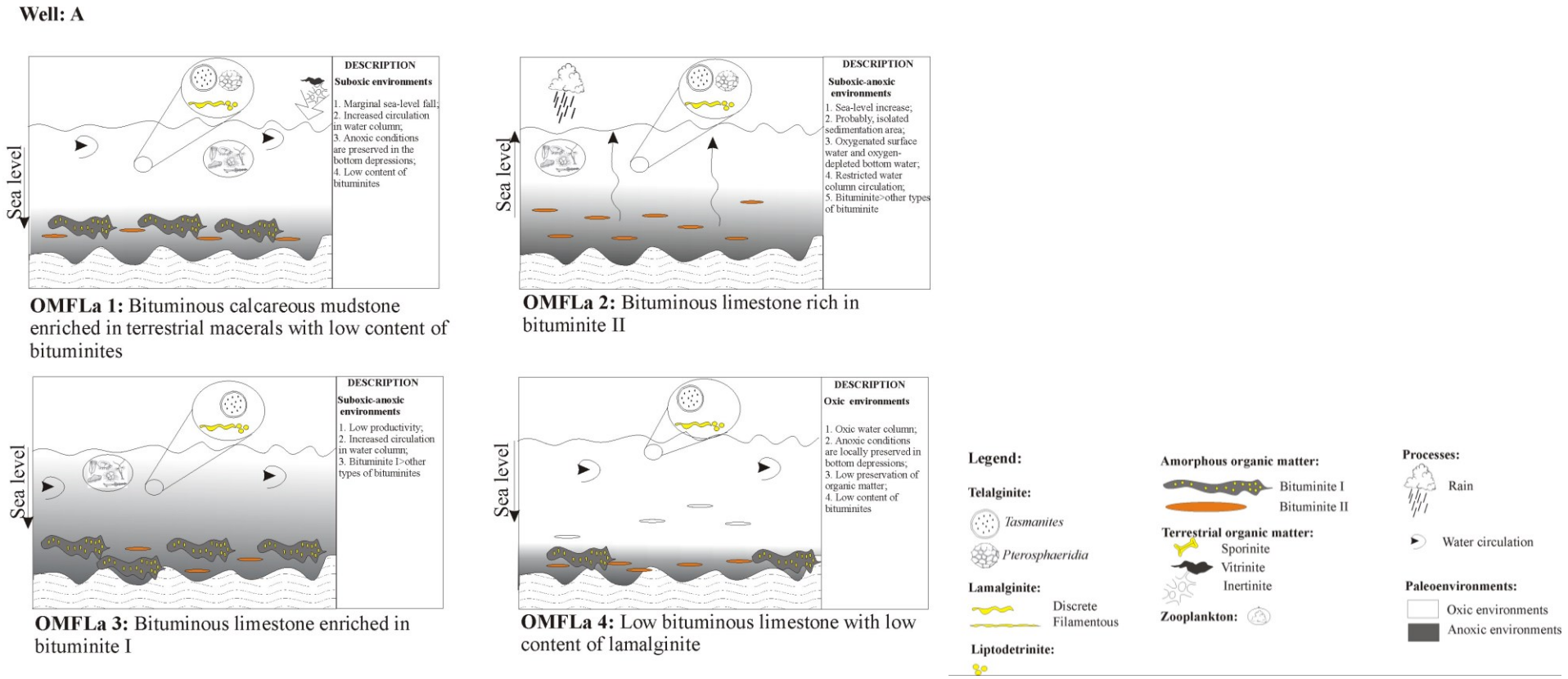

Fig. 6-4: Schematic illustration of different scenarios of organic matter sedimentation for each organo-mineral microfacies from well A of the Lower Saxony Basin.

In well D, the water column is well oxygenated (14-25 mg CO_2/g TOC) with a great water dynamic, which results in the low thickness of the Posidonia Shale reaching only 7 m. However, the low thickness of the Posidonia Shale in well D might be caused by erosion as well. HI and TOC do not vary significantly between the organo-mineral microfacies, indicating a resemblance of the environments in which they were formed.

6.2.3. The South German Basin

6.2.3.1. Evolution of the organic microfacies

6.2.3.1.1. Dotternhausen-1001 well

On the basis of organic petrography, 5 different organo-mineral microfacies were distinguished. The changes of organo-mineral microfacies from the bottom to the top of the investigated succession of Posidonia Shale indicate the variations in depositional paleoenvironments, which reflects the sea-level fluctuations (Fig. 6-5).

Organo-mineral microfacies enriched in bituminite I (OMFDot 2) was probably deposited in anoxic paleoenvironments, reflecting an increasing sea level with restricted water circulation (APPENDIX B.5). It is marked sedimentologically by the occurrence of laminated layers. The decreased content of zooclasts and the poor diversity of telalginite and lamalginite demonstrate the expansion of the oxygen-minimum zone into the photic zone. This microfacies is overlaid by the OMFDot1, indicating short-term oxygenated period which was later changed again by suboxic-anoxic environments (OMFDot 2). This organic-rich succession comprises a depth ranging from 47.83 to 46.15 m. It is in agreement with the bituminous facies A defined by Küspert (1983), which is characterised by very light $\delta^{13}C_{org}$ and $\delta^{13}C_{carb}$ (Küspert, 1983; Röhl and Schmid-Röhl, 2005).

After OMFDot 2, which indicates that suboxic-anoxic conditions appeared after a short sea-level decrease (Fig.6-5, OMFDot 2 A and B scenarios), the short term oxygenation event led to the formation of OMFDot 5, which was followed by OMFDot1. These organo-mineral microfacies indicate oxygenated environments with increasing water column circulation that prevents the sedimentation of the organic matter in high amounts. Anoxic conditions (OMFNDot 2-3) later established led to mass mortality of the fauna. Therefore, in overlying organic OMFDot 2–3, bituminite III was identified in higher concentration than in other organo-mineral microfacies. The origin of this bituminite III is still questionable. It

probably occurs when well-oxygenated environments were changed by strong anoxic conditions. These rapid changes were only observed in the South German Basin.

Later, anoxic paleoenvironments were changed again by conditions corresponding to high oxygen availability. This is reflected in the decreased content of bituminite I and bituminite II (OMFDot 3 or OMFDot 4) (Fig. 6-5). This microfacies succession, ranging from 44.38 to 38.71 m, coincides with the facies B defined by Küspert (1983).

Finally, the organo-mineral microfacies described above are overlaid by those which are enriched in zooclasts, indicating oxygenation of the water column (OMFDot 1). This part of the Posidonia Shale is attributed by Küspert (1983) to facies C.

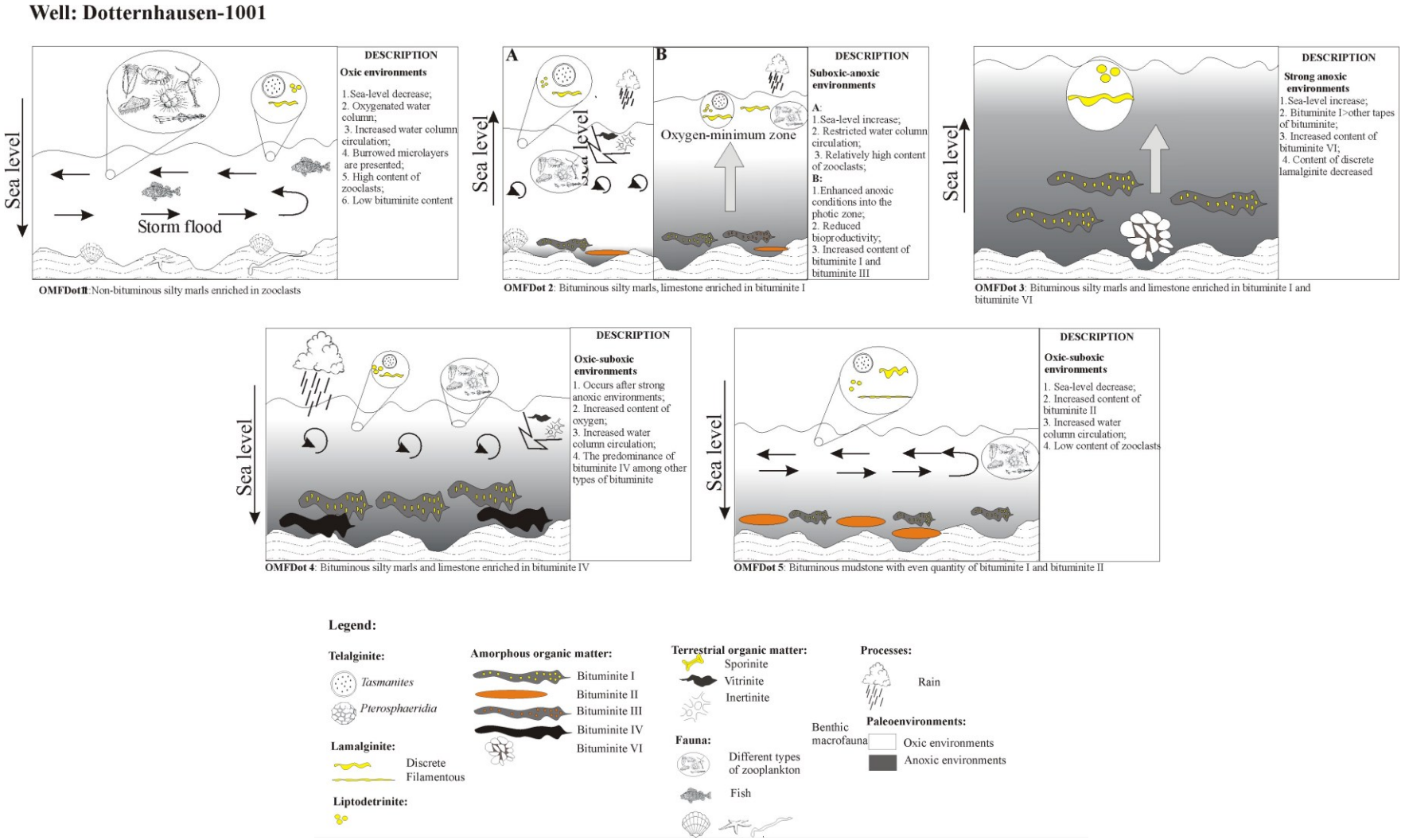

Fig. 6-5: Schematic illustration of the different scenarios of organic matter sedimentation for each organo-mineral microfacies from the Dotternhausen-1001 well of the South German Basin.

6.2.3.1.2. Bisingen-1002 well

OMFBis 9 indicates that the increasing water column circulation prevented sedimentation of the organic matter and its subsequent incorporation in the sediments (Appendix B.7). This explains the low bioproductivity rate and, as a result, the low values of TOC and HI. The depositional conditions of OMFBis 9 were oxygenated in the long term and resemble those of the organo-mineral microfacies OMFDot 1 from the Dotternhausen-1001 well (Fig. 6-5). Sedimentologically, it is marked by the high zooclast and inertinite contents, and the presence of burrows in the sediments. The Lias epsilon is represented by a sea-level rise and the establishment of anoxic conditions, which led to mass mortality of the fauna. This unit consists of organo-mineral microfacies enriched in lamalginite, bituminite I, and liptodetrinite (OMFBis 8). The following organo-mineral microfacies indicates a continuous rise of the sea level (OMFBis 6). This was, however, interrupted by a short-term oxygenation event, represented by OMFBis 1. OMFBis 3, OMFBis 6 and OMFBis 8 resemble a transitional stage between scenario A and scenario B of OMFDot 2. OMFBis 3 is similar to scenario A, whereas OMFBis 6 is similar to scenario B with low biomass productivity. OMFBis 8 is a transitional stage between these two organo-mineral microfacies, indicating the highest values of TOC (av. 6.3 %) and HI (av. 522 mg HC/g TOC) among these organo-mineral microfacies.

OMFBis 1 resembles OMFDot 1. However, in the Bisingen-1002 well, the oxygenation event was brief, caused by a rapid sea-level fall. In these environments, anoxia was still present in depressions. These can explain the deposition of a greater amount of vitrinite. OMFBis 7 and OMFBis 5 indicate a continuous rise of the sea level and the expansion of the anoxia into the photic zone. The OMFBis 5 results from the maximum of the flooding event, coinciding with the order of *falciferum* and *bifrons* zones (Röhl and Schmid-Röhl, 2005). This corresponds to the low TOC values reaching 0.4 %, which probably indicate low biomass productivity. The overlying organo-mineral microfacies indicates regression and changes in paleoenvironments from anoxic to dysoxic conditions. These changes are marked by the following organo-mineral microfacies of OMFBis 3, OMFBis 2 and OMFBis 1, which comprise the sediments of the Dogger alpha at the top of the Posidonia Shale succession. OMFBis 2 and OMFBis 1 both indicate dysoxic conditions. Nevertheless, OMFBis 2 is characterised by higher oxygen availability, which does not allow good preservation of the organic matter. This is in an agreement with low TOC values (av. 0.3 %).

Similarly to the Dotternhausen-1001 well, Küspert (1983) also identified three facies units A, B, C in the Bisingen-1002 well. These facies are in agreement with gradual changes of the organo-mineral microfacies, indicating anoxic to dysoxic and oxic conditions.

6.2.3.1.3. Notzingen-1017 well

Similarly to the Bisingen-1002 well, the Lias delta begins with the sedimentation of the organo-mineral microfacies enriched in terrestrial organic matter and zooclasts (OMFNot 7) (Appendix B.6.). However, contrary to OMFBis 9 in the Bisingen-1002 well, in OMFNot 7 terrestrial organic matter is represented by vitrinite, indicating suboxic conditions. Due to a short transportation, vitrinite was incorporated into sediments in greater quantities than in the Bisingen-1017 well. The continued rise of the sea level led to sedimentation of the OMFNot 4. The model of depositional environment is close to that described for OMFBis 1. The presence of zooclasts in the Notzingen-1017 well indicates the oxygen availability. However, the later oxic-suboxic conditions turned into suboxic-anoxic, indicated by the increasing content of the bituminite (OMFNot 5). The maximum transgression attained by OMFNot 3 with a high bituminite and liptodetrinite content, and simultaneously low quantity of zooclasts. This evidence is in agreement with high TOC and HI values reaching 11.2 % and 701 mg HC/g TOC respectively. After the maximum flooding event, the sedimentation of the following microfacies resulted in a gradual regression (Appendix B.6.). Increasing water mixing caused oxygenation of the water column. This led to decreasing content of bituminite, but increasing content of liptodetrinite.

The OI in this well indicates oxygen-depleted paleoenvironments. It does not change considerably through the well, showing average values from 9.8–13 [mg CO/g TOC]. The exception is only OMFNot7, containing a value of 42 [mg CO/g TOC] (Chapter 4).

6.3. Discussion of the depositional models for investigated sedimentary basins

Previously proposed depositional models of the black shales are based on the suggestion that bituminous shales were deposited in deep-water environments in conditions of sediment starvation (Hallam and Bradshaw, 1979; Wignall, 1991; Hesselbo and Jenkyns, 1995; Jenkyns *et al*., 2001). The occurrence of such paleoenvironments was caused by rapid sea-level rise or/and high basin subsidence rates. These models can explain the formation of organo-mineral microfacies from the West Netherlands Basin and the Lower Saxony Basin. However, they fail in the explanation of the occurrence of reworking layers in the South German Basin (Röhl and Schmid-Röhl, 2005). This confirms that deposition of the Posidonia Shale in southern Germany developed under shallow-water conditions. The shallow-water depositional model was also proposed by several authors (Wignall, 2001; Wignall and Newton, 2001; Röhl and Schmid-Röhl, 2005).

The depositional features of the Posidonia Shale succession differ from area to area. In southern Germany, it was deposited in shallow-water environments with good communication between all three sedimentation basins, whereas those in the Netherlands were far more isolated from each other. Sub-basins of the Lower Saxony Basin represent two different examples of organic matter accumulation and preservation. If in well A environments more resemble deep-sea environments with restricted water circulation, then the scenario of well D is opposed to the well A scenario. In well D, the water dynamic was far greater, leading to oxygenation of the water column. Therefore, it increases the diversity and content of the telalginite and lamalginite, however, decreases the amount of amorphous organic matter, which remains were still preserved in depressions of the sea-bottom relief.

None of the proposed depositional models, which were described in detail in Chapter 1. Introduction, can totally explain all the reconstructed scenarios for each organo-mineral microfacies. The sedimentation of the Posidonia Shale is rather a combination of two and more depositional models.

The “upwelling” model cannot explain the formation of bituminous shales within isolated silled basins (Röhl and Schmid-Röhl, 2005). In addition, according to Röhl and Schmid-Röhl (2005), it fails to explain the evidence for the extensive reworked layers associated with unconformities.

The "stagnant" depositional model cannot completely explain the occurrence of the highly bituminous shale. The deposition of the organo-mineral microfacies in environments with restricted water column circulation will lead to expansion of the anoxia into the photic zone and the mortality of organisms. This decreases incorporation of the organic matter in the sediments. Moreover, this model fails to explain the presence of burrowed sediments in southern Germany.

The "expanding puddle" model is a developed version of the "irregular bottom topography basin". It is the best model to explain the accumulation of the organo-mineral microfacies enriched in bituminite I and bituminite II. Nevertheless, it fails in the same way as the "stagnant" depositional model. Increasing sea level leads to the establishment of strong anoxic conditions, which triggers the mortality of organisms and reduces the biomass productivity.

The depositional "transgressive chemoclines" model proposed by Röhl and Schmid-Röhl (2005) is the model based on sea-level fluctuation and climatically induced variations. This model can explain variations in organo-mineral microfacies in all the sedimentary basins.

6.4. Different types of graphic visualisation of the obtained organo-petrographic results

Graphics is one method of the visual representation of the obtained results. The choice of graphic is crucial for the author and the objectives of the study (Tyson, 1995). For this study, two types of graphic are used to illustrate two different approaches to organo-mineral microfacies analysis. The first is the "classic" ternary diagram, widely used in organic petrography to illustrate maceral composition, and the second is the scatter plot. The ternary diagram is based on three different selected macerals or their assemblage and represents not only the paleoenvironments in the sediments, but in the water column, including the dynamic. The scatter plot is based on the calculation of the Oxidation and Degradation Indices. It has been developed to show the paleoenvironments favouring the formation of bituminous shales.

6.4.1. Ternary diagram

The ternary diagram is a very useful tool for data visualisation. However, the efficiency of this type of representation of results depends on the selection of the three main constituents. Indeed, the common assemblage of macerals of the three main groups — vitrinite-liptinite-inertinite — is widely used in coals. However, this assemblage is not

appropriate for analysing marine organic-rich sediments. In marine sediments, opposed to terrestrial ones, vitrinite-inertinite groups of macerels and sporinite are transported into the sediments by the wind or currents. Their content is rather low in the sediments deposited under calm conditions, whereas it increases with the increase of water energy. In this study, the bituminite-liptodetrinite-alginite maceral assemblage has been selected as the main indicator of paleoenvironmental variations (Fig. 6-6).

Bituminite and alginite represent two different paleoenvironmental conditions (Fig. 6-6). While the algenite indicates oxic conditions and, theoretically, in a maximum extreme it represents calm conditions with a well-oxygenated water column, the high content of bituminite indicates anoxic conditions. However, it is important to take into account that the extension of the anoxia led to reduced oxygen availability in a photic zone and mortality of the fauna. Once there is no more supply of organic matter, the content of the bituminite decreases significantly.

Another important issue is related to the liptodetrinite origin. Many authors did not pay much attention to the content of this maceral in marine sediments. The assumption that it is a product of bacterial degradation and/or is partly derived from minute algae, authorised them to group liptodetrinite together with alginite (Tyson, 1995). However, current research challenges this statement and shows that the liptodetrinite content decreases when that of bituminites (AOM) increases (Fig. 6-1D). If it is taken into account that it mostly already occurs in the water column, liptodetrinite more significantly indicates energetic oxygenated environments than those with restricted water circulation (Fig. 6-6).

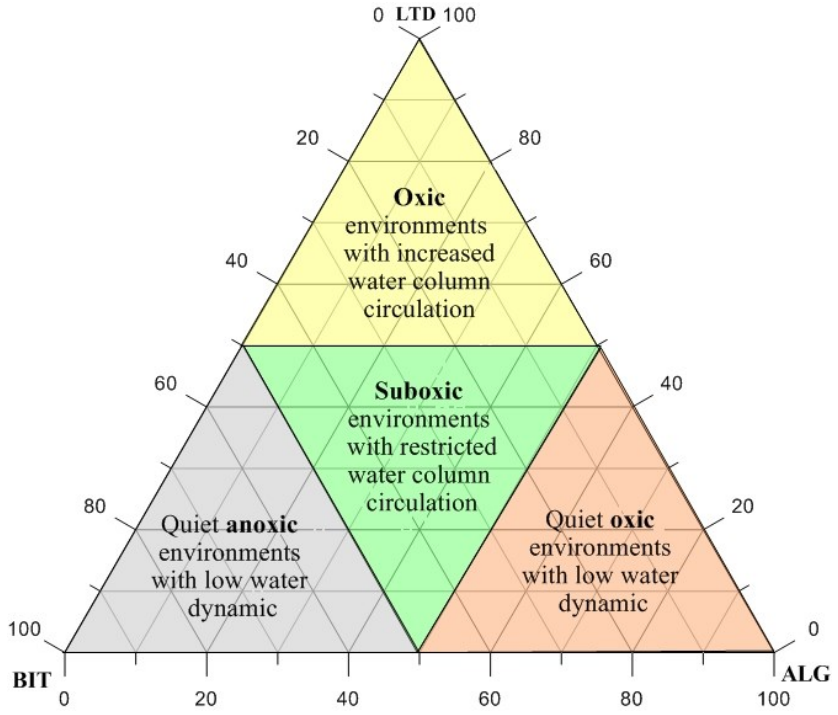

Fig. 6-6: Schematic representation of different paleoenvironmental conditions on the ternary diagram. LTD: liptodetrinite; ALG: alginite; BIT: bituminite.

6.4.1.1. Ternary diagram and organo-mineral microfacies

Organic petrological results, plotted into the ternary diagram are presented in Fig. 6-7 and Fig. 6-8. These diagrams demonstrate the distribution of marine liptinites (alginite, liptodetrinite, bituminite) in Posidonia Shale from the West Netherlands, Lower Saxony and South German Basins. On these ternary diagrams, organo-mineral microfacies are illustrated together with characterising their composition of bituminites, depicted in pie charts. Indeed, the pie chart does not represent the real concentration of bituminites, but shows the "evolution" in the composition of the bituminite "group" depending on the distinct paleoenvironmental condition.

The scatter pattern of the identified organo-mineral microfacies is in agreement with the previously defined paleoenvironments. It is easily recognised that bituminous shale from wells E and A were deposited under more quiet oxygen-depleted environments than those in wells M and D (Figs. 6-7 A-D). Moreover, in bituminous organo-mineral microfacies in wells E and A, the distinct type of bituminites may act as an indicator of the paleoenvironments. For instance, organo-mineral microfacies enriched in bituminite I and bituminite II fall into the area, indicating suboxic paleoenvironments, whereas those rich in bituminite V demonstrate more oxygen-exhausted conditions than were previously discussed. Organo-mineral microfacies from wells M and D contain a higher amount of liptodetrinite and lower content

of bituminites than wells E and A. As was mentioned before, the increased content of liptodetrinite demonstrates the increased water column circulation. In this paleoenvironment, bituminites were preserved only in relief depressions, where suboxic-anoxic conditions were still present (Figs. 6-7 B, D).

Organo-mineral microfacies from wells of the South German Basin show considerable scatterings (Fig. 6-8). This verifies the previous suggestions that paleoenvironments vary considerably from oxic to suboxic-anoxic. Those organo-mineral microfacies enriched in zooclasts are located in the upper part of the diagram, whereas scattering, characterising organo-mineral microfacies rich in amorphous organic matter organisms, are shifted to the centre of the diagram or to the lower part.

The distribution of macerals of terrestrial origin (macerals of the vitrinite and inertinite groups and sporinite) does not contradict the defined organo-mineral microfacies and paleoenvironments they indicate (Fig. 6-9). However, the presence of terrestrial macerals in a relatively high quantity in bituminous organo-mineral microfacies, which indicates suboxic-anoxic conditions, may demonstrate the close proximity of continental landmasses to the sedimentation area.

6.4.1.2. The distribution of TOC and HI according to the maceral composition of the investigated Posidonia Shale

Organic petrography in conjunction with the results of the geochemical analysis provide a comprehensive characterisation of organic matter. In Fig. 6-10 and Fig. 6-11, the distribution of TOC and HI are illustrated according to the main maceral assemblages: bituminite-liptodetrinite-alginite. It is apparent that almost all investigated samples of Posidonia Shale contain TOC values of more than 5 %, except wells of the South German Basin (Fig. 6-10). It is apparent that in these wells strong anoxic conditions had never been established. The oxygenated water column with good water mass circulation probably did not favour the preservation of organic matter and increased its oxidation.

In addition, in Fig. 6-10 it is clearly demonstrated that TOC values increase towards the alginite “corner” or are concentrated in the middle of the diagram. These parts of the ternary diagram indicate the biomass productivity. When paleoenvironmental conditions allowed organic matter supply, both provided by zooplankton and algae, and its preservation, the organic-rich sediments contain high TOC values.

As illustrated in Fig. 6-11, the quality of organic matter, indicated by HI, differs among the investigated wells. The HI index may not be correlated to TOC values,

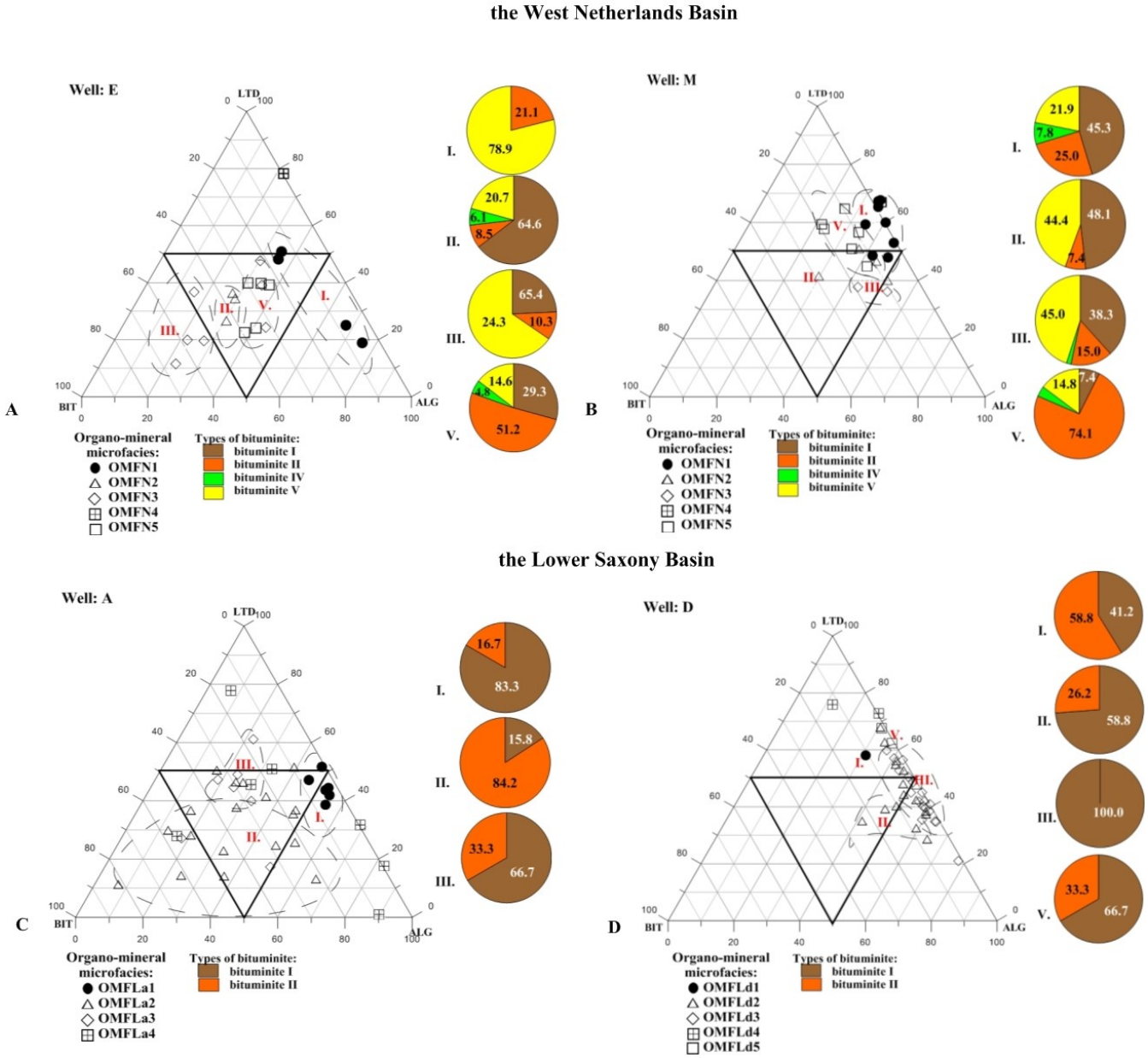

Fig. 6-7: Ternary diagrams illustrating the distribution of organo-mineral microfacies in wells of the West Netherlands Basin (A, B) and the Lower Saxony Basin (C, D). Pie charts show representative bituminite pattern within each microfacies.
Ternary diagram: Bit (sum of all bituminites)+LTD(liptodetrinite)+ALG(telalginite and lamalginite)=100 [vol.%]. Pie chart: Sum of all bituminites=100 [vol.%].

Organo-mineral microfacies from the West Netherlands Basin. OMFN 1: Low bituminous limestone with low content of bituminite; OMFN 2: Bituminous marly limestone enriched in bituminite I; OMFN3: Bituminous calcareous mudstone and marly limestone enriched in bituminite V; OMFN 4: Low bituminous limestone rich in liptodetrinite and discrete lamalginite; OMFN 5: Bituminous calcareous mudstone and limestone enriched in bituminite II. **Organo-mineral microfacies from the Lower Saxony Basin.** Well A. OMFLa 1: Bituminous calcareous mudstone enriched in terrestrial macerals with low content of bituminites; OMFLa 2: Bituminous limestone enriched in bituminite II; OMFLa 3: Bituminous limestone enriched in bituminite I; OMFLa 4: Bituminous limestone with low content of lamalginite. Well B. OMFLd 1: Bituminous limestone enriched in bituminite II; OMFLd 2: Bituminous limestone enriched in bituminite I; OMFLd 3: Bituminous limestone with high content of filamentous lamalginite and decreased content of bituminites; OFLd 4: Low bituminous limestone with low diversity of macerals; OMFLd 5: Bituminous limestone with low content of discrete, filamentous lamalginite and bituminites.

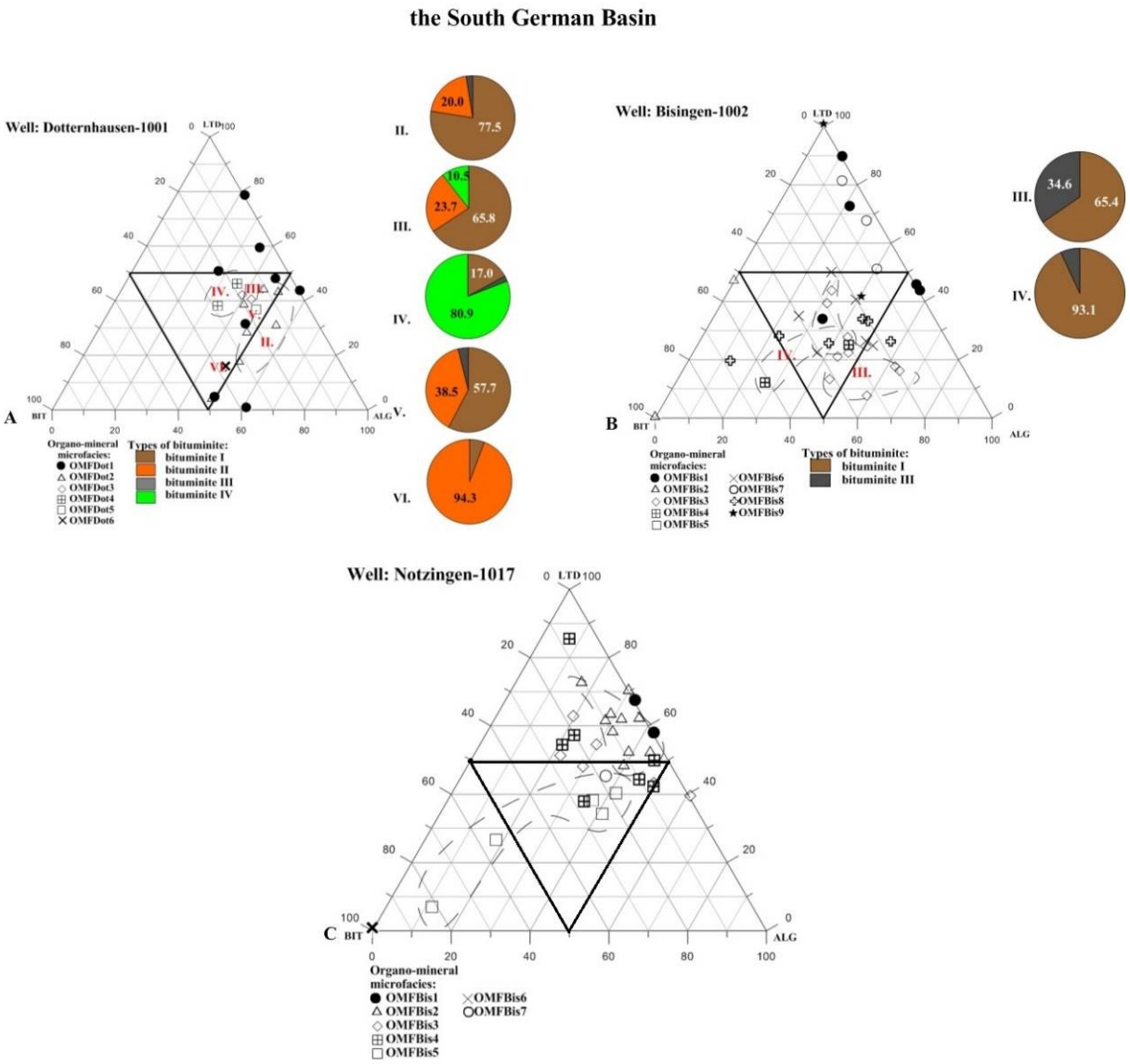

Fig. 6-8: Distribution of organo-mineral microfacies in the Dotternhausen-1001 well (A), Bisingen-1002 well (B) and Notzingen-1017 (C) of the South German Basin.
Note: the maceral composition data of the Bisingen 1002 well after Prauss *et al*., (1991); maceral composition data of Notzingen-1017 well after Ligouis, (unpublished).
Pie charts illustrate the distribution of the bituminites within the individual organo-mineral microfacies.
Ternary diagram: Bit (sum of all bituminites)+LTD(liptodetrinite)+ALG(telalginite and lamalginite)=100 [vol.%]. Pie chart: Sum of all bituminites=100 [vol.%].

Organo/mineral microfacies from the South German Basin:

Dotternhausen-1001 well: OMFDot 1: Non-bituminous silty marls enriched in zooclasts; OMFDot 2: Bituminous silty marls, limestone enriched in bituminite I; OMFDot 3: Bituminous silty marls and limestone enriched in bituminite I and bituminite VI; OMFDot 4: Bituminous silts marls and limestone enriched in bituminite IV; OMFDot 5: Bituminous mudstone with even quantity of bituminite I and bituminite II.

Bisingen-1002 well: OMFBis 1: Claystones and calcareous shales with high input of vitrinite maceral and suppressed content of zooclasts; OMFBis 2: Calcareous shales and limestone enriched in vitrinite and with a high content of zooclasts; OMFBis 3: Bituminous shales enriched in bituminite I with moderate content of zooclasts; OMFBis 4: Bituminous shales with high content of zooclasts; OMFBis 5: Bituminous limestone poor in organic matter; OMFBis 6: Bituminous shales enriched in bituminite I with low content of zooclasts; OMFBis 7: Bituminous limestone with high content of lamalginite and liptodetrinite; OMFBis 8: Bituminous shales with high content of lamalginite, bituminite I and liptodetrinite; OMFBis 9: Calcareous shales with high content of inertinite and zooclasts.

Notzingen-1017 well: OMFNot 1: Calcareous shales with high input of terrestrial organic matter; OMFNot 2: Bituminous limestone and bituminous calcareous shales with low content of zooclasts and increased content of sporinite and telalginite; OMFNot 3: Bituminous shales and limestone with increased content of liptodetrinite and bituminites; OMFNot 4: Bituminous shales and calcareous shales, characterised by increased content of telalginite together with inertinite; OMFNot 5: Bituminous shales and calcareous shales enriched in telalginite, bituminite and sporinite; OMFNot 6: Calcareous shales enriched in inertinite; OMFNot 7: Bituminous calcareous shales enriched in vitrinite.

demonstrating that the quality of the organic matter depends on the maceral type. Each of the distinct macerals is characterised by different generation properties.

The samples from the West Netherlands Basin are characterised by values of HI more than 500 mg HC/g TOC, indicating good quality source rocks. However, Posidonia Shale in well D also shows equally high values of HI. As was mentioned before, the samples from well D contain a large quantity of liptodetrinite, but a lower content of bituminite than the Posidonia Shale from wells E and M. This enables the assumption that the high generation properties of the source rocks are provided not only by bituminites (AOM), but probably by alginite and liptodetrinite, concentrated in source rocks in high quantities.

Posidonia Shale from well A is characterised by a high content of bituminites. However, it shows lower values of HI than wells E, M and D. The maturity level in samples from well A is higher than those from wells E and M. If it is taken into account that diagenetically transformed bituminite yields oil earlier than macerals of the alginite group, then the Posidonia Shale in well A has already undergone oil expulsion (Teichmüller and Ottenjann, 1977).

HI varies in the wells of the South German Basin. In the Bisingen-1002 well, it is lower than in the Notzingen-1017 well. This difference can probably be explained by a variation in paleoenvironmental conditions. In the Notzingen-1017 well, those were more oxygen-depleted than the Bisingen-1002 well.

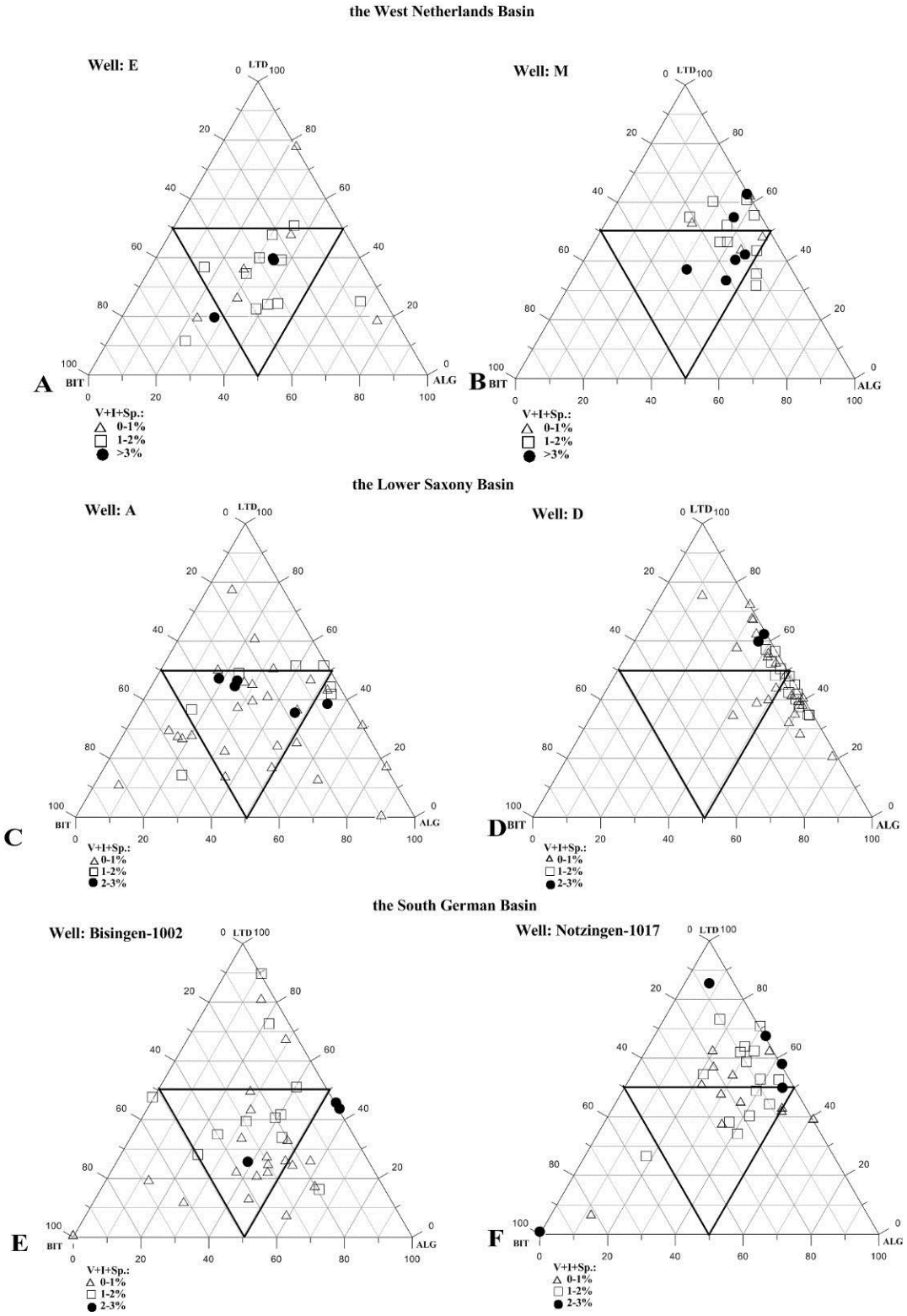

Fig. 6-9: Ternary diagram showing distribution of the organic matter of terrestrial origin in wells from the West Netherlands Basin (A, B), the Lower Saxony Basin (C,D) and the South German Basin (E,F).
Note that Bit (sum of all bituminites)+LTD(liptodetrinite)+ALG(telalginite and lamalginite)=100 [vol.%].
V-macerals of vitrinite group; I-macerals of inertinite group; Sp.-sporinite.

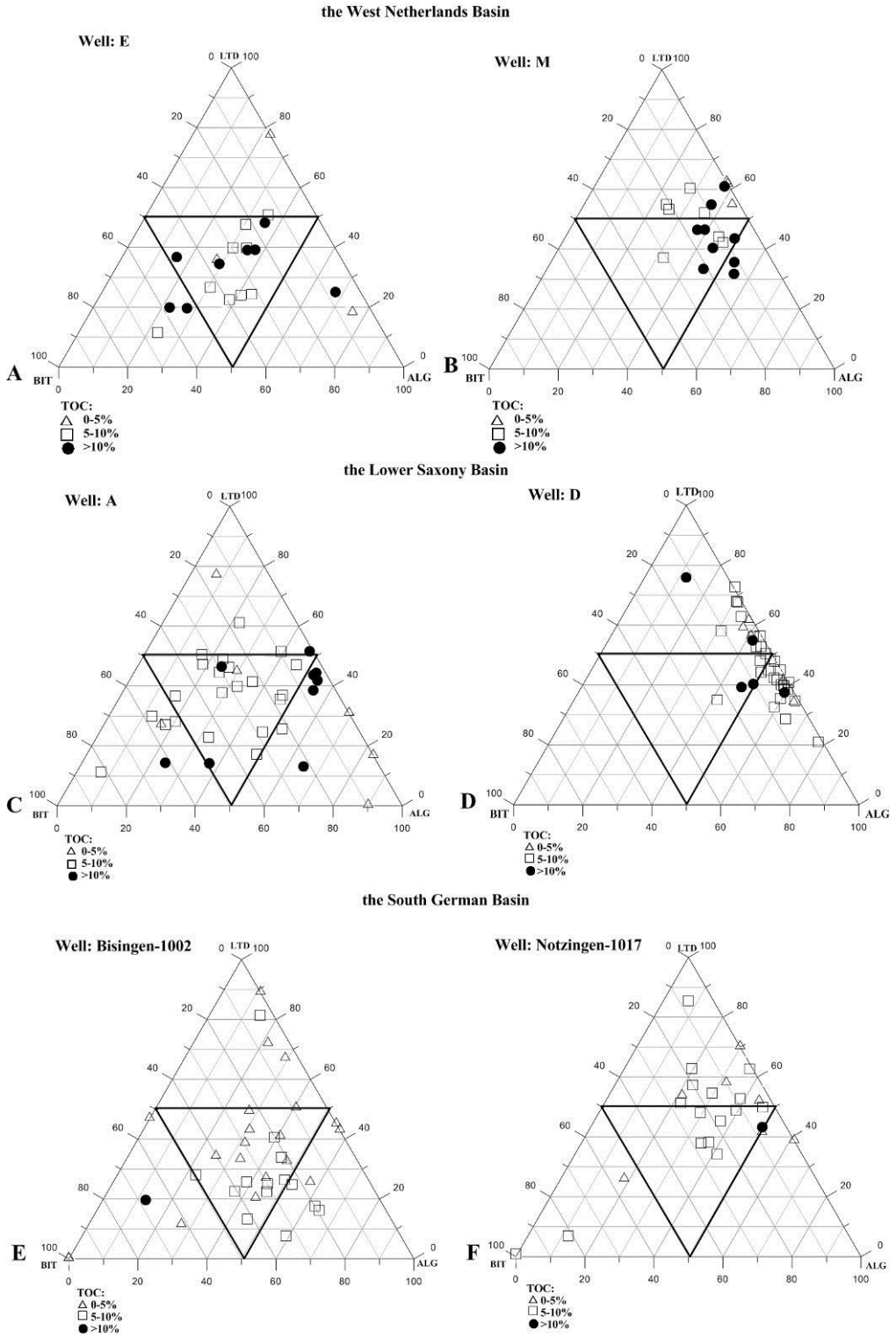

Fig. 6-10: Distribution of TOC values in Posidonia Shale of the West Netherlands Basin (A,B), the Lower Saxony Basin (C,D) and the South German Basin (E,F).
Note that Bit (sum of all bituminites)+LTD(liptodetrinite)+ALG(telalginite and lamalginite)=100 [vol.%].

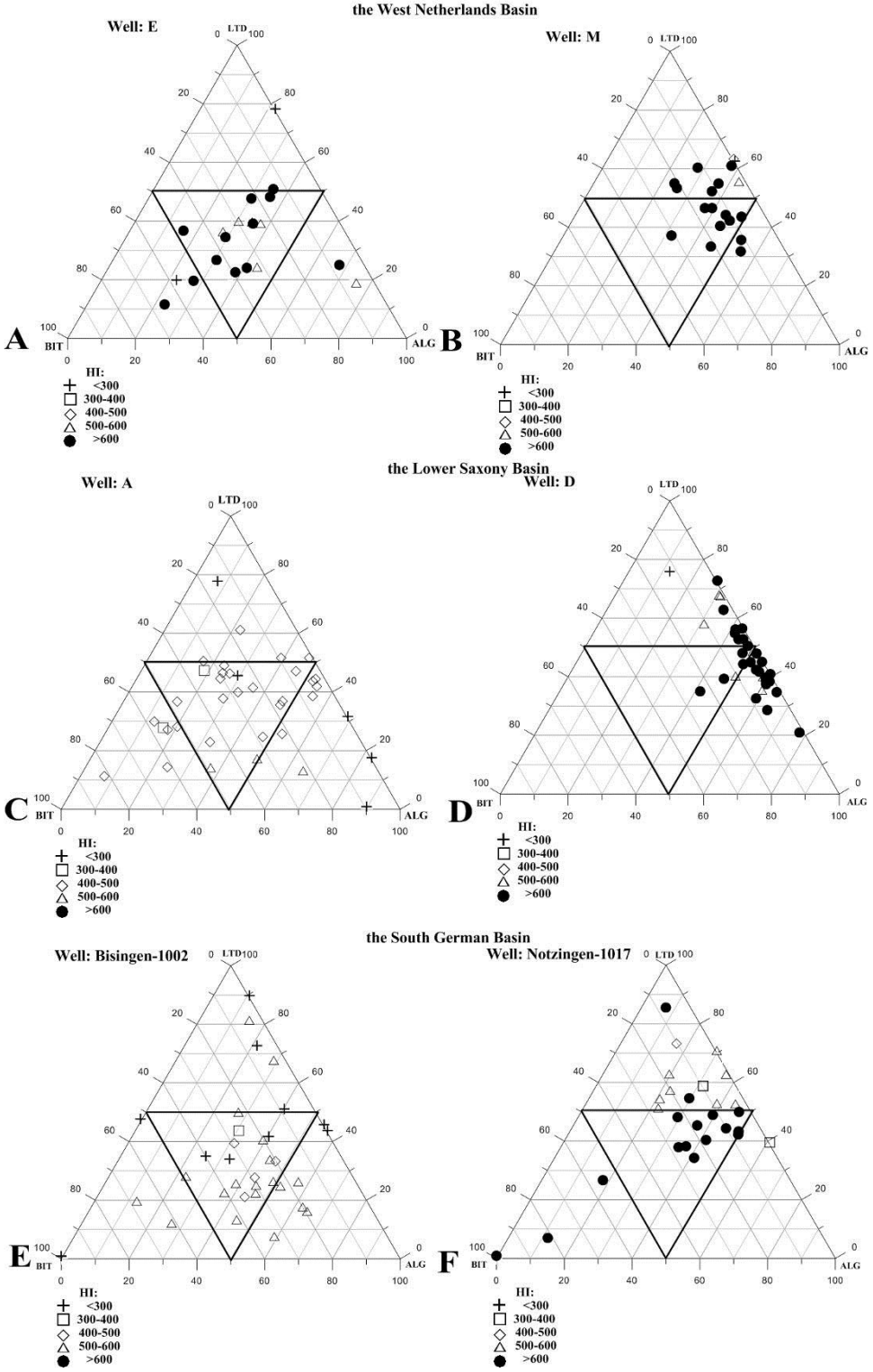

Fig. 6-11: Distribution of HI values in Posidonia Shale from the West Netherlands Basin (A, B), the Lower Saxony Basin (C, D) and the South German Basin (E, F).
Note: Bit (sum of all bituminites)+LTD (liptodetrinite)+ALG(telalginite and lamalginite)=100 [vol.%]. HI [mg HC/g TOC].

6.4.2. The scatter plot

The other method proposed in this study for data visualisation is the scatter plot. Contrary to the ternary diagram, the scatter plot describes the oxidation and degradation processes which have already taken place in the sediments.

As mentioned in the Introduction, organic matter accumulation and preservation is controlled by biologic productivity, sediment mineralogy and oxygenation of the bottom water and sediments (McCarthy *et al*., 2011). Within depositional settings, fluctuation in oxygen content in the water column is perhaps the most important parameter. The increased availability of oxygen favours the concentration of organic matter in the sediments, while its deficiency ensures the preservation of organic matter (McCarthy *et al*., 2011).

Because of the thermodynamically unstable nature of organic matter, the latter suffers modifications caused by bacterial degradation once it has started to sink. Bacterial degradation proceeds quickly and efficiently in well-oxygenated water. Once the oxygen supply becomes exhausted, degradation of organic matter continues by anaerobic bacteria using sulfates as an oxygenation agent (Demaison and Moore, 1980). Anaerobic degradation is thermodynamically less efficient than aerobic decomposition. Moreover, it results in more lipid-rich substances (hydrogen-rich) than in aerobic degradation (Demaison and Moore, 1980). In other words, macerals of the vitrinite group are more likely to be bacterially oxidised than those of the liptinite group. Therefore, an increased content of bituminites (AOM) is an indicator of enhanced anoxic environments.

Our study on the Posidonia Shale shows the relationships between identified organo-mineral microfacies and four depositional areas, describing a variety of paleoenvironmental conditions (Fig. 6-11). These areas are empirically established according to the organo-petrographic results. The calculation is based on the data set of quantitative and qualitative maceral analysis, using two indices proposed in this study: Degradation Index and Oxidation Index. The Degradation Index is the ratio of macerals derived by anaerobic bacteria degradation to those non-degraded (Eq. 1). When the Degradation Index shows values of more than 1, the conditions change from suboxic to anoxic. The Oxidation Index is the ratio between macerals, indicating oxygenated, dynamically active paleoenvironments, and those macerals which demonstrate quiet anoxic conditions (Eq. 2). In addition, it may provide information on the remoteness of the sedimentation area from landmasses. Therefore, the denominator includes oxidised vitrinite and liptodetrinite. Oxidised vitrinite, indeed, might already have been formed on the continent. However, the presence of this maceral

incorporated in the sediments may suggest strong currents as well as the presence of liptodetrinite. The relationship between liptodetrinite and alginite, liptodetrinite and bituminites has been demonstrated above. In Fig. 6-1 it is clearly recognisable that liptodetrinite acts as an indicator of oxygenated conditions.

The denominator of the Oxidation Index includes indigenous vitrinite and bituminites. As previously mentioned, vitrinite is a maceral of terrestrial origin, transported into marine environments. However, well-preserved indigenous vitrinite along with bituminites may indicate suboxic-anoxic environments. On the one hand, it indicates rather close proximity to the landmasses; on the other hand, it demonstrates oxygen-depleted environments favouring the preservation of vitrinite particles.

The areas distinguished in Fig. 6-12 reflect transitions between oxic and anoxic depositional conditions. Each of the identified areas shows paleoenvironments which favour the occurrence of organo-mineral microfacies with a predominance of one distinct type of bituminite among others (areas II, III, IV), or those organo-mineral microfacies which contain a low concentration of bituminites (area I).

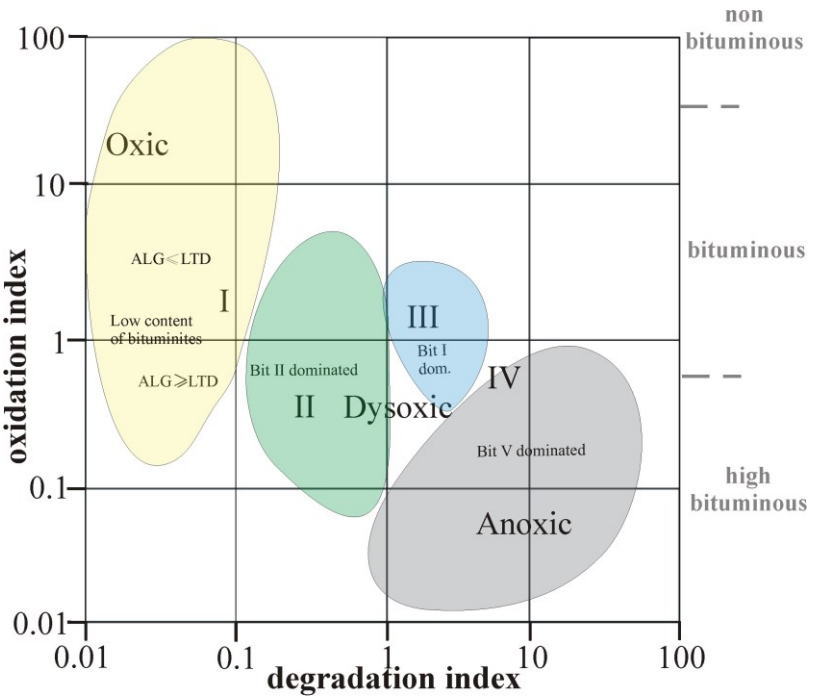

Fig. 6-12: Diagram showing the distribution of the organo-mineral microfacies according to the calculated Oxidation and Degradation Indices.

$$\textbf{Degradation Index} = \frac{\sum Bituminites}{Sp.+Alg.}$$

(Eq. 1)

$$\textbf{Oxidation Index} = \frac{V\ (oxidised)+LTD}{V\ (indigenous)+\sum Bituminites}$$

(Eq. 2).

As shown in Fig. 6-13, the distribution of the points in the diagram is in agreement with the previously discussed results of the maceral analysis. The low bituminous shales in wells M and D were deposited under oxic-suboxic paleoenvironmental conditions, while those in wells E and A indicate suboxic-anoxic conditions, by shifting the scatterings to the middle or right lower part of the diagram. The distribution of the areas is appropriate only for bituminous and high bituminous organic- rich sediments and in agreement with the organo-mineral microfacies identified in wells E and A.

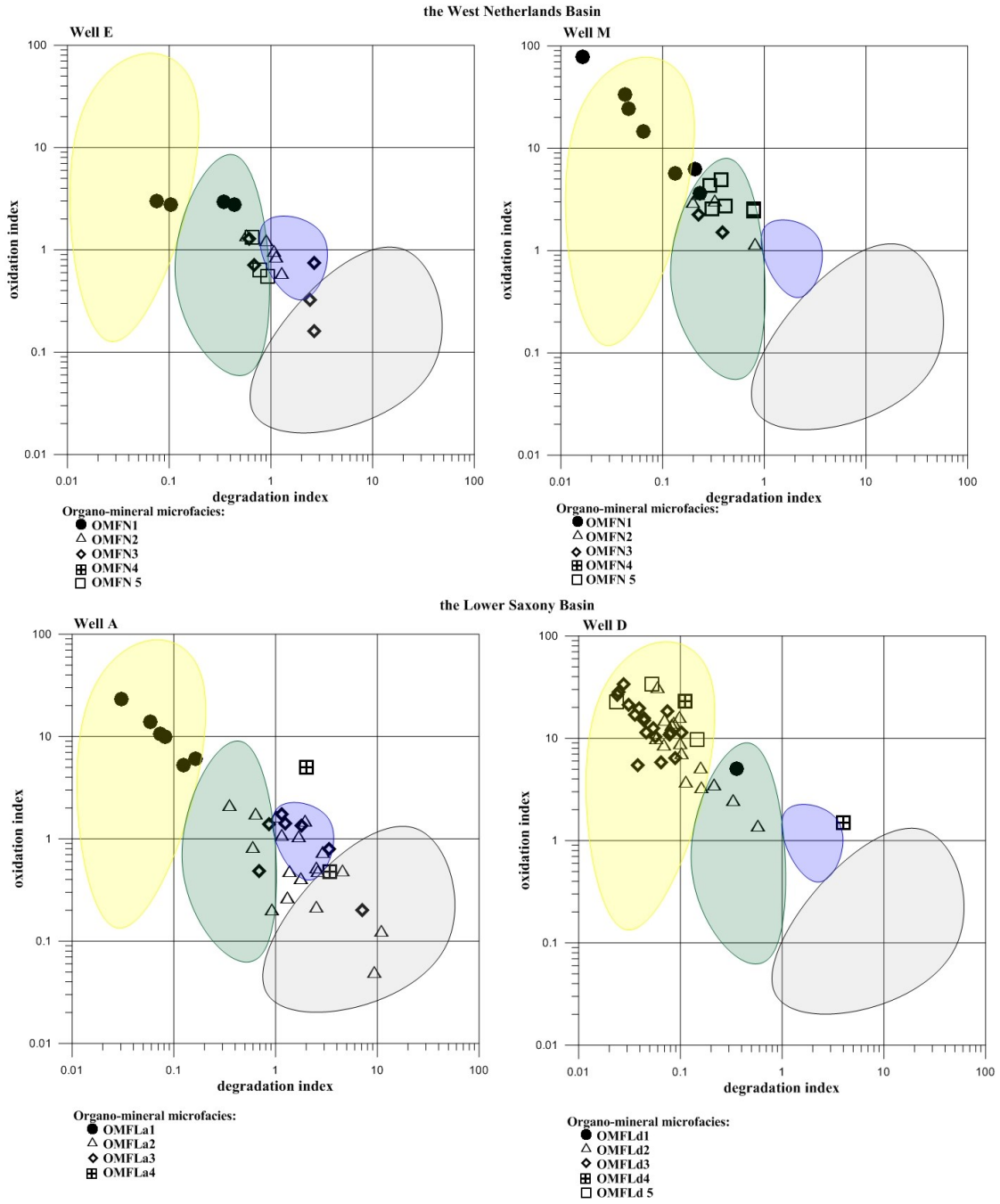

Fig. 6-13: Scatter plot illustrating the distribution of the organo-mineral microfacies of the West Netherlands (A, B) and Lower Saxony Basins (C, D).

Organo-mineral microfacies from the West Netherlands Basin. OMFN 1: Low bituminous limestone with low content of bituminites; OMFN 2: Bituminous marly limestone enriched in bituminite I; OMFN 3: Bituminous calcareous mudstone and marly limestone enriched in bituminite V; OMFN 4: Low bituminous limestone rich in liptodetrinite and discrete lamalginite; OMFN 5: Bituminous calcareous mudstone and limestone enriched in bituminite II.

Organo-mineral microfacies from the Lower Saxony Basin. Well A. OMFLa 1: Bituminous calcareous mudstone enriched in terrestrial macerals with low content of bituminites; OMFLa 2: Bituminous limestone enriched in bituminite II; OMFLa 3: Bituminous limestone enriched in bituminite I; OMFLa 4: Bituminous limestone with low content of lamalginite. Well B. OMFLd 1: Bituminous limestone enriched in bituminite II; OMFLd 2: Bituminous limestone enriched in bituminite I; OMFLd 3: Bituminous limestone with high content of filamentous lamalginite and decreased content of bituminites; OFLd 4: Low bituminous limestone with low diversity of macerals; OMFLd 5: Bituminous limestone with low content of discrete, filamentous lamalginite and bituminites.

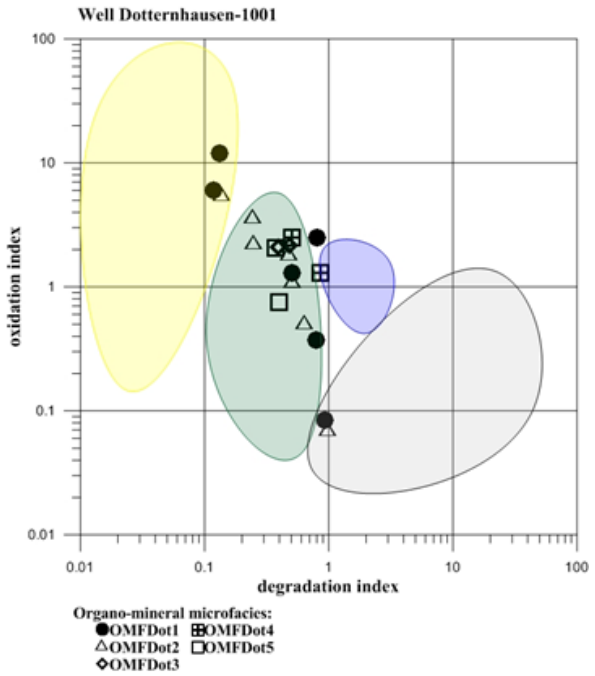

Fig. 6-14: Scatter plot illustrating the distribution of the organo-mineral microfacies in the Dotternhausen-1001 well of southern Germany.
OMFDot 1: Non-bituminous silty marls enriched in zooclasts; OMFDot 2: Bituminous silty marls, limestone enriched in bituminite I; OMFDot 3: Bituminous silty marls and limestone enriched in bituminite I and bituminite VI; OMFDot 4: Bituminous silty marls and limestone enriched in bituminite IV; OMFDot 5: Bituminous mudstone with even quantity of bituminite I and bituminite II.

In southern Germany, such a detailed maceral analysis was only done on Posidonia Shale samples from the Dotternhausen-1001 well. Fig. 6-14 illustrates that scatterings are gathered in areas indicating oxic and suboxic paleoenvironments. As was mentioned before, variations in organo-mineral microfacies are high compared to those from the West Netherlands Basin and the Lower Saxony Basin. This resulted from frequent changes in paleoenvironments, favouring the formation of the identified organo-mineral microfacies. These changes did not allow the establishment of distinct environments over a long time. Therefore, the organo-mineral microfacies do not show a distinct concentration within one specific area (Fig. 6-13).

This diagram is crucial for the interpretation and reconstruction of paleoenvironmental conditions. Moreover, it is an essential clue to the understanding of the origin of bituminites. For instance, in high bituminous shales, organo-mineral microfacies enriched in bituminite I are concentrated in the middle of the plot, where the suboxic conditions favour the sedimentation and preservation of organic matter. This supports the suggestion by

Teichmüller and Ottenjann (1977) that bituminite I probably originates from the bacterial degradation of algae.

Organo-mineral microfacies enriched in bituminite II are located in the middle part, but in a lower position than those rich in bituminite I. Rullkötter *et al*. (1992) stated that faecal pellets may act as a precursor of bituminite II. Important factors for these organo-mineral microfacies are both the oxygenated water surface, controlling bioproductivity, and suboxic-anoxic conditions which govern the preservation of organic matter. Organo-mineral microfacies in which bituminite V prevails among other bituminites are located in the right lower area, in which paleoenvironmental conditions turn anoxic. In these harsh conditions, there is no longer a high supply of organic matter and only bacteria can survive. Therefore, bituminite V possibly originated from bacterial mats itself (?).

It is clear that a better understanding of the origin of bituminites is one of the main challenges of organic petrology. A better understanding of the main factors controlling the accumulation and preservation of organic matter would certainly provide an important clue. For this reason, more work is required to confirm these hypotheses.

CHAPTER 7. CONCLUSIONS AND PERSPECTIVES

CONTENTS

It is well-known that Lower Toarcian Posidonia Shale was deposited in a wide epicontinental sea flooded in central and northern Europe. However, despite the widespread character of anoxic conditions at that time (AOE), which launched the occurrence of bituminous shales, organo-mineral microfacies may vary significantly. Seemingly homogeneous from a macroscopic point of view, Posidonia Shale is more heterogeneous on the microscopic scale.

In this PhD study, detailed high-resolution organic petrography was performed on Posidonia Shale from three different sedimentary basins. Posidonia Shale exhibits vertical and lateral organo-mineral microfacies variations that are largely related to the changes in paleoenvironmental conditions, which, in turn, differ from one sedimentary basin to another. Laterally, these patterns of organo-mineral microfacies are slightly correlated to each other, indicating restricted communication between the indicated basins. The paleoenvironmental features and reconstruction of the sedimentary model of Posidonia Shale deposition are summarised herein.

Apart from the organo-mineral microfacies and depositional paleoenvironments, the maturity of the bituminous shales from each of the aforementioned sedimentary basins was determined. Among early mature and mature levels, the post-mature Posidonia Shale was investigated. The thermal evolution of the macerals from the main organic groups was studied in particular and described in detail.

7.1. Lateral and vertical organo-mineral microfacies variations of Posidonia Shale

All the identified organo-mineral microfacies include the specific assemblage of individual terrestrial and marine macerals and related minerals. These organo-mineral microfacies reflect sea-level fluctuation and, as a consequence, different paleoenvironmental conditions. However, in the paleoenvironmental reconstruction, uncertainty of bituminites (AOM) and liptodetrinite origin complicates the interpretation of the obtained results.

In the Posidonia Shale from the West Netherlands Basin, the variation of the telalginite and lamalginite is very low. However, the identified bituminite V in high quantities was represented only in this area.

Telalginite and lamalginite from the Lower Saxony Basin exhibit the highest variability among all the investigated wells. Moreover, the content of the bituminite II in well

A reaches a high of 58.0 vol.%. This demonstrates the quiet paleoenvironments with restricted water column circulation. The Posidonia Shale in well D contains the highest amount of liptodetrinite among all the investigated wells, probably indicating the increased water dynamic and oxygen availability.

While the organo-mineral microfacies from the West Netherlands and northwestern Germany are characterised by gradual vertical transition, those from southern Germany changed rapidly from oxic-suboxic to anoxic conditions. This led to mass mortality of the fauna recorded in the organo-mineral microfacies. Moreover, high input of the terrestrial macerals, together with the wavy fabric of the sediments emphasised by the zooclasts, probably indicate water currents. In addition, bituminite III was encountered in higher concentration only in the organo-mineral microfacies of Posidonia Shale from the South German Basin.

Some individual macerals are linked to a specific mineral groundmass. Specifically, bituminite I is more frequently found in the clayey-rich groundmass, whereas other bituminites are more common in the calcareous-rich matrix.

7.2. Depositional paleoenvironments

7.2.1. Organo-mineral microfacies as an indicator of the paleoenvironmental changes and their relationship to the oil generation potential

7.2.1.1. The West Netherlands Basin

Lateral variation in maceral assemblage comprising organo-mineral microfacies indicates that all three sedimentary basins were enclosed, hosting specific paleoenvironments. In the West Netherlands Basin, organo-mineral microfacies from well E and well M show a resemblance. However, oxygen availability and the water dynamic in well M is greater than in well E, as well as the depth. This is echoed by the increased content of liptodetrinite in well M, which is inversely proportional to that of the bituminite.

The marly groundmass in the investigated bituminous shale, probably indicates evaporitic environments which are characterised by high biomass productivity (Curial *et al*., 1990). Nevertheless, in an enclosed sedimentary basin, the establishment and the spread of anoxic events is more efficient than in well-communicated basins. This led to an increased amount of amorphous organic matter and suppressed organic matter variability. The

established oxygen-depleted paleoenvironments decreased the content of telalginite and lamalginite, which were represented mostly by *Tasmanite*-derived algae and discrete lamalginite respectively. In addition, these depositional environments favoured the rapid burial of organic matter in the sediments without major reworking (Curial *et al.,* 1990).

The thickness of the Lias epsilon is high and comprises 29.91 and 31.37 m for well E and well M respectively, indicating a low water mass circulation and the absence of the rapid fluctuation of the sea level. Presumably, the water dynamic increased when a storm event occurred. Therefore, sub-basins of well M and well E were in communication. However, they were separated by a morphological barrier.

These are in good agreement with the geochemical results integrated in the study, which reveal that Posidonia Shale from the West Netherlands Basin contains the highest values of TOC and HI, reaching 16.6 % and 689 mg HC/g TOC and 16.8 % and 737mg HC/g TOC in wells E and M respectively. It is clear that bioproductivity in well M was marginally higher than in well E, as well as organic matter preservation. In addition, the highest quality of organic matter increases significantly when the content of bituminite V rises as well.

7.2.1.2. The Lower Saxony Basin

Wells A and D represent other depositional environments. Well A is presumed to be a significantly deeper sedimentary basin than all the other investigated areas. It was probably separated from the ocean water masses. However, an increasing water flux in storm periods influenced the distribution of oxygen in the water column: the water surface was more oxygenated than the bottom water. This can explain the high productivity of organic matter and its good preservation (Busson, 1979).

The thickness of the Lias epsilon in well A is the highest among all the investigated wells at 34.15 m, whereas that in well D and well B are 6.96 and 5.30 m respectively. In well D, thickness and microfabrics may indicate the increased circulation of the water column and close location to the landmasses. These environments induce the reworking of organic matter, prevent its rapid burial and the occurrence of amorphous organic matter as well. However, reduced thickness may be linked to post-sedimentation erosion as well. In the case of well B, it is difficult to reconstruct the depositional environments as the sediments have undergone a high thermal maturation, which complicates the maceral analysis and paleoenvironmental reconstructions in such sediments.

In the Lower Saxony Basin, Posidonia Shale is characterised by a lower TOC and HI, comprising a maximum of 14.4 % and 539 mg HC/g TOC and 11.3 % and 654 mg HC/g TOC in wells A and D respectively. In these two wells, the predominant macerals are different. While in well A it is bituminite II, in well D it is liptodetrinite and discrete lamalginite with a low content of bituminite. Moreover, the optical properties of bituminite II indicate the thermal alteration of the sediments, which triggered the generation of oil from the amorphous organic matter. It is well established that oil generation from liptodetrinite and algae occurs under higher maturity than that of bituminites (AOM). Therefore, this evidence led to lower values of the HI in well D than in well A.

7.2.1.3. The South German Basin

Organo-mineral microfacies from the South German Basin demonstrate rapid changes of the paleoenvironments from oxic to suboxic-anoxic leading to the mass mortality of the fauna. This is in agreement with the thicknesses in the investigated wells. These thicknesses are 11.38, 11.92 and 4.92 m in the Dotternhausen-1001, Bisingen-1002 Notzingen-1017 wells respectively. In addition, the considerable variation from one environment to another enables both productivity of the organic matter and its rapid burial in the sediments. Among all the wells from the South German Basin, the stronger anoxic conditions were observed in the Notzingen-1017 well.

The Posidonia Shale from southern Germany yields variable values of TOC and HI. In the Notzingen-1017 well, the TOC and HI reach 11.2 % and 701mg HC/g TOC, whereas those in the Bisingen-1002 well are lower, comprising 8.5 % and 586 mg HC/g TOC respectively. These are in agreement with the organo-mineral microfacies, which were discussed in Chapter 4, and the above-mentioned conclusion.

7.3. Maturity and changes in optical properties of the macerals in the Posidonia Shale from early mature to post-mature stage.

The maturity of the Posidonia Shale in the investigated wells expressed by vitrinite reflectance varies from 0.4 to 0.5 %VRr, indicating the early mature to mature stage. However, the vitrinite reflectance in well B climbed to a high of 3.5 %, caused by the thermal influence of adjacent intrusive bodies. In order to define the optical properties of the macerals in the post-mature well, those were compared to the macerals from well A, which is located

44 km from well B. The results demonstrate that the telalginite bodies (named post-mature telalginite in this study), as well as bituminite I (named post-mature bituminite I in this study), bituminite II (named post-mature bituminite II in this study) and sporinite (named post-mature sporinite in this study) are still recognisable by their shape in the post-mature Posidonia Shale.

The benefits of the use of these terms in the maceral analysis of post-mature oil shale are the following (see Gorbanenko and Ligouis, 2014):

- Identification of carbon residues left by the hydrocarbon generation from telalginite, bituminite I, bituminite II, sporinite made possible by the recognition of the post-mature telalginite, post-mature bituminite I, post-mature bituminite II and post-mature sporinite, based on morphological criteria of the secondary forms of replacement.
- Appraisal of the telalginite content and of the contents of bituminite I (in part), of bituminite II, as well as the content in sporinite of the shale in the early mature stage.
- Identification of the mineral phases filling the spaces in these macerals once oil generation is achieved and expelled. Localisation and distribution of the porosity associated with these mineral phases.
- Recording of the modifications of size and morphology of these macerals resulting in oil generation and the crystallisation of minerals.
- Recognition of the disappearance of primary macerals, of the appearance of secondary macerals. Genetic relationships between primary macerals in mature bituminous shales and their replacements in post-mature Posidonia Shales.
- Characterisation of the organic-mineral fabric of the post-mature shale.
- Recognition of the modification of the mineral contents between mature and post-mature Posidonia Shales. Increase of the carbonate content.
- The secondary forms of replacement of alginite macerals in the maceral analysis of post-mature Posidonia Shales through the use of these terms can considerably improve the interpretation of the results of maceral analysis of post-mature source rocks.

In addition, this approach could offer new perspectives in pluridisciplinary works, by allowing a better integration of the results of organic petrology in a broader interpretation of the characteristics of oil and gas source rocks, which usually also takes into account the results of organic geochemistry and especially of Rock-Eval pyrolysis.

7.3.1. Graphical representation of the data in service of the depositional reconstruction

To ensure that the interpretation of the obtained maceral analysis results are more efficient, two types of diagram are proposed. The first is a ternary diagram, whereas the second is a scatter plot. In the ternary diagram, the interpretation was based on the fact that the liptodetrinite, alginite and bituminite indicate different paleoenvironments, which are either dynamic with increased oxygen availability or quiet with available oxygen and oxygen-depleted with restricted water circulation respectively. This diagram reflects the paleoenvironments not only regarding the sediments, but more significantly, the water column as well.

In contrast, the principles of the visualisation data on the scatter diagram are based on the reflection of the paleoenvironments regarding the sediments. In this case, macerals were selectively combined in the Oxidation and Degradation Indices, which describe different paleoenvironmental conditions governing the deposition and preservation of organic matter.

These results exhibit good agreement on the distribution of organo-mineral microfacies and the specific assemblages of macerals. In particular, the increased content of liptodetrinite and zooclasts exhibits a good correlation with the increased terrestrial input. Whereas bituminite V, which seems to be composed of bacterial mats, indicates significant anoxic conditions, bituminite II is associated with a high content of coccoliths and zooclasts. This indicates temporary oxygenation of the water surface, probably caused by a short-term storm event, which increased the water column circulation. In this case, the anoxic conditions are still present in the bottom water, favouring the preservation of organic matter.

Therefore, it enables the conclusion to be reached that sedimentation of Posidonia Shale in the Lower Saxony Basin occurred in suboxic environments, whereas those in the West Netherlands Basin were almost shifted to anoxic. The range of the paleoenvironments in South Germany is highly variable, indicating a rapid change in the paleoenvironments from oxic to suboxic-anoxic.

The variation of the organo-mineral microfacies, their deposition and preservation are in agreement with the model developed by Röhl and Schmid-Röhl (2005). This model described not only the morphological features of the sedimentary basin and the water column circulation as an important factor controlling the sedimentation and preservation of the Posidonia Shale, but more significantly, the sea-level fluctuation and climatic variations which promoted the changes in the deep-water redox conditions.

The plotting on the diagram of the results of geochemical analysis provides insights into the chemical properties of each of the selected maceral assemblages. In addition, it evaluates the contribution of distinct macerals in the generation properties of source rocks.

7.4. Perspectives and implications of high-resolution organic petrography

7.4.1. Perspectives and future plans

This study provides insights into the main constituents of the organic-rich sediments in the case of Posidonia Shale, which act as the main indicators of different paleoenvironments. However, the uncertainty of origin of some of them, such as liptodetrinite and bituminite, complicates the interpretation. These macerals originated from a variety of precursors and, consequently, have different petrographic, physical and chemical properties. Knowing these precursors provides some clue to the understanding of the depositional settings which favour the formation of organic-rich sediments. The theories and hypothesis proposed in this work have a theoretical character and still require the results of the biomarker analysis to prove them valid or invalid.

7.4.2. Implications of high-resolution organic petrography

Organic petrography is a fairly quick method that provides direct information on the organic constituents in the hydrocarbon source rocks. The use of quantitative and qualitative methods enables comprehensive characterisation of the organic matter, including the determination of the maturity of the source rocks. Moreover, this technique is crucial in the understanding of the relationships between the identified organo-mineral microfacies and the different paleoenvironmental conditions which favoured organic matter sedimentation in marine paleoenvironments.

Organic petrography is complementary to organic geochemistry. It does not replace the results obtained by geochemical methods, but provides considerable details. For instance, the results of geochemical analysis are based on the investigation of powdered samples. They show the average data of one selected sample. By contrast, for high-resolution organic petrography, pieces of rock cut perpendicular to the bedding plane are used. The results obtained using this technique provide information not only on the main constituents in the

samples, but a detailed description of sedimentological features. This increases the accuracy and, as a consequence, the quality of the interpretation. Moreover, organic petrography as a paleoenvironmental implication is widely useful in those sediments where the sedimentological transition is not easily recognisable.

REFERENCES

Abraham, H., 1938. Asphalts and allied substances, their occurrence, modes of production, uses in the arts and methods of testing. D. Van Nostrand Co., New York.

Alpern, B., 1980. Pétrographie du kérogéne, in: Durand, B. (Ed.), Kerogen: Insoluble Organic Matter from Sedimentary Rocks. Technip, Paris, pp. 339–371.

Alpern, B., Cheymol, D., 1978. Réflectance et fluorescence des organoclastes du Toarcien du bassin de Paris en fonction de la profondeur et de la température. Rev. Inst. Fr. Pét. 33, 515–535.

Alpern, B., Oudin, J.L., Pinheiro, H.J., Pitton, J.-L., Zhu, X., 1994. Optical study method of hydrocarbon extracted and fixed by the embedding resin of polished rock samples. Influence of the richness in oil on the reflectance of kerogen. Bull.Centres Rech. Explor. 15–35.

Arntz, W.E., Tarazona, J., Gallardo, V.A., Flores, L.A., Salzwedel, H., 1991. Benthos communities in oxygen deficient shelf and upper slope areas of the Peruvian and Chilean Pacific coast, and changes caused by El Niño, in: Tyson, R. V, Pearson, T.H. (Eds.), Modern and Ancient Continental Shelf Anoxia. Geol. Soc. Spec. Publ., London, pp. 131–154.

Baldaschuhn, R., Best, G., Kockel, F., 1991. Inversion tectonics in the north-west German basin, in: Spencer, A.M. (Ed.), Generation, Accumulation and Production of Europe´s Hydrocarbons I. Spec. Publ. Eur. Assoc. Pet. Geosci., pp. 149–159.

Barker, C., 1974. Pyrolysis techniques for source-rock evaluation. AAPG Bull. 58, 2349–2361.

Barker, C., Pawlewicz, M., Buntebarth, G., Stegena, L., 1986. The correlation of vitrinite reflectance with maximum temperature in humic organic matter. Paleogeothermics 5, 79–93.

Barker, C., Pawlewicz, M.J., 1993. An empirical determination of the minimum number of measurements needed to estimate the mean random vitrinite reflectance of disseminated organic matter. Org. Geochem. 20, 643–651.

Bartenstein, H., Teichmüller, M., Teichmüller, R., 1971. Die Umwandlung der organischen Substanz im Dach des Bramscher Massivs. Fortschr. Geol. Rheinld. Westf. 18, 501–538.

Batten, D.J., 1985. Coccolith moulds in sedimentary organic matter and their use in palynofacies analysis. J.Micropalaeontol. 4, 111–116.

Bernard, S., Horsfield, B., Schulz, H.M., Wirth, R., Schreiber, A., Sherwood, N., 2012. Geochemical evolution of organic-rich shales with increasing maturity: A STXM and TEM study of the Posidonia Shale (Lower Toarcian, northern Germany). Mar. Pet. Geol. 31, 70–89.

Berner, R.A., 1984. Sedimentary pyrite formation: An update. Geochim. Cosmochim. Ac. 48, 605–615.

Berner, R.A., 1964. Distribution and diagenesis of sulfur in some sediments from the Gulf of California. Mar. Geol. 1, 117–140.

Bertrand, R., 1993. Standartization of solid bitumen reflectance to vitrinite in some Paleozoic Sequences of Canada. Energy Sourc. 15, 269–287.

Betz, D., Führer, F., Greiner, G., Plein, E., 1987. Evolution of the Lower Saxony Basin. Tectonophysics 137, 127–170.

Beurlen, K., Gall, H., Schairer, G., 1992. Die Alb und ihre Fossilien. Sonderausgabe. Geologie und Paläontologie der Schwaben- und Frankenalb. Gondrom Verlag GmbH.

Binot, F., Gerling, P., Hiltmann, W., Kockel, F., Wehner, H., 1993. The petroleum system in the Lower Saxony Basin III, in: Spencer, A.M. (Ed.), Generation, Accumulation and Production of Europe's Hydrocarbons. Springer Verlag, Berlin-Heidelberg, pp. 121–139.

Bodenhausen, J.W.A., Ott, W.F., 1981. Habitat of the Rijswijk oil province, onshore, the Netherlands., in: Illing, L. V, Hobson, G.D. (Eds.), Petroleum Geology of the Continental Shelf of North-West Europe. Institute of Petroleum, London, pp. 301–309.

Boggs, S., 2009. Petrology of sedimentary rocks, Cambridge University Press. Cambridge.

Boigk, H., 1968. Gedanken zur Entwicklung des Niedersächsischen Tectogens. Geol. Jahrb 85, 861–900.

Boigk, H., Hark, H.H., Meyer, H.J., Wehner, H., 1974. Beziehungen zwischen Gechemie, Migration und Lagerstättengenese im Niedersächsischen Becken (westlich der Weser). Erdöl Erdgas Kohle 24, 98–113.

Bordenave, M.L., Espitalié, J., Leplat, P., Oudin, J.L., Vandenbroucke, M., 1993. Screening techniques for source rock evaluation, in: Bordenave, M.L. (Ed.), Applied Petroleum Geochemistry. Éditions technip, Paris, pp. 217–279.

Borrego, A.G., Araujo, C.V., Balke, A., Cardott, B., Cook, A.C., David, P., Flores, D., Hámor-Vidó, M., Hiltmann, W., Kalkreuth, W., Koch, J., Kommeren, C.J., Kus, J., Ligouis, B., Marques, M., Mendonça Filho, J.G., Misz, M., Oliveira, L., Pickel, W., Reimer, K., Ranasinghe, P., Suárez-Ruiz, I., Vieth, A., 2006. Influence of particle and surface quality on the vitrinite reflectance of dispersed organic matter: Comparative exercise using data from the qualifying system for reflectance analysis working group of ICCP. Int.J.Coal Geol. 68, 151–170.

Botz, R., Schmidt, M., Kus, J., Ostertag-Henning, C., Ehrhardt, A., Olgun, N., Garbe-Schönberg, D., Scholten, J., 2011. Carbonate recrystallisation and organic matter maturation in heat-affected sediments from the Shaban Deep, Red Sea. Chem. Geol. 280, 126–143.

Boussafir, M., Lallier-Vergès, E., 1997. Accumulation of organic matter in the Kimmeridge Clay formation (KCF): an update fossilisation model for marine petroleum source-rocks. Mar. Pet. Geol. 14, 75–83.

Brauckmann, F.J., 1984. Hochdiagenese im Muschelkalk der Massive von Bramsche und Vlotho. Ruhr-Univ.

Brinkmann, R., Kayser, E., 1991. Abriss der Geologie, B2 ed. Enke, Stuttgart.

Büchner, M., 1986. Geothermisch bedingte Veränderungen in Rhät- und Jura-Gesteinen des Unteren Weserberlandes als Folge des Vlothoer Glutflußmassivs. Ber. Naturwiss. Ver. Biefeld Umgebung 28, 109–138.

Buntebarth, G., 1985. Das Temperaturgefälle im Dach des Bramscher Massivs aufgrund von Inkohlungsuntersichingen im Karbon von Ibbenbüren. Fortschr. Geol. Rheinld. Westf. 33, 255–264.

Busson, G., 1979. Couches laminées riches en matiére organique et précédant les roches salines: les enseignements d´un enchalinement de faciés. Doc. des Lab. la Fac. des Sci. Lyon 75, 5–18.

Carr, A.D., Williamson, J.E., 1990. The relationship between aromaticity, vitrinite reflectance and maceral composition of coals: Implications for the use of vitrinite reflectance as a maturation parameter. Org. Geochem. 16, 313–323.

Caspers, H., 1957. Black Sea and Sea of Azov, in: Hedgepeth, J. (Ed.), Treatise of Marine Ecology and Paleoecology. Geol. Soc. Am. Mem., pp. 801–890.

Clementz, D.M., 1979. Effect of oil and bitumen saturation on source rock pyrolysis. Am. Assoc. Pet. Geol. Bull. 63, 2227–2232.

Cook, A., Hutton, A.C., Sherwood, N.R., 1981. Classification of oil shales. Bull. Centres Rech. Explor. 5, 353–381.

Cook, A.C., 1982. Organic facies in the Eromanga Basin, in: Moore, P.S., Mount, T.J. (Eds.), Eromanga Basin Symposium. Geol. Soc. Austr. And Pet. Explr. Soc. Austr., Adelaide, pp. 234–257.

Creaney, S., 1980. The organic peîrology ofthe Upper Cretaceous Boundary Creekformatìon, Beaufort-Mackenzie basin. B. Can. Pet. Geol. 28, l12–l19.

Cuomo, M.C., Bartholomew, P.R., 1991. Pelletal black shale fabrics: their origin and significance. Geol. Soc. London Spec. Pub. 58, 221–232.

Curial, A., Dumas, D., Dromart, G., 1990. Organic matter and evaporates in the Paleogene West European Rift: the Bresse and Valence Salt Basins (France)., in: Huc, A.Y. (Ed.), Deposition of Organic Facies. AAPG Stud.Geol. 30, Tulsa. Oklahoma, U.S.A., pp. 119–132.

Curiale, J.A., 1986. Origin of solid bitumens, with emphasis on biological marker results. Org. Geochem. 10, 559–580.

De Jager, J., Doyle, M.A., Grantham, P.J., Mabillard, J.E., 1996. Hydrocarbon habitat of the West Netherlands Basin, in: Rondeel, H.E., Batjes, D. A. J. Nieuwenhuijs, W.H. (Eds.),

Geology of Gas and Oil under the Netherlands. Kluwer Academic Publishers, Dordrecht, pp. 191–209.

De Jager, J., Geluk, M.C., 2007. Petroleum geology, in: Wong, T.E., Batjes, D.A.J., De Jager, J. (Eds.), Geology of the Netherlands. DutchAcademy of Arts and Sciences, Amsterdam, pp. 237–260.

Degens, E.T., Mopper, K., 1976. Factors controlling the distribution and early diagenesis of organic material in marine sediments. Chem. Ocean. 6, 11–59.

Degens, E.T., Ross, D.A., 1974. The Black Sea: Geology, chemistry, biology. AAPG Mem. 20, 183–199.

Dellisanti, F., Pini, G.A., Baudin, F., 2010. Use of Tmax as a thermal maturity indicator in orogenic successions and comparison with clay mineral evolution. Clay Miner. 45, 115–130.

Demaison, G.J., Moore, G.T., 1980. Anoxic environments and oil source bed genesis. Org. Geochem. 2, 9–31.

Deutloff, O., Teichmüller, M., Teichmüller, R., Wolf, H., 1980. Inkohlungsuntersuchung im Mesozoikum des Massivs von Vlotho (Niedersächsiches Tektogen). Neues Jahrb. Geol. Paläontol. 321–341.

Dias, J.M., Pilkey, O.H., Heilweil, V., 1984. Detrital mica: Environmental significance in north Portugal Continental Shelf sediments. Comun. Serv. Eol. Port. . 70, 93–101.

Dorning, K.J., 1981. Silurian acritarchs distribution in the Ludlovian shelf sea of South Wales and the Welsh Borderland., in: Neale, J.W., Brasier, M.D. (Eds.), Microfossils from Recent and Fossil Shelf Seas (British Micropalaeontological Society). Ellis Horwood, Chichester, pp. 6–31.

Düppenbecker, S.J., Welte, D.H., 1989. Effects of heating rates on generation and expulsion of hydrocarbons, Lower Saxony Basin, Federal Republic of Germany, in: 28th Int. Geol. Congr,. Washington D. C., pp. 228–229.

Durand, B., Alpern, B., Pittion, J.L., Pradier, B., 1986. Reflectance of vitrinite as a control of thermal history of sediments, in: Burrus, J. (Ed.), Thermal Modeling in Sedimentary Basins. Technip, Paris, pp. 441–474.

Durand, B., Espitalié, J., Nicaise, G., Combaz, A., 1972. Ètude de la matiére organique insoluble (kérogéne) des argiles du oarcien du Bassin de Paris: I. ètude par les proceeds optiques, analyse élémentaire, etude en microscopie et microdiffraction électoniques. Rev. Inst. Fr. Pét. 27, 865–884.

Espitalié, J., 1986a. La pyrolyse rock-eval et ses application, troisiéme partie. Rev. Inst. Fr.Pét. 41, 73–89.

Espitalié, J., 1986b. Use of Tmax as a maturation index for different types of organic matter. Comparison with vitrinite reflectance., in: Burrus, J. (Ed.), Thermal Modelling in Sedimentary Basins. Technip, Paris, pp. 475–496.

Espitalié, J., Marquis, F., Barsony, I., 1984. Geochemical logging, in: Voorhees, K.J. (Ed.), Analytical Pyrolysis: Techniques and Applications. Butterworth, Boston, pp. 276–304.

Espitalié, J., Marquis, F., Sage, I., Barsony, I., 1977. Méthode rapide de caractérisation des roches mères, de leur potential pétrolier et de leur degré d´évolution. Rev. Inst. Franç.du Pétr. 32, 23–45.

Fang, H., Jianyu, C., 1992. The cause and mechanism of vitrinite reflectance anomalies. J. Pet. Geol. 15, 419–434.

Faraj, B.S.M., Mackinnon, I.D.R., 1993. Micrinite in southern hemisphere sub-bituminous and bituminous coals: Redefined as fine grained kaolinite. Org. Geochem. 20, 823–841.

Farrimond, P., Eglinton, G., Brassell, S.C., Jenkyns, H.C., 1989. Toarcian anoxic event in Europe: An organic geochemical study. Mari. Pet. Geol. 6, 136–147.

Farrimond, P., Eglinton, G., Brassell, S.C., Jenkyns, H.C., 1988. The Posidonia black shale event in northern Italy. Org. Geochem. 13, 823–832.

Flügel, E., 2004. Microfacies of carbonate rocks: Analysis, interpretation and application. Springer Verlag, Berlin-Heidelberg-New-York.

Geyer, M., Nitsch, E., Simon, T., 2011. Geologie von Baden-Württemberg. Schweizerbart, Stuttgart.

Godoi, R.H.M., Aerts, K., Harlay, J., Kaegi, R., Ro, C., Chou, L., van Grieken, R., 2009. Organic surface coating on Coccolithophores - Emiliania huxleyi: Its determination and implication in the marine carbon cycle. Microchem. J. 91, 266–271.

Goldman, M., 1924. “Black shale” formation in and about Chesapeake Bay. Am. Assoc. Pet. Geol. Bull. 8, 195–201.

Golubic, S., 1976. Organisms that build stromatolites, in: Walter, M.R. (Ed.), Stromatolites. Developments in Sedimentology 20. Elsevier, Amsterdam, pp. 113–126.

Gonçalves Sá da Silva, P.A., 2014. Characterisation of organic facies and identification of potential source rocks in Jurassic sedimentary sequences of the Lustanian Basin (Portugal). FCUL.

Gorbanenko, O.O., Ligouis, B., 2014. Changes in optical properties of liptinite macerals from early mature to post mature stage in Posidonia Shale (Lower Toarcian, NW Germany). Int. J. Coal Geol. 133, 47–59.

Götz, A.E., Feist-Burkhardt, S., 2012. Phytoplankton associations of the Anisian Peri-Tethys Basin (Central Europe): Evidence of basin evolution and palaeoenvironmental change. Palaeogeogr. Palaeocl. 337-338, 151–158.

Gutjahr, C.C.M., 1983. Introduction to incident light microscopy of oil and gas source rocks. Geol. Mijnb. 62, 417–425.

Hallam, A., Bradshaw, M.J., 1979. Bituminous shales and oolithic ironstones as indicator of transgressions and regressions. Geol. Soc. London 136, 157–164.

Herngreen, G.F.W., Kouwe, W.F.P., Wong, T.E., 2003. The Jurassic of the Netherlands. Geol. Surv. Denmark Greenl. Bull. 1, 217–229.

Hesselbo, S.P., Jenkyns, H.C., 1995. A comparision of Hettangian to Bajocian successions of Dorset and Yorkshire., in: Taylor, P.D. (Ed.), Field Geology of the British Jurassic. Geol. Soc. Publishing House, Bath, UK, pp. 105–150.

Heybroek, P., 1974. Explanation to tectonic maps of the Netherlands. Geol.Mijnbouw. 53, 43–50.

Hollander, D.J., Bessereau, G., Belin, S., Huc, A.Y., Houzay, J., 1991. Organic matter in the Early Toarcian shales, Paris Basin, France: a response to environmental changes. Rev. Inst. Fr. Pét. 32, 703–718.

Huc, A.Y., 1990. Understanding organic facies: A key to improved quantitative petroleum evaluation of sedimentary basins, in: Huc, A.Y. (Ed.), Deposition of Organic Microfacies. AAPG Stud. Geol. 30, Tulsa, Oklahoma, U.S.A., pp. 1–11.

Huc, A.Y., 1977. Contribution de la géochimie organique à une esquisse paléoécologique des schistes bitumineux du Toarcian de l´est du Bassin de Paris. Étude de la matiére organique insoluble (kérogène). Rev. Inst. Fr. Pét. 32, 703–718.

Hunt, C.O., 1987. Dinoflagellate cyst and acritarch assemblages in shallow-marine and marginal-marine carbonates; the Portland Sand Portland Stone and Purbrck Formation (Upper Jurassic/ Lower Cretaceous) of southern England and northern France., in: Hart, M.B. (Ed.), Micropaleontology of Carbonate Environments. Ellis Horwood, Chichester, pp. 25–208.

Hunt, J.M., 1979. Petroleum geochemistry and geology. Freeman and Co., San Francisco, C.A.

Hutton, A.C., 1987. Petrographic classification of oil shales. Int. J. Coal Geol. 8, 203–231.

Hutton, A.C., Cook, A.C., 1980. Influence of alginate on the reflectance of vitrinite from Joadja N.S.W. and some other coals and oil shales containing alginate. Fluel 59, 711–714.

Hutton, A.C., Rob, T., 1994. Chemical and petrographic classification of kerogen / macerals. Energ. Fuel. 1478–1488.

ICCP, 2001. New inertinite classification (ICCP System 1994). Fuel 80, 459–471.

ICCP, 1993. Int. Handbook Coal Petr. 3d Suppl. To 2nd Ed. . University of Newcastle , Tyne.

ICCP, 1975. Int. Handbook Coal Petr., 2nd Suppl. To 2nd Ed. Centre national de la Recherche scientifique, Paris.

ICCP, 1971. Int. Handbook Coal Petr., 2nd Suppl. to 2nd Ed. Centre national de la Recherche scientifique, Paris.

Jacob, H., 1989. Classification, structure, genesis and particles importance of natural solid oil bitumen (migrabitumen). Int. J. Coal Geol. 54, 125–136.

Jacob, H., 1983. Neuere Untersuchungen zur Genesis natürlicher, fester Erdölbitumina. Geol. Jahrb. D, 3–61.

Jenkyns, H.C., 1985. The early Toarcian and Cenomanian-Turonian anoxic events in Europe: comparisons and contrasts. Geol. Rundsch. 74, 505–518.

Jenkyns, H.C., 1980. Cretaceous anoxic events: from continents to oceans. J. Geol. Soc. London 137, 171–188.

Jenkyns, H.C., Clayton, C.J., 1997. Lower Jurassic epicontinental arbonates and mudstones from England and Wales: chemostratigraphic signals and the early Toarcian anoxic event. Sedimentology 44, 687–706.

Jenkyns, H.C., Gröcke, D.R., Hesselbo, S.P., 2001. Nitrogen isotope evidence for water mass denitrification during the early Toarcian (Jurassic) oceanic anoxic event. Paleoceanography 16, 593–603.

Jørgensen, B.B., Revsbech, N.P., 1985. Diffusive boundary layers and the oxygen uptake of sediments and detritus. Limnol. Ocean. 30, 111–122.

Kalkreuth, W., 1982. Prelimenary results on rank and composition of coals from the Gething Formation north of Peace River, northeastern British Columbia. Curr. Res. Part C. Geol. Surv. Can. 82, 65–69.

Katz, B.J., 1983. Limitations of “Rock-Eval” pyrolysis for typing organic matter. Org. Geochem. 4, 195–199.

Kauffman, E.G., 1981. Ecological reappraisal of the German Posidonienschiefer and the Stagnant Basin Model, in: Gray, J., Boucot, A.J., Berry, W.B.N. (Eds.), Communities of the Past. Hutchinson Ross, Stroudsburg, pp. 311–381.

Kauffman, E.G., 1978. Benthic environments and paleoecology of the Posidonienschiefer (Toarcian). N. Jb. Geol. Paläont. 157, 18–36.

Kauffman, E.G., Sageman, B.B., 1990. Biological sensing of benthic environments in dark shales and related oxygen-restricted facies. CRER 121–138.

Kaufmann, G., Romanov, D., 2007. Cave development in the Swabian Alb, south-west Germany: A numerical perspective. J. Hydrol. 349, 302–317.

Klubov, B.A., 1993. A new scheme for the formation and classification of bitumens. J.Petrol.Geol. 16, 335–344.

Koch, J., Arnemann, H., 1975. Die Inkohlung in Gesteinen des Rhät und Lias im südlichen Nordwestdeutschland. Geol. Jb. 29, 33–43.

Kockel, F., Wehner, H., Gerling, P., 1994. Petroleum systems of the Lower Saxony Basin, Germany., in: Magoon, L.B.D., Dow, W.G. (Eds.), The Petroleum System-from Source to Trap. AAPG Mem. 60, Tulsa, Oklahoma, U.S.A., pp. 573–586.

Kulicki, C., Szaniawski, H., 1972. Cephalopod arm hooks from Jurassic of Poland. Palaeontol. Pol. 17, 379–419.

Kus, J., Cramer, B., Kockel, F., 2005. Effects of a Cretaceous structural inversion and a postulated high heat flow event on petroleum system of the western Lower Saxony Basin and the charge history of the Apeldorn gas field. Neth. J. Geosci. 84, 3–24.

Küspert, W., 1983. Faziestypen des Posidonienschiefers Toarcium, Süddeutschland, Eine isotopengeologische, organisch-chemische und petrographisches Studie. Univesity of Tübingen.

Kwiecińska, B., Petersen, H.I., 2004. Graphite, semi-graphite, natural coke, and natural char classification-ICCP system. Int. J.Coal Geol. 57, 99–116.

Landis, C.R., Castaño, J.R., 1995. Maturation and bulk chemical properties of a suite of solid hydrocarbons. Org. Geochem. 22, 137–149.

Leckie, D.A., Singh, C., Goodarzi, F., Wall, J.H., 1990. Organic-rich, radioactive marine shale; a case study of a shallow-water condensed section, Cretaceous Shaftesbury Formation, Alberta, Canada. J. Sediment. Res. 60, 101–117.

Leischner, K., Welte, D.H., Littke, R., 1993. Fluid inclusions and organic maturity parameters as calibration tools in basin modeling, in: Doré, A.G., Augstson, J.H., Hermann, C., Steward, D.J., Sylta, O. (Eds.), Basin Modelling: Advances and Applications. Elsevier Science, pp. 161–172.

Leventhal, J.S., 1982. Limitations of Rock-Eval Pyrolysis assay to characterize kerogen. AAPG Bul. 64, 593–598.

Leythaeuser, D., Littke, R., Radke, M., Schaefer, R.G., 1988. Geochemical effects of petroleum migration and expulsion from Toarcian source rocks in the Hils syncline area, NW-Germany. Org. Geochem. 13, 489–502.

Lipson-Benitah, S., Flexer, A., Rosenfeld, A., Honigstein, A., Conway, B., Eris, H., 1990. Dysoxic sedimentation in the Cenomanien-Turonian Daliyya Formation, Israel, in: Huc, A.Y. (Ed.), Deposition of Organic Facies. AAPG Stud. Geol. 30, Tulsa, Oklahoma, U.S.A., pp. 27–39.

Littke, R., 1993. Deposition, diagenesis and weathering of organic matter-rich sediments, Lecture notes in Earth Science. Springer Verlag, Berlin-Heidelberg.

Littke, R., Rotzal, H., Leythaeuser, D., Baker, D.R., 1991. Lower Toarcian Posidonia Shale in Southern Germany (Schwäbische Alb). Organic facies, depositional environment, and maturity. Erdöl Kohle Erdgas 44, 407–414.

Littke, R., Rullkötter, J., 1987. Mikroskopische und makroskopische Unterschiede zwischen Profilen unreifen und reifen Posidonienschiefers aus der Hilsmulde. Facies 17, 171–179.

Littke, R., Urai, J.L., Uffmann, A.K., Risvanis, F., 2012. Reflectance of dispersed vitrinite in Palaeozoic rocks with and without cleavage: Implications for burial and thermal history modeling in the Devonian of Rursee area, northern Rhenish Massif, Germany. Int. J. Coal Geol. 89, 41–50.

Lo, H.B., 1992. Identification of indigenous vitrinites for improved thermal maturity evaluation. Org. Geochem. 18, 359–364.

Loh, H., Maul, B., Prauss, M., Riegel, W., 1986. Primary production, maceral formation and carbonate species in the Posidonia Shale of NW Germany, in: Degens, E.T., Meyers, P.A., Brassell, S.C. (Eds.), Biogeochemistry of Black Shales. Mitt. Geol. Paläont. Inst. Univ. Hamburg 60, Hamburg, pp. 397–364.

Mädler, K., 1963. Die figurierten organischen bestandteile der Posidonienschiefer. Beih. Geol. Jahrb. 58, 287–406.

Malinconico, M.L., 2000. Using reflectance crossplots and rotational polarization for determining first-cycle vitrinite for maturation studies. Int. J.Coal Geol. 43, 105–120.

Masran, T., Pocock, S.A., 1981. The classification of plant-derived particulate organic matter in sedimentary rocks, in: Organic Maturation Studies and Fossil Fuel Exploration. Academic Press, London-New York, pp. 145–175.

McCann, T., 2008. The Geology of Central Europe: Mesozoic and Cenozoic. Geol. Soc. London, London.

McCarthy, K., Rojas, K., Niemann, M., Palmowski, D., Peters, K.E., Stankiewicz, A., 2011. Basic Petroleum Geochemistry for Source Rock Evaluation. Oilf. Rev. 23, 32–43.

McClay, K.R., Ellis, P.G., 1983. Deformation and recrystallization of pyrite. Miner. Mag. 47, 527–538.

Mørk, A., Bromley, R.G., 2008. Ichnology of a marine regressive systems tract: The Middle Triassic of Svalbard. Polar Res. 27, 339–359.

Mukhopadhyay, P.K., 1992. Maturation of organic matter as revealed by microscopic method: applications and limitation of vitrinite reflectance, and continuous spectral and pulsed laser fluorescence spectroscopy, in: Wolf, K.H., Chilingarin, G. V. (Eds.), Diagenesis, III. Elsevier, Amsterdam, pp. 435–510.

Mukhopadhyay, P.K., Hagemann, H.W., Gormly, J.R., 1985. Characterization of kerogens as seen under the aspect of maturation and hydrocarbon generation. Erdöl Kohle Erdgas 38, 7–18.

Muntendam-Bos, A.G., Wassing, B.B.T., ter Heege, J.H., van Bergen, F., Schavemaker, Y.A., van Gessel, S.F., de Jong, M.L., 2009. Inventory non-conventional gas.

Newman, J., Newman, N.A., 1982. Reflectance anomalies in Pike River coals: evidence of variability in vitrinite type, with implications for maturation studies and "Suggate rank." New Zeal. J. Geol. Geop. 25, 233–243.

Nzoussi-Mbassani, P., Copard, Y., Disnar, J.R., 2005. Vitrinite recycling: Diagnostic criteria and reflectance changes during weathering and reburial. Int. J. Coal Geol. 61, 223–239.

Oschmann, W., 2000. Microbes and black shales, in: Riding, R.E., Awramik, S.M. (Eds.), Microbial Sediments. Springer Verlag, Berlin-Heidelberg, pp. 137–148.

Palliani, R.B., Mattioli, E., Riding, J.B., 2002. The response of marine phytoplankton and sedimentary organic matter to the early Toarcian (Lower Jurassic) oceanic anoxic event in northern England. Mar. Micropaleontol. 46, 223–245.

Palliani, R.B., Riding, J.B., 1999. Relationships between the early Toarcian anoxic event and organic-walled phytoplankton in Central Italy. Mar. Micropaleontol. 37, 101–116.

Pasley, M.A., Hazel, J.E., 1989. Use of organic petrology and graphic correlation of biostratigraphic data in sequence stratigraphic interpretations: example from the Eocene-Oligocene boundary section, St. Stephens Quarry, Alabama. GCAGS Trans. 40, 661–683.

Pedersen, T.F., Calvert, S.E., 1990. Anoxia vs. productivity: What controls the formation of organic- carbon-rich sediments and sedimentary rocks? AAPG Bull. 74, 454–466.

Peniguel, G., Couderc, R., Seyve, C., 1989. Les microalgues actuelles et fossils-intérêts stratigraphique et pétrolier. Bull. Cent. Rech. Explor. Prod. 13, 455–482.

Peters, K.E., 1986. Guidelines for evaluating petroleum source rock using programmed pyrolysis. AAPG Bull. 70, 318–329.

Peters, K.E., Cassa, M.R., 1994. Applied source rock geochemistry, in: The Petroleum System-from Source to Trap. AAPG Bull. 60, Tulsa, Oklahoma, U.S.A., pp. 93–117.

Peters, K.E., Walters, C.C., Moldowan, J.M., 2005. Origin of preservation of organic matter, in: Peters, K.E., Walters, C.C., Moldowan, J.M. (Eds.), The Biomarker Guide: Vol. 1, Biomarker and Isotopes in the Environments. Cambridge University Press, Cambridge, pp. 3–18.

Petersen, H.I., Schovsbo, N.H., Nielsen, A.T., 2013. Reflectance measurements of zooclasts and solid bitumen in Lower Paleozoic shales, southern Scandinavia: Correlation to vitrinite reflectance. Int. J. Coal Geol. 114, 1–18.

Petmecky, S., Meier, L., Reiser, H., Littke, R., 1999. High thermal maturity in the Lower Saxony Basin: Intrusion or deep burial? Tectonophysics 304, 317–344.

Plein, E., 1985. Entwicklung und Bedeutung der Erdöl/Erdgasfinde zwischen Weser und Ems. Oldenburg. Jahrb. 85, 267–311.

Pletsch, T., Appel, J., Botor, D., Clayton, C.J., Duin, E.J.T., Faber, E., Górecki, W., Kombrink, H., Kosakowski, P., Kuper, G., Kus, J., Lutz, R., Mathiesen, A., Ostertag-Henning, C., Papiernek, B., van Bergen, F., 2010. Petroleum generation and migration, in: Doornenbal, J.C., Stevenson, A.G. (Eds.), Petroleum Geological Atlas of the Southern Permian Basin Area. EAGE Publications, Houten, pp. 225–253.

Pompeckj, J.F., 1901. Der Jura zwischen Regnsburg und Regenstauf. Geognost. Jahresh. 14, 139–220.

Porter, K.G., Robbins, E.I., 1981. Zooplankton fecal pellets link fossil fuel and phosphate deposits. Sci. 212, 931–933.

Powell, T.G., Creaney, S., Snowdon, L.R., 1982. Limitations of use of organic petrographic techniques for identification of petroleum source rocks. AAPG Bull. 66, 430–435.

Pratt, L.M., 1984. Influence of paleoenvironmental factors on preservation of organic matter in Middle Cretaceous. AAPG Bull. 68, 1146–1159.

Prauss, M., 1996. The Lower Toarcian Posidonia Shale of Grimmen, northwest Germany. Neues Jahrb. Geol. P. 200, 107–132.

Prauss, M., Ligouis, B., Luterbacher, H., 1991. Organic matter and palynomorphs in the "Posidonienschiefer" (Toarcian, Lower Jurassic) of southern Germany. Geolo. Soc. Spec. Pub. 58, 335–351.

Pugmire, R.J., Zilm, K.W., Woolfenden, W.R., Grant, D.M., Dyrkacz, G.R., Bloomquist, C.A.A., Horwitz, E.P., 1982. Carbon-13 NMR spectra of macerals separated from individual coals. Org. Geochem. 4, 79–84.

Ramsden, A.R., 1983. Microscopic petrography of oil shales at Julia Creek, northwestern Queensland. J. Geol. Soc. Aust. 30, 17–23.

Riediger, C.L., 1993. Solid bitumen reflectance and Rock-Eval Tmax as maturation indices: an example from the "Nordegg Member", Western Canada Sedimentary Basin. Int. J. Coal Geol. 22, 295–315.

Riegel, W., Loh, H., Maul, B., Prauss, M., 1986. Effects and causes in a black shale event — the Toarcian Posidonia Shale of NW Germany, in: Walliser, O.H. (Ed.), Global Bio-Events: A Critical Approach Proceedings of the First International Meeting of the IGCP Project 216. Springer, pp. 267–276.

Riegraf, W., 1985. Mikrofauna, Biostratigraphie und Fazies im Unteren Toarcium Südwestdeutschlands und Vergleiche mit benachbarten Gebieten. Tüb. Mikropaläont. Mitt., Tübingen.

Röhl, H.-J., Schmid-Röhl, A., 2005. Lower Toarcian (Upper Liassic) Black Shales of the Central European Epicontinental Bason: A Sequence stratigrphic case study from the SW German Posidonia Shale. Spec. Pub.-SEPM. 82, 165–189.

Röhl, H.-J., Schmid-Röhl, A., Oschmann, W., Frimmel, A., Schwark, L., 2001. The Posidonia Shale (Lower Toarcian) of SW-Germany: An oxygen-depleted ecosystem controlled by sea level and palaeoclimate. Palaeogeogr. Palaeoecol. 165, 27–52.

Rosenberg, R., 1977. Benthic macrofaunal dynamics, production, and dispersion in an oxygen-deficient estuary of west Sweden. J. Exp. Mar. Biol. Ecol. 26, 107–133.

Rosenberg, R., Arntz, W.E., de Flores, E.C., Flores, L.A., Carbajal, G., Finger, I., Tarazona, J., 1983. Benthos biomass and oxygen deficiency in the upwelling system off Peru. J. Mar. Res. 41, 263–279.

Rullkötter, J., Leythaeuser, D., Horsfield, B., Littke, R., Mann, U., Müller, P.J., Radke, M., Schaefer, R.G., Schenk, H.-J., Schwochau, K., Witte, E.G., Welte, D.H., 1988. Organic matter maturation under the influence of a deep intrusive heat source: A natural experiment for quantitation of hydrocarbon generation and expulsion from a petroleum source rock (Toarcian shale, northern Germany). Org. Geochem. 13, 847–856.

Rullkötter, J., Littke, R., Radke, M., Disko, U., Horsfield, B., Thurow, J., 1992. Petrography and geochemistry of organic matter in Triassic and Cretaceous deep-sea sediments from the Wombat and Exmouth plateous and nearby abyssal plains off NW Australia. Proc. Ocean Drilli. Prog. Sci. Results 122, 317–333.

Rullkötter, J., Marzi, R., 1988. Natural and artificial maturation of biological markers in a Toarcian shale from northern Germany. Org. Geochem. 13, 639–645.

Schegg, R., 1993. Thermal maturity and history of sediments in the North Alpine Foreland Basin (Switzerland, France). Université de Genève, Genéve.

Schlager, W., 1981. The paradox of drowned reefs and carbonate platforms. Geol. Soc. Am. Bull. 92, 197–211.

Schlanger, S.O., Jenkyns, H.C., 1976. Cretaceous oceanic anoxic events: Causes and consequences. Geol. Minjnbouw 55, 179–184.

Schmitz, U., Wenzlow, B., 1990. Maturity anomalies of the western Lower Saxony Basin in their regional contex. Zbl. Geol. Paläontol. Teil I, 1091–1103.

Schoenherr, J., Littke, R., Urai, J.L., Kukla, P.A., Rawahi, Z., 2007. Polyphase thermal evolution in the Infra-Cambrian Ara Group (South Oman Salt Basin) as deduced by maturity of solid reservoir bitumen. Org. Geochem. 38, 1293–1318.

Schwarz, H.-U., 2012. Das Schwäbisch-Fränkische Bruchmuster. Z. dt. Ges. Geowiss. 163, 411–446.

Senglaub, Y., Brix, M.R., Adriasola, A.C., Littke, R., 2005. New information on the thermal history of the southwestern Lower Saxony Basin, northern Germany, based on fission track analysis. Int. J. Earth. Sci. 94, 876–896.

Shewrood, N.R., Cook, A.C., 1986. Organic matter in the Toolebuc Formation, in: 12 Proc. Eromanga Basin Symp. Geol. Soc. Austr. Special Publ., pp. 255–265.

Sielacher, A., 1982. Ammonite shells as habitats in the Posidonia Shales of Holzmaden-floats or benthic islands? N. Jb. Geol. Paläont. 98–114.

Smith, C.R., Hamilton, S.C., 1983. Epibenthic megafauna of a bathyal basin of Southern California: pattern of abundance, biomass and dispersion. Deep. Res. 30, 907–928.

Stach, E., 1953. Der Inkohlungssprung im Ruhrkarbon. Brennst.-Chem. 34, 353–355.

Stach, E., Mackowsky, M.-T., Teichmüller, M., Taylor, G.H., Chandra, D., Teichmüller, R., 1982. Coal petrology. Gebrüder Borntraeger, Berlin-Stuttgart.

Stadler, G., Teichmüller, R., 1971. Zusammenfassender Überblick über die Entwicklung des Bramscher Massivs und des Niedersächsischen Tektogens. Fortschr. Geol. Rheinld. Westf. 18, 547–564.

Stasiuk, L.D., 1994. Oil-prone alginite macerals from organic-rich Mesozoic and Palaeozoic strata, Saskatchewan, Canada. Mar. Pet. Geol. 11, 208–217.

Stasiuk, L.D., Goodarzi, F., 1988. Organic petrology of second white speckled shale, Saskatchewan, Canada - a possible link between bituminite and biogenic gas? B. Can.Petrol.Geol. 36, 397–406.

Suárez-Ruiz, I., 2012. Organic petrology: an overview, in: Ali Ismail Al-Juboury (Ed.), Petrology-New Perspectives and Applications. InTech, Rijeka, pp. 199– 224.

Swanson, V.E., 1961. Geology and geochemistry of uranium in marine black shales. A review. Uranium in Carbonaceous rocks. U.S. Government Printing Office, Washington D. C.

Taylor, G.H., Liu, S.Y., 1989. Micrinite — its nature, origin and significance. Int. J. Coal Geol. 14, 29–46.

Taylor, G.H., Liu, S.Y., Teichmüller, M., 1991. Bituminite — A TEM view. Int. J. Coal Geol. 18, 71–85.

Taylor, G.H., Teichmüller, M., Davis, A., Diessel, C.F.K., Littke, R., Robert, P., 1998. Organic petrology: a new handbook incorporating some revised parts of Stach's Textbook of coal petrology. Gehrüder Borntraeger, Berlin, Stuttgart.

Teerman, S.C., Cardott, B.J., Harding, R.W., Lemos De Sousa, M.J., Logan, D.R., Pinheiro, H.J., Reinhardt, M., Thompson-Rizer, C.L., Woods, R.A., 1995. Source rock/dispersed organic matter characterization—TSOP research subcommittee results. Org. Geochem. 22, 11–25.

Teichmüller, M., 1990. The genesis of coal from the viewpoint of coal geology. Int. J.Coal Geol. 16, 121–124.

Teichmüller, M., 1974. Uber Neue Macerale der Liptin-Gruppe und dei Entstehung des Micrinite. Fortschr. Geol. Rheinl. Westfalen 24, 37–64.

Teichmüller, M., Durand, B., 1983. Fluorescence microscopical rank studies on liptinites and vitrinites in peat and coals, and comparison with results of the rock-eval pyrolysis. Int. J. Coal Geol. 2, 197–230.

Teichmüller, M., Ottenjann, K., 1977. Liptinit und lipoid Stoffe in einem Erdolmuttergestein. Type and diagenesis of liptinites and lipoid-substances in an oil source rock on the basis of fluorescence microscopical studies. Erdöl, Erdgas, Kohle 30, 387–398.

Teichmüller, M., Teichmüller, R., 1968. Geological aspects of coal metamorphism, in: Murchison, D.G., Westoll, T.S. (Eds.), Coal and Coal-Bearing Strata. Oliver and Boyd, Edinburgh, pp. 233–267.

Teichmüller, M., Teichmüller, R., 1951. Inkohlungsfragen im Osnabrüker Raum. N. Jb. Geol. Pal. 69–85.

Teichmüller, M., Teichmüller, R., 1950. Das Inkohlungsbild des Niedersächsischen Wealdenbeckens. Z. Dtsch. Geol. Ges. 100, 498–517.

Teichmüller, R., Teichmüller, M., 1985. Inkohlungsgradienten in der Anthrazitfolge des Ibbenbürener Karbons. Fortschr. Geol. Rheinld. Westf. 33, 231–253.

Thompson, B., Mullins, H.T., Newton, C.R., Vercoutere, T.L., 1985. Alternative biofacies model for dysaerobic communities. Lethaia 18, 167–179.

Tissot, B.P., Welte, D.H., 1978. Petroleum Formation and Occurrence. Springer Verlag, Berlin, Heidelberg.

Tissot, B.P., Welte, D.H., Durand, B., 1987. The role of geochemistry in exploration risk evaluation and decision making, in: 12th World Petroleum Congress. World Petroleum Congress, Houston, Texas, USA, pp. 99–112.

Trabucho-Alexandre, J., Dirkx, R., Veld, H., Klaver, G., de Boer, P.L., 2012. Toarcian Black Shales In the Dutch Central Graben: Record of Energetic, Variable Depositional Conditions During An Oceanic Anoxic Event. J. Sediment. Res. 82, 104–120.

Traverse, A., 2005. Sedimentation of organic particles. Cambridge University Press, Cambridge.

Tyson, R. V., 1995. The nature of organic matter in sediments, in: Tyson, R. V (Ed.), Sedimentary Organic Matter. Charman & Hall, London, p. 615.

Ulrichs, M., Wild, R., Ziegler, B., 1979. Fossilien aus Holzmaden. Stutt. Beitr. Naturkd. 11, 1–34.

Van Balen, R.T., van Bergen, F., de Leeuw, C., Pagnier, H., Simmelink, H., van Wees, J.D., Verweij, J.M., 2000. Modeling the hydrocarbon generation and migration in the West Netherlands Basin, the Netherlands. Neth. J. Geosci. 79, 29–44.

Van Bergen, F., Zijp, M., Nelskamp, S., Kombrink, H., 2013. Shale gas evaluation of the Early Jurassic Posidonia Shale Formation and the Carboniferous Epen Formation in the Netherlands. AAPG. Mem. 103, 1–24.

Van Bergen, M.J., Sissingh, W., 2007. Magmatism in the Netherlands: Expression of the north-west European rifting history, in: Wong, T.E., Batjes, D.A.J., De Jager, J. (Eds.), Geology of the Netherlands. R. Neth. Acad. of Arts and Sci., Amsterdam, p. 354.

Van den Hoek, C., Jahns, H.M., Mann, D.G., 1993. Algen. 3. Neubearbeitete Auflage. Georg Thieme Verlag, Stuttgart.

Van Wijhe, D.H., 1987. Structural evolution of inverted basins in the Dutch offshore. Tectonophysics 137, 171–219.

Vigran, J.O., Mørk, A., Forsberg, A.W., Weiss, H.M., Weitschat, W., 2008. Tasmanites algae-contributors to the Middle Triassic hydrocarbon source rocks of Svalbard and the Barents Shelf. Polar Res. 27, 360–371.

Walter, R., 2007. Geologie von Mitteleuropa. Nägele u. Obermiller, Stuttgart.

Wehner, H., Hufnagel, H., 1986. Some characteristics of the inorganic and organic composition of oil shales from Jordan. Mitt. Geol. Paläont. Inst. Univ. Hambg. 60, 381–395.

Wignall, P.B., 1991. Model for transgressive black shales? Geology 19, 167–170.

Wignall, P.B., Newton, R., 2001. Black shales on the basin margin: A model based on examples from the Upper Jurassic of the Boulonnais, northern France. Sed. Geol. 144, 335–356.

Wilde, P., Quinby-Hunt, M., Berry, W., 1990. Vertical advection from oxic or anoxic water from the main pycnocline as a cause of rapid extinction or rapid radiations, in: Kaufmann, E.G., Walliser, O.H. (Eds.), Extinction Events in Earth History. Springer Verlag, Berlin, pp. 85–98.

Williams, H., Turner, F.J., Gilbert, C.M., 1982. Petrography. An Introduction to the study of rocks in thin section. W.H. Freeman and Company, New-York.

Wolf, M., 1966. Petrographische Beobachtingen an den Uran und Thorium führenden Bpgheadschiefern von Autun (Saöne-et-Loire) unter besnderer Berücksichtigung von Ergebnissen der Fluoreszenzmikroskopie. Brennstoff-Chemie 11–14.

Wong, T.E., 2007. Jurassic, in: Wong, T.E., Batjes, D.A.J., de Jager J (Eds.), Geology of the Netherlands. Royal Netherlands Academy of Arts and Sciences, Amsterdam, pp. 107–125.

Ziegler, P.A., 1990. Geological atlas of Western and Central Europe, 2nd ed. Shell Int. Petrol. Mij. and Geol Soc., London.

Ziegler, P.A., 1988. Evolution of the Arctic-North Atlantic and the Western Tethys, AAPG Mem.

Ziegler, P.A., 1982. Triassic rifts and facies pattern in Western and Central Europe. Int. J. Earth Sci. 71, 747–772.

Zilm, K.W., Pugmire, R.J., Larter, S.R., Allan, J., Grant, D.M., 1981. Carbon – 13 CP/MAS spectroscopy of coal macerals. Fuel 60, 717–722.

Zimmerman, H., Boersma, A., McCoy, F.W., 1987. Carbonaceous sediments and paleoenvironment of the Creataceous South Antlantic Ocean, in: Brooks, J., Fleet, A.J. (Eds.), Marine Petroleum Source Rocks. Geol.Soc. London. Spec. Pub. 26, London, pp. 271–286.

APPENDIX A. TABLES OF THE RESULTS OF ORGANO-PETROGRAPHIC AND ORGANO-GEOCHEMICAL ANALYSES

CONTENTS

Appendix A1: Well E

ORGANIC PETROGRAPHY – Organic matter [vol.%]

Sample/ Depth, m	Lithology	Age (Local names)	Vitrinite (V) [vol.%] autochthonous heterogeneous el.	autochthonous heterogeneous eq.	autochthonous homogeneous el.	autochthonous homogeneous eq.	recycled homogeneous el.	recycled homogeneous eq.	Liptinite (L) [vol.%] Spor.	Alginite Tel.	Alginite lamalginite discrete	lamalginite fil.	lamalginite layered	Liptd.	Bit. I	Bit. II	Bit. III	Bit. IV	Bit. V	Bit. VI	Migrabitumen homog.	Migrabitumen heter.	Oil drop.	Inertinite (I) [vol.%] Fus.	Semifus.	Secret.	Intd.	Micr.
2460-2461	limestone, bituminous	Lias zeta	-	-	-	-	0.1	-	0.3	0.3	22.4	1.6	0.6	5.9	-	0.4	-	-	1.5	-	-	-	-	-	-	0.1	-	-
2478.95	limestone, strong bituminous	Lias epsilon	-	-	-	-	-	-	0.8	1.0	7.5	1.1	-	12.1	4.6	3.3	-	-	1.4	-	-	-	0.1	0.2	0.1	-	0.2	0.2
2480.05	calcareous mudstone, strong bituminous		-	-	-	-	0.1	-	0.7	0.8	5.8	0.9	0.1	7.7	2.3	1.5	-	0.1	0.9	-	-	-	-	0.5	0.1	-	-	-
2482.05	limestone, strong bituminous		-	-	-	-	-	-	0.7	0.5	5.3	1.2	-	7.9	7.2	0.8	-	-	0.6	-	-	-	-	0.4	0.1	-	-	1.6
2482.48			-	-	0.1	0.2		0.3	0.8	0.6	3.8	1.0	0.1	6.1	1.2	2.1	-	0.2	0.6	-	-	-	-	0.6	-	-	0.1	2.2
2485.14			-	-	0.2	-	0.1	-	1.3	0.4	5.2	1.1	0.1	7.3	1.5	0.1	-	-	3.4	-	-	-	0.1	0.7	0.1	-	-	1.9
2487.50			-	-	-	-	-	-	0.9	0.1	4.2	1.2		7.7	0.5	0.3		0.1	1.3	-	-	-	-	0.1	0.1		0.1	1.1
2488.32			0.1	-	-	-	-	-	0.5	0.2	3.4	2.3	-	4.9	5.3	0.7	-	0.5	1.7	-	-	-	0.2	-	-	-	-	-
2489.13	calcareous mudstone, strong bituminous		-	-	-	-	-	-	1.1	0.5	9.7	0.5	-	6.0	0.6	5.0	-	0.2	3.4	-	-	-	0.3	-	0.1	-	0.2	0.1
2490.35			-	-	-	-	-	0.1	0.7	0.2	5.7	1.0	-	15.2	2.8	4.1	-	0.2	13.2	-	-	-	0.4	0.3	-	-	-	0.2
2491.49	limestone, bituminous		-	-	-	-	-	-	0.3	0.1	5.6	0.4	-	8.0	1.0	0.6	-	-	1.2	-	-	-	-	0.1	-	-	-	0.2
2494.10			0.1	-	-	-	0.3	0.1	0.7	0.3	11.1	0.5	-	6.3	1.8	2.0	-	0.5	4.4	-	-	-	-	0.2	0.5	-	-	0.2
2495.95			-	-	-	-	-	-	1.1	0.3	9.2	2.8	0.1	4.4	0.3	0.2	-	-	0.9	-	-	-	-	0.1	-	-	0.1	-
2498.46	marly limestone, strong bituminous		-	-	-	-	0.1	-	0.7	0.2	2.9	0.3	-	4.3	3.0	0.2	-	-	1.2	0.1	-	-	0.5	-	0.1	-	-	-
2500.47	limestone, strong bituminous		-	-	-	-	-	-	0.5	0.2	8.2	0.3	-	7.3	10.5	1.2	-	-	10.7	-	-	-	0.5	-	0.1	-	-	-
2501.43	marly limestone, strong bituminous		-	0.1	-	-	-	0.1	1.2	0.2	10.9	0.7	-	6.6	5.6	5.3	-	-	1.2	-	-	-	0.6	-	-	-	-	-
2503.35			-	-	-	-	-	-	0.3	0.1	3.2	1.5	-	2.2	3.3	1.4	-	-	8.9	-	-	-	1.1	-	-	-	-	-
2504.85	calcareous mudstone, strong bituminous		-	-	-	-	0.1	-	4.5	0.6	7.4	0.9	-	6.0	3.0	2.1	-	-	12.0	-	-	-	0.1	-	0.1	-	-	-
2506.55	limestone, strong bituminous		-	-	-	-	0.1	-	1.2	0.3	7.6	0.8	-	13.2	0.7	0.1	-	-	5.5	-	-	-	0.2	-	-	-	-	-
2508.86			-	-	0.1	-	-	0.1	0.2	-	1.1	0.1	-	4.1	-	-	-	-	-	-	-	-	-	0.2	-	-	-	0.1

ORGANIC PETROGRAPHY – Mineral matter [vol. %]; Vitrinite reflection, %VRo; ORGANIC GEOCHEMISTRY

Sample/ Depth, m	Mineral groundmass calcareous bits.	calcareous l.-bits.	n.-bits.	clayey bits.	clayey l.-bits.	mic.-r.	F.g. pel.	C.g. pel.	Carbonates is. cry.	Carbonates coccol.	dol.	Glauc.	Gyps.	Detrital minerals qtz	Detrital minerals mica	Pyrite crys.	Pyrite framb.	Pyrite epig.	Zooclasts shell	Zooclasts fish r.	Zooclasts biocl.	Vitrinite reflection mean	s.d.	n	TOC [%]	S1 *	S2 *	HI ~	OI ~~	Tmax °C
2460-2461	24.4	-	1.4	11.3	-	-	-	-	20.3	-	0.1	-	-	2.1	1.3	0.9	2.4	0.9	-	0.3	1.3	-	-	-	3.4	0.5	18.7	548	16	434
2478.95	15.5	-	-	20.7	-	-	0.6	-	13.7	-	0.2	-	-	2.8	1.3	6.5	3.7	1.0	-	0.6	0.8	-	-	-	7.7	1.5	44.7	583	18	429
2480.05	12.1	-	-	39.3	-	-	-	-	10	-	0.2	-	-	0.6	0.4	5.2	9.3	0.3	0.3	0.1	0.5	-	-	-	13.5	3.5	77.1	572	15	431
2482.05	9.6	-	-	18.8	-	-	5.1	0.4	14	1.3	0.5	-	-	0.7	0.4	10.9	9.7	0.1	0.5	0.3	1.3	-	-	-	11.0	3.8	66.2	601	16	433
2482.48	31.3	-	-	20.4	-	-	1.8	0.1	9.4	2.4	-	-	-	0.5	0.8	5.5	5.2	0.2	-	1.9	0.5	0.44	0.02	9	7.8	1.7	45.8	589	20	433
2485.14	13.8	-	-	24.8	-	-	2	-	7.1	7.6	-	-	-	0.5	0.4	11.8	6.4	0.0	-	0.6	1.5	0.45	0.02	9	10.9	3.5	66.6	613	19	425
2487.50	44.6	-	-	10.2	-	-	5.2	0.5	5.7	2.6	0.2	-	-	0.2	0.6	3.6	6.4	0.0	0.6	0.2	1.6	-	-	-	7.1	2.0	43.0	606	25	428
2488.32	10.6	-	-	11.6	-	-	15.7	0.1	2.4	26.2	0.2	-	-	0.7	0.1	4.3	5.6	0.8	-	1.3	0.4	-	-	-	9.9	3.3	63.3	640	22	428
2489.13	9.1	-	0.9	29.4	-	-	0.6	-	10.7	-	0.4	-	-	-	0.3	3.9	4.6	0.0	0.1	3.7	7.8	-	-	-	8.3	2.6	55.4	667	22	430
2490.35	3.8	-	-	23.3	-	-	0.6	-	5.5	-	-	-	-	1.3	0.5	10.3	8.6	0.2	0.8	0.2	0.8	-	-	-	13.1	5.1	88.2	671	16	431
2491.49	8.2	-	-	38.9	-	-	7.8	-	6.1	4	0.2	-	-	0.7	-	8.6	4.7	0.4	0.1	0.2	2.6	0.46	0.04	11	11.5	3.8	77.0	670	19	428
2494.10	3.9	-	0.9	29.3	-	-	0.1	-	21.5	-	0.4	-	-	0.3	0.2	6.6	6.1	0.0	-	0.5	1.1	0.43	0.01	9	8.2	2.4	48.5	594	25	429
2495.95	3.3	-	-	38.1	-	-	0.2	-	28.2	-	0.2	-	-	0.3	0.9	5.1	3.5	0.5	-	-	0.2	-	-	-	13.4	5.0	90.5	676	14	431
2498.46	10.7	-	0.1	1.1	-	-	0.7	-	5.6	-	53.8	-	-	0.3	0.3	4.6	3.2	0.2	0.4	1.7	1.2	-	-	-	2.8	0.9	14.1	510	24	425
2500.47	2.8	-	2	25.1	-	-	4.1	-	14.8	-	0.8	-	-	-	0.4	3.1	6.1	0.0	-	0.2	0.9	-	-	-	16.6	3.6	71.8	432	9	431
2501.43	2	-	0.1	11.6	-	-	-	-	11.5	-	28.3	-	-	0.5	0.4	6.1	5.4	0.9	-	0.2	0.5	-	-	-	9.9	3.2	63.4	640	14	427
2503.35	1.2	-	0.1	1.9	-	-	-	-	11.1	-	55.6	-	-	-	-	1.6	4.1	1.4	-	-	0.8	-	-	-	7.9	3.0	54.5	689	15	428
2504.85	4	-	0.5	26.6	-	-	2.2	-	11.6	-	0.5	-	-	0.6	0.4	6.6	7.7	0.3	0.4	0.1	1.6	-	-	-	11.4	3.8	71.5	627	19	430
2506.55	19	-	0.2	14	-	-	4	-	12.7	-	0.1	-	-	1.9	0.6	5.5	11	0.1	0.1	-	1.1	-	-	-	5.3	1.1	32.1	609	20	429
2508.86	-	-	79.1	0.2	-	-	-	-	5.1	0.2	-	-	-	2	4.2	0	0.1	0.3	0.4	0.2	2.2	0.44	0.01	8	0.9	0.2	2.3	239	65	444

ORGANIC PETROGRAPHY

el.-elongated; eq.-equidimensional; Spor.- sporinite; Tel.- telalginite; fil.-filamentous; Liptd.-liptodetrinite; Bit. I- bituminite I; Bit. II-bituminite II; Bit. III- bituminite III; Bit. IV- bituminite IV; Bit. IV- bituminite IV; Bit.V- bituminite V; Bit.VI- bituminite VI; homog.-homogeneous; heter.-heterogeneous; Oil drop.-oil droplets; Fus.-fusinite; Semifus.-semifusinite; Secret.-secretinite; Intd.-inertodetrinite; Micr.- micrinite; fish r.-fish remains; biocl.-bioclasts; bits.-bituminous; l.-bits.-low bituminous; n.-bits.-non-bituminous; mic.-r.- micrinite-rich; F.g.pel.-Fine-grained peloids; C.g. pel.-Coarse-grained peloids; is. cry.-isolated crystals; coccol.-coccoliths; dol.-dolomite; Glauc.-Glauconite; qtz.-quartz; Gyps.-Gypsum; cryst.-crystals ; framb.-framboidal; epig.-epigenetic.

mean-mean value; s.d.-standart deviation; n-total number of measurements.

ORGANIC GEOCHEMISTRY

*-[mg HC/g],~-[mg HC/g TOC], ~~-[mg CO2/g TOC].

**Lithology has been taken from unpublished BEB reports

Appendix A2: Well M

ORGANIC PETROGRAPHY – Organic matter [vol.%]

Sample/ Depth, m	Lithology	Age (Local names)	Vitrinite (V) [vol.%] autochthonous heterogeneous el.	autochthonous heterogeneous eq.	autochthonous homogeneous el.	autochthonous homogeneous eq.	recycled homogeneous el.	recycled homogeneous eq.	Liptinite (L) [vol.%] Spor.	Alginite Tel.	Alginite lamalginite discrete	lamalginite fil.	lamalginite layered	Liptd.	Bit. I	Bit. II	Bit. III	Bit. IV	Bit. V	Bit. VI	Exsud.	Migrabitumen homog.	Migrabitumen heter.	Oil drop.	Inertinite (I) [vol.%] Fus.	Semifus.	Secret.	Intd.	Char	Micr.
2074-2075	limestone, bituminous	Lias epsilon	-	-	-	-	-	-	0.6	0.1	8	1.5	-	15.9	-	-	-	-	-	-	-	-	-	-	0.1	0.1	0.1	-	-	-
2078.23			-	-	-	-	0.1	-	0.3	-	4.5	2.8	0.1	7.2	-	0.5	-	-	-	-	0.1	-	-	-	-	-	-	-	-	-
2087.33	limestone, strong bituminous		-	-	-	-	-	-	1.2	0.2	8.6	0.8	-	12.2	-	0.4	-	0.1	-	-	0.1	-	-	-	-	0.1	-	-	-	0.1
2088.30			-	-	-	-	-	-	1.0	0.10	6.60	1.6	-	11.6	0.2	2	-	0.1	0.4	-	-	-	-	0.1	0.1	0.1	-	-	-	-
2089.33			-	-	-	-	-	-	0.7	0.2	5	0.7	-	12.3	0.1	2.3	-	-	0.1	-	-	-	-	-	0.2	-	-	-	-	0.2
2090.55			-	-	-	-	-	-	1.0	0.2	7.8	2.8	0.3	13.5	1.3	2.9	-	0.1	0.7	-	-	-	-	0.1	0.1	0.1	-	0.1	0.1	0.3
2091.55			-	-	-	-	0.1	-	0.6	0.1	3.3	1.1	-	10	0.2	3.1	-	0.6	0.1	-	-	-	-	-	0.2	-	-	-	0.2	-
2092.43			-	-	-	-	-	-	0.5	0.2	5.2	1.5	-	14	1	4.4	-	0.2	0.2	-	0.1	-	-	0.2	0.2	-	-	0.1	0.1	-
2093.40			-	-	-	-	-	-	1.3	0.3	5.2	0.9	0.2	7.4	2.9	1.6	-	0.5	1.4	-	-	-	-	0.1	0.7	0.1	-	-	-	0.4
2095.10			-	-	-	-	-	-	1.5	0.1	9.3	3.5	0.1	18.8	0.5	1.6	-	0.3	0.6	-	-	-	-	-	0.2	-	-	-	-	0.4
2096.13			-	-	-	-	-	-	1.4	0.2	6.9	5.6	-	20	-	-	-	-	0.6	-	-	-	-	-	-	-	-	0.1	-	-
2097.13			-	-	-	-	-	-	1.5	0.4	9.9	2.9	0.1	11.7	1.7	1.2	-	-	0.4	-	-	-	-	0.3	0.4	0.1	-	-	-	0.1
2098.15			-	-	-	-	-	-	1.9	0.2	13.9	1.4	-	13.6	1.1	3	-	0.5	0.7	-	-	-	-	-	0.9	-	-	-	-	0.3
2099.39			-	-	-	-	-	-	3.0	0.1	8.3	0.9	-	15.5	-	0.2	-	-	-	-	-	-	-	-	0.4	0.2	-	-	-	0.1
2100.49			-	-	-	-	-	-	1.6	0.6	14.8	3.1	0.2	10.4	0.1	0.1	-	-	4.4	-	-	-	-	0.2	0.2	0.1	-	-	-	-
2101.52			-	-	-	-	-	-	1.0	0.6	8.6	2.9	0.4	8.1	1.3	0.2	-	-	1.2	-	-	-	-	-	0.1	-	-	-	-	0.1
2102.50			-	-	-	-	-	-	1.6	2.3	7	1.9	-	9.6	0.2	0.6	-	0.1	0.8	-	-	-	-	0.1	-	-	-	-	-	-
2103.45	marly limestone, bituminous		-	-	-	-	-	-	1.8	-	11	2.2	-	15.2	4.2	0.1	-	0.1	0.5	-	-	-	-	0.2	-	-	-	-	-	-
2104.27	limestone, bituminous		-	-	-	-	-	-	2.7	0.1	8.6	3.4	0.6	9	2.3	0.9	-	0.1	2.7	-	-	-	-	0.3	-	-	-	-	-	0.1
2105.37	marly limestone, bituminous		-	-	-	-	-	-	1.2	0.6	5.5	2.5	0.1	8.4	0.8	0.6	-	0.1	0.8	-	-	-	-	0.6	0.1	-	-	-	-	0.1
2116.2-2117.2	limestone, bituminous	Lias delta	-	-	-	-	-	-	-	0.1	1.9	0.8	-	4.5	-	-	-	-	-	-	-	-	-	-	-	-	-	-	0.1	-

ORGANIC PETROGRAPHY – Mineral matter [vol. %]; Vitrinite reflection, %VRo; ORGANIC GEOCHEMISTRY

Sample/ Depth, m	Mineral groundmass calcareous bits.	calcareous l.-bits.	calcareous n.-bits.	clayey bits.	clayey l.-bits.	clayey mic.-r.	F.g. pel.	C.g.pel.	Carbonates is. cry.	Carbonates coccol.	Carbonates dol.	Glauc.	Gyps.	Detrital minerals qtz	Detrital minerals micas	Pyrite crys.	Pyrite framb.	Pyrite epig.	Zooclasts shell	Zooclasts fish r.	Zooclasts biocl.	Vitrinite reflection mean	s.d.	n	TOC [%]	S1 *	S2 *	HI ~	OI ~~	Tmax °C
2074-2075	-	61.6	-	0.3	-	-	0.3	-	2.2	0.3	-	-	-	0.1	1.6	2.2	1.0	1.4	0.3	0.6	1.7	-	-	-	3.3	0.5	14.4	434	27	433
2078.23	-	67.6	-	0.2	-	-	1.9	-	4.7	0.1	-	-	-	0.5	3.1	0.7	0.6	2.9	-	0.5	1.6	-	-	-	-	-	-	-	-	-
2087.33	57.3	-	0.1	1.2	-	-	4.7	-	1.1	4.6	-	-	-	0.2	1.2	2.6	2.4	0.2	-	-	0.6	-	-	-	4.8	1.1	26.0	547	25	428
2088.30	57.7	-	-	0.4	-	-	3.6	-	2.9	0.9	-	-	-	0.1	2.1	4.2	2.0	1.2	-	0.2	0.8	-	-	-	6.2	1.7	37.7	604	20	427
2089.33	55.6	-	-	0.8	-	-	0.5	-	5.4	1.9	-	-	-	0.1	1.6	6.3	4.0	0.2	0.1	1.7	-	-	-	-	7.5	2.3	46.2	614	17	430
2090.55	43.9	-	-	3.7	-	-	0.6	0.6	3.5	3.5	0.2	-	-	0.8	1.0	3.1	3.4	0.9	-	0.7	2.7	-	-	-	11.1	3.7	75.5	679	11	430
2091.55	52.0	-	-	0.5	-	-	4.9	0.5	4.0	0.4	0.4	-	-	0.2	0.5	3.5	2.6	0.4	-	1.1	9.3	-	-	-	6.3	2.1	41.6	661	16	430
2092.43	40.4	-	-	0.3	-	-	6.6	0.2	3.3	7.3	1.2	-	-	-	0.5	4.1	4.3	0.4	0.1	0.8	2.6	-	-	-	8.1	3.0	54.1	668	18	429
2093.40	28.3	-	-	4.7	-	-	6.5	0.2	1.9	21.8	0.2	-	-	0.9	1.0	2.7	7.6	0.1	-	0.6	0.5	-	-	-	10.0	3.6	65.5	655	17	427
2095.10	36.3	-	-	0.9	-	-	1.0	0.1	3.3	0.9	-	-	-	0.4	0.9	8.4	6.2	1.2	0.1	1.6	1.8	-	-	-	11.4	3.9	75.3	661	15	429
2096.13	45.0	-	-	1.2	-	-	0.2	0.2	3.5	0.1	-	-	-	0.4	1.5	4.3	5.6	0.4	-	0.1	2.7	-	-	-	14.1	4.9	102.8	728	8	429
2097.13	23.7	-	-	4.0	-	-	5.8	0.2	2.2	15.6	0.3	-	-	0.9	0.6	8.6	4.2	0.2	0.8	0.3	1.9	-	-	-	9.5	3.8	65.0	681	14	429
2098.15	14.6	-	-	9.4	-	-	1.3	0.4	3.5	16.1	-	-	-	1.2	2.7	4.6	7.2	0.1	-	0.2	1.2	-	-	-	13.1	5.4	96.6	737	10	428
2099.39	25.8	-	-	10.7	-	-	0.4	5.9	3.8	1.3	-	-	-	0.8	4.4	6.6	9.9	0.4	0.3	0.4	0.6	-	-	-	-	-	-	-	-	-
2100.49	26.2	-	-	11.0	-	-	-	2.4	3.7	-	-	-	0.4	1.6	1.5	7.0	8.6	0.2	1.4	0.2	-	-	-	-	11.4	3.6	76.9	674	13	429
2101.52	47.7	-	-	5.2	-	-	0.1	0.5	1.8	7.6	-	-	0.2	0.4	1.9	3.5	5.8	-	-	0.4	0.4	-	-	-	10.1	3.6	62.5	619	14	427
2102.50	45.6	-	-	3.0	-	-	0.9	0.3	3.7	4.3	0.2	-	-	0.4	1.9	5.2	9.4	-	0.1	0.3	0.5	-	-	-	10.8	4.0	70.3	651	15	430
2103.45	21.7	-	-	0.9	-	-	2.7	0.1	7.4	-	16.2	-	-	-	1.4	5.8	6.2	1.0	-	0.1	1.2	-	-	-	12.5	4.6	87.3	700	8	427
2104.27	48.3	-	-	2.5	-	-	-	-	3.7	-	0.1	-	-	0.8	0.9	2.2	9.2	0.4	-	-	1.1	-	-	-	16.8	6.2	119.5	710	9	430
2105.37	35.7	-	-	3.6	-	-	0.7	0.1	5.0	-	22.3	-	-	0.1	0.8	3.1	6.0	0.4	0.1	-	0.8	-	-	-	7.7	3.1	51.9	675	12	426
2116.2-2117.2	-		79.9	-	-	-	-	0.1	3.0	-	0.3	-	-	0.8	2.7	0.5	0.8	3.2	0.1	0.2	1.0	-	-	-	0.9	0.2	1.6	170	186	437

ORGANIC PETROGRAPHY

el.-elongated; eq.-equidimensional; Spor.- sporinite; Tel.- telalginite; fil.-filamentous; Liptd.-liptodetrinite; Bit. I- bituminite I; Bit. II-bituminite II; Bit. III- bituminite III; Bit. IV- bituminite IV; Bit. IV- bituminite IV; Bit.V- bituminite V; Bit.VI- bituminite VI; homog.-homogeneous; heter.-heterogeneous; Oil drop.-oil droplets; Fus.-fusinite; Semifus.-semifusinite; Secret.-secretinite; Intd.-inertodetrinite; Micr.- micrinite; fish r.-fish remains; biocl.-bioclasts; bits.-bituminous; l.-bits.-low bituminous; n.-bits.-non-bituminous; mic.-r.- micrinite-rich; F.g.pel.-Fine-grained peloids; C.g. pel.-Coarse-grained peloids; is. cry.-isolated crystals; coccol.-coccoliths; dol.-dolomite; Glauc.-Glauconite; qtz.-quartz; Gyps.-Gypsum; cryst.-crystals ; framb.-framboidal; epig.-epigenetic.

mean-mean value; s.d.-standart deviation; n-total number of measurements.

ORGANIC GEOCHEMISTRY

*-[mg HC/g],~-[mg HC/g TOC], ~~-[mg CO2/g TOC].

Appendix A3: Well A

Sample/ Depth, m	Lithology	Age	Local names	ORGANIC PETROGRAPHY: Organic matter: Vitrinite (V) [vol.%]: autochthonous: heterogeneous: el.	autochthonous: heterogeneous: eq.	autochthonous: homogeneous: el.	autochthonous: homogeneous: eq.	recycled: homogeneous: el.	recycled: homogeneous: eq.	Spor.	Alginite: Tel.	Alginite: lamalginite: discrete	Alginite: lamalginite: fil.	Alginite: lamalginite: layered	Liptd.	Bit. I	Bit. II	Bit. III	Bit. IV	Bit. V	Bit. VI	Migrabitumen: homog.	Migrabitumen: heter.	Oil drop.	Fus.	Semifus.	Secret.	Intd.	Micr.
2328.20				0.1	-	-	-	-	-	-	0.9	10.3	4.0	1.7	11.5	0.2	-	-	0.2	-	1.7	-	-	-	-	0.1	-	0.3	2.2
2328.30	calcareous mudstone, bituminous			-	-	-	-	-	0.1	-	0.5	8.5	2.0	-	8.9	0.6	-	-	-	-	0.3	-	-	-	0.1	0.1	-	0.2	0.2
2328.60				0.1	-	-	-	-	-	-	1.1	2.7	2.7	0.1	7.0	0.1	-	-	-	-	0.1	-	-	-	-	-	-	1.4	0.4
2328.80	limestone, bituminous			-	-	-	-	-	-	-	1.1	3.4	2.0	0.2	6.7	0.1	0.5	-	-	-	0.5	-	-	-	-	-	-	0.2	-
2331.20	calcareous mudstone			-	-	-	-	0.2	0.2	-	1.1	7.0	3.8	0.3	9.1	0.5	0.1	-	-	-	0.3	-	-	-	0.1	0.1	-	0.5	0.2
2331.80	bituminous			-	-	-	-	-	-	-	1.0	7.2	2.1	-	8.4	0.5	-	-	-	-	0.1	-	-	-	0.3	0.2	-	1.2	0.1
2333.70				-	-	-	-	-	-	-	0.5	3.3	2.1	0.1	4.0	0.6	7.6	-	-	-	-	-	-	-	0.3	-	-	0.4	0.2
2336.05				-	-	-	-	-	-	-	0.9	3.9	2.2	-	3.5	0.9	3.3	-	-	-	-	-	-	-	-	-	-	0.1	0.3
2337.10				-	-	-	-	-	-	-	1.0	3.3	1.0	0.1	4.1	0.3	1.6	-	-	-	-	-	-	-	0.1	-	-	-	-
2338.20				-	-	-	-	-	-	-	0.4	3.7	0.8	0.1	8.7	3.1	3.1	-	-	-	-	-	-	0.1	-	-	-	0.6	1.8
2339.00				-	-	-	-	0.1	-	-	0.6	4.8	1.3	-	8.0	3.0	0.6	-	-	-	2.2	-	-	-	0.1	-	-	0.2	-
2340.30				-	-	-	-	-	-	-	0.5	3.5	0.5	0.2	5.9	0.2	2.9	-	-	-	2.3	-	-	-	0.1	-	-	0.3	0.2
2342.40				-	-	-	-	-	-	-	1.0	4.8	1.7	0.2	8.6	0.1	1.9	-	-	-	2.9	-	-	-	-	0.1	-	0.2	-
2343.20				-	-	-	-	-	-	-	0.5	4.0	1.5	0.2	10.4	0.2	4.1	-	-	-	2.0	-	-	-	-	-	-	-	-
2344.60				-	-	-	-	-	-	-	0.6	2.0	2.4	0.9	7.8	0.2	11.7	-	-	-	3.0	-	-	-	-	-	-	0.1	0.5
2345.40				-	-	-	-	-	-	-	0.6	2.5	1.3	-	12.7	0.5	5.5	-	-	-	2.5	-	-	-	-	-	-	0.2	0.4
2345.70				0.1	-	-	-	-	-	-	0.4	4.1	1.2	-	7.3	0.4	13.5	-	-	-	1.0	-	-	-	0.1	0.1	-	0.3	0.5
2345.80				-	-	-	-	-	-	-	0.3	2.9	2.0	0.1	11.6	0.2	14.2	-	-	-	1.1	-	-	-	-	-	-	0.2	1.6
2345.90				-	-	-	-	-	-	-	0.3	0.7	0.3	-	2.9	-	0.1	-	-	-	5.8	-	-	0.6	-	-	-	0.1	0.4
2346.20				-	-	-	-	-	-	-	0.1	1.3	0.6	-	5.3	1.0	5.2	-	-	-	0.5	-	-	-	-	-	-	0.3	-
2350.40				-	-	-	-	-	-	-	0.5	4.4	1.3	0.2	12.8	4.5	0.2	-	-	-	2.7	-	-	0.4	0.3	-	-	0.5	0.4
2352.05				-	-	-	-	0.1	-	-	0.2	4.6	1.0	-	14.1	7.0	0.4	-	-	-	3.1	-	-	0.3	0.2	-	-	0.8	1.1
2352.15	limestone, bituminous			-	-	-	-	-	-	-	-	4.8	3.5	0.3	4.7	2.2	0.5	-	-	-	18.9	-	-	0.1	0.1	0.1	-	0.5	0.4
2352.90				-	-	-	-	-	-	-	0.2	4.4	1.7	0.8	5.2	0.6	9.9	-	-	-	2.1	-	-	-	0.5	-	-	0.5	4.6
2353.35				-	-	-	-	-	-	-	1.2	2.8	0.8	0.1	7.0	10.6	19.9	-	-	-	4.2	-	-	0.1	-	-	-	0.4	0.2
2353.90				-	-	-	-	-	-	-	1.6	3.2	1.4	0.4	3.1	2.1	59	-	-	-	0.7	-	-	-	-	-	-	0.1	0.5
2355.30				-	-	-	-	-	-	-	0.5	1.7	1.7	0.1	5.5	4.7	22.1	-	-	-	16.7	-	-	-	0.1	-	-	0.2	0.4
2356.55				-	-	-	-	-	-	0.1	0.5	3.0	1.3	0.0	8.8	1.8	2.6	-	0.1	-	3.8	-	-	-	0.1	-	-	0.8	2.4
2358.80				-	-	-	-	-	-	-	0.4	5.6	10.4	6.0	4.2	0.7	12.8	-	-	-	7.0	-	-	-	-	-	-	0.2	0.3
2359.20				-	-	-	-	-	-	-	-	1.1	0.2	0.0	2.1	0.4	0.6	-	-	-	3.4	-	-	0.7	-	-	-	0.1	0.3
2359.65				-	-	-	-	-	-	-	0.1	4.0	3.8	2.0	3.5	2.8	2	-	-	-	8.2	-	-	0.2	-	-	-	-	-
2361.10				-	-	-	-	-	-	-	0.1	3.4	3.1	1.0	2.5	3.9	-	-	-	-	1.3	-	-	-	-	-	-	-	-
2362.15				0.1	-	-	-	-	-	-	-	1.2	0.2	-	2.1	0.9	0.4	-	-	-	0.2	-	-	0.3	0.1	0.1	-	-	-
2362.25				-	-	-	-	-	-	-	-	1.8	0.2	-	3.0	0.8	0.1	-	-	-	0.2	-	-	0.4	-	-	-	0.3	-
2362.35				-	-	-	-	-	-	-	0.1	0.2	0.2	-	0.1	-	-	-	-	-	-	-	-	-	-	-	-	-	-
2366.30				-	-	-	0.1	-	-	-	3.7	2.0	0.6	0.1	-	0.6	0.2	-	-	-	-	-	-	0.2	-	-	-	0.2	0.1
2367.40		Lias delta		-	-	-	-	-	-	-	-	0.1	0.0	-	1.0	0.2	-	-	-	-	-	-	-	0.2	-	-	-	0.1	-
2373.00				-	-	-	-	-	-	-	-	0.6	0.3	-	0.4	-	-	-	-	-	-	-	-	0.1	-	-	-	0.3	0.1

Sample/ Depth, m	Lithology	Age	Local names	ORGANIC PETROGRAPHY: Liptinite (L) [vol.%]: Bit. I	Bit. II	Bit. III	Bit. IV	Bit. V	Bit. VI	Inertinite (I) [vol.%]: Fus.	Semifus.	Secret.	Intd.	Micr.	Mineral matter, [vol. %]: Mineral groundmass: calcareous: bits.	calcareous: 1-bits.	calcareous: n.-bits.	clayey: bits.	clayey: 1-bits.	clayey: mic.-r.	F.g. pel.	C.g. pel.	Carbonates: is. cry.	Carbonates: coccol.	Carbonates: dol.	Glauc.	Gyps.	Detrital minerals: qtz	Detrital minerals: mica	Pyrite: crys.	Pyrite: framb.	Pyrite: epig.	Zooclasts: shell	Zooclasts: fish r.	Zooclasts: biocl.	Vitrinite reflection, %VRo: mean	s.d.	n
2328.20															4.1	-	-	34.3	-	-	-	0.1	-	-	0.2	-	-	1.3	0.3	16.7	6	3.7	-	-	0.1	0.54	0.03	4
2328.30	calcareous mudstone, bituminous														6.9	-	-	35.4	-	-	-	0.1	4.7	-	-	-	-	0.8	0.1	18.9	6.8	4.7	-	-	-	-	-	-
2328.60															10.4	-	-	31.9	-	-	-	0.8	5.8	-	-	-	-	0.8	0.4	23.8	8.6	1.1	-	-	0.1	-	-	-
2328.80	limestone, bituminous														41.2	-	-	16.2	-	-	-	0.4	2.3	-	-	-	-	0.6	0.1	17.3	6	0.9	-	-	-	0.6	0.5	13
2331.20	calcareous mudstone														5.9	-	-	32.6	-	-	-	0.7	3.2	-	-	-	-	0.5	-	16.4	16.5	0.3	-	-	0.1	-	-	-
2331.80	bituminous														7.1	-	-	30.8	-	-	-	1	6.5	-	-	-	-	0.4	0.3	18.1	13.9	0.5	-	-	-	-	-	-
2333.70															64.1	-	0.4	4.5	-	-	-	1.2	-	-	-	-	-	0.7	0.3	5.1	4.2	0.4	-	-	-	-	-	-
2336.05															48.4	-	-	13.2	-	-	-	0.2	1.6	-	0.1	-	-	0.1	0.2	6.3	12.5	0.4	0.3	-	1.5	-	-	-
2337.10															68.8	-	-	4.8	-	-	-	0.5	0.6	-	-	-	-	0.7	0.3	4.8	6.7	0.5	0.3	-	-	-	-	-
2338.20															47.6	-	-	4	-	-	-	0.5	3.8	-	-	-	1.6	-	-	9	6.8	0.9	1.6	-	1.8	-	-	-
2339.00															60.4	-	-	6.5	-	-	-	0.7	0.6	-	-	-	-	0.1	-	4.8	4.6	1.3	0.1	-	-	-	-	-
2340.30															65.2	-	-	1.3	-	-	-	2.8	1.3	-	-	-	0.1	0.2	-	5.9	6	0.6	-	-	-	-	-	-
2342.40															61.4	-	-	0.7	-	-	-	4.6	0.5	-	-	-	-	0.1	-	4.2	7	0	-	-	-	-	-	-
2343.20															64.3	-	-	0.3	-	-	-	4.4	0.9	-	-	-	-	-	-	2.8	3.8	0.6	-	-	-	-	-	-
2344.60															55.5	-	-	0.5	-	-	-	6.2	1	-	-	-	-	-	-	3.1	3.6	0.7	0.1	-	0.1	-	-	-
2345.40															47.3	-	-	2.6	-	-	-	8.1	2.2	-	0.2	-	-	-	-	4	6.4	1.1	0.4	1.1	0.3	-	-	-
2345.70															46.4	-	0.1	1.2	-	-	-	6.8	7.2	-	0.1	-	-	-	-	2.7	4.7	0.8	0.4	0.1	0.5	0.54	0.02	15
2345.80															39.4	-	-	6.8	-	-	-	10.1	-	-	-	-	-	-	-	2.4	5.9	0.7	-	0.2	0.3	-	-	-
2345.90															3.9	-	-	1	-	-	-	0.2	12.1	-	0.1	-	60.4	-	-	3.3	3.8	2.8	-	0.2	0.5	-	-	-
2346.20															60.6	-	-	0.9	-	-	-	2	2.2	-	-	-	-	-	-	2	2.6	1.7	-	12	1.7	-	-	-
2350.40															52.5	-	-	1.8	-	-	-	1.7	3.2	-	-	-	0.1	0.8	0.4	4.7	5.4	0.6	-	-	-	-	-	-
2352.05															12.4	-	-	15.1	-	-	-	3.2	13.1	-	0.3	-	0.1	-	-	9.6	12.4	0.8	-	-	-	-	-	-
2352.15	limestone, bituminous														13.5	-	-	8.4	-	-	-	8.4	10.5	-	0.1	-	0.3	-	0.2	6	15.6	0.4	0.2	-	0.2	-	-	-
2352.90															52.4	-	0.2	0.4	-	-	-	3.9	4.3	-	0.1	-	-	-	-	1.7	5	0.7	-	-	0.8	0.55	0.03	11
2353.35															27.3	-	0.5	1.9	-	-	-	6.5	5.5	-	0.2	-	-	-	0.1	2	8.2	0.2	-	-	0.3	0.54	0.02	7
2353.90															12.2	-	0.6	1.5	-	-	-	3.9	3.3	-	0.1	-	-	0.3	-	0.9	4.6	0.2	-	-	0.3	-	-	-
2355.30															26.1	-	0.1	1.9	-	-	-	2.4	7.7	-	-	-	-	-	-	3.4	2.9	0.9	0.1	0.2	0.5	-	-	-
2356.55															53.2	-	0.5	0.5	-	-	-	8.3	1.8	-	0.2	-	-	-	0.1	0.9	8.9	0	-	-	0.3	-	-	-
2358.80															36.9	-	0.1	-	-	-	-	6.9	1.1	-	-	-	-	-	0.1	0.6	5.4	0.2	0.4	0.1	0.6	-	-	-
2359.20															1.7	-	0.9	0.3	-	-	-	76.2	-	-	9.4	-	0.3	-	-	-	1.2	1	0.1	-	-	-	-	-	-
2359.65															34.2	-	5.4	-	-	-	-	18.5	3.5	-	4	-	-	0.6	0.3	0.2	6.2	0.3	0.1	-	0.1	-	-	-
2361.10															34	-	17.8	-	-	-	-	22.4	4.7	-	0.9	-	-	0.5	0.2	-	2.9	0.6	0.2	-	0.5	-	-	-
2362.15															73.3	-	8	-	-	-	-	0.1	7.8	-	0.2	-	-	0.2	0.3	-	1	2.8	0.2	-	0.5	-	-	-
2362.25															75.2	-	3.1	-	-	-	-	1.9	6	-	0.4	-	-	0.3	0.4	0.1	1.7	3.6	-	-	0.5	-	-	-
2362.35															50.1	-	-	0.8	-	-	-	26.1	0.2	-	-	-	2.9	-	-	1.2	0.1	13.5	-	-	4.5	-	-	-
2366.30															84.1	-	-	-	-	-	-	0.4	5	-	-	-	0.1	-	0.8	0.5	0.6	0.1	-	-	0.5	-	-	-
2367.40		Lias delta													1.7	-	51.1	-	-	-	-	-	39	-	0.1	-	3.3	-	0.2	0.2	-	2.3	-	0.1	0.4	-	-	-
2373.00															0.3	-	94.6	-	-	-	-	-	2.7	-	-	-	0.3	0.1	0.5	-	-	-	-	-	0.1	-	-	-

ORGANIC PETROGRAPHY

el.-elongated; eq.-equidimensional; Spor.- sporinite; Tel.- telalginite; fil.-filamentous; Liptd.-liptodetrinite; Bit. I- bituminite I; Bit. II-bituminite II; Bit. III- bituminite III; Bit. IV- bituminite IV; Bit. IV- bituminite IV; Bit.V- bituminite V; Bit.VI- bituminite VI; homog.-homogeneous; heter.-heterogeneous; Oil drop.-oil droplets; Fus.-fusinite; Semifus.-semifusinite; Secret.-secretinite; Intd.-inertodetrinite; Micr.- micrinite; fish r.-fish remains; biocl-bioclasts; bits.-bituminous; l-bits.-low bituminous; n.-bits.-non-bituminous; mic.-r.- micrinite-rich; F.g.pel.-Fine-grained peloids; C.g. pel.-Coarse-grained peloids; is. cry.-isolated crystals; coccol.-coccoliths; dol.-dolomite; Glauc.-Glauconite; qtz.-quartz; Gyps.-Gypsum; cryst.-crystals ; framb.-framboidal; epig.-epigenetic.
mean-mean value; s.d.-standart deviation; n-total number of measurements.

Sample/ Depth, m	Lithology	Age	Local names	ORGANIC GEOCHEMISTRY: TOC [%]	S1 *	S2 *	HI ~	OI ~~	Tmax °C
2328.20				10.8	4.0	52.9	488	5	449
2328.30	calcareous mudstone, bituminous			10.5	3.6	51.5	492	4	448
2328.60				11.2	3.8	54.9	491	5	450
2328.80	limestone, bituminous			8.1	3.6	38.8	482	6	448
2331.20	calcareous mudstone			10.9	4.0	49.5	456	4	447
2331.80	bituminous			10.7	3.7	50.3	470	6	448
2333.70				8.0	3.5	37.3	464	8	446
2336.05				7.4	3.5	34.3	464	8	447
2337.10				5.6	2.9	24.3	433	11	446
2338.20				6.2	2.9	27.9	452	10	448
2339.00				5.5	3.3	24.3	441	10	447
2340.30				6.4	3.6	29.3	458	10	445
2342.40				7.1	3.8	31.8	448	8	449
2343.20				6.6	2.7	27.2	413	8	447
2344.60				6.7	2.7	28.3	423	8	448
2345.40				7.2	3.1	30.5	423	7	448
2345.70				7.6	2.8	31.3	414	8	446
2345.80				7.2	2.9	29.5	408	7	447
2345.90				6.4	2.4	25.8	406	9	446
2346.20				6.8	3.3	28.5	422	9	447
2350.40				9.6	2.9	39.8	416	6	446
2352.05				9.1	2.7	36.0	396	6	445
2352.15	limestone, bituminous			10.4	2.9	42.6	410	6	448
2352.90				8.8	3.1	43.5	494	9	446
2353.35				8.3	2.8	37.9	456	10	447
2353.90				7.4	4.4	37.0	497	8	442
2355.30				8.9	3.6	42.7	479	7	447
2356.55				10.7	3.5	50.0	469	7	448
2358.80				14.4	3.8	77.4	539	6	447
2359.20				2.5	2.0	8.4	340	20	443
2359.65				11.4	3.3	60.7	534	8	443
2361.10				8.7	2.5	46.5	535	8	447
2362.15				1.9	0.6	5.2	270	46	445
2362.25				-	-	-	-	-	-
2362.35				2.4	0.4	2.3	96	46	436
2366.30				1.2	0.2	2.7	232	32	446
2367.40		Lias delta		0.7	0.2	0.8	116	84	444
2373.00				0.9	0.1	1.5	155	50	447

ORGANIC GEOCHEMISTRY

*-[mg HC/g],~-[mg HC/g TOC], ~~-[mg CO2/g TOC].

Appendix A4: Well B

Sample/ Depth, m	Lithology	Age	ORGANIC PETROGRAPHY: Organic matter																										Mineral matter, [vol. %]																					Reflection, %Ro									ORGANIC GEOCHEMISTRY: TOC	S1	S2	HI	OI	Tmax
		Local names	Meta-vitrinite (V) [vol.%]						Meta-liptinite (L) [vol.%]															Inertinite (I) [vol.%]					Mineral groundmass						F.g. pel.	C.g. pel.	Carbonates		dol.	Glauc.	Gyps.	Detrital minerals		Pyrite			Zooclasts			Bitumen						Vitrinite			[%]	*	*	~	~~	°C
			autochthonous				recycled		M.Spor.	M.Tel.	M.Alginite			M. Liptd.	M.Bit. I	M.Bit. II	M.Bit. III	M.Bit. IV	M.Bit. V	M.Bit. VI	Migrabitumen		Oil drop.	Fus.	Semifus.	Secret.	Intd.	Micr.	calcareous			clayey					is. cry.	coccol.				qtz	mica	crys.	framb.	epig.	shell	fish r.	biocl.	homogeneous			heterogeneous			mean	s.d.	n						
			heterogeneous		homogeneous		homogeneous				M.lamalginite										homog.	heter.							bits.	l.-bits.	n.-bits.	bits.	l.-bits.	mic.-r.																mean	s.d.	n	mean	s.d.	n									
			el.	eq.	el.	eq.	el.	eq.			discrete	fil.	layered																																																		
1227.10			-	-	-	-	-	-	0.1	0.8	-	-	-	-	-	2.4	-	-	-	-	1.4	0.2	-	0.2	-	-	0.6	21.7	0.2	-	-	-	-	18.8	0.2	-	37.4		-	-	-	-	0.1	6.5	2.2	0.5	-	-	6.9	3.43	0.30	19	-	-	-	-	-	-	5.7	1.3	0.6	11	21	-
1227.20			-	-	-	-	-	0.2	-	0.6	-	-	-	-	0.1	12.6	-	-	-	-	0.3	0.0	-	0.1	-	-	-	12.3	0.1	-	-	-	-	28.2	0.1	-	27.9		-	-	-	-	0.3	11.3	3.6	0.8	1.3	-	0.4	-	-	-	1.10	0.10	10	-	-	-	5.6	1.2	0.8	14	23	-
1227.27			-	-	-	-	-	-	0.1	0.8	-	-	-	-	1.1	11.2	-	-	-	-	0.3	0.1	-	-	-	-	-	18.1	0.1	-	-	-	-	19.9	-	-	26.2		-	-	-	-	0.3	16.2	3.7	0.6	1.3	-	-	-	-	-	-	-	-	3.33	0.60	100	5.7	1.2	0.6	11	20	-
1227.37			-	-	-	-	-	-	0.1	1.4	-	-	-	-	0.1	3.7	-	-	-	-	0.8	0.4	-	0.4	-	0.1	0.1	21.7	-	-	-	-	-	24.5	0.2	-	24.5		-	-	-	-	0.1	11.8	4.6	2.1	-	-	3.4	-	-	-	-	-	-	-	-	-	5.3	0.3	0.2	5	22	-
1227.56			0.1	-	-	-	-	-	-	0.5	-	-	-	-	1.4	2.8	-	-	-	-	0.2	-	-	0.2	-	-	0.2	19.9	-	-	-	-	-	30.8	-	-	22.1		0.1	-	-	-	-	15.0	1.4	3.0	1.8	-	0.6	-	-	-	-	-	-	-	-	-	4.9	0.2	0.0	1	31	-
1227.62			0.1	-	-	-	-	-	-	0.3	-	-	-	-	0.3	7.3	-	-	-	-	0.3	-	-	0.5	-	-	0.1	17.1	-	-	-	-	-	26.1	-	-	23.3		-	-	-	-	0.1	14.3	6.0	1.3	2.2	-	0.7	-	-	-	-	-	-	-	-	-	5.4	0.2	0.1	1	24	-
1227.87			-	-	-	-	-	-	-	0.4	-	-	-	-	0.3	1.7	-	-	-	-	0.4	0.1	-	0.1	-	0.1	0.1	27.8	-	-	-	-	-	21.8	-	-	18.6		-	-	-	-	0.2	17.9	3.3	4.0	-	-	3.2	-	-	-	-	-	-	-	-	-	5.5	0.5	0.3	5	21	-
1227.95			-	-	-	-	-	-	0.1	0.9	-	-	-	-	0.4	10.8	-	-	-	-	0.1	-	-	0.1	-	-	0.2	20.2	0.1	-	-	-	-	23.2	-	-	28.2		-	-	-	-	0.5	8.6	2.8	2.0	1.4	-	0.2	-	-	-	-	-	-	-	-	-	5.6	0.4	0.4	7	21	-
1228.02			-	-	-	-	-	-	-	0.2	-	-	-	-	1.8	5.2	-	-	-	-	0.2	-	-	0.4	-	-	0.1	20.4	0.1	-	-	-	-	18.8	-	-	27.7		-	-	-	-	-	13.0	5.0	3.0	-	-	4.1	-	-	-	-	-	-	3.52	0.36	100	5.7	0.7	0.3	6	23	-
1228.07			-	-	-	-	-	-	-	0.5	-	-	-	-	0.2	0.9	-	-	-	-	0.2	0.1	-	0.2	-	-	-	25.2	-	-	-	-	-	30.4	-	-	19.7		-	-	-	-	-	15.0	2.3	2.7	-	-	3.1	3.53	0.20	20	-	-	-	-	-	-	5.6	1.2	0.6	11	18	-
1228.12			-	-	-	-	-	-	0.1	1.4	-	-	-	-	0.5	1.1	-	-	-	-	0.2	-	-	0.8	-	0.1	0.4	21.8	0.1	-	-	-	-	27.7	-	-	21.2		0.1	-	-	-	-	15.9	3.2	1.0	-	-	4.4	-	-	-	-	-	-	-	-	-	5.5	0.3	0.1	2	24	-
1228.18			-	-	-	-	-	-	-	1.0	-	-	-	-	0.8	2.1	-	-	-	-	0.7	0.1	-	-	-	0.1	-	21.5	-	-	-	-	-	22.2	-	-	28.0		-	-	-	-	0.2	11.0	4.4	1.4	-	-	6.5	-	-	-	-	-	-	-	-	-	5.8	0.7	0.4	7	21	-
1228.25			-	-	-	-	-	-	0.1	0.8	-	-	-	-	-	6.4	-	-	-	-	0.8	-	-	0.4	-	0.1	0.3	22.3	-	-	-	-	-	21.3	-	-	30.8		-	-	-	-	0.1	10.4	1.0	2.8	1.8	-	0.5	-	-	-	-	-	-	-	-	-	-	-	-	-	-	-
1228.34			-	-	-	-	-	-	0.1	1.0	-	-	-	-	-	3.0	-	-	-	-	0.4	-	-	0.3	-	-	-	22.8	-	-	-	-	-	26.2	0.1	-	25.6		-	-	-	-	0.2	12.9	2.7	0.1	0.1	-	4.5	-	-	-	-	-	-	-	-	-	5.9	0.2	0.0	1	22	-
1228.40			-	-	-	-	-	-	0.1	1.1	-	-	-	-	-	8.0	-	-	-	-	0.3	0.1	-	0.1	-	-	0.1	14.0	-	-	-	-	-	13.9	-	-	31.3		0.1	-	-	-	0.6	21.6	4.5	0.6	3.0	-	0.6	-	-	-	-	-	-	-	-	-	6.1	0.6	0.5	8	20	-
1228.64			-	-	-	-	-	0.2	0.2	0.9	-	-	-	-	0.3	7.6	-	-	-	-	0.2	0.3	-	0.2	-	-	0.5	23.0	0.2	-	-	-	-	22.5	0.1	-	22.1		-	-	-	-	-	13.4	3.5	2.0	0.7	-	2.0	-	-	-	-	-	-	-	-	-	6.3	0.1	0.0	0	22	-
1228.84			-	-	-	-	-	-	-	0.9	-	-	-	-	-	6.3	-	-	-	-	0.4	-	-	0.2	-	0.1	-	18.2	-	-	-	-	-	30.2	-	-	21.3		0.1	-	-	-	0.1	14.5	4.7	1.5	0.9	-	0.6	-	-	-	-	-	-	-	-	-	6.7	0.4	0.3	4	21	-
1229.06	mudstone, calcareous with pyrite inclusions, plant remains	Lias epsilon	-	-	-	-	-	-	-	1.4	-	-	-	-	-	6.1	-	-	-	-	1.4	0.1	-	0.2	-	0.1	0.1	10.6	-	-	-	-	-	31.1	0.2	-	26.2		-	-	-	-	0.1	13.7	3.3	1.9	2.6	-	0.9	-	-	-	-	-	-	-	-	-	6.7	0.7	0.5	7	19	-
1229.14			-	-	-	-	-	-	0.1	0.7	-	-	-	-	0.9	10.2	-	-	-	-	0.5	0.1	-	-	-	-	0.3	18.2	-	-	-	-	-	17.0	-	-	24.7		-	-	-	-	0.2	15.9	4.0	3.2	1.1	-	2.9	-	-	-	-	-	-	-	-	-	6.7	0.7	0.3	5	21	-
1229.28			-	-	-	-	-	0.1	-	0.4	-	-	-	-	0.4	5.1	-	-	-	-	0.2	-	-	0.5	-	-	0.3	22.0	-	-	-	-	-	21.5	0.1	-	24.9		-	-	-	0.1	0.1	13.9	4.6	2.7	2.0	-	1.1	-	-	-	-	-	-	-	-	-	-	-	-	-	-	-
1229.43			-	-	-	-	-	-	0.2	1.9	-	-	-	-	-	6.0	-	-	-	-	-	-	-	0.2	-	-	-	26.9	-	-	-	-	-	17.4	-	-	29.5		0.1	-	-	-	0.3	9.7	3.4	1.0	2.1	-	1.2	-	-	-	-	-	-	-	-	-	6.5	0.2	0.1	2	23	-
1229.61			-	-	-	-	-	-	0.6	1.8	-	-	-	-	1.3	1.2	-	-	-	-	-	-	-	0.4	-	0.1	0.2	27.1	-	-	-	-	-	30.1	-	-	19.8		-	-	-	-	0.3	9.4	1.8	1.5	-	-	4.4	-	-	-	-	-	-	-	-	-	6.7	0.4	0.4	5	21	-
1229.75			-	-	-	-	-	-	-	1.0	-	-	-	-	3.3	0.1	-	-	-	-	-	0.4	-	0.4	-	0.1	-	32.4	2.0	-	-	-	-	32.4	-	-	13.3		-	-	-	0.1	0.0	4.0	1.4	4.8	0.1	-	4.2	-	-	-	-	-	-	3.51	0.65	100	7.0	0.1	0.0	1	19	-
1229.83			-	-	-	-	-	-	-	1.0	-	-	-	-	0.4	0.3	-	-	-	-	0.1	-	-	0.8	-	-	-	28.6	-	-	-	-	-	31.6	-	-	19.9		-	-	-	-	-	7.0	3.6	1.9	-	-	4.8	-	-	-	-	-	-	-	-	-	-	-	-	-	-	-
1229.93			-	-	-	-	-	-	-	0.9	-	-	-	-	0.2	1.2	-	-	-	-	0.6	-	-	0.3	-	0.1	-	21.5	-	-	-	-	-	25.7	-	-	29.3		-	-	-	-	0.1	9.8	1.9	0.4	-	-	8.0	-	-	-	-	-	-	3.66	0.35	100	6.8	0.1	0.0	1	21	-
1230.00			-	-	-	-	-	-	-	0.7	-	-	-	-	0.5	0.1	-	-	-	-	0.4	-	-	0.7	0.1	-	-	31.3	-	-	-	-	-	33.4	-	-	12.9		-	-	-	-	-	9.8	0.8	3.1	-	-	6.2	-	-	-	-	-	-	-	-	-	7.3	1.0	0.8	11	18	-
1230.10			-	-	-	-	-	-	-	0.8	-	-	-	-	0.2	1.1	-	-	-	-	0.8	-	-	0.4	-	-	0.2	27.9	-	-	-	-	-	15.9	-	-	19.5		-	-	-	-	-	20.7	4.3	2.1	0.1	-	6.0	-	-	-	-	-	-	-	-	-	6.7	0.4	0.3	4	19	-
1230.18			-	-	-	-	-	-	-	1.4	-	-	-	-	-	8.7	-	-	-	-	0.5	-	-	0.1	-	-	-	22.0	-	-	-	-	-	20.5	-	-	24.9		-	-	-	-	0.1	7.5	3.7	6.7	3.2	-	0.7	-	-	-	-	-	-	-	-	-	7.2	0.5	0.3	4	25	-
1230.50			-	-	-	-	-	-	-	-	-	-	-	-	0.2	2.9	-	-	-	-	0.5	0.3	-	0.3	-	-	-	18.4	-	-	-	-	-	16.3	0.1	-	22.9		-	-	-	-	0.5	26.1	6.8	1.4	2.2	-	0.8	-	-	-	-	-	-	-	-	-	6.7	0.2	0.1	1	20	-
1230.74			-	-	-	-	-	-	0.1	0.4	-	-	-	-	0.6	7.4	-	-	-	-	0.6	0.1	-	-	-	-	0.1	18.4	-	-	-	-	-	17.0	-	-	26.6		-	-	-	-	-	21.8	2.5	0.7	1.5	-	2.2	-	-	-	1.07	0.10	16	-	-	-	4.9	1.2	0.6	12	21	-
1230.94			-	-	-	-	-	-	-	0.2	-	-	-	-	-	0.6	-	-	-	-	-	0.1	-	-	-	-	-	-	75.1	-	-	-	-	4.7	-	-	1.7		-	-	-	-	-	2.1	0.1	14.1	-	-	1.3	-	-	-	-	-	-	-	-	-	-	-	-	-	-	-
1231.14			-	-	-	-	-	-	-	0.8	-	-	-	-	0.6	7.5	-	-	-	-	0.2	0.1	-	0.3	-	0.1	0.1	25.5	-	-	-	-	-	21.6	1.2	-	24.5		-	-	-	-	0.1	8.1	5.5	0.3	-	-	3.5	-	-	-	-	-	-	-	-	-	7.2	0.7	0.6	8	15	-
1231.30			-	-	-	-	-	-	-	0.3	-	-	-	-	0.5	2.5	-	-	-	-	0.3	0.1	-	0.2	-	0.2	-	22.5	0.2	-	-	-	-	20.1	0.8	-	27.1		-	-	-	-	0.1	13.9	4.9	4.7	0.3	-	1.3	-	-	-	-	-	-	-	-	-	6.0	0.6	0.4	6	22	-
1231.53			-	-	-	-	-	-	-	0.1	-	-	-	-	0.1	7.1	-	-	-	-	1.3	0.1	-	0.2	-	0.1	0.6	15.5	-	-	-	-	-	11.5	-	-	43.1		-	-	-	-	0.4	5.4	5.6	1.6	1.3	-	5.8	-	-	-	-	-	-	-	-	-	6.0	0.9	0.4	7	19	-
1231,73 o			-	-	-	-	-	-	-	0.7	-	-	-	-	0.2	1.4	-	-	-	-	1.5	-	-	0.3	-	-	-	20.9	-	-	-	-	-	33.5	-	-	26.4		-	-	-	-	-	5.3	2.6	-	-	-	6.4	-	-	-	-	-	-	-	-	-	6.7	0.6	0.2	4	19	-
1231.93			-	-	-	-	-	-	-	0.8	-	-	-	-	0.9	2.5	-	-	-	-	0.3	0.5	-	0.1	-	0.1	0.0	21.8	0.1	-	-	-	-	39.1	0.2	-	18.0		-	-	-	0.3	-	3.4	2.4	-	1.0	-	6.1	-	-	-	-	-	-	-	-	-	6.7	0.3	0.2	2	19	-
1231.84-1232.2			-	-	-	-	-	-	-	0.3	-	-	-	-	0.1	6.3	-	-	-	-	0.7	0.4	-	-	-	-	1.0	20.0	-	-	-	-	-	20.1	0.2	-	29.5		-	-	-	-	0.2	9.1	4.5	1.1	4.1	-	2.4	-	-	-	1.21	0.10	30	-	-	-	6.3	0.3	0.1	1	18	-
1231.84-1232.3			-	-	-	-	-	-	-	0.9	-	-	-	-	0.3	4.5	-	-	-	-	0.7	0.3	-	0.1	-	-	-	25.0	0.2	-	-	-	-	21.5	-	-	30.7		0.1	-	-	-	0.3	5.9	4.3	1.8	2.5	-	0.9	-	-	-	1.10	0.10	17	3.26	0.44	100	5.9	0.3	0.2	4	20	-
1231.84-1232.4			0.1	-	-	-	-	-	-	0.9	-	-	-	-	0.1	4.9	-	-	-	-	0.3	0.3	-	0.3	-	-	-	18.0	0.2	-	-	-	-	21.0	0.9	-	31.4		-	-	-	-	0.2	11.9	6.5	0.9	2.0	-	0.8	-	-	-	-	-	-	-	-	-	-	-	-	-	-	-

ORGANIC PETROGRAPHY

el.-elongated; eq.-equidimensional; M.Spor.- meta-sporinite; M.Tel.- meta-telalginite; fil.-filamentous; M.Liptd.-meta-liptodetrinite; M.Bit. I-meta-bituminite I; M.Bit. II-meta-bituminite II; M.Bit. III-meta-bituminite III; M.Bit. IV- meta-bituminite IV; M.Bit. IV- meta-bituminite IV; M.Bit.V- meta-bituminite V; M.Bit.VI- meta-bituminite VI; homog.-homogeneous; heter.-heterogeneous; Oil drop.-oil droplets; Fus.-fusinite; Semifus.-semifusinite; Secret.-secretinite; Intd.-inertodetrinite; Micr.- micrinite; fish r.-fish remains; biocl.-bioclasts; bits.-bituminous; l.-bits.-low bituminous; n.-bits.-non-bituminous; mic.-r.- micrinite-rich; F.g.pel.-Fine-grained peloids; C.g. pel.-Coarse-grained peloids; is. cry.-isolated crystals; coccol.-coccoliths; dol.-dolomite; Glauc.-Glauconite; qtz.-quartz; Gyps.-Gypsum; cryst.-crystals ; framb.-framboidal; epig.-epigenetic.

mean-mean value; s.d.-standart deviation; n-total number of measurements.

ORGANIC GEOCHEMISTRY

*-[mg HC/g],~-[mg HC/g TOC], ~~-[mg CO2/g TOC].

Appendix A5: Well D

Sample/ Depth, m	Lithology	Age / Local names	ORGANIC PETROGRAPHY – Organic matter: Meta-vitrinite (V) [vol.%]						Meta-liptinite (L) [vol.%]															Inertinite (I) [vol.%]					Mineral matter, [vol. %]																					Reflection, %Ro									ORGANIC GEOCHEMISTRY: TOC [%]	S1 *	S2 *	HI ~	OI ~~	Tmax °C
			autochthonous heterogeneous		autochthonous homogeneous		recycled homogeneous		M.Spor.	M.Tel.	M.Alginite: M.lamalginite			M. Liptd.	M.Bit. I	M.Bit. II	M.Bit. III	M.Bit. IV	M.Bit. V	M.Bit. VI	Migrabitumen		Oil drop.	Fus.	Semifus.	Secret.	Intd.	Micr.	Mineral groundmass: calcareous			Mineral groundmass: clayey			F.g. pel.	C.g. pel.	Carbonates			Glauc.	Gyps.	Detrital minerals		Pyrite			Zooclasts			Bitumen: homogeneous			Bitumen: heterogeneous			Vitrinite								
			el.	eq.	el.	eq.	el.	eq.			discrete	fil.	layered								homog.	heter.							bits.	l.-bits.	n.-bits.	bits.	l.-bits.	mic.-r.			is. cry.	coccol.	dol.			qtz	mica	crys.	framb.	epig.	shell	fish r.	biocl.	mean	s.d.	n	mean	s.d.	n	mean	s.d.	n						
1227.10			-	-	-	-	-	-	0.1	0.8	-	-	-	-	-	2.4	-	-	-	-	1.4	0.2	-	0.2	-	-	0.6	21.7	0.2	-	-	-	-	18.8	0.2	-	37.4		-	-	-	-	0.1	6.5	2.2	0.5	-	-	6.9	3.43	0.30	19	-	-	-	-	-	-	5.7	1.3	0.6	11	21	-
1227.20			-	-	-	-	-	0.2	-	0.6	-	-	-	-	0.1	12.6	-	-	-	-	0.3	0.0	-	0.1	-	-	-	12.3	0.1	-	-	-	-	28.2	0.1	-	27.9		-	-	-	-	0.3	11.3	3.6	0.8	1.3	-	0.4	-	-	-	1.10	0.10	10	-	-	-	5.6	1.2	0.8	14	23	-
1227.27			-	-	-	-	-	-	0.1	0.8	-	-	-	-	1.1	11.2	-	-	-	-	0.3	0.1	-	-	-	-	-	18.1	0.1	-	-	-	-	19.9	-	-	26.2		-	-	-	-	0.3	16.2	3.7	0.6	1.3	-	-	-	-	-	-	-	-	3.33	0.60	100	5.7	1.2	0.6	11	20	-
1227.37			-	-	-	-	-	-	0.1	1.4	-	-	-	-	0.1	3.7	-	-	-	-	0.8	0.4	-	0.4	-	0.1	0.1	21.7	-	-	-	-	-	24.5	0.2	-	24.5		-	-	-	-	0.1	11.8	4.6	2.1	-	-	3.4	-	-	-	-	-	-	-	-	-	5.3	0.3	0.2	5	22	-
1227.56			0.1	-	-	-	-	-	-	0.5	-	-	-	-	1.4	2.8	-	-	-	-	0.2	-	-	0.2	-	-	0.2	19.9	-	-	-	-	-	30.8	-	-	22.1		0.1	-	-	-	-	15.0	1.4	3.0	1.8	-	0.6	-	-	-	-	-	-	-	-	-	4.9	0.2	0.0	1	31	-
1227.62			0.1	-	-	-	-	-	-	0.3	-	-	-	-	0.3	7.3	-	-	-	-	0.3	-	-	0.5	-	-	0.1	17.1	-	-	-	-	-	26.1	-	-	23.3		-	-	-	-	0.1	14.3	6.0	1.3	2.2	-	0.7	-	-	-	-	-	-	-	-	-	5.4	0.2	0.1	1	24	-
1227.87			-	-	-	-	-	-	-	0.4	-	-	-	-	0.3	1.7	-	-	-	-	0.4	0.1	-	0.1	-	0.1	0.1	27.8	-	-	-	-	-	21.8	-	-	18.6		-	-	-	-	0.2	17.9	3.3	4.0	-	-	3.2	-	-	-	-	-	-	-	-	-	5.5	0.5	0.3	5	21	-
1227.95			-	-	-	-	-	-	0.1	0.9	-	-	-	-	0.4	10.8	-	-	-	-	0.1	-	-	0.1	-	-	0.2	20.2	0.1	-	-	-	-	23.2	-	-	28.2		-	-	-	-	0.5	8.6	2.8	2.0	1.4	-	0.2	-	-	-	-	-	-	-	-	-	5.6	0.4	0.4	7	21	-
1228.02			-	-	-	-	-	-	-	0.2	-	-	-	-	1.8	5.2	-	-	-	-	0.2	-	-	0.4	-	-	0.1	20.4	0.1	-	-	-	-	18.8	-	-	27.7		-	-	-	-	-	13.0	5.0	3.0	-	-	4.1	-	-	-	-	-	-	3.52	0.36	100	5.7	0.7	0.3	6	23	-
1228.07			-	-	-	-	-	-	-	0.5	-	-	-	-	0.2	0.9	-	-	-	-	0.2	0.1	-	0.2	-	-	-	25.2	-	-	-	-	-	30.4	-	-	19.7		-	-	-	-	-	15.0	2.3	2.7	-	-	3.1	3.53	0.20	20	-	-	-	-	-	-	5.6	1.2	0.6	11	18	-
1228.12			-	-	-	-	-	-	0.1	1.4	-	-	-	-	0.5	1.1	-	-	-	-	0.2	-	-	0.8	-	0.1	0.4	21.8	0.1	-	-	-	-	27.7	-	-	21.2		0.1	-	-	-	-	15.9	3.2	1.0	-	-	4.4	-	-	-	-	-	-	-	-	-	5.5	0.3	0.1	2	24	-
1228.18			-	-	-	-	-	-	-	1.0	-	-	-	-	0.8	2.1	-	-	-	-	0.7	0.1	-	-	-	0.1	-	21.5	-	-	-	-	-	22.2	-	-	28.0		-	-	-	-	0.2	11.0	4.4	1.4	-	-	6.5	-	-	-	-	-	-	-	-	-	5.8	0.7	0.4	7	21	-
1228.25			-	-	-	-	-	-	0.1	0.8	-	-	-	-	-	6.4	-	-	-	-	0.8	-	-	0.4	-	0.1	0.3	22.3	-	-	-	-	-	21.3	-	-	30.8		-	-	-	-	0.1	10.4	1.0	2.8	1.8	-	0.5	-	-	-	-	-	-	-	-	-	-	-	-	-	-	-
1228.34			-	-	-	-	-	-	0.1	1.0	-	-	-	-	-	3.0	-	-	-	-	0.4	-	-	0.3	-	-	-	22.8	-	-	-	-	-	26.2	0.1	-	25.6		-	-	-	-	0.2	12.9	2.7	0.1	0.1	-	4.5	-	-	-	-	-	-	-	-	-	5.9	0.2	0.0	1	22	-
1228.40			-	-	-	-	-	-	0.1	1.1	-	-	-	-	-	8.0	-	-	-	-	0.3	0.1	-	0.1	-	-	0.1	14.0	-	-	-	-	-	13.9	-	-	31.3		0.1	-	-	-	0.6	21.6	4.5	0.6	3.0	-	0.6	-	-	-	-	-	-	-	-	-	6.1	0.6	0.5	8	20	-
1228.64			-	-	-	-	-	0.2	0.2	0.9	-	-	-	-	0.3	7.6	-	-	-	-	0.2	0.3	-	0.2	-	-	0.5	23.0	0.2	-	-	-	-	22.5	0.1	-	22.1		-	-	-	-	-	13.4	3.5	2.0	0.7	-	2.0	-	-	-	-	-	-	-	-	-	6.3	0.1	0.0	0	22	-
1228.84			-	-	-	-	-	-	-	0.9	-	-	-	-	-	6.3	-	-	-	-	0.4	-	-	0.2	-	0.1	-	18.2	-	-	-	-	-	30.2	-	-	21.3		0.1	-	-	-	0.1	14.5	4.7	1.5	0.9	-	0.6	-	-	-	-	-	-	-	-	-	6.7	0.4	0.3	4	21	-
1229.06	mudstone, calcareous with pyrite inclusions, plant remains	Lias epsilon	-	-	-	-	-	-	-	1.4	-	-	-	-	-	6.1	-	-	-	-	1.4	0.1	-	0.2	-	0.1	0.1	10.6	-	-	-	-	-	31.1	0.2	-	26.2		-	-	-	-	0.1	13.7	3.3	1.9	2.6	-	0.9	-	-	-	-	-	-	-	-	-	6.7	0.7	0.5	7	19	-
1229.14			-	-	-	-	-	-	0.1	0.7	-	-	-	-	0.9	10.2	-	-	-	-	0.5	0.1	-	-	-	-	0.3	18.2	-	-	-	-	-	17.0	-	-	24.7		-	-	-	-	0.2	15.9	4.0	3.2	1.1	-	2.9	-	-	-	-	-	-	-	-	-	6.7	0.7	0.3	5	21	-
1229.28			-	-	-	-	-	0.1	-	0.4	-	-	-	-	0.4	5.1	-	-	-	-	0.2	-	-	0.5	-	-	0.3	22.0	-	-	-	-	-	21.5	0.1	-	24.9		-	-	-	0.1	0.1	13.9	4.6	2.7	2.0	-	1.1	-	-	-	-	-	-	-	-	-	-	-	-	-	-	-
1229.43			-	-	-	-	-	-	0.2	1.9	-	-	-	-	-	6.0	-	-	-	-	-	-	-	0.2	-	-	-	26.9	-	-	-	-	-	17.4	-	-	29.5		0.1	-	-	-	0.3	9.7	3.4	1.0	2.1	-	1.2	-	-	-	-	-	-	-	-	-	6.5	0.2	0.1	2	23	-
1229.61			-	-	-	-	-	-	0.6	1.8	-	-	-	-	1.3	1.2	-	-	-	-	-	-	-	0.4	-	0.1	0.2	27.1	-	-	-	-	-	30.1	-	-	19.8		-	-	-	-	0.3	9.4	1.8	1.5	-	-	4.4	-	-	-	-	-	-	-	-	-	6.7	0.4	0.4	5	21	-
1229.75			-	-	-	-	-	-	-	1.0	-	-	-	-	3.3	0.1	-	-	-	-	-	0.4	-	0.4	-	0.1	-	32.4	2.0	-	-	-	-	32.4	-	-	13.3		-	-	-	0.1	0.0	4.0	1.4	4.8	0.1	-	4.2	-	-	-	-	-	-	3.51	0.65	100	7.0	0.1	0.0	1	19	-
1229.83			-	-	-	-	-	-	-	1.0	-	-	-	-	0.4	0.3	-	-	-	-	0.1	-	-	0.8	-	-	-	28.6	-	-	-	-	-	31.6	-	-	19.9		-	-	-	-	-	7.0	3.6	1.9	-	-	4.8	-	-	-	-	-	-	-	-	-	-	-	-	-	-	-
1229.93			-	-	-	-	-	-	-	0.9	-	-	-	-	0.2	1.2	-	-	-	-	0.6	-	-	0.3	-	0.1	-	21.5	-	-	-	-	-	25.7	-	-	29.3		-	-	-	-	0.1	9.8	1.9	0.4	-	-	8.0	-	-	-	-	-	-	3.66	0.35	100	6.8	0.1	0.0	1	21	-
1230.00			-	-	-	-	-	-	-	0.7	-	-	-	-	0.5	0.1	-	-	-	-	0.4	-	-	0.7	0.1	-	-	31.3	-	-	-	-	-	33.4	-	-	12.9		-	-	-	-	-	9.8	0.8	3.1	-	-	6.2	-	-	-	-	-	-	-	-	-	7.3	1.0	0.8	11	18	-
1230.10			-	-	-	-	-	-	-	0.8	-	-	-	-	0.2	1.1	-	-	-	-	0.8	-	-	0.4	-	-	0.2	27.9	-	-	-	-	-	15.9	-	-	19.5		-	-	-	-	-	20.7	4.3	2.1	0.1	-	6.0	-	-	-	-	-	-	-	-	-	6.7	0.4	0.3	4	19	-
1230.18			-	-	-	-	-	-	-	1.4	-	-	-	-	-	8.7	-	-	-	-	0.5	-	-	0.1	-	-	-	22.0	-	-	-	-	-	20.5	-	-	24.9		-	-	-	-	0.1	7.5	3.7	6.7	3.2	-	0.7	-	-	-	-	-	-	-	-	-	7.2	0.5	0.3	4	25	-
1230.50			-	-	-	-	-	-	-	-	-	-	-	-	0.2	2.9	-	-	-	-	0.5	0.3	-	0.3	-	-	-	18.4	-	-	-	-	-	16.3	0.1	-	22.9		-	-	-	-	0.5	26.1	6.8	1.4	2.2	-	0.8	-	-	-	-	-	-	-	-	-	6.7	0.2	0.1	1	20	-
1230.74			-	-	-	-	-	-	0.1	0.4	-	-	-	-	0.6	7.4	-	-	-	-	0.6	0.1	-	-	-	-	0.1	18.4	-	-	-	-	-	17.0	-	-	26.6		-	-	-	-	-	21.8	2.5	0.7	1.5	-	2.2	-	-	-	1.07	0.10	16	-	-	-	4.9	1.2	0.6	12	21	-
1230.94			-	-	-	-	-	-	-	0.2	-	-	-	-	-	0.6	-	-	-	-	-	0.1	-	-	-	-	-	-	75.1	-	-	-	-	4.7	-	-	1.7		-	-	-	-	-	2.1	0.1	14.1	-	-	1.3	-	-	-	-	-	-	-	-	-	-	-	-	-	-	-
1231.14			-	-	-	-	-	-	-	0.8	-	-	-	-	0.6	7.5	-	-	-	-	0.2	0.1	-	0.3	-	0.1	0.1	25.5	-	-	-	-	-	21.6	1.2	-	24.5		-	-	-	-	0.1	8.1	5.5	0.3	-	-	3.5	-	-	-	-	-	-	-	-	-	7.2	0.7	0.6	8	15	-
1231.30			-	-	-	-	-	-	-	0.3	-	-	-	-	0.5	2.5	-	-	-	-	0.3	0.1	-	0.2	-	0.2	-	22.5	0.2	-	-	-	-	20.1	0.8	-	27.1		-	-	-	-	0.1	13.9	4.9	4.7	0.3	-	1.3	-	-	-	-	-	-	-	-	-	6.0	0.6	0.4	6	22	-
1231.53			-	-	-	-	-	-	-	0.1	-	-	-	-	0.1	7.1	-	-	-	-	1.3	0.1	-	0.2	-	0.1	0.6	15.5	-	-	-	-	-	11.5	-	-	43.1		-	-	-	-	0.4	5.4	5.6	1.6	1.3	-	5.8	-	-	-	-	-	-	-	-	-	6.0	0.9	0.4	7	19	-
1231,73 o			-	-	-	-	-	-	-	0.7	-	-	-	-	0.2	1.4	-	-	-	-	1.5	-	-	0.3	-	-	-	20.9	-	-	-	-	-	33.5	-	-	26.4		-	-	-	-	-	5.3	2.6	-	-	-	6.4	-	-	-	-	-	-	-	-	-	6.7	0.6	0.2	4	19	-
1231.93			-	-	-	-	-	-	-	0.8	-	-	-	-	0.9	2.5	-	-	-	-	0.3	0.5	-	0.1	-	0.1	0.0	21.8	0.1	-	-	-	-	39.1	0.2	-	18.0		-	-	-	0.3	-	3.4	2.4	-	1.0	-	6.1	-	-	-	-	-	-	-	-	-	6.7	0.3	0.2	2	19	-
1231.84-1232.2			-	-	-	-	-	-	-	0.3	-	-	-	-	0.1	6.3	-	-	-	-	0.7	0.4	-	-	-	-	1.0	20.0	-	-	-	-	-	20.1	0.2	-	29.5		-	-	-	-	0.2	9.1	4.5	1.1	4.1	-	2.4	-	-	-	1.21	0.10	30	-	-	-	6.3	0.3	0.1	1	18	-
1231.84-1232.3			-	-	-	-	-	-	-	0.9	-	-	-	-	0.3	4.5	-	-	-	-	0.7	0.3	-	0.1	-	-	-	25.0	0.2	-	-	-	-	21.5	-	-	30.7		0.1	-	-	-	0.3	5.9	4.3	1.8	2.5	-	0.9	-	-	-	1.10	0.10	17	3.26	0.44	100	5.9	0.3	0.2	4	20	-
1231.84-1232.4			0.1	-	-	-	-	-	-	0.9	-	-	-	-	0.1	4.9	-	-	-	-	0.3	0.3	-	0.3	-	-	-	18.0	0.2	-	-	-	-	21.0	0.9	-	31.4		-	-	-	-	0.2	11.9	6.5	0.9	2.0	-	0.8	-	-	-	-	-	-	-	-	-	-	-	-	-	-	-

ORGANIC PETROGRAPHY

el.-elongated; eq.-equidimensional; M.Spor.- meta-sporinite; M.Tel.- meta-telalginite; fil.-filamentous; M.Liptd.-meta-liptodetrinite; M.Bit. I-meta-bituminite I; M.Bit. II-meta-bituminite II; M.Bit. III-meta-bituminite III; M.Bit. IV- meta-bituminite IV; M.Bit. IV- meta-bituminite IV; M.Bit.V- meta-bituminite V; M.Bit.VI- meta-bituminite VI; homog.-homogeneous; heter.-heterogeneous; Oil drop.-oil droplets; Fus.-fusinite; Semifus.-semifusinite; Secret.-secretinite; Intd.-inertodetrinite; Micr.- micrinite; fish r.-fish remains; biocl.-bioclasts; bits.-bituminous; l.-bits.-low bituminous; n.-bits.-non-bituminous; mic.-r.- micrinite-rich; F.g.pel.-Fine-grained peloids; C.g. pel.-Coarse-grained peloids; is. cry.-isolated crystals; coccol.-coccoliths; dol.-dolomite; Glauc.-Glauconite; qtz.-quartz; Gyps.-Gypsum; cryst.-crystals ; framb.-framboidal; epig.-epigenetic.
mean-mean value; s.d.-standart deviation; n-total number of measurements.

ORGANIC GEOCHEMISTRY

*-[mg HC/g],~-[mg HC/g TOC], ~~-[mg CO2/g TOC].

Appendix A6: Dotternhausen-1001 well

ORGANIC PETROGRAPHY

Organic matter

Sample	Depth, m	Lithology	Age / Local names	Vitrinite (V) [vol.%] autochthonous heterogeneous el.	autochthonous heterogeneous eq.	autochthonous homogeneous el.	autochthonous homogeneous eq.	recycled homogeneous el.	recycled homogeneous eq.	Liptinite (L) [vol.%] Spor.	Alginite Tel.	Alginite lamalginite discrete	lamalginite fil.	lamalginite layered	Liptd.	Bit. I	Bit. II	Bit. III	Bit. IV	Bit. V	Bit. VI	Migrabitumen homog.	Migrabitumen heter.	Oil drop.	Inertinite (I) [vol.%] Fus.	Semifus.	Secret.	Intd.	Micr.
22-29	34.15	mudstone, dark gray	Lias zeta	-	-	0.1	-	0.1	-	-	0.3	0.9	-	-	0.9	-	-	-	-	-	-	-	-	-	-	-	-	-	-
23-95	35.58	silty marls	Lias zeta	-	-	-	-	0.1	-	-	-	0.5	-	-	0.9	-	-	-	-	-	0.4	-	-	-	-	-	-	-	-
24-0.3	35.59		Lias zeta	-	-	-	-	-	-	-	-	0.5	0.3	-	-	-	-	-	0.1	-	0.4	-	-	-	-	-	-	-	-
24-65	36.44	marly shale, bituminous	Lias zeta	-	-	-	-	-	-	0.1	0.4	4.6	1.0	-	9.6	0.3	0.1	-	0.1	-	0.3	-	-	-	-	0.1	-	0.2	0.1
24-82	36.45		Lias epsilon	0.1	-	-	-	0.1	-	-	0.4	0.9	0.4	-	1.7	-	-	-	-	-	0.2	-	-	-	-	-	-	-	-
25-0.6	36.62		Lias epsilon	-	0.1	0.1	-	0.1	-	-	1.3	7.8	1.2	0.8	10.7	2.3	-	-	0.1	-	0.3	-	-	-	-	-	-	0.2	0.4
26-0.3	37.65		Lias epsilon	-	-	0.1	-	0.1	-	-	0.7	3.8	0.6	0.6	3.8	2.6	-	-	0.3	-	0.0	-	-	-	0.1	-	-	-	0.5
27-11	38.71		Lias epsilon	-	-	0.1	-	-	-	-	0.5	1.4	0.4	-	2.1	0.2	0.1	-	0.1	-	0.5	-	-	-	-	-	-	-	0.1
28-81	40.42	limestone, bituminous	Lias epsilon	-	-	0.1	-	0.2	-	-	0.4	4.8	0.4	0.5	6.7	0.8	-	0.1	3.8	-	0.5	-	-	-	-	-	-	0.2	0.7
30-56	42.17	silty marls, weakly bituminous	Lias epsilon	-	-	-	-	-	0.2	0.1	0.4	4.2	0.5	0.7	7.3	0.7	0.9	-	1.4	-	-	-	-	0.1	-	0.2	-	0.1	0.1
31-40	43.02	silty marls, bituminous, laminated	Lias epsilon	0.1	-	-	-	0.2	-	-	1.1	5.2	1.5	0.1	8.2	2.5	0.9	-	0.4	-	-	-	-	-	-	0.3	-	-	0.4
31-64	43.24	limestone, bituminous, poor laminated	Lias epsilon	-	-	-	-	0.1	-	-	0.1	4.3	0.9	-	2.9	0.1	0.2	-	0.3	-	0.7	-	1.0	0.2	-	-	-	-	-
32-90	44.38	silty marls, bituminous, laminated	Lias epsilon	-	-	-	-	-	-	-	0.7	3.9	0.9	0.8	0.5	3.3	0.4	-	-	-	2.2	-	-	1.8	-	-	-	-	-
33-21	44.82	limestone,bituminous, strong laminated	Lias epsilon	0.1	-	0.1	-	-	-	-	0.2	2.8	1.1	-	0.3	3.1	0.8	0.1	-	-	-	-	-	-	-	-	-	-	-
34-27	45.85		Lias epsilon	-	-	-	-	-	-	-	0.5	2.3	0.6	0.9	3.3	0.7	0.7	0.2	-	-	-	-	-	-	-	-	-	-	-
34-44 a	46.03	silty marls, bituminous	Lias epsilon	-	-	0.1	-	-	-	-	0.5	4.6	0.9	0.5	3.8	3.2	0.1	-	-	-	-	-	-	-	-	-	-	-	-
34-44 b	46.03		Lias epsilon	0.2	-	0.1	-	-	-	-	0.1	0.1	-	-	0.7	-	-	-	-	-	-	-	-	-	-	-	-	-	-
34-55	46.15	silty marls, weakly bituminous	Lias epsilon	-	-	0.1	-	-	-	-	1.0	4.3	0.7	0.5	2.2	4.0	-	0.1	-	-	-	-	-	-	-	-	-	0.3	-
34-60	46.2	silty marls, bituminous	Lias epsilon	0.1	-	0.1	-	-	-	-	1.3	1.4	2.8	1.0	2.1	1.5	1.0	0.1	-	-	-	-	-	-	-	-	-	0.1	-
34-73	46.34	silty marls, brownish, bituminous	Lias epsilon	-	-	0.1	-	-	-	0.1	1.2	5.7	0.6	0.5	6.8	1.0	-	-	0.1	-	-	-	-	0.1	-	-	-	0.5	-
35-55	47.16	silty marls	Lias epsilon	0.1	0.1	0.1	-	-	-	-	3.9	0.7	0.1	-	1.5	0.2	3.3	-	-	-	0.2	-	-	0.1	-	-	-	-	-
36-27	47.83	silty marls, bituminous	Lias epsilon	-	-	0.1	-	-	0.1	0.1	0.6	4.0	1.0	0.2	5.3	2.7	0.1	-	-	-	-	-	-	-	-	0.1	-	0.2	-

Mineral matter, [vol. %]

Sample	Depth, m	Mineral groundmass calcareous bits.	calcareous l.-bits.	calcareous n.-bits.	clayey bits.	clayey l.-bits.	clayey mic.-r.	F.g. pel.	C.g. pel.	Carbonates is. cry.	Carbonates coccol.	Carbonates dol.	Glauc.	Gyps.	Detrital minerals qtz	Detrital minerals mica	Pyrite crys.	Pyrite framb.	Pyrite epig.	Zooclasts shell	Zooclasts fish r.	Zooclasts biocl.	VR [%] mean	VR s.d.	VR n
22-29	34.15	76.1	-	8.2	2.9	0.7	-	-	0.7	-	-	0.3	-	-	0.3	0.2	0.1	-	0.3	5.9	-	2.0	-	-	-
23-95	35.58	7.9	-	68.4	0.7	1.0	-	-	-	-	-	6.0	-	-	0.2	0.3	0.5	0.1	4.9	0.7	-	7.4	-	-	-
24-0.3	35.59	1.8	-	83.3	0.3	0.4	-	-	-	-	-	5.9	-	-	0.2	0.1	-	-	0.6	0.1	0.1	5.9	-	-	-
24-65	36.44	27.0	-	37.2	3.1	0.2	-	-	0.4	-	-	0.7	-	-	1.4	0.1	1.5	0.1	2.6	3.4	0.1	5.3	-	-	-
24-82	36.45	7.3	-	57.3	4.6	0.8	-	-	-	-	-	-	-	-	0.1	0.1	1.3	0.1	5.2	4.0	1.3	14.1	-	-	-
25-0.6	36.62	2.7	34.5	5.0	14.3	0.5	-	-	2.4	-	-	0.4	-	-	3.9	0.6	2.9	2.2	3.4	1.4	0.1	0.3	0.47	0.06	-
26-0.3	37.65	20.1	-	4.9	9.3	5.2	-	-	0.3	-	-	0.1	-	-	0.3	-	1.4	0.4	3.3	40.6	0.6	0.3	-	-	-
27-11	38.71	64.1	-	24.8	1.9	1.1	-	-	0.2	-	-	-	-	-	0.1	-	-	0.5	1.7	-	-	0.1	-	-	-
28-81	40.42	46.7	-	2.6	13.5	1.1	-	-	3.5	-	-	0.1	-	-	2.0	-	2.7	0.7	3.0	2.9	0.2	1.8	0.44	0.04	5
30-56	42.17	40.5	-	11.1	14.3	8.3	-	-	2.7	-	-	-	-	-	1.9	0.4	1.2	1.1	1.5	-	-	0.1	-	-	-
31-40	43.02	21.5	-	10.8	22.7	4.7	-	-	5.7	0.1	-	-	-	-	2.5	0.3	4.8	2.6	3.2	0.1	0.1	-	-	-	-
31-64	43.24	59.1	-	20.0	0.9	0.3	-	-	0.3	-	-	0.1	-	-	-	-	0.7	0.1	7.5	0.2	-	-	-	-	-
32-90	44.38	40.1	-	28.7	9.2	1.6	-	-	0.2	-	-	-	-	-	0.2	0.3	0.6	2.6	1.9	-	-	0.1	-	-	-
33-21	44.82	2.1	-	9.6	34.2	19.7	-	-	7.6	-	-	-	-	-	6.2	0.4	3.7	7.2	-	-	0.1	0.6	0.4	0.04	71
34-27	45.85	3.1	-	5.1	30.8	32.9	-	-	5.1	0.1	-	-	-	-	4.5	0.3	1.2	6.8	0.1	-	0.5	0.3	-	-	-
34-44 a	46.03	2.9	-	5.2	36.6	15.4	-	-	9.0	-	-	-	-	-	5.8	0.3	0.8	7.8	2.1	0.1	0.3	-	-	-	-
34-44 b	46.03	5.5	-	77.5	0.1	2.8	-	-	0.2	-	-	7.9	-	-	0.3	0.7	0.4	0.2	0.1	0.1	2.3	0.7	-	-	-
34-55	46.15	8.1	-	12.7	47.9	6.9	-	-	0.8	-	-	-	-	-	2.1	0.1	2.5	2.9	0.0	2.2	0.4	0.2	-	-	-
34-60	46.2	3.0	-	3.0	64.7	6.0	-	-	1.0	-	-	-	-	-	3.1	-	0.4	6.4	-	0.9	-	-	-	-	-
34-73	46.34	31.2	-	5.6	19.8	2.0	-	-	0.7	-	-	0.1	-	-	2.6	0.3	6.4	4.2	10.2	-	0.1	0.1	-	-	-
35-55	47.16	47.2	-	26.7	5.6	4.6	-	-	0.1	-	-	2.1	-	-	0.3	0.8	0.7	0.1	1.1	-	-	0.4	-	-	-
36-27	47.83	48.1	-	5.5	13.1	7.5	-	-	1.0	-	-	0.1	-	-	2.9	0.4	3.1	1.6	2.1	0.1	-	-	-	-	-

ORGANIC PETROGRAPHY

el.-elongated; eq.-equidimensional; Spor.- sporinite; Tel.- telalginite; fil.-filamentous; Liptd.-liptodetrinite; Bit. I- bituminite I; Bit. II-bituminite II; Bit. III- bituminite III; Bit. IV- bituminite IV; Bit. IV- bituminite IV; Bit.V- bituminite V; Bit.VI- bituminite VI; homog.-homogeneous; heter.-heterogeneous; Oil drop.-oil droplets; Fus.-fusinite; Semifus.-semifusinite; Secret.-secretinite; Intd.-inertodetrinite; Micr.- micrinite; fish r.-fish remains; biocl.-bioclasts; bits.-bituminous; l.-bits.-low bituminous; n.-bits.-non-bituminous; mic.-r.- micrinite-rich; F.g.pel.-Fine-grained peloids; C.g. pel.-Coarse-grained peloids; is. cry.-isolated crystals; coccol.-coccoliths; dol.-dolomite; Glauc.-Glauconite; qtz.-quartz; Gyps.-Gypsum; cryst.-crystals ; framb.-framboidal; epig.-epigenetic.
mean-mean value; s.d.-standart deviation; n-total number of measurements.

ORGANIC GEOCHEMISTRY

*-[mg HC/g],~-[mg HC/g TOC], ~~-[mg CO2/g TOC].

Appendix A7: Notzingen-1017 well

Sample/ Depth, m	Lithology	Age	Local names	ORGANIC PETROGRAPHY: Organic matter: Vitrinite (V) [vol.%]	Liptinite (L) [vol.%]: Spor.	Alginite: Tel.	Alginite: Lamalg.	Liptd.	Bit.	Bitumen	Oil d.	(I) [vol.%]	Mineral matter, [vol. %]: Min.g.	Pyrite	Zooclasts	Reflection, %Ro: Bitumen: mean	Bitumen: s.d.	Bitumen: n	Bitumen-Jet: mean	Bitumen-Jet: s.d.	Bitumen-Jet: n	Vitrinite: mean	Vitrinite: s.d.	Vitrinite: n	ORGANIC GEOCHEMISTRY: TOC [%]	S1 *	S2 *	HI ~	OI ~~	Tmax °C
26.09	calcareous shale	Lias zeta		3.0	-	-	3.7	4.1	-	-	-	0.7	81.1	1.4	6.0	0.22	-	1	0.42	-	2	0.54	0.20	12	-	-	-	-	-	-
26.76				1.4	-	-	1.1	2.1	-	-	-	1.1	90.2	2.2	1.9	0.32	-	1	0.44	0.02	3	0.55	0.20	6	-	-	-	-	-	-
26.92	bituminous shale burrowed	Lias epsilon		-	0.5	0.6	8.8	15.0	3.0	0.1	-	0.5	64.4	4.0	3.1	0.24	0.50	28	0.43	0.03	11	0.56	0.20	4	1.4	0.2	5.15	348	22	431
27.05	bituminous shale			0.2	0.6	0.5	7.3	16.6	2.8	-	-	0.6	66.4	3.5	1.6	0.22	0.03	20	0.41	0.04	13	0.56	0.20	10	-	-	-	-	-	-
27.55				-	0.5	0.2	9.0	10.7	0.7	-	-	1.3	73.1	4.1	0.3	0.22	0.03	8	0.42	0.04	25	0.55	0.20	16	3.8	0.8	20.5	510	11	430
28.02	calcareous shale burrowed			0.1	0.5	0.1	7.9	9.6	2.4	-	-	0.8	72.6	5.6	0.2	0.25	0.02	4	0.43	0.04	32	0.55	0.20	6	7.3	2	44.2	618	10	429
28.18	bituminous shale			0.1	0.1	-	4.0	6.7	0.1	-	-	0.4	84.9	3.0	0.5	0.24	0.02	4	0.43	0.04	25	0.54	0.20	8	5.2	1.3	28.9	549	12	428
28.32	bituminous limestones			-	0.1	0.1	4.6	9.0	0.9	-	-	1.2	80.8	3.0	0.3	0.24	0.03	12	-	-	-	0.44	0.03	68	-	-	-	-	-	-
28.57	bituminous shales			0.3	0.5	0.1	7.5	10.2	1.8	-	-	0.9	74.3	4.3	0.2	0.24	0.03	12	-	-	-	0.47	0.06	38	9.9	4.1	60.2	557	7	428
28.80	bituminous limestone			0.0	0.5	-	3.0	7.1	-	-	-	0.8	81.7	6.9	0.0	0.22	0.03	31	0.40	0.05	23	0.53	0.02	5	2.8	0.5	15.4	527	12	431
29.05	bituminous shale			0.3	0.3	0.4	3.1	14.9	2.2	-	-	0.6	73.1	4.6	0.5	0.23	0.02	25	-	-	-	0.43	0.06	47	-	0.5	11.4	466	19	430
29.34				0.1	0.8	0.8	4.7	12.1	1.5	-	-	0.7	73.3	5.1	0.8	0.23	0.04	26	-	-	-	0.44	0.05	59	-	-	-	-	-	-
29.40	bituminous limestone			-	-	0.2	4.6	3.0	-	-	-	0.5	88.1	3.5	0.1	0.23	0.04	16	-	-	-	0.44	0.05	27	1.4	0.2	4.6	322	27	430
29.60	bituminous shale			-	0.1	0.7	4.7	14.6	4.8	-	-	0.4	69.0	5.5	0.3	0.22	0.00	1	-	-	-	0.42	-	2	7.8	2.4	49.8	585	7	432
29.90				-	0.2	-	6.7	13.7	8.0	-	-	-	67.2	4.0	0.2	0.26	0.04	36	0.39	0.02	16	0.51	0.04	10	6.3	1.9	36.2	559	10	431
30.06	bituminous limestone			0.1	-	0.1	12.8	10.9	1.9	-	-	-	70.0	3.9	0.2	0.21	0.03	14	0.39	0.03	28	0.49	0.02	14	11.2	5.8	66.8	615	13	430
30.25	bituminous shale			0.1	-	-	10.2	14.1	6.5	-	-	-	63.5	4.0	1.5	0.27	0.03	21	-	-	-	0.45	0.03	52	8.0	2.7	52.8	701	9	430
30.41				0.3	0.1	0.1	7.5	12.5	4.1	-	-	0.1	70.2	4.2	0.9	0.25	0.02	28	0.37	0.02	25	0.44	0.02	28	9.3	5.7	63.6	615	10	429
30.54	bituminous shale/coquina			0.3	0.3	1.2	9.7	9.8	8.6	0.1	-	0.4	60.8	4.0	4.8	0.27	0.04	18	0.40	0.02	20	0.52	0.03	45	5.5	4.1	39.6	615	9	430
30.72	bituminous calcareous shale			0.2	-	-	6.1	5.4	1.4	-	-	1.8	78.5	5.4	1.2	-	-	-	0.37	0.00	1	0.54	0.02	4	-	3.8	60.7	626	11	427
30.80	bituminous shale			0.7	0.2	0.5	5.4	6.1	0.5	-	-	2.0	81.7	2.9	-	0.26	0.03	13		-		0.47	0.04	38	8.0	3.5	51.1	668	9	431
30.90	bituminous shale burrowed			0.2	0.4	-	1.1	2.8	1.3	0.2	-	1.3	89.5	2.8	0.5	0.30	0.03	10	0.41	0.02	5	0.57	0.06	47	1.8	0.8	11.7	583	14	431
31.20	calcareous shale			0.7	-	0.4	-	4.1	0.4	-	-	1.9	87.2	4.9	0.5	0.25	0.05	5	0.41	0.02	4	0.58	0.05	18	7.1	2.8	44.7	682	11	430
31.35	bituminous shale burrowed			-	-	0.2	1.8	4.9	1.8	-	-	0.4	85.7	4.7	0.4	0.27	0.03	8	0.41	0.02	4	0.54	0.04	30	8.8	3.8	53.5	594	10	429
31.38	calcareous bituminuos shale			0.2	-	0.5	5.4	4.8	0.9	-	-	0.5	83.3	4.1	0.3	0.26	0.05	12	0.41	0.02	13	0.54	0.05	41	1.8	0.8	12.8	670	16	430
31.44	bituminous shale burrowed			-	-	0.6	3.3	1.9	11.1	0.2	-	0.8	66.2	15.9	-	0.27	0.03	12	0.44	0.03	29	0.60	0.05	16	7.2	3.1	46.7	630	12	429
31.50	calcareous shale			-	0.4	0.2	0.8	0.8	0.6	-	-	0.6	94.7	1.8	-	-	-	-	0.37	0.06	10	0.61	0.05	27	5.0	1.7	34.1	671	12	429
31.63	calcareous shale burrowed			-	0.4	0.3	1.6	2.7	5.8	0.1	-	0.6	84.6	3.5	0.3	-	-	-	0.40	0.09	22	0.57	0.04	45	3.2	0.8	18.8	603	18	429
31.76	bituminous shale			0.8	0.1	0.4	2.8	3.2	2.2	0.1	-	0.8	87.4	2.2	0.1	-	-	-	0.37	0.08	33	0.56	0.04	35	5.8	2	35.8	656	13	430
31.84	calcareous shale burrowed			0.5	0.3	0.3	2.4	2.6	1.2	0.2	-	0.5	88.7	3.1	0.2	-	-	-	0.34	0.08	31	0.56	0.03	56	-	2.6	44.3	619	10	432
32.20	calcareous shale	Lias delta		0.8	-	-	-	-	0.8	-	-	1.7	93.8	2.5	0.4	-	-	-	0.35	0.07	10	0.57	0.03	6	10.0	4.2	66.3	624	9	433
32.33	bituminous shale burrowed			-	-	-	2.3	2.8	1.2	-	-	0.2	89.7	2.9	0.9	-	-	-	0.35	0.08	13	0.56	0.04	44	9.7	4.5	62.89	630	10	432
32.44	calcareous shale			5.1	-	-	-	-	-	-	-	-	89.9	4.0	1.0	-	-	-	0.42	0.05	10	0.62	0.04	8	-	-	-	-	-	-
32.65				4.0	-	-	-	-	-	-	-	-	92.1	2.6	1.3	-	-	-	0.47	0.05	2	0.64	0.03	9	0.7	0.1	1.5	201	42	431

ORGANIC PETROGRAPHY

Spor.- sporinite; Tel.- telalginite; Lamalg.-lamalginite;Liptd.-liptodetrinite; Bit.- sum of bituminites; Oil d.-oil droplets; I-inertinite group; Min.g.-mineral groundmass.

mean-mean value; s.d.-standart deviation; n-total number of measurements.

ORGANIC GEOCHEMISTRY

*-[mg HC/g],~-[mg HC/g TOC], ~~-[mg CO2/g TOC].

Appendix A8: Bisingen-1002 well

Sample	Depth, m	Lithology	Age	ORGANIC PETROGRAPHY																							ORGANIC GEOCHEMISTRY				
				Organic matter											Mineral matter, [vol. %]				Reflection, %Ro								TOC	S1	S2	HI	Tmax
				Vitrinite	Liptinite (L) [vol.%]									(I)					Bitumen			Vitrinite				[%]	*	*	~	°C
			Local names	(V) [vol.%]	Spor.	Alginite		Liptd.	Bit.I	Bit.II	Bit.III	Bitumen	Oil d.	[vol.%]	Min.g.		Pyrite	Zooclasts	mean	s.d.	n	mean	s.d.	n							
						Tel.	Lamalg.								Clayey	Calc.															
343	21.22			2.0	1.3	-	0.3	-	-	-	-	-	-	0.8	95.4	0.1	2.0	0.5	0.37	0.06	11	0.53	0.05	19	0.9	0.2	0.8	88	438
341	22.63	Claystone	Dogger alpha	2.5	0.6	-	0.8	-	-	-	-	-	-	-	96.7	0.0	1.0	0.6	0.37	0.07	10	0.53	0.05	12	0.8	0.1	0.9	108	439
3a	24.61			1.5	0.3	-	0.6	1.2	0.2	-	0.5	-	-	-	96.4	0.0	1.0	0.9	0.43	0.06	16	0.58	0.05	10	0.7	0.2	0.6	89	436
346	25.87	Calcareous		1.7	-	-	-	0.6	0.1	-	-	-	-	0.6	41.1	56.4	2.0	2.3	0.38	0.05	8	0.55	0.05	9	0.4	0.1	0.4	102	437
344	26.44	shale		1.0	-	-	-	-	-	-	-	-	-	-	58.5	35.7	1.0	6.0	0.37	0.04	5	0.54	0.04	11	0.3	0.1	0.3	93	437
3a1	26.83	Limestone	Lias zeta	0.2	0.2	-	0.2	-	-	-	-	-	-	-		97.3	1.0	3.4	0.42	0.00	1	0.62	0.03	6	0.1	0.1	0.1	75	437
3a2	26.92	Calcareous shale		0.8	0.2	-	-	0.2	0.2	-	-	-	-	0.2	4.4	80.6	1.0	14.6	0.38	0.04	9	0.54	0.05	12	0.2	0.1	0.3	123	436
3a3	27.02	Bituminous limestone		0.5	-	-	-	0.2	0.1	-	-	-	-	-	22.7	65.6	4.0	13.4	-	-	-	-	-	-	0.5	0.2	1.1	211	433
3a4	27.06			0.2	0.9	-	1.4	2.9	0.9	-	0.3	-	-	0.8	60.0	32.4	3.0	2.9	-	-	-	-	-	-	1.9	0.4	6.8	365	435
3b	27.18			-	0.5	-	1.7	3.1	1.5	-	0.1	-	-	0.5	77.3	16.0	2.0	1.3	0.38	0.05	16	0.57	0.07	33	2.7	0.6	11.0	401	433
3c	27.49			-	0.2	0.1	3.6	3.6	1.6	-	0.9	-	-	0.7	60.9	28.6	2.0	1.4	-	-	-	-	-	-	3.3	0.8	15.3	467	433
311	28.13			0.2	1.2	0.2	4.3	3.7	2.2	-	0.8	-	-	0.2	46.3	38.2	2.0	5.3	-	-	-	-	-	-	5.1	1.7	27.4	538	431
319	28.71	Bituminous shale		-	-	-	7.3	8.1	6.0	-	0.7	-	-	0.4	58.9	21.1	2.0	4.2	-	-	-	-	-	-	6.6	2.6	35.7	542	433
3d	29.14			-	-	0.4	4.0	11.2	9.4	-	0.5	-	-	0.4	34.9	31.3	2.0	18.4	-	-	-	-	-	-	4.0	1.9	23.9	597	432
3c	29.45			0.2	-	-	8.8	8.6	4.3	-	0.7	-	-	0.2	33.0	51.4	4.0	1.2	-	-	-	-	-	-	6.0	2.9	35.0	580	433
318	29.91			-	-	0.3	3.9	3.6	2.6	-	0.2	-	-	0.3	32.7	42.5	3.0	17.6	0.28	0.04	20	0.49	0.04	36	5.6	2.4	31.7	567	430
320	30.85			-	-	0.4	10.6	4.8	2.9	-	0.5	-	-	0.6	44.2	39.0	3.0	1.0	-	-	-	-	-	-	7.0	3.3	37.7	540	432
3n	31.27	Bituminous limestone		-	-	-	-	-	-	-	-	-	-	-	3.0	96.0	1.0	-	-	-	-	-	-	-	0.4	0.1	0.8	200	435
3f	31.35			0.4	0.2	0.4	9.0	3.8	2.7	-	0.3	-	-	0.8	47.1	34.0	2.0	3.8	-	-	-	-	-	-	6.6	2.8	35.9	548	430
3g	31.56			0.3	0.3	-	6.2	6.5	4.2	-	0.9	-	-	-	19.4	57.9	3.0	9.9	-	-	-	-	-	-	4.8	1.7	23.1	484	429
323	31.92	Bituminous		-	0.2	0.2	8.6	5.4	3.3	-	0.5	-	-	0.2	45.8	36.8	3.0	1.4	-	-	-	-	-	-	6.1	3.0	33.6	548	429
314	32.76	shale		0.2	0.0	0.2	9.2	6.4	4.0	-	0.7	-	-	0.2	51.8	29.2	3.0	0.9	-	-	-	-	-	-	7.3	3.8	39.7	542	430
312	33.62			0.3	0.3	0.3	8.4	13.4	9.0	-	0.5	-	-	-	38.0	38.3	4.0	0.3	-	-	-	-	-	-	7.8	3.4	40.8	524	432
3m	34.09		Lias epsilon	-	0.5	0.3	8.9	7.6	4.2	-	0.6	-	-	-	16.4	62.0	5.0	0.3	0.27	0.06	11	0.49	0.04	58	5.2	2.2	28.1	542	431
324	34.34	Bituminous limestone		-	-	-	2.5	1.4	0.3	-	-	-	-	0.4	0.6	93.1	4.0	-	-	-	-	-	-	-	1.3	0.5	7.2	569	428
313	34.79	Bituminous shale		0.2	0.2	-	4.2	5.9	2.9	-	0.6	-	-	0.8	53.1	31.7	4.0	0.4	-	-	-	-	-	-	4.4	1.3	23.4	538	432
322	34.98	Bituminous limestone		-	-	-	1.8	1.3	0.5	-	-	-	-	0.3	0.2	90.7	4.0	-	0.27	0.04	21	0.45	0.06	72	6.5	2.9	36.2	557	431
315	35.66			-	-	-	5.4	30.3	28.5	-	0.1	-	-	-	41.9	13.8	5.0	0.5	0.23	0.05	117	0.45	0.04	206	11.6	6.7	67.9	586	430
317	36.73	Bituminous		0.3	0.3	-	10.5	7.7	5.0	-	0.1	-	-	-	57.1	19.0	6.0	1.5	0.26	0.04	186	0.49	0.04	267	7.7	3.4	44.8	585	431
316a	37.37	shale		-	0.0	1.2	5.8	8.5	6.3	0.1	0.0	-	-	0.2	51.9	28.1	3.0	3.0	-	-	-	-	-	-	8.5	4.4	42.6	503	431
316b	37.52			0.4	0.4	0.4	12.2	6.5	3.7	-	0.1	-	-	1.1	64.8	8.8	11.0	0.4	-	-	-	-	-	-	4.2	1.1	22.1	531	434
342	37.95	Calcareous shale		0.7	-	-	3.4	-	-	-	-	-	-	1.4	89.0	6.0	4.0	0.7	-	-	-	-	-	-	0.8	0.2	0.8	91	430
3o	38.38	Bituminous shale		-	0.3	0.3	9.0	8.5	4.1	-	-	-	-	0.6	73.1	6.2	9.0	0.9	-	-	-	-	-	-	4.0	1.0	16.3	408	430
3h	38.56	Calcareous shale		1.8	-	-	1.1	0.6	0.1	-	0.2	-	-	0.2	89.7	4.6	2.0	0.5	-	-	-	-	-	-	0.9	0.3	0.8	84	431
3i	38.79	Bituminous		-	0.3	-	4.5	11.5	6.1	0.1	0.9	-	-	0.8	74.4	6.4	6.0	-	0.33	0.05	22	0.59	0.06	37	1.7	0.4	4.2	251	434
340	38.94	shale		-	1.1	0.6	4.2	15.7	10.2	-	-	-	-	0.3	69.0	7.9	5.0	0.6	-	-	-	-	-	-	7.4	2.6	38.3	519	429
347	39.37	Calcareous shale		-	-	-	0.2	0.2	0.1	-	-	-	-	1.3	91.7	6.0	1.0	1.0	-	-	-	-	-	-	0.5	0.1	0.3	62	433
3j	39.49	Bituminous shale	Lias delta	-	-	-	3.3	2.4	0.5	-	0.2	-	-	1.2	82.0	10.7	4.0	-	-	-	-	-	-	-	0.9	0.2	1.5	164	432
3k	39.64			-	-	-	-	-	-	-	-	-	-	1.5	88.0	9.9	1.0	1.9	0.37	0.04	12	0.53	0.04	15	0.6	0.1	0.6	100	428
349	40.42	Calcareous shale		-	-	-	-	-	-	-	-	-	-	1.9	78.3	18.7	2.0	4.7	0.38	0.05	8	0.55	0.05	15	0.2	0.1	0.1	60	430
31	41.3			-	-	-	-	-	-	-	-	-	-	0.8	67.7	21.6	2.0	0.0	-	-	-	-	-	-	0.3	0.1	0.2	77	439

ORGANIC PETROGRAPHY

Spor.- sporinite; Tel.- telalginite; Lamalg.-lamalginite;Liptd.-liptodetrinite; Bit I, II, III.-bituminite I, bituminite II, bituminite III; Oil d.-oil droplets; I-inertinite group; Min.g.-mineral groundmass; Calc.-calcareous.
mean-mean value; s.d.-standart deviation; n-total number of measurements.

ORGANIC GEOCHEMISTRY

*-[mg HC/g],--[mg HC/g TOC].

APPENDIX B. SUMMARISING DIAGRAMS ILLUSTRATING THE DISTRIBUTION OF MACERALS; ORGANO-MINERAL MICROFACIES AND ORGANO-GEOCHEMICAL PARAMETERS WITH THE DEPTH

CONTENTS

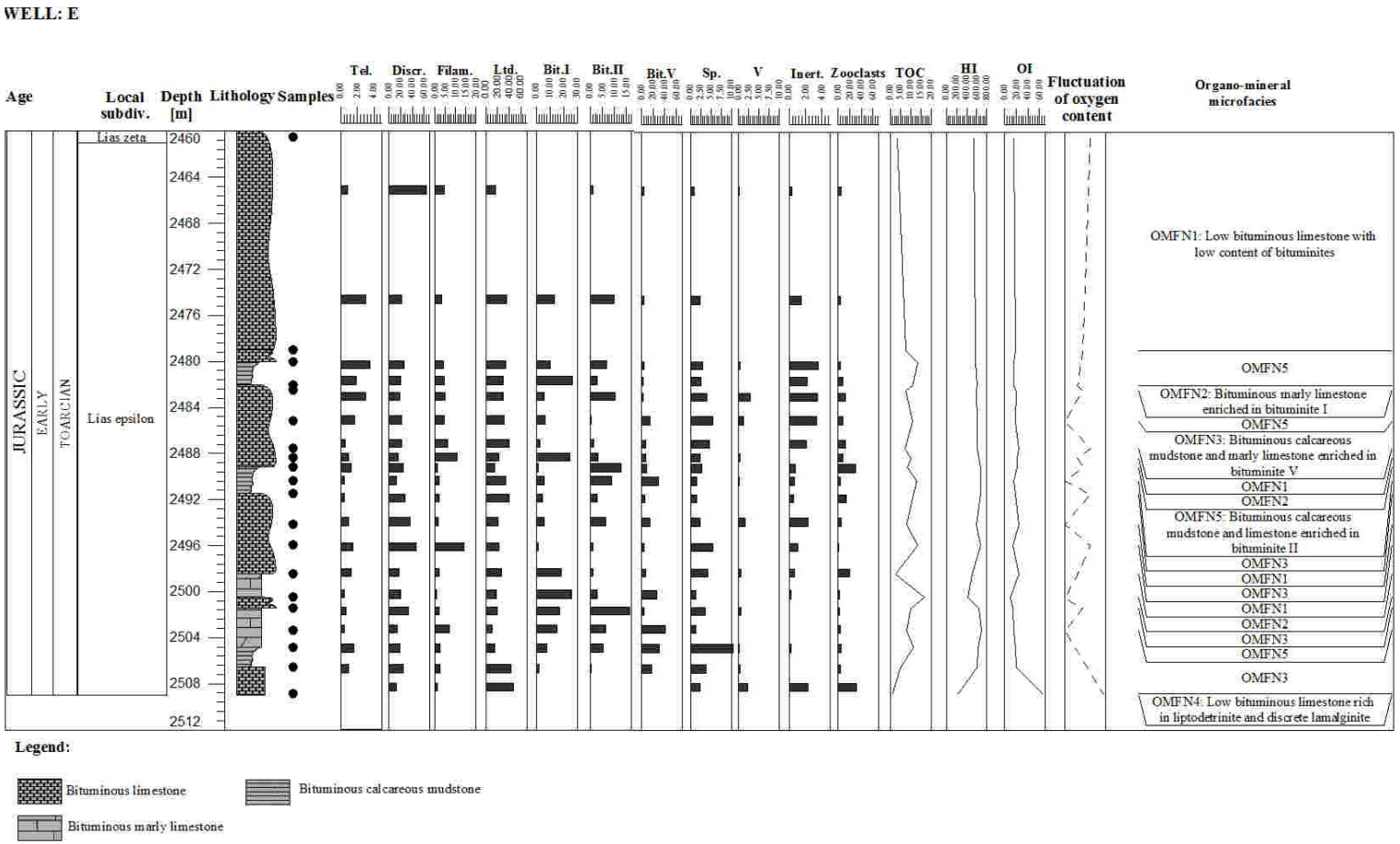

Appendix B1: Distribution of the individual macerals' organo-mineral microfacies with the depth in well E (the West Netherlands Basin). On the Figure: Tel. – telalginite; Discr. – discrete lamalginite; Filam. – filamentous lamalginite; Ltd. – liptodetrinite; Bit. – bituminite; Sp. – sporinite; V. – vitrinite; Inert. – inertinite.

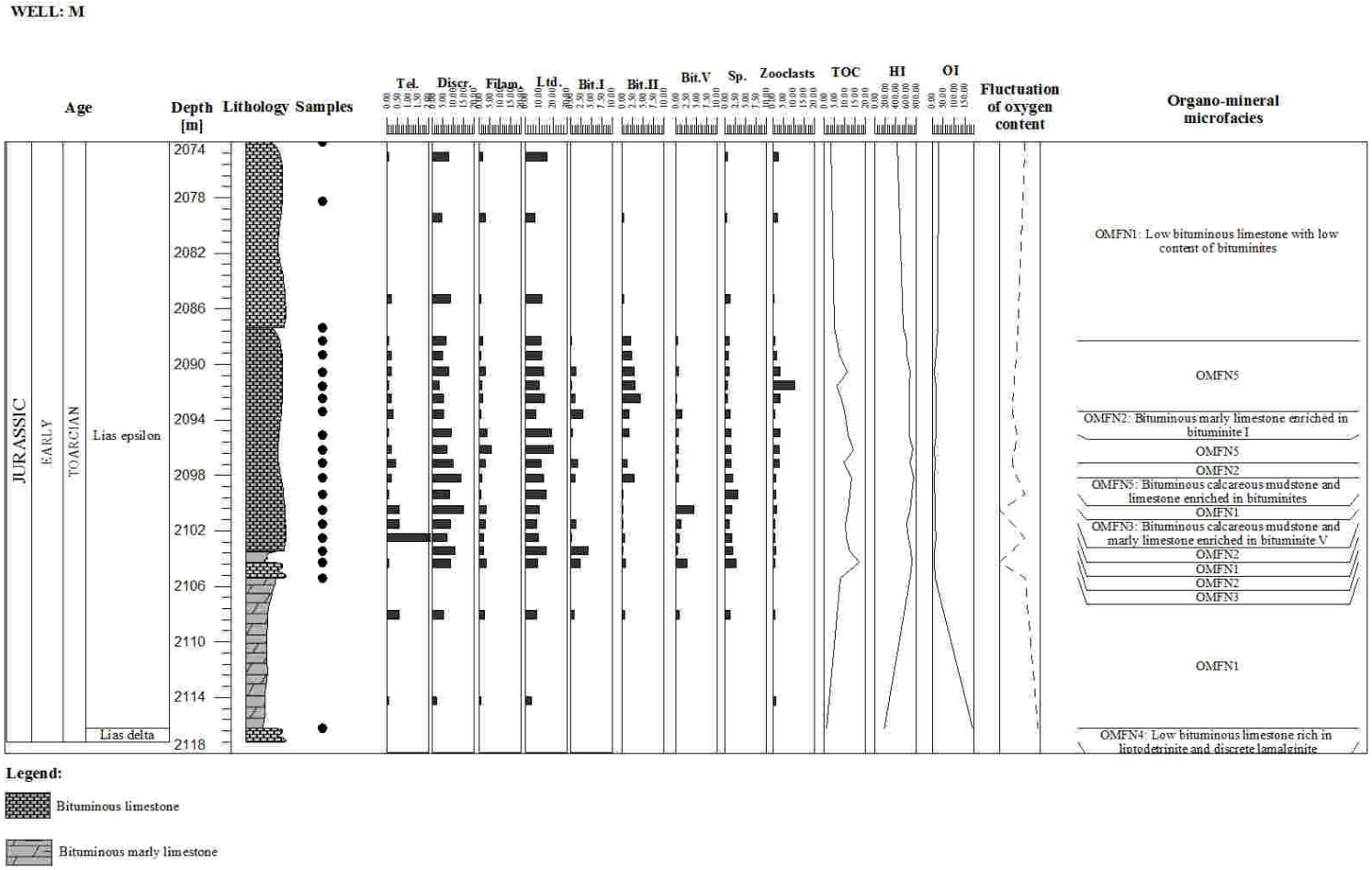

Appendix B2: Distribution of the individual macerals' organo-mineral microfacies with the depth in well M (the West Netherlands Basin). On the Figure: Tel. – telalginite; Discr. – discrete lamalginite; Filam. – filamentous lamalginite; Ltd. – liptodetrinite; Bit. – bituminite; Sp. – sporinite.

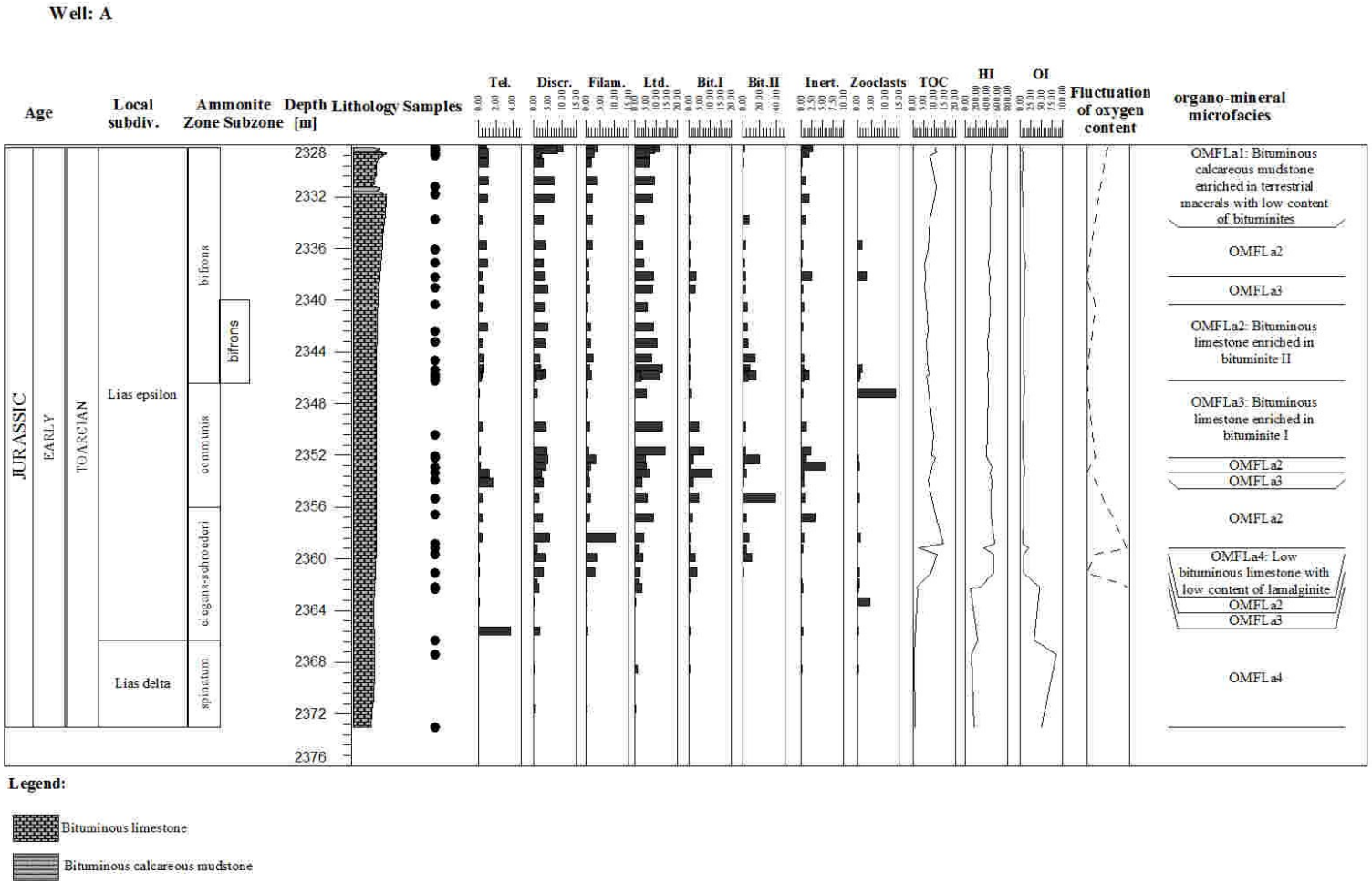

Appendix B3: Distribution of the individual macerals' organo-mineral microfacies with the depth in well A (the Lower Saxony Basin). Lithostratigraphic data are from unpublished BEB reports – BEB Erdöl und Erdgas GmbH. On the Figure: Tel. – telalginite; Discr. – discrete lamalginite; Filam. – filamentous lamalginite; Ltd. – liptodetrinite; Bit. – bituminite; Sp. – sporinite; Inert. – inertinite.

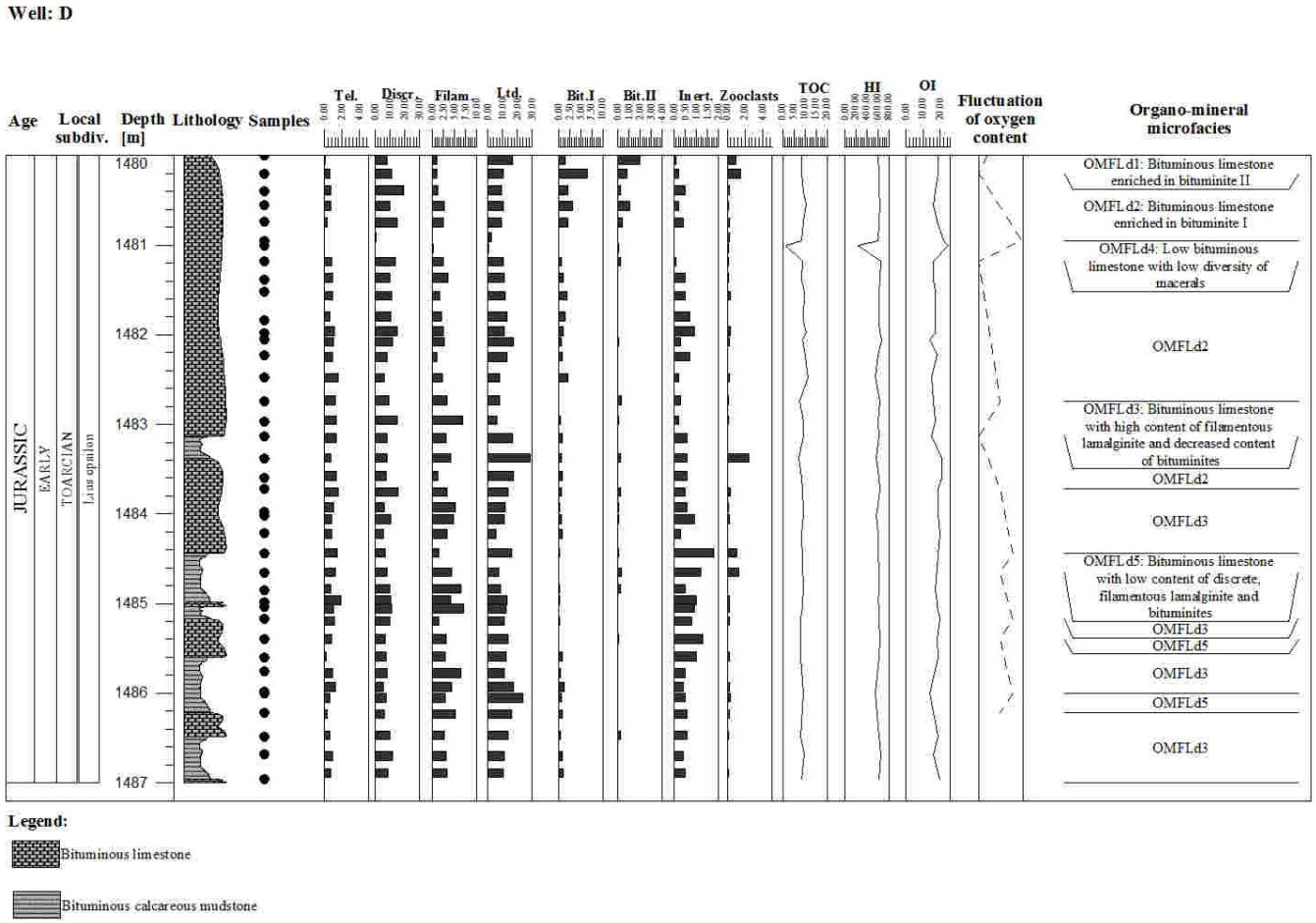

Appendix B4: Distribution of the individual macerals' organo-mineral microfacies with the depth in well D (the Lower Saxony Basin).

On the Figure: Tel. – telalginite; Discr. – discrete lamalginite; Filam. – filamentous lamalginite; Ltd. – liptodetrinite; Bit. – bituminite; Sp. – sporinite; Inert. – inertinite.

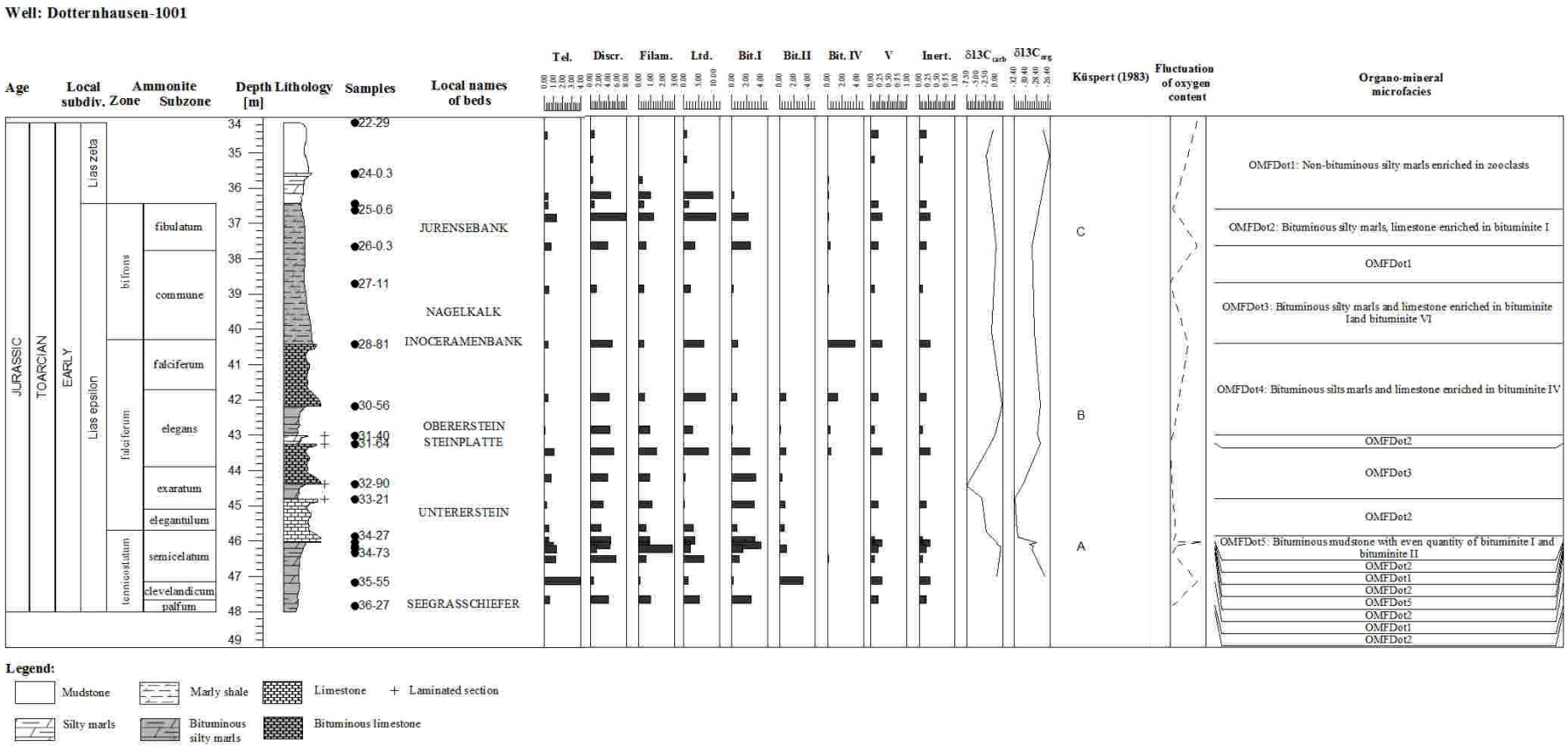

Appendix B5: Distribution of the individual macerals' organo-mineral microfacies with the depth in well Dotternhausen-1001 (the South German Basin).

On the Figure: Tel. – telalginite; Discr. – discrete lamalginite; Filam. – filamentous lamalginite; Ltd. – liptodetrinite; Bit. – bituminite; Sp. – sporinite; V. – vitrinite; Inert. – inertinite.

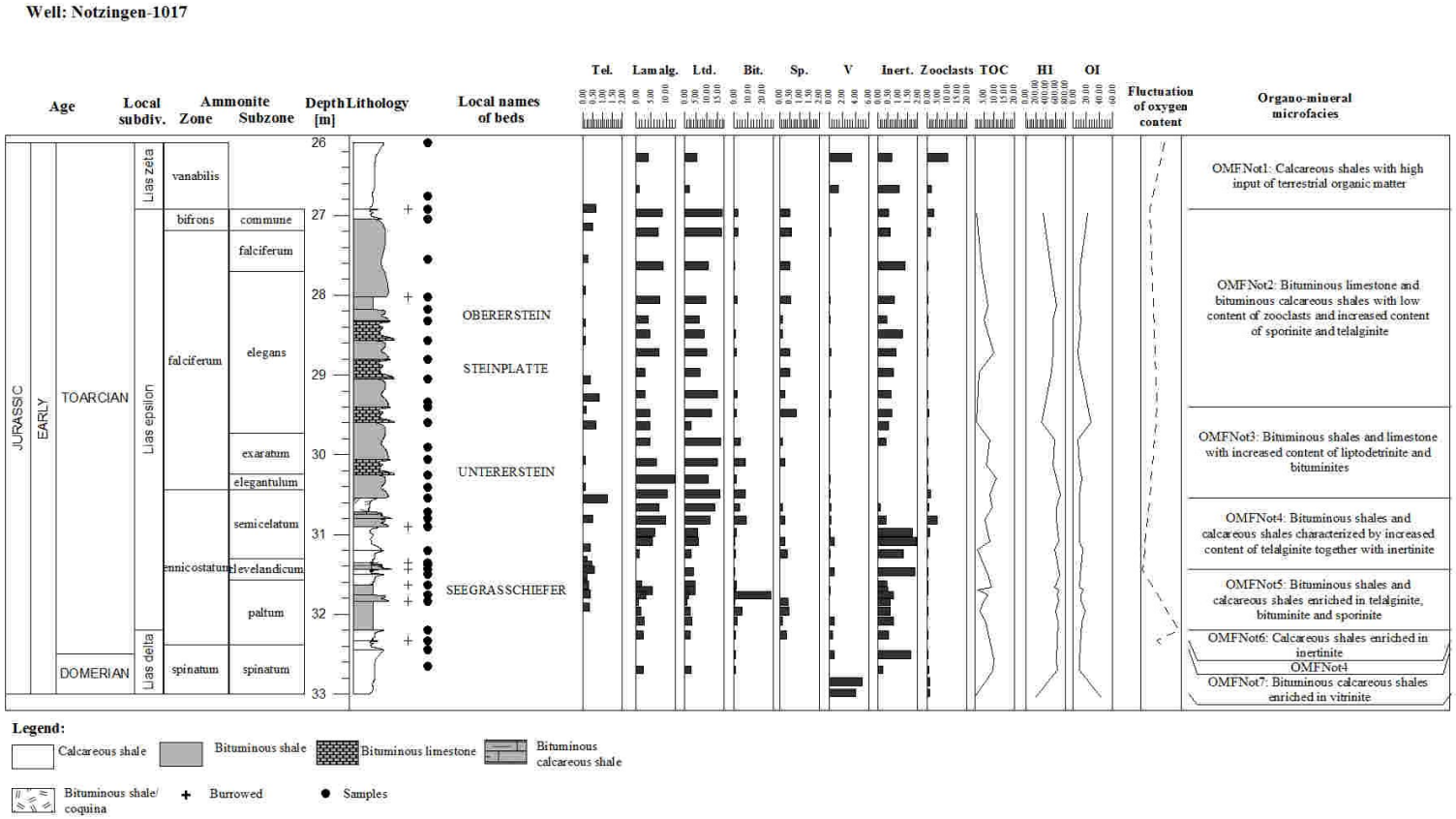

Appendix B6: Distribution of the individual macerals' organo-mineral microfacies with the depth in Notzingen-1017 well (the South German Basin).

On the Figure: Tel. – telalginite; Lamalg. – sum of lamalginite; Ltd. – liptodetrinite; Bit. – bituminite; Sp. – sporinite; V. – vitrinite; Inert. – inertinite.

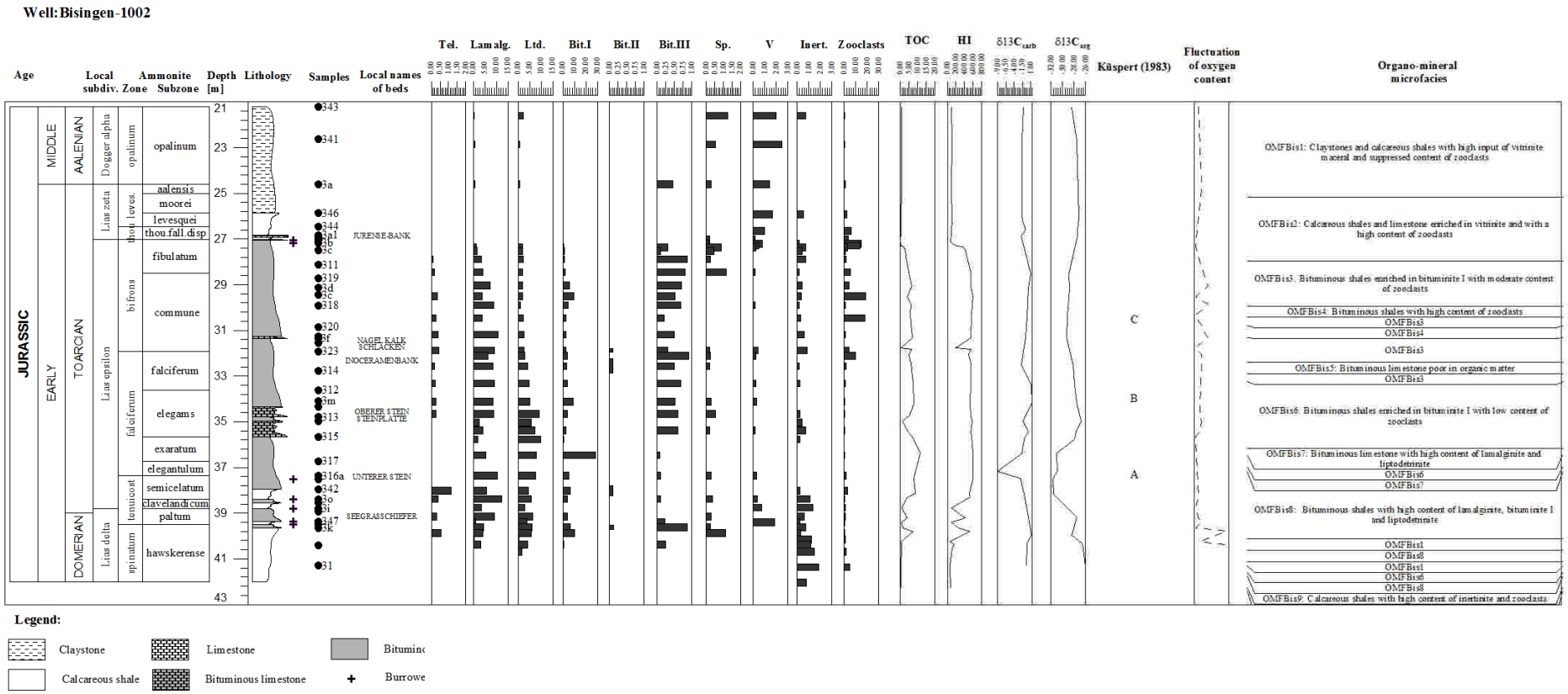

Appendix B7: Distribution of the individual macerals' organo-mineral microfacies with the depth in Bisingen-1002 well (the South German Basin).

On the Figure: Tel. – telalginite; Lamalg. – sum of lamalginite; Ltd. – liptodetrinite; Bit. – bituminite; Sp. – sporinite; V. – vitrinite; Inert. – inertinite.